Universiteit Antwerpen

Universitaire Instelling Antwerpen

Departement Scheikunde

Eindverslag: Addenda D t.e.m. F

Studie van de geochemische cycli van particulaire zware metalen en organische micropolluenten in het Noordzeemilieu

Oktober 1992- september 1996

R. Van Grieken, promotor
W. Jambers
L. De Bock
K. Torfs
K. Gysels
J. Injuk
H. Struyf
S. Hoornaert
H. Van Malderen

Eindverslag in het kader van het Impulsprogramma Zeewetenschappen, voor rekening van de Belgische Staat - Diensten van de Eerste Minister - Federale Diensten voor Wetenschappelijke, Technische en Culturele Aangelegenheden
(contract MS/06/050)

Oktober 1996

Addendum D

Artikels in Press en in Voorbereiding

Lijst met artikels in press, submitted en in voorbereiding in het kader van dit project gedurende de periode oktober 1992- september 1996.

In press en submitted (manuscript bijgevoegd)

1. Jambers W. en Van Grieken R., Environmental problems, in "Handbook of microscopy: applications in material science, solid-state physics and chemistry (Eds. Amelinckx S., Van Dyck D., Van Landuyt J.F. en Van Tenderloo G.), in press.

2. De Bock L. A., Jambers W. en Van Grieken R. E., Micro-analysis of individual aerosol particles using lectron, proton and laser beams, S. Afr. J Chem, in press.

3. De Bock L.A., Treiger B., Van der Auwera L. en Van Grieken R.E., Extraction of environmental information from large aerosol data sets through combined application of cluster and factor analyses, Anal. Chim. Acta, submitted.

4. Injuk J., De Bock L. en Van Grieken R., Structural heterogeneity within airborne particles, in "Environmental particles Vol IV: Atmospheric particles" (Eds. Harrison R.M. en Van Grieken R.), submitted.

5. Injuk J., Van Grieken R. en De Leeuw G., Deposition of atmospheric trace elements into the North Sea: coastal, ship, platform measurements and model predictions, Atmos. Environ., submitted.

6. Hoornaert S., Treiger B., Van Grieken R. en Laane R., Trend analysis of the published concentration of heavy metals in aerosols above the North Sea and The Channel for the period 19971-1994, Mar. Pol. Bul., submitted.

7. Jambers W. en Van Grieken R., Single particle characterisation of inorganic and organic North Sea suspension, Env. Sci. Techn., submitted.

In voorbereiding

1. Jambers W. en Van Grieken R., Single particle characterisation of North Sea suspension using EPXMA and STEM.

2. De Bock L. en Van Grieken R., Characterisation of individual aerosols collected above the North Sea.

3. Jambers W. en Van Grieken R., Characterisation of rainwater collected above the North Sea.

4. Jambers W., De Bock L. en Van Grieken R., Study of heavy metals in particulate matter in the North Sea environment.

Hoofdstuk in "Handbook of microscopy: applications in
material science, solid-state physics and chemistry"
Eds. : Amelinckx S., Van Dyck D., Van Landuyt J.F. en
Van Tendeloo G.

4 Environmental Problems

Wendy Jambers and René Van Grieken

4.1 Introduction

Although microbeam techniques are very useful for the analysis of individual environmental particles, they are still seldom used. This is surprising and may be related to the high cost of some of the instruments. Yet, the importance of particulate matter in the environment is well known: many components of environmental particles are toxic, particles are the major material carriers in water and air, atmospheric aerosols influence the visibility and the global climate, etc. Individual particle analysis is a very useful complement to conventional bulk analysis, because it can provide detailed information on the origin, formation processes, transport, reactivity, transformation reactions, and environmental impact of particles.

However, specific problems arise which are often related to the small size of the samples. Quantitative analyses are difficult to perform because the small dimension of the particles make the determination of the interaction volume uncertain and because of the absence of suitable standards. Statistically relevant results can only be obtained by the analysis of large numbers of particles per sample, which makes this very time consuming. This problem has already partly been solved by the recent developments in automation and computerization, and computer-controlled electron probe X-ray microanalysis (EPXMA) is the most advanced example of this technology. However, the major drawback of most microbeam techniques is the necessity to operate in vacuum, which implicates loss or transformation of most volatile and unstable compounds. Fourier transform infrared microscopy (FT-IR) and micro-Raman spectrometry both operate under atmospheric pressure, and are thus the only ones suitable for the analysis of these particles. Moreover, all microbeam techniques have specific limitations and they mostly complement each other with respect to detectable elements, detection limits, lateral resolution, etc. Hence, an optimal characterization of a sample is only possible by combining different microbeam techniques with bulk analysis.

This Chapter gives an overview of the recent applications of microbeam techniques, discussed in Vol. I of this book, on individual environmental particles. Environmental applications of microanalytical techniques have been reviewed by Grasserbauer [1], Van Grieken et al. [2], Van Grieken and Xhoffer [3], Xhoffer et al. [4], and Jambers et al. [5].

4.2 Scanning Microanalysis

As the differences between EPXMA and scanning electron microscopy/energy dispersive X-ray detection (SEM-EDX) have been minimized over the years to a slightly different instrumental set-up, both techniques can to some extent be used for both chemical and morphological studies. The applications of both are discussed together.

4.2.1 Automation

By combining an EPXMA ~~and~~ SEM-EDX system with a system for automated particle recognition and characterization (PRC), ~~high~~ amounts of individual particles can be analyzed in a few hours. At the Micro and Trace Analysis Center (MiTAC) of the University of Antwerp, this automation has been achieved using home-made software. The particles are located by performing successive horizontal line scans over the selected sample area. During this scan, the contour points of all detected particles are saved. When all contour points of a certain particle are found, the area, perimeter, and equivalent diameter (i.e. the diameter of a circle which has the same area as the particle) are calculated. According to the preselected parameters, ~~an~~ X-ray spectrum is recorded at the center of the particle or during a star scan over the particle. After this location, sizing, and characterization, the horizontal line scans are resumed until the next particle is detected. Since this technique produces a huge data matrix, combination with multivariate techniques and/or cluster analysis is necessary.

4.2.2 Applications to Aerosols

EPXMA and SEM-EDX have been used successfully for the analysis of aerosols collected in sampling places ranging from remote to workplace environments.

The most remote place on Earth is probably the Antarctic continent, and it is thus the ideal site at which to collect background aerosols. Early research on single Antarctic aerosols from different locations have shown that the background aerosols mainly exist of sulfur rich particles (probably formed by gas-to-particle conversion), sea salt particles (formed by bubble bursting and wave action in the ocean), aluminosilicates (Earth crust dust and/or particles from local sources, such as volcanos and geysers), and iron rich particles (long-range transport anthropogenic particles and/or meteoric dust) [6–11]. The relative concentrations of these particle types vary with season, meteorological conditions, and sampling site. Aerosols collected on the coast of the Antarctic continent are dominated by marine components in both the fine and coarse fractions [12–15]. In a significant number of sea salt particles, small amounts of sulfur were detected, indicating a possible reaction with gaseous sulfur compounds. In most particles larger than 0.1 μm, sulfur is present as gypsum. Manual analysis indicated that some aerosols are an internal mixture of marine components and silicates. An example of the dependence of the season is the dominance, by number and mass, of ~~sulfur~~ particles during the summer [8–14, 17]. Some researchers

[9, 16] have also detected H_2SO_4 and $(NH_4)_2SO_4$ particles.

By combining SEM analysis with chemical tests for the characterization of individual aerosols from Cape Grim (Tasmania), the Mauna Loa Observatory (Hawaii) and Point Barrow (Alaska), Bigg [16] found that the majority of the particles were composed of sulfuric acid or ammonium sulfate. The sulfuric acid particles dominated the samples from Barrow and Mauna Loa, while at the Antarctic and Cape Grime sites ammonium sulfate was dominant.

Siberia is characterized by both very remote areas and some strongly polluted regions. Since aerosols from this huge subcontinent have an impact on the Arctic and on the global climate, studies have been started to investigate the production, transport, and deposition of both natural and pollution aerosols at the local, regional and long-range levels [18].

Analysis of volcanic loess on Hawaii has given new evidence ~~to~~ the long-range transportation of particles [19]. In late Quaternary loess deposits of the Pahala Formation at Pu'u Mahana, quartz grains were found which are virtually unknown in the basalt of Hawaii. The study was done by combining X-ray diffraction of bulk samples with SEM-EDX measurements on single mineral grains and X-ray mappings of particles in a grain matrix. Figure 1 shows a silicon and an iron X-ray mapping of the same particles. The intensity of the particles in these maps gives an indication of the elemental concentration. Note that the quartz grains in Fig. 1a (some are indicated by arrows) are dark in color in Fig. 1b. Only the iron containing minerals, including basaltic glass, are lighter in color. Numerous 1–10 µm and some 60 µm quartz particles were found, with a total deposit contribution of 1–3%. It is assumed that these particles originate from Asia and were carried over more than 10 000 km by late Quaternary storms.

Patterson et al. [20] analyzed remote continental and marine aerosols, collected with an aircraft at altitudes ranging from the air–sea exchange zone to the free troposphere. For the continental aerosols no significant differences were noted as a function of altitude. The aerosol mass with a diameter greater than 0.5 µm mainly consisted of soil dust particles, ~~which~~ the sulfate particles dominated the small fraction (diameter <0.5 µm). However, the composition of the samples from the Pacific showed large variations with altitude. Also noticeable was a decrease in the crustal components from the northern towards the southern Pacific.

Individual aerosol particles were sampled over the Amazon Basin and analyzed using automated EPXMA [13, 15, 21]. The results were used to estimate the chemical processes occurring in the Amazon Basin atmosphere and the aerosol and gas emission of the forest. The two main components, soil dust and biological derived material, could be linked to local sources.

Pacific aerosols were analyzed with manual and automated EPXMA. Manual analysis of central Pacific aerosols revealed that a large amount of aluminosilicates was present as an internal mixture with sea salt aerosols [22]. These mixtures are probably the result of a coagulation of aluminosilicates and sea salt particles inside the clouds. Automated analysis of more than 5000 individual particles from the Eastern Pacific showed that more than 45% of all particles were 'pure' sulfur (no other detectable elements) [23]. The morphology and the diameter of these particles were used to discriminate between submicrometer particles which evaporated under the electron beam and which are most probably ammonium sulfate and less volatile particles with a mean diameter of 2 μm and more spherical in shape. A considerable portion of the particles has only characteristic calcium and phosphorus X-ray signals. Their abundance seemed to show some increase as the sampling location approached the continent, but no final conclusions could be drawn.

For several years automated EPXMA has been used to characterize individual North Sea aerosols [24]. During a first research period, 2500 particles sampled from a research vessel were sized, chemically analyzed and classified [25]. Sea salt particles dominate in air masses which originate from above the Atlantic Ocean. When the air has been above land for a considerable time, the amounts of aluminosilicates (mostly spherical fly ash particles), carbonates, gypsum, and spherical iron oxides increase. During the following 4 years more than 25 000 particles from over the North Sea and the English Channel were collected on board a research vessel [26]. The combination of single-particle analysis and hierarchical clustering revealed that the majority of the North Sea aerosols are composed of sea salt, sulfur-rich particles, silicates, and gypsum. Meteorological conditions and sampling locations influence the abundance of the particle types. A study of the difference between the samples was based on principal component analysis (PCA) of the abundances of the different particle types. A division in components was found and all could be source appointed. The marine derived aerosols were the first group, and their importance grows with increasing wind speed (sea salt aerosol formation is dominated by the breaking of waves, which is dependent on wind speed) and sampling at more marine locations. Anthropogenic derived gypsum, which seemed to be of more importance when the air originated from above southern England, formed the second component. The samples in the third group were characterized by particles with a high silicate and sulfur content. A second PCA differentiated between the two sources of this last group, namely a mixed marine/continental origin and a truly continental one.

The aerosol composition at different heights above the North Sea was studied by the automated EPXMA of 50 000 particles which were collected at six different altitudes [27]. The continental air masses were dominated by aluminosilicates, gypsum, and iron rich particles. Due to the turbulence of the atmosphere no major difference in main particle types with altitude were noted for either western or marine air masses. Aluminosilicates, iron rich particles, ~~and~~ sea salt enriched with lead, and organic materials were the major particle types in these air masses. Combustion or energy-generation processes seemed to be responsible for about 60% of the ~~analysis~~ particles.

analyzed

The modification of particle composition by air–sea interactions was examined by analyzing aerosol and rain water samples, which were collected on two research vessels located on the diameter of a 200 km circle one downwind from the other in the central part of the North Sea [28]. Automated EPXMA in combination with hierarchical clustering revealed three to eight different particle types and a principal factor analysis (PFA) appointed these groups to four major sources. As the air is crossing the North Sea the quantity of aluminosilicate particles is reduced and replaced by sea salt and sea-water crystallization products. No shrinking of the particle diameter was observed. Manual EPXMA was used to study the relation between particle composition, origin, and shape. For most particle types a shape-based characterization was possible. The collected rainwater showed serious variation in composition and diameter.

Giant aerosols have a diameter >1 μm. The amount of these particles in the lower troposphere is small compared with the condensation-mode particles, but their contribution to atmospheric deposition is of great importance [29–31]. A slow realization of the importance of these particles, the sampling difficulties and the measurement errors have made the giant aerosol a new and still little explored research domain. The importance of these giant aerosols in the North Sea atmosphere was tested using samples which were collected on an impactor rod on top of an aircraft [32]. These samples were analyzed by a combination of EPXMA with different multivariate techniques. PFA revealed aluminosilicate dispersal, combustion processes, industrial activity, and marine origin as the major sources for these giant aerosols. Samples associated with marine and continental air masses could be differentiated by means of clustering analysis. The size distribution of the main particle types fitted a log–normal size distribution curve well, with an average diameter of about 3 μm. Only aluminosilicates had a bimodal size distribution and average size maxima at 4 and 15 μm.

Studies of volcanic ash particles using a combination of SEM and X-ray photoelectron spectroscopy (XPS) have been reported by several researchers [33–35]. The EDX spectra of these particles show major aluminum, calcium, potassium, and silicon peaks, and small contributions for iron, manganese, and titanium. Rampino and Self [36] have proven that these volcanic aerosols are a fraction of the terrestrial particles released directly into the stratosphere. Other sources of stratospheric particles are sulfuric acid nucleation, sapphires, and meteorites [37]. The major particle types are aluminum metal particles and Al_2O_3 spheres. Sulfate particles of terrestrial origin dominate the submicrometer aerosol mass [38]. Volcanic eruptions also emit large amounts of sulfur. The thin sulfate coating on ash particles is probably the result of reaction with this sulfur in stratospheric clouds [39].

The influence of the huge oil fires in Kuwait in 1991 on the local and global environment was studied by analyzing aerosol samples collected on board an aircraft at different altitudes in the plumes [40]. Analysis of transport smoke clouds revealed more small sulfate particles, which are most probably produced by the oxidation and nucleation of sulfur oxide. In areas where rarefication of the plumes has occurred, large soot, salt, and dust particles are coated with sulfur and become active cloud condensation nuclei (CCN). The CCN initiate the formation of cloud, haze, fog, and smog droplets. In the absence of rain showers, black carbon particles, such as those formed by these fires, have a tendency to remain airborne and can undergo long-range transportation. Air trajectory studies show that there were periods when the aerosols generated by the oil fires could have reached China.

The relation between the fires in Kuwait and the severe rainfall in China at the end of May and the beginning of June will have to be proven with more research.

Individual stack fly ash particles from a Hungarian power station [41] and Hungarian background aerosols [42] have both been analyzed using EPXMA. In the power-plant aerosol fraction of particles <2 μm, two unexpected particle types were found: barium rich particles and arsenic rich gypsum particles. Anthropogenic sources also seemed to be the major origin of the 0.3–20 μm background aerosols. Air back-trajectories confirm this statement.

The urban aerosol composition is highly variable and depends on geographical location and local activities and industries. Aerosols from the city of Khartoum, Sudan, have been analyzed using different bulk techniques and automated EPXMA for single-particle analysis [43]. The majority of these aerosols were identified as soil dust, namely aluminosilicates and smaller amounts of quartz and calcium carbonate. This enormous amount of natural airborne dust has, to our knowledge, the lowest concentration of sulfur, chlorine, zinc, bromine, and lead in urban aerosols ever reported. The daily variation in the concentration of bromine, lead, and crustal elements indicates that the production is from traffic. Aerosol particles were also collected 4 km west of Santiago, Chile, and analyzed using automated EPXMA [44]. Both the coarse and the fine fraction could be classified into eight particle types. The coarse-particle fraction was dominated by soil dust particles, while anthropogenic particles were predominant in the fine mode. Although a large amount of particles contain sulfur, they are not all of one particle type but represent six ~~of eight~~ groups. The automated EPXMA of 15 000 aerosols from Antwerp, Belgium, showed that soil dust dominates these samples [45, 46]. Sulfates, lead-rich particles, and other anthropogenic particles are also often detected. The combustion of leaded fuel is the main source of lead containing particles. Post and Buseck [47] used SEM analysis to characterize 8000 individual urban aerosols from Phoenix, Arizona. The coarse fraction consisted of crustal material and a minor fraction of biological material, sulfur rich and lead rich particles. Some 60–80% of the fine fraction were sulfur containing particles, presumably ammonium sulfates.

Hunt et al. [48] used SEM-EDX to study lead containing particles in the floor dust of 16 houses in the London borough of Richmond, England. The identification of the different particle types was based on a classification scheme which was constructed by analyzing different types of lead source particles [49]. Lead rich particles with diameters ranging from 0 to 64 μm were identified as paint, road dust, and garden soil. Paint was also the major contributor to the lead containing dust in the size range 64–100 μm. The contribution of the major sources seemed to be independent of the age of the houses.

A combination of SEM and transmission electron microscopy (TEM) with thin-film chemical tests was used to determine the nature and morphology of methane sulfonic acid (MSA) particles, which were collected over Sakushima Island, Japan [50]. Dimethyl sulfate, which is transferred from the sea surface into the atmosphere, is oxidized to MSA and sulfur dioxide. MSA containing particles dominate in the coarse fraction of very humid air masses. These mixed particles are produced by heterogeneous nucleation reactions of gaseous MSA with sea salt and soil particles. The submicrometer fraction is dominated by sulfate particles and contains no MSA particles.

Pardess et al. [51] have recently developed a new method for determining the sulfur content in single particles by SEM. Artificially generated sulfur particles of known composition were used to calculate the calibration curves. These curves give a reasonably accurate determination of the sulfur mass in particles larger than 0.4 μm and with a minimum of 10^{-13} g of sulfur. This method can also be used to estimate the sulfur contents of heterogeneous particles.

Industrial and workplace aerosols, especially fly ash, are often analyzed using EPXMA and SEM [52–63]. The term 'fly ash' is used for a variety of particles which are emitted during combustion processes. Both the micrometer and the submicrometer size particles have silicon, aluminum, potassium, iron, titanium, manganese, and sulfur as their major elements, and minor contributions from calcium, phosphorus, sodium, chlorine, and nickel. The fly ash particles are known to have a characteristic spherical shape, although irregularly shaped particles were also observed [63]. Power plants running on oil or coal produce different fly ashes [64–67]. Oil fly ash particles contain considerably more sulfur and substantial concentrations of vanadium and nickel. Over 90% of the particles contribute to the fine fraction. The long exposure to heat and oxidants make their morphology variable from nearly spherical to lacy and spongy lumps [68]. These spongy structures easily break down into smaller aggregates. Over 90% of coal fly ash is in the coarse particle fraction [66]. They have a smooth mineral spherical morphology and contain less cenospheres.

4.2.3 Applications to Suspensions and Sediments

Sedimentation processes, interactions between the water column and the sediments, and physicochemical reactions of suspended and sedimented particles have been studied extensively using EPXMA. Initially, manual SEM-EDX was used for the chemical and morphological characterization of aquatic particles [69–72]. Bishop, Biscaye, and coworkers [73, 74] were the first to report results of automated EPXMA on aquatic particles. They analyzed individual particles from the nepheloid layer of the Atlantic Ocean and classified them according to their silicon/aluminum ratio.

EPXMA and SEM were used to identify the sources and study the lateral distribution of suspended matter collected around Sumbawa Island, Indonesia [75]. Iron rich particles, probably of volcanic origin, dominate samples collected from the northern side of the island. Suspended matter from Saleh Bay, a huge bay on the Sumbawa Island near to the Tambora volcano, is characterized by a high content of tin rich particles. Considerable amounts of tin rich particles have also been found in the Flores Sea and the Makasar Strait [76, 77]. There are possible regional sources of tin, but other sources cannot be excluded. A morphological study of aggregates showed that these exist only in the presence of biogenic material such as diatoms and coccolithophorids. The correlation between aggregates and the presence of diatoms has been reported previously [76, 78]. The flocculated particles are probably held together by a gummy organic material produced by the diatoms [75].

North Sea bulk water and corresponding surface microlayer samples have been characterized by a combination of EPXMA and laser microprobe mass spectrometry (LMMS) [79]. Due to the roughness of the sea, only small differences in particle type and abundance could be found between the collected surface microlayer and the underlying bulk samples. Organic particulate matter was more abundant in the microlayer and showed a correlation with the metal-rich fraction. Figures 2 and 3 show the secondary electron image and the X-ray spectrum of a fly-ash particle (aluminosilicate rich in iron, calcium, manganese, and sulfur) and a diatom (a silicon rich skeleton with a small aluminum fraction), both found in the surface microlayer of the North Sea. These marine samples were also compared with the corresponding aerosol samples. Since no chemical analogs for calcium rich aluminosilicates were observed above the North Sea, they must be of aquatic origin. Titanium rich particles, however, have a similar marine and atmospheric fraction and are thus deposited from the air.

Silty and clayey sediment samples from the Baltic Sea were analyzed with automated EPXMA and conventional bulk techniques [80, 81]. Automated EPXMA showed nine particle types which could be identified as different minerals. Quartz and aluminosilicates were the most abundant particle types, but they are not characteristic for the geochemistry of the Baltic sediments. Anoxic sediment environments, such as the Gotland Deep, are characterized by reduced species, like iron sulfides and rhodochrosite. Iron and manganese oxides/hydroxides indicate oxic environments such as Kattegat. In regions with periodic redox changes, sulfides and oxides/hydroxides are both present. Calcium rich particles are only detected in the transition zone between the Baltic Sea and the North Sea. The clear gradient from the North Sea to the Baltic Sea indicates the inflow of calcium rich particles from the North Sea [80]. The high abundance of titanium rich particles near the coast of Germany and southern Poland could be the result of erosion or of anthropogenic deposits [81].

Automated EPXMA has also been used to study deposition, remobilization, and mixing of materials from different origins in estuaries. Analysis of suspended matter from the Ems estuary (at the border of Germany and The Netherlands) revealed mixing with marine material in the freshwater zone and the transport of this marine suspension across the salt wedge [82]. No net flux of marine suspended matter into the estuaries of the Garone or Rhône (France) was found [83, 84]. This is probably due to the different natures of these estuaries. Sediment samples from a longitunal profile and suspended matter from a maximum peak flow were collected in the Elbe river (Germany) [85]. The mixing ratio of marine and fluvial sediments could be based on the variation in abundance of calcium carbonate, and the results are comparable with those found for the Ems river. Load transport, characteristic of discharge events, and erosion of settled mud particles are the major sources of suspended matter transported during peak events.

The nature of the inorganic colloidal and suspended matter transported by the Magela Creek, northern Australia, was studied during a small flood event [86]. Only a small difference was noticed between the inorganic composition of the coarse colloidal matter (0.1–1 μm) and the suspended particulate matter (>1 μm). Both are dominated by weathering products.

Computer-controlled SEM (CCSEM) was used to analyze suspended matter from Onondaga Lake, New York [87]. The size and composition of these particles are directly related to biological production, precipitation in the water column, and transport of suspended matter by the lake tributaries (especially after runoff events). The total amount of suspended matter and the relative abundance of the different particle types are exposed to strong temporal variations.

Organic particles can be investigated using automated SEM-EDX analysis, by staining the samples with ruthenium tetroxide. However, in EDX spectra serious interference occurs between the ruthenium L_α peak and the chlorine K_α peak. This interference is not limiting for aquatic samples, because chlorine is usually removed during their preparation. Suspended samples from the Sargasso Sea were prepared using this stain [88]. Analysis showed that over 70% of the particles were organic and the major components of the inorganic fraction were iron, calcium, sulfur, and silicon rich particles.

The correlation between the occurrence of suspended and sedimented barite and the intensity of previous biological activity [89] was confirmed by manual EPXMA of suspended matter from the Scotia Sea–Weddel Sea confluence [90]. In the surface waters, barite is mainly contained within large bioaggregates. These aggregates disperse in the subsurface zone and the barite crystals become individual particles. No association of barite with phytoplankton was found. The pelagic barite is thus most probably formed through passive precipitation in a saturated microenvironment. Manual EPXMA has also been used to distinguish the different structures of manganese [91] and the different species of pyrite [92].

The morphological characterization of environmental particles with SEM has been reported by several researchers [75, 93–95].

4.3 Scanning Transmission Electron Microscopy

Publications on the characterization of environmental particles with scanning transmission electron microscopy–energy dispersive X-ray detection (STEM-EDX) are limited. To our knowledge no articles on aerosol research have been published.

Recently, a study has been started to characterize individual submicrometer indoor aerosol particles using STEM-EDX [96]. The aim of this study is to identify those aerosol particles which are responsible for the staining of paintings in the Correr Museum, Venice. Preliminary results show the presence of silicon and sulfur rich particles, titanium rich particles, and aluminosilicates.

Leppard [97] has reviewed the application of electron microscopy (EM) to aquatic colloids. STEM-EDX was used for the characterization of mineral and mineral–

organic colloids. The crucial point of the EM analysis of aquatic particles is sample preparation. Simple and powerful preparation techniques which reduce the amount of artifacts are described by Leppard [97] and Perret et al. [98].

Iron oxyhydroxides in the sediments of eight lakes were analyzed after preparation with Nanoplast resin [99]. A combination of STEM-EDX with ~~ED~~ electron diffraction and X-ray diffraction revealed that crystalline iron(III) oxyhydroxides were only present as poorly ordered ferrihydrite and lepidocrocite. Deposition of these iron oxyhydroxides in the lake sediments also seemed to occur on bacterial cells and their exopolymers. This explains the significant amount of organic carbon found in the diagenetic iron(III) oxyhydroxides.

Identification of the mineral structure of crystalline particles is possible by combining STEM-EDX with selected-area ED. This combination has been tested on Nanoplast-embedded micrometer-sized suspended particles collected in the Southern Bight of the North Sea, and the results are promising [100]. As a preliminary result of this research the transmission electron image, electron diffraction pattern, and X-ray spectrum of a sodium chloride (halite) particle are shown in Fig. 4.

4.4 Electron Energy-Loss Spectrometry

Electron energy-loss spectrometry (EELS) has only been recently commercialized and for environmental applications it is still in an experimental stage. The few applications published on this subject are briefly discussed.

Standard test aerosols of inorganic salts were analyzed by serial and parallel EELS (SEELS and PEELS) [101]. Even at cryogenic temperatures there were distinct losses and structure reorganizations of the inorganic salts. PEELS can be used to analyze these beam-sensitive samples, but only for qualitative purposes.

PEELS analysis of atmospheric aerosols indicated that the majority of the ultrafine particles consist of carbon [102]. The carbonaceous aerosols collected in Phoenix, Arizona, are smaller than 2 μm and contain 10–100 aggregated spheres [103, 104]. Information on the electronic state of the carbon edge showed the presence of a mixture of graphitic and amorphous carbon within and among the individual aggregate particles. The graphite is probably part of the primary soot, while the amorphous carbon is the result of hydrocarbon condensation during aggregation. During the summer, some particles are coated with sulfates and nitrates. Visual evidence of these sulfur coatings was provided by element-specific imaging (ESI) [104]. Since coated and uncoated aggregates have the same structural variations, it is presumed that they are from the same source.

The combination of EELS with ESI is very useful in studying the inhomogeneous composition of nanometer-range, surface-modified asbestos fibers [105, 106]. Carbon maps or organosilane coated chrysolite fibers showed that the coating was not distributed homogeneously over the fibers. Some fibers even seem to be unaffected by the treatment. The surface modification, necessary for the reduction of the toxicity of the fibers, is thus only partially efficient.

The oxygen peaks from $TiCl_3$ modified fiber spectra have a pre-edge which indicates bonding between oxygen and titanium. The titanium chloride is thus chemically bound to the fiber. ESI maps of titanium reveal the encapsulation of the material and thus full coverage of the fibers. Elemental mappings of titanium in a cross-section of a $TiCl_3$ treated fiber embedded in Spurr resin are shown in Fig. 5.

4.5 Micro-Raman Spectrometry

Although micro-Raman spectrometry is a very slow analytical method, it offers great potential for environmental particle analysis. Environmental researchers are fairly unfamiliar with this technique and its possibilities, which has resulted in a very small amount of publications on environmental applications.

Raman microprobe measurements on Antarctic aerosols showed that the sulfur rich fine fraction is dominated by H_2SO_4, $(NH_4)HSO_4$, $(NH_4)_2SO_4$, or a mixture of more complex species [107]. The particulate aerosol fraction from oil and coal power plants has also been examined [108, 109]. Vanadium oxide was found to be a major component of the oil-derived particles, and only a minor one in the coal ashes.

A combination of Raman and infrared spectrometry was used to characterize large individual dust particles from an office–laboratory area [110]. Not surprisingly, many of the analyzed dust particles originated from paper products.

4.6 Fourier Transform Infrared Spectrometry

FT-IR spectroscopy and FT-IR microspectroscopy have rarely been used for environmental applications. Long-path FT-IR spectroscopy has been reported for the measurement of atmospheric trace gases [111], the monitoring of airborne gases and vapours [112–114], the study of atmospheric pollutants [115], and the characterization of organic components in aerosols [116].

FT-IR microspectroscopy has been used as a direct method to analyze the organic contents of size-fractionated atmospheric aerosols [117] and size-segmented aerosol particles and clusters [118]. In these publications it is stated that FT-IR microspectroscopy has three major advantages for the analysis of single aerosol particles: only small sample masses are required, sample dilution is not necessary, and direct analysis of the impactor stages after aerosol collection is possible. These statements were tested by the analysis of giant North Sea aerosols with FT-IR microspectroscopy and EPXMA [96]. The first results were not promising. The analyzed particles were dominated by inorganic salts which only absorb partially in the middle IR region. Most marine giant aerosols contain a mixture of components which leads to peak overlap in the spectra and to interpretation difficulties.

Acknowledgements

This work was partially prepared in the framework of the Impulse Programme in Marine Sciences, supported by the Belgian State–Prime Minister's

Service–Services for Scientific, Technical and Cultural Affairs (contract MS/06/050).

4.7 References

[1] M. Grasserbauer, *Mikrochim. Acta* **1983,** *III*, 415.
[2] R. Van Grieken, P. Artaxo, P. Bernard, L. Leysen, P. Otten, H. Stroms, A. Van Put, L. Wouters, C. Xhoffer, ~~*Chem. Anal.*~~ **1990,** *35*, 75.
[3] R. Van Grieken, C. Xhoffer, *J. Anal. Atom. Spectrom.* **1992,** *7*, 81.
[4] C. Xhoffer, L. Wouters, P. Artaxo, A. Van Put, R. Van Grieken in *Environmental Particles, Vol. I* (Eds.: J. Buffle, H. P. Van Leeuwen), Lewis, Chelsea MI **1992,** Chap. 3.
[5] W. Jambers, L. De Bock, R. Van Grieken, *Analyst*, ~~in press.~~
[6] R. Cadle, W. Fisher, E. Frank, J. Lodge, *J. Atmos. Sci.* **1967,** *25*, 100.
[7] F. Parungo, B. Bodhaine, J. Bortnak, *J. Aerosol Sci.* **1981,** *12*, 367.
[8] G. E. Shaw, *Atmos. Environ.* **1983,** *17*, 329.
[9] T. Ito, *J. Atmos. Chem.* **1985,** *3*, 69.
[10] B. A. Bodhaine, M. E. Murphy, *J. Aerosol Sci.* **1980,** *11*, 305.
[11] B. A. Bodhaine, J. J. Deluisi, J. M. Harris, *Tellus* **1986,** *38B*, 223.
[12] P. Artaxo, M. L. C. Rabello, W. Maenhaut, R. Van Grieken, *Tellus* **1992,** *44B*, 318.
[13] P. Artaxo, R. Van Grieken, F. Watt, M. Jakšić in *Proc. Second World Congress on Particle Technology*, Society of Powder Technology, Kyoto **1990,** pp. 421–426.
[14] R. E. Van Grieken, P. Artaxo, C. Xhoffer in *Proc. Fiftieth Annual Meeting by the Electron Microscopy Society of America* (Eds.: G. W. Bailey, J. Bentley, J. A. Small), San Francisco Press, San Francisco, CA **1992,** pp. 1482–1483.
[15] H. Storms, *Ph.D. Thesis*, University of Antwerp, Antwerp **1988.**
[16] E. Bigg, *J. Appl. Meteorol.* **1980,** *19*, 521.
[17] W. Cunningham, W. Zoller, *J. Aerosol Sci.* **1981,** *12*, 367.
[18] H. Van Malderen, R. Van Grieken, T. Khodzher, ~~M. Grachev~~, V. Bufetov, K. P. Koutzenogii, *Ocean and Atmospheric Optics*, in press.
[19] E. J. Begét, M. Keskinen, K. Severin, *Sediment. Geol.* **1993,** *84*, 189.
[20] E. M. Patterson, C. S. Kiang, A. C. Delany, A. F. Artburg, A. C. D. Leslie, B. J. Huebert, *J. Geophys. Res.* **1980,** *8*, 7361.
[21] P. Artaxo, H. Stroms, F. Bruynseels, R. Van Grieken, W. Maenhaut, *J. Geophys. Res.* **1988,** *93*, 1605.
[22] M. O. Andreae, R. J. Charlson, F. Bruynseels, H. Storms, R. Van Grieken, W. Maenhaut, *Science* **1986,** *232*, 1620.
[23] C. Xhoffer, *M.Sc. Thesis*, University of Antwerp, Antwerp **1987.**
[24] H. Van Malderen, L. De Bock, J. Injuk, C. Xhoffer, R. Van Grieken in *Progress in Belgian Oceanographic Research*, Royal Academy of Belgium, Brussels **1993,** pp. 119–135.
[25] F. Bruynseels, H. Storms, R. Van Grieken, L. Van Der Auwera, *Atmos. Environ.* **1988,** *22*, 2593.
[26] C. Xhoffer, P. Bernard, R. Van Grieken, L. Van Der Auwera, *Environ. Sci. Technol.* **1991,** *25*, 1470.
[27] C. M. Rojas, R. Van Grieken, *Atmos. Environ.* **1992,** *26A*, 1231.
[28] L. A. De Bock, H. Van Malderen, R. Van Grieken, *Environ. Sci. Technol.* **1994,** *28*, 1513.
[29] R. Jaenicke, *Ann. NY Acad. Sci.* **1980,** *338*, 317.
[30] R. Jaenicke in *Chemistry of the Unpolluted and Polluted Troposphere*, 1st edn. (Eds.: W. Georgii, W. Jaeschke), D. Reidel, Dordrecht **1982,** pp. 341–374.
[31] H. L. Dedeurwaerder, *Ph.D. Thesis*, Free University of Brussels, Brussels **1988.**
[32] H. Van Malderen, C. Rojas, R. Van Grieken, *Environ. Sci. Technol.* **1992,** *26*, 750.
[33] J. Fruchter, *Science* **1980,** *209*, 1116.
[34] J. P. Wightman, *Colloid. Surf.* **1982,** *4*, 401.
[35] J. L. Gooding, U. S. Clanton, E. M. Gabel, J. L. Warren, *Geophys. Res. Lett.* **1983,** *10*, 1033.
[36] M. R. Rampino, S. Self, *Sci. Am.* **1984,** *250*, 48.
[37] D. E. Brownlee, ~~*Microbeam Anal.* **1980**~~, 199. Proc Annual Conference on Microbeam Analysis Society 1980,
[38] R. D. Cadle, G. W. Grams, *Rev. Geophys. Space Phys.* **1975,** *13*, 475.
[39] L. D. R. Mackinnon, J. L. Gooding, D. S. McKay, U. S. Clanton, *J. Volcanol. Geotherm. Res.* **1984,** *23*, 125.
[40] F. Parungo, B. Kopcewicz, C. Nagamoto, R. Schnell, P. Sheridan, C. Zhu, J. Harris, *J. Geophys. Res.* **1992,** *97*, 15867.
[41] S. Sándor, S. Török, C. Xhoffer, R. Van Grieken in *Proc. Twelfth International Congress for Electron Microscopy* (Eds.: L. D. Peachy, P. B. Williams), San Francisco Press, San Francisco, CA **1990,** pp. 245–255.
[42] S. Török, S. Sándor, C. Xhoffer, R. Van Grieken, E. Mészáros, A. Molnar, *Idojaras* **1993,** *96*, 223.
[43] M. A. H. Eltayeb, C. F. Xhoffer, P. J. Van Espen, R. E. Van Grieken, *Atmos. Environ.* **1993,** *27B*, 67.
[44] C. M. Rojas, P. Artaxo, R. Van Grieken,

Atmos. Environ. **1990,** *24B*, 227.
[45] W. Van Borm, F. Adams, W. Maenhaut, *Atmos. Environ.* **1989,** *23*, 1139.
[46] W. Van Borm, L. Wouters, R. Van Grieken, F. Adams, *Sci. Total Environ.* **1990,** *90*, 55.
[47] J. E. Post, P. R. Buseck, *Environ. Sci. Technol.* **1985,** *18*, 35.
[48] A. Hunt, D. L. Johnson, I. Thornton, J. M. Watt, *Sci. Total Environ.* **1993,** *138*, 183.
[49] A. Hunt, D. L. Johnson, J. M. Watt, I. Thornton, *Environ. Sci. Technol.* **1992,** *26*, 1513.
[50] G.-W. Qian, Y. Ishizaka, *J. Geophys. Res. Oceans* **1993,** *98*, 8459.
[51] D. Pardess, Z. Levin, E. Ganor, *Atmos. Environ.* **1992,** *26A*, 675.
[52] G. Bonafede, L. T. Kiss, *Am. Soc. Mech. Eng.* **1973,** 73-WA/CD-7.
[53] J. E. Baker, C. A. Evans, A. Loh, D. F. S. Natush, *Proc. Annual Conference on Microbeam Analysis Society* **1975,** *10*, 33A.
[54] D. L. Gibbon, *Scanning Electron Microsc.* **1979,** *I*, 501.
[55] R. L. Carpenter, R. D. Clark, Y.-F. Su, *J. Air Pollut. Control Assoc.* **1980,** *30*, 679.
[56] D. Lichtman, S. Mroczkowski, *Environ. Sci. Technol.* **1985,** *19*, 274.
[57] L. M. Middleman, J. D. Geller, *Scanning Electron Microsc.* **1976,** 171.
[illegible]
[58] J. A. Small, W. H. Zoller, *NBS Monogr. (US)* **1977,** *464*, 651.
[59] G. L. Fisher, B. A. Prentice, D. Silberman, J. M. Ondov, *Environ. Sci. Technol.* **1978,** *12*, 447.
[60] F. Parungo, E. Ackerman, H. Proulx, R. Pueschel, *Atmos. Environ.* **1978,** *12*, 929.
[61] T. L. Hayes, J. B. Pawley, G. L. Fisher, *Scanning Electron Microsc.* **1978,** *I*, 239.
[62] R. Capron, P. Haymann, F. Pellerin, *C.R. Hebd. Seances Acad. Sci.* **1979,** *C289*, 313.
[63] N. Kaufherr, D. Lichtman, *Environ. Sci. Technol.* **1984,** *18*, 544.
[64] J. Wagman in *Colloid and Interface Science, Vol. II: Aerosols, Emulsions and Surfactants*, Academic Press, New York **1976.**
[65] E. Denoyer, T. Mauney, D. F. S. Natusch, F. Adams, ~~*Microbeam. Anal.* **1982,**~~ 191.
[illegible]
52, [illegible]
[66] Y. Mamane, J. L. Miller, T. G. Dzubay, *Atmos. Environ.* **1986,** *20*, 2125.
[67] B. Raeymaekers, *Ph.D. Thesis*, University of Antwerp, Antwerp **1987.**
[68] W. C. McCrone, J. G. Delly, *The Particle Atlas, Vol. II*, 2nd edn, Ann Arbor Science, Ann Arbor, MI **1973,** p. 543.
[69] F. Dehairs, R. Chesselet, J. Jedwab, *Earth Planet. Sci. Lett.* **1980,** *49*, 528.
[70] J. Jedwab, *Earth Planet. Sci. Lett.* **1980,** *49*, 551.
[71] J. M. Skei, S. Melson, *Estuarine, Coast. Shelf Sci.* **1982,** *14*, 61.
[72] B. N. Sundby, N. Silverberg, R. Chesselet, *Geochim. Cosmochim. Acta* **1984,** *45*, 293.
[73] J. K. B. Bishop, P. E. Biscaye, *Earth Planet. Sci. Lett.* **1982,** *58*, 265.
[74] C. E. Lambert, J. K. B. Bishop, P. E. Biscaye, R. Chesselet, *Earth Planet. Sci. Lett.* **1984,** *70*, 237.
[75] D. Eisma, A. Van Put, R. Van Grieken, *Mitt. Geol.-Paläont. Inst. Univ. Hamberg* **1992,** *70*, 137.
[76] D. Eisma, J. Kalf, M. Karmini, W. G. Mook, A. Van Put, P. Bernard, R. Van Grieken, *Neth. J. Sea Res.* **1989,** *24*, 383.
[77] A. Van Put, D. Eisma, R. Van Grieken, unpublished results.
[78] D. Eisma in *Facets of Modern Biogeochemistry* (Eds.: V. Ittekkot, S. Kempe, W. Michaelis, A. Spitzy), Springer Verlag, Heidelberg **1990,** pp. 127–146.
[79] C. Xhoffer, L. Wouters, R. Van Grieken, *Environ. Sci. Technol.* **1992,** *26*, 2151.
[80] P. C. Bernard, R. E. Van Grieken, L. Brügmann, *Mar. Chem.* **1989,** *26*, 155.
[81] F. Belmans, R. Van Grieken, L. Brügmann, *Mar. Chem.* **1993,** *42*, 223.
[82] P. Bernard, R. Van Grieken, D. Eisma, B. Hudec, *Environ. Sci. Technol.* **1986,** *20*, 467.
[83] D. Eisma, P. Bernard, J. Boon, R. Van Grieken, J. Kalf, W. Mook, *Mitt. Geol.-Paläont. Inst. Univ. Hamburg* **1985,** *58*, 397.
[84] D. Eisma, P. Bernard, G. Cadee, V. Ittekot, J. Kalf, R. Laane, J. Martin, W. Mook, A. Van Put, T. Schumacher, *Neth. J. Sea Res.* **1991,** *28*, 193.
[85] A. Van Put, R. Van Grieken, R.-D. Wilken, B. Hudec, *Wat. Res.* **1994,** *28*, 643.
[86] B. T. Hart, G. B. Douglas, R. Beckett, A. Van Put, R. E. Van Grieken, *Hydrol. Proc.* **1993,** *7*, 105.
[87] D. L. Johnson, J. Jiao, S. G. DosSantos, S. W. Effler, *Environ. Sci. Technol.* **1991,** *25*, 736.
[88] D. M. Lavoie, *Deep-Sea Res.* **1992,** *39*, 1655.
[89] J. Bishop, *Nature (London)* **1988,** *332*, 341.
[90] N. Stroobants, F. Dehairs, L. Goeyens, N. Vanderheijden, R. Van Grieken, *Mar. Chem.* **1991,** *35*, 411.
[91] J. Middelburg, G. De Large, H. Van der Sloot, P. Van Emburg, S. Sophiah, *Mar. Chem.* **1989,** *23*, 353.
[92] G. Luther, A. Meyerson, J. Krajewski, R. Heres, *J. Sediment. Petrol.* **1980,** *50*, 1117.
[93] A. Tucan, S. Pamukcu in *Proc. Mediterranean Conference on Environmental Geotechnology* (Eds.: Usmen, Acer), Balkema, Rotterdam A. B. Y. B. **1992,** pp. 109–121.

[94] E. Tipping, C. Woof, K. Clarke, *Hydrol. Proc.* **1993,** *7*, 263.
[95] J. M. Oades, A. G. Waters, *Aust. J. Soil Res.* **1991,** *29*, 815.
[96] L. A. De Bock, R. E. Van Grieken, unpublished work.
[97] G. G. Leppard in *Environmental Particles, Vol. I* (Eds.: J. Buffle, H. P. Van Leeuwen), Lewis, Chelsea, MI **1992,** Chap. 6.
[98] D. Perret, G. G. Leppard, M. Müller, N. Belzile, R. De Vitre, J. Buffle, *Water Res.* **1991,** *25*, 1333.
[99] D. Fortin, G. G. Leppard, A. Tessier, *Geochim. Cosmochim. Acta* **1993,** *57*, 4391.
[100] W. Jambers, ~~unpublished work.~~
[101] C. Xhoffer, *Ph.D. Thesis*, University of Antwerp, Antwerp **1993,** pp. 189–204.
[102] A. D. Maynard, L. M. Brown, *J. Aerosol Sci.* **1992,** *23*, S433.
[103] C. Xhoffer, *Ph.D. Thesis*, University of Antwerp, Antwerp **1993,** pp. 205–233.
[104] K. A. Katrinak, P. Rez, P. R. Buseck, *Environ. Sci. Technol.* **1992,** *26*, 1967.
[105] C. Xhoffer, P. Berghmans, I. Muir, W. Jacob, R. Van Grieken, F. Adams, *J. Microsc.* **1991,** *162*, 179.
[106] P. Berghmans, J. Injuk, R. Van Grieken, F. Adams, *Anal. Chim. Acta* **1994,** *297*, 27.
[107] E. Etz, G. Rosasco in *Proc. 5th International Conference on Raman Spectroscopy*, Hans Ferdinand Schulz Verlag, Freiburg **1976,** pp. 776–777.
[108] E. Etz, G. Rosasco, J. Blaha in *Environmental Pollutants: Detection and Measurements* (Eds.: T. Toribara, J. Coleman, B. Dahneke, I. Feldman), Plenum Press, New York **1978,** p. 413.
[109] E. Etz, G. Rosasco, K. Heinrich, *EPA Report, EPA-600/2-78-193* **1978.**
[110] P. Lang, J. Katon, A. Bonanno, *Appl. Spectrosc.* **1988,** *42*, 313.
[111] R. A. Nyquist, M. A. Leugers, M. L. McKelvy, R. R. Papenfuss, C. L. Putzig, L. Yurga, *Anal. Chem.* **1990,** *62*, 223R.
[112] J. Gosz, C. Dahm, P. Risser, *Ecology* **1988,** *69*, 1326.
[113] S. Levine, Y. Li-Shi, C. Strang, X. Hong-Kui, *Appl. Ind. Hyg.* **1989,** *4*, 180.
[114] Y. Li-Shi, S. Levine, *Anal. Chem.* **1989,** *61*, 677.
[115] G. Small, R. Kroutil, J. Ditillo, W. Loerop, *Anal. Chem.* **1988,** *60*, 264.
[116] R. Gordon, N. Trivedi, B. Singh, *Environ. Sci. Technol.* **1988,** *22*, 672.
[117] M. Dargler, S. Burke, S. Hering, D. Allen, *Atmos. Environ.* **1987,** *21*, 1001.
[118] R. Kellner, H. Malissa, *Aerosol Sci. Technol.* **1989,** *10*, 397.

Figure 1. (a) Silicon (SiK_α) and (b) iron (FeK_α) X-ray mappings of a grain mount of silt particles from Pu'u o Mahana, Hawaii [19]. Reproduced by permission of Elsevier Science Publishers B.V.

Figure 2. Secondary electron image and X-ray spectrum of a fly-ash particle collected from the surface microlayer of the North Sea [79]. Reproduced by permission of the American Chemical Society.

Figure 3. Secondary electron image and X-ray spectrum of a diatom skeleton present in the surface microlayer of the North Sea [79]. Reproduced by permission of the American Chemical Society.

Figure 4. Transmission electron image, electron diffraction pattern, and X-ray spectrum of a sodium chloride particle (halite) collected in the Southern Bight of the North Sea ~~[100]~~

Figure 5. Element-specific imaging of titanium in a cross-section of a $TiCl_3$ treated asbestos fiber. (a) Net titanium image obtained by subtracting an extrapolated image at 460 eV (calculated from the 435 and 445 eV images) from the 460 eV image. (b) Combination of the binary titanium distribution image (black) and the grey reference electron specific image at 435 eV (scale bar = 25 nm) [106]. Reproduced by permission of Elsevier Science Publishers B.V.

Fig 1a

JAMBERS & VAN GRIEKEN
FIG. 1a

Fig 1c
C

JAMBERS & VAN GRIEKEN
FIG. 1b

~~Fig Ac~~ Fig 2

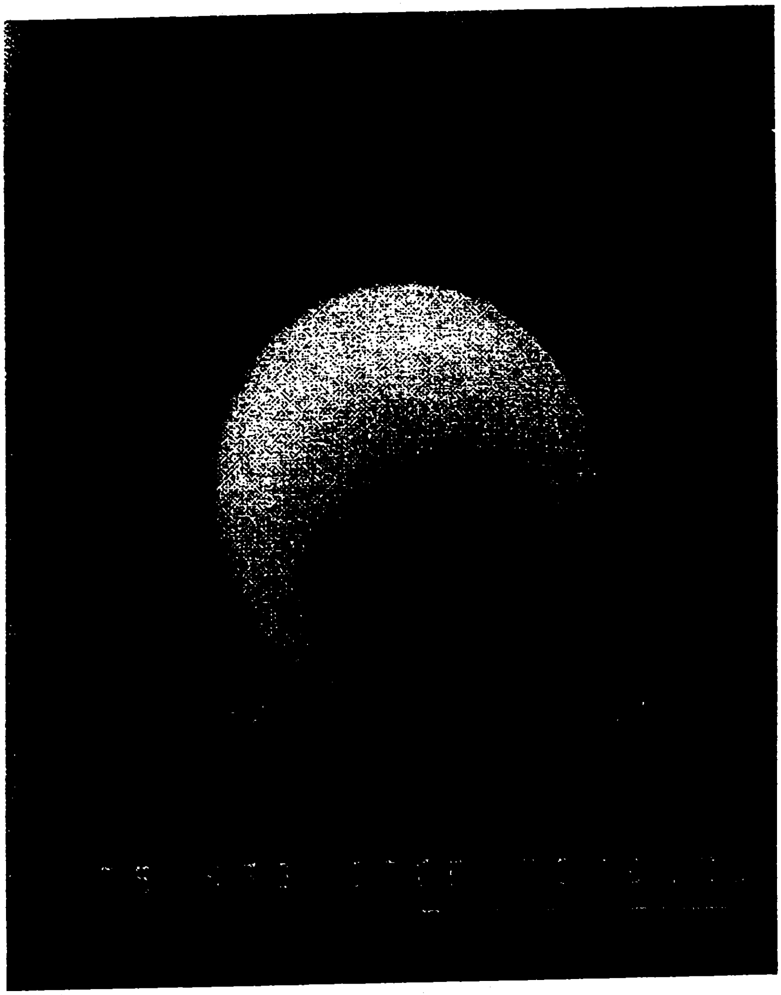

JAMBEKE & VAN GIEKEN
FIG 2 (part 1)

Fig 2 ~~Fig 3~~

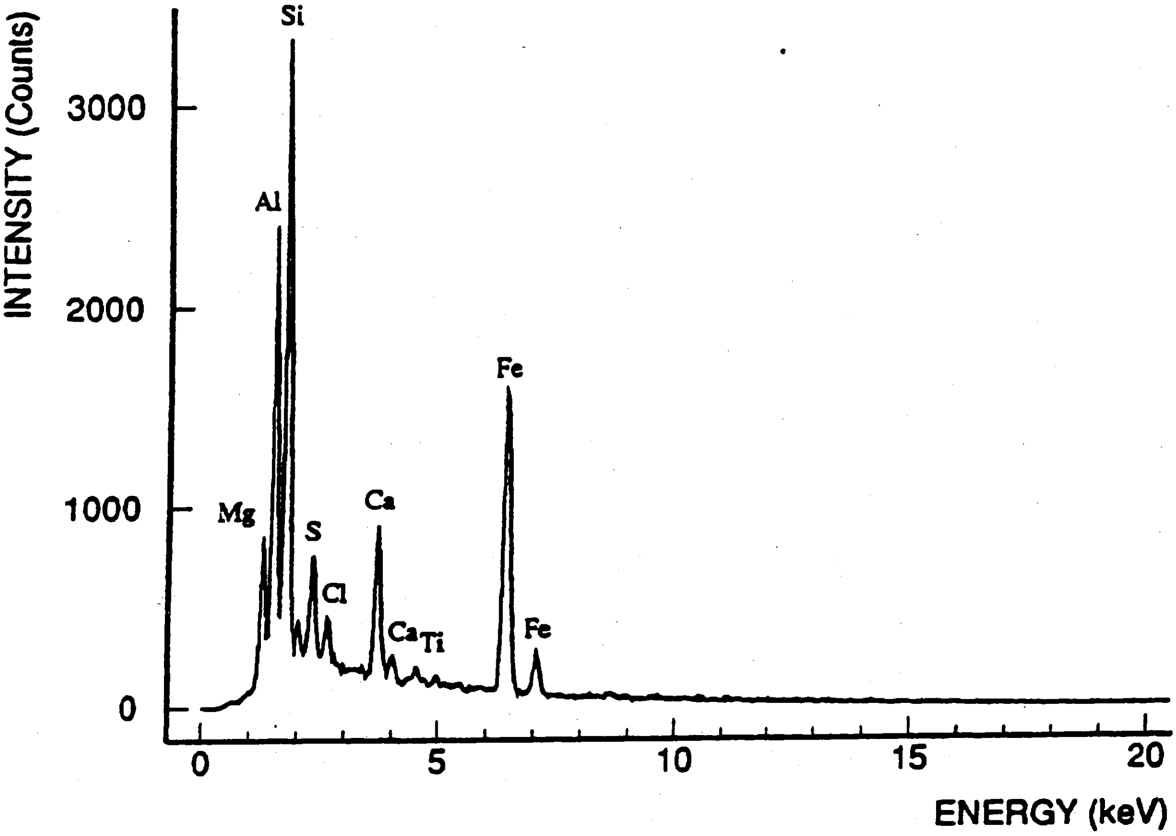

JAMBERS & IAN SPRIECEN

FIG. 2 [illegible]

Fig 3

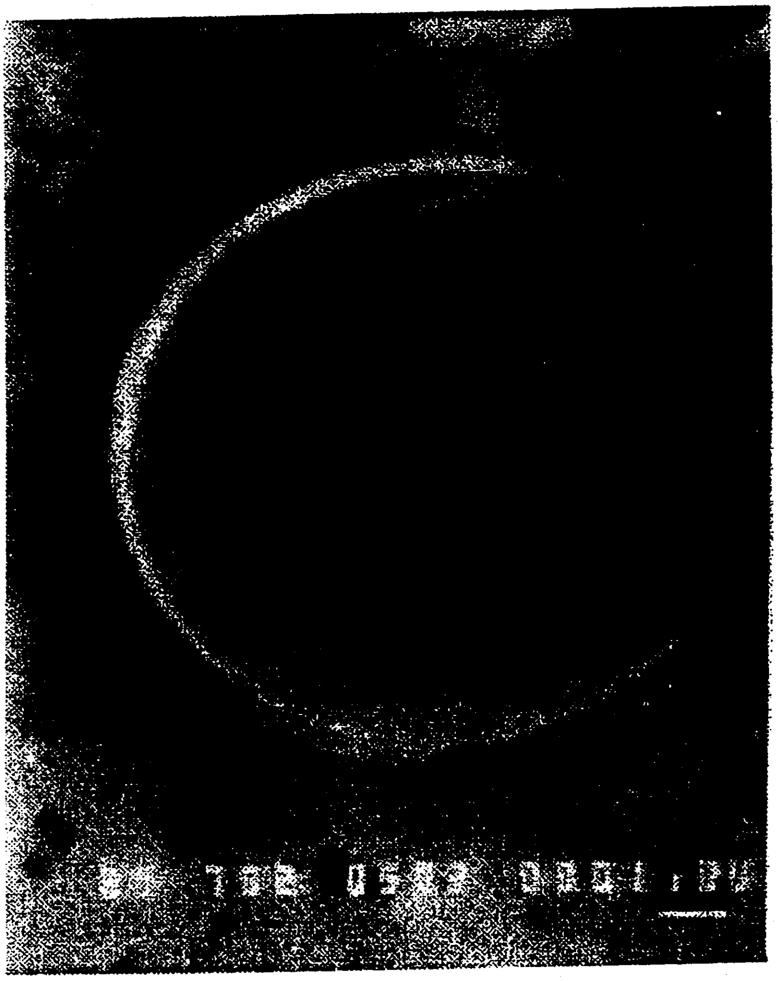

JAMBE[illegible] & [illegible]

Fig. 2(part [illegible])

5.3

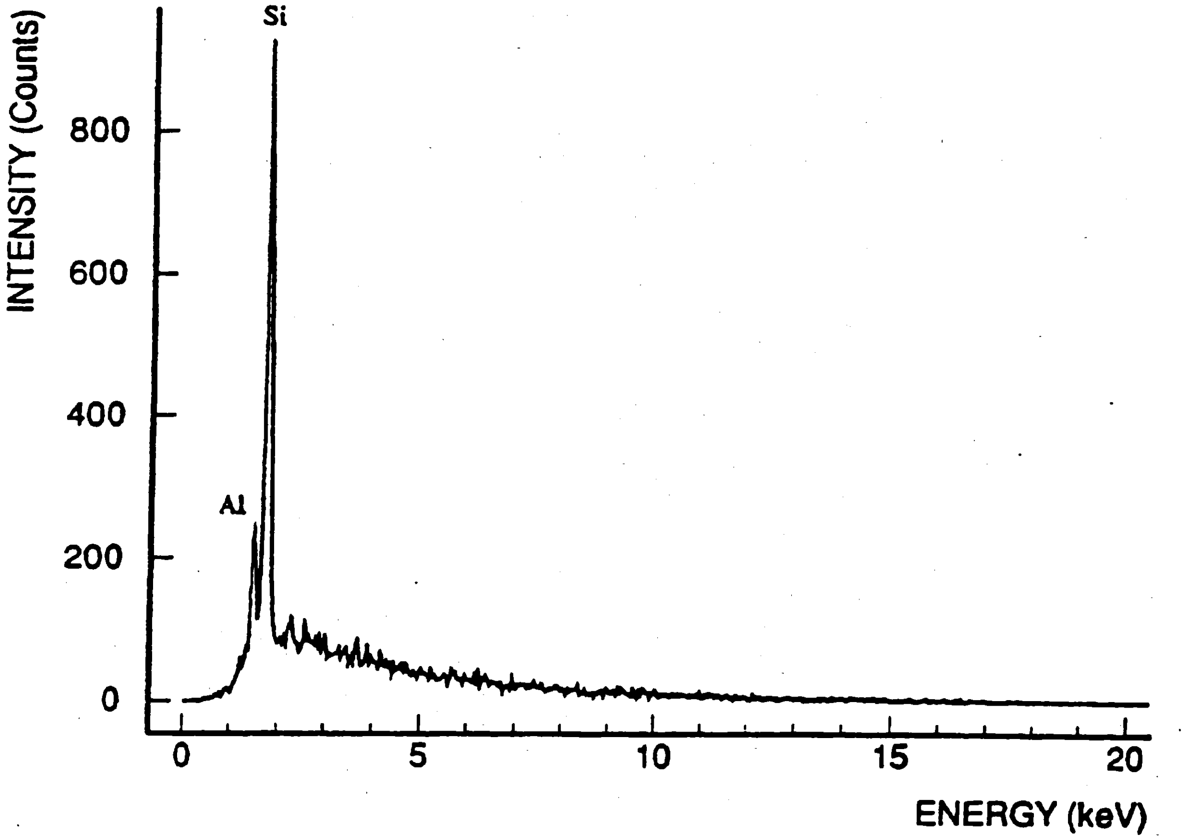

JAMBERS & VAN GRIEKEN

FIG. 3(a)

Fig 4

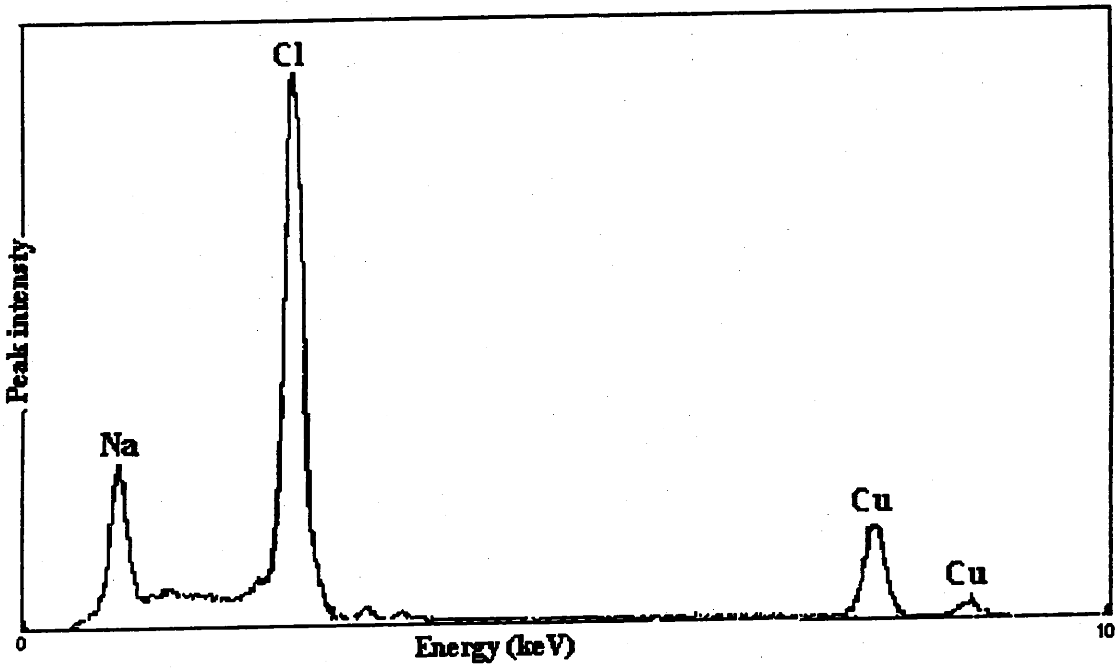

[illegible]

[illegible]

Fig 5a

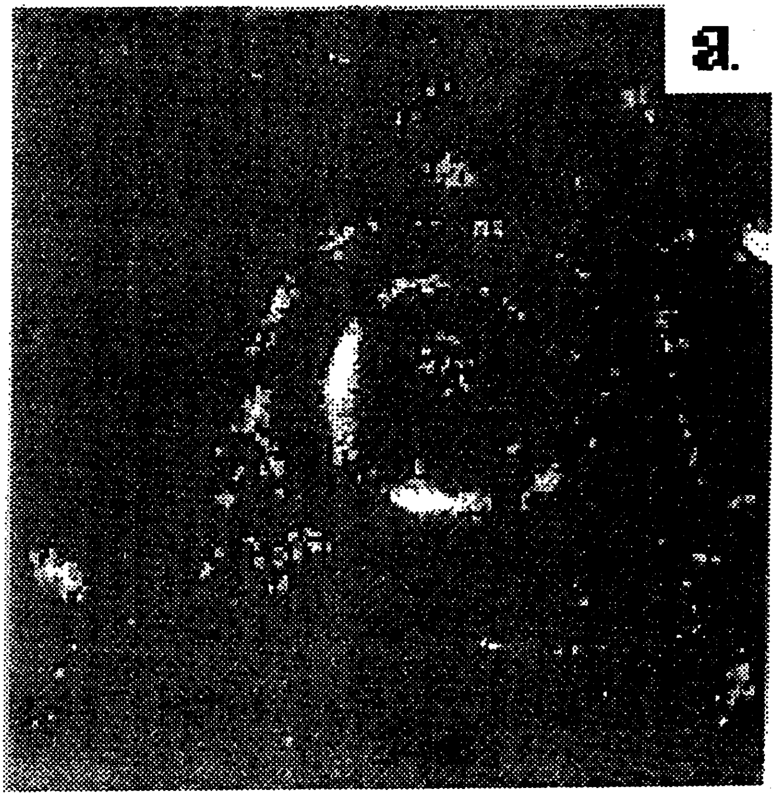

[illegible]

[illegible]

Fig 5b

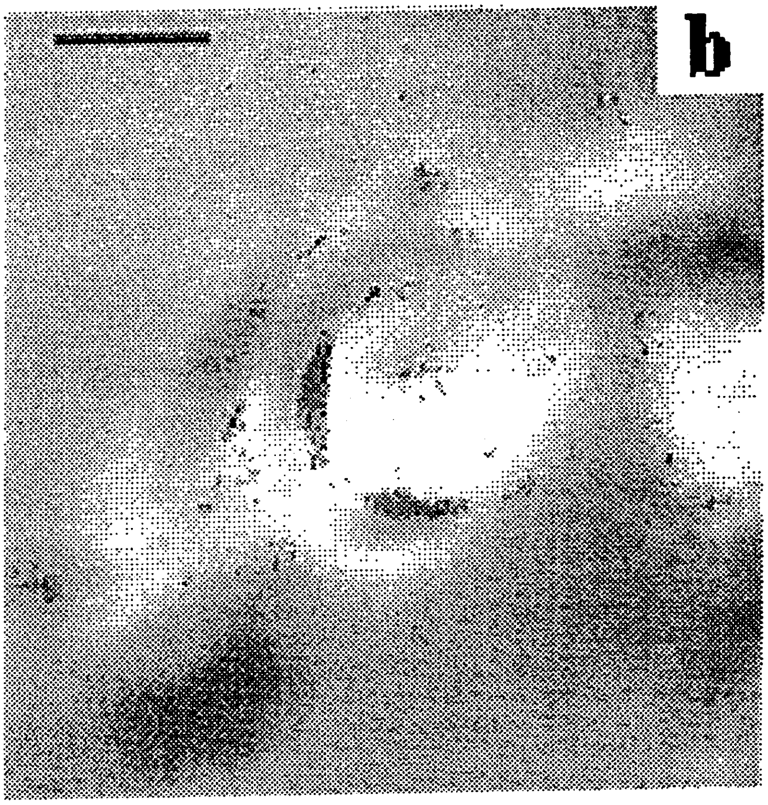

[illegible] & [illegible]

[illegible]

, ꝁ V 4

Review

3166

Micro-analysis of individual aerosol particles using electron, proton and laser beams

Lieve A. De Bock, Wendy Jambers and René E. Van Grieken*
Department of Chemistry, University of Antwerp (UIA), Universiteitsplein 1, B- 2610 Antwerpen, Belgium

Received 24 July 1995

This paper is based on a plenary lecture delivered during ANALYTIKA 94, the 2nd National Symposium on Analytical Science, Stellenbosch, 8–13 December 1994

The applications of electron probe X-ray micro-analysis, scanning electron microscopy, laser microprobe mass spectrometry and micro-particle-induced X-ray emission in the field of individual environmental aerosol particle analysis are reviewed for the period 1990–1995.

Although several micro-analysis beam techniques have been developed specifically for the analysis of individual particles and were recognized to be very useful as a complement to bulk analysis, their applications in the environmental field are still limited. Yet there exists no doubt about the importance of particulate matter in the environment: particles are considered to be the major material carriers in water and air, the visibility and the global climate are influenced by atmospheric aerosols, a significant number of components present in environmental particles are highly toxic, etc. Single particle analysis can reveal detailed information on different particle aspects like origin, formation processes, reactivity, whether they have undergone transformation reactions, and environmental impact.

The specific problems of different micro-analytical techniques can often be reduced to analysis problems in the small particle-size range. Quantitative information is limited because the variable particle geometry introduces several complications which are not present in the analysis of polished specimens, and because suitable standards are lacking. Moreover, to obtain statistically relevant results, large numbers of particles per sample should be analysed, which may be very time consuming. The major problem with most micro-analysis techniques is the necessity to operate under vacuum conditions, resulting unfortunately in loss or transformation of most volatile and unstable compounds.

Because all techniques are limited in one way or another but can be complementary to each other with respect to detection limits, lateral and depth resolution, detectable elements, and so forth, the optimal characterization of a sample can be obtained by using several micro-beam techniques in combination with bulk analysis.

The present review discusses the applications of the most frequently used micro-beam techniques in the field of individual environmental aerosol particle analysis. The article is based on a computer search of the literature published during the time period January 1990 to March 1995. Detailed descriptions of micro-analytical techniques can be found in earlier reviews on this subject, published by Grasserbauer,[1] Van Grieken and Xhoffer,[2] Xhoffer *et al.*[3] and Jambers *et al.*[4]

Electron probe X-ray micro-analysis and scanning electron microscopy

In electron-probe X-ray micro-analysis (EPXMA) and scanning electron microscopy (SEM), a nanometer-sized electron probe generates various signals upon sample interaction. The detection of the emitted characteristic X-rays by wavelength- or energy-dispersive spectrometers (WDX and EDX respectively) as well as the backscattered electron image provide compositional information on the sample. Morphological studies are based on the detection of backscattered and secondary electrons. Since the differences between EPXMA and scanning electron microscopy coupled to an energy-dispersive X-ray analysis system (SEM/EDX) have been reduced over the years to only a slightly different instrumental set-up, both techniques are nowadays to some extent used for chemical and morphological studies. Their applications are therefore discussed together.

Recent developments in computerization and automation offer the possibility of obtaining statistically rele-

---

*To whom correspondence should be addressed.

vant results by analysing large numbers of individual particles in a very short time period. The computer-controlled SEM-EDX is the most highly evolved example of this technology. The JEOL JSM-6300 scanning electron microscope at the Micro and Trace Analysis Centre (MiTAC) of the University of Antwerp is equipped with a PGT (Princeton Gamma Tech) energy-dispersive X-ray detector. The IMIX software, available for X-ray collection and image processing, runs on a SUN workstation. The particle analysis program PA 6300 can be applied for automated particle analysis. Using this program, the area of interest on the sample is subdivided in different fields and the program starts with the collection of a BSE image of each field. The area, perimeter and diameter of the particles within the field are calculated from the image and compared with a selection criterion (e.g. diameter > 0.2 μm). Based on the particle's contour, the X-ray spectrum is accumulated by rastering the electron beam on 40 points within its contour. A top-hat filter is applied for spectrum evaluation. BSE images and spectra are stored on an optical disk, allowing re-evaluation of the obtained data. An automated SEM is, in combination with multivariate techniques, a powerfull method for the determination of the chemical composition and characterization of a large number of individual particles in a very short time.

Applications

Aerosol particles collected at widely divergent places were successfully identified, classified and apportioned to their different sources by the application of EPXMA and SEM.

The increasing industrialization together with long-range transport of pollutants has reduced the possibility of locating and characterizing the composition of 'pure' aerosols in the absence of any pollution. The Antarctic continent belongs to the few locations where the so-called background aerosols can still be found. In the fine- and coarse-mode fraction of coastal Antarctic aerosols, marine components were identified by EPXMA as a dominant particle type and only a minor crustal component could be detected.[5-8] Evidence of possible reactions with gaseous S compounds was found in the small amounts of S present in several NaCl and $MgCl_2$ particles. In the majority of particles larger than 0.1 μm, S is present as gypsum and these sulphate particles showed a seasonal variability with maximum number and mass during the summer. Manual analysis revealed that some of the aerosols were internal mixtures of marine components and silicates. The second location, which is characterized in this case by both very remote as well as strongly polluted areas, but until recently was almost inaccessible for Western scientists, is Siberia. Since practically no experimental data exist and scientists believe that western and central Siberia could have an important impact on the Arctic region as well as on the global climate, studies were set up to determine processes responsible for the production, transport and fate of both natural and pollution aerosols. The investigations take place at local, regional and long-range level.[9]

Automated particle analysis was performed to study the composition of individual aerosol particles sampled over the Amazon Basin.[8] Based on the data obtained, chemical mechanisms occurring in the Amazon Basin's atmosphere and processes involving aerosol and gas emission of the forest as well as long-range transport were investigated. The majority of identified particles was produced by two local sources; they consisted of soil dust and biologically derived material.

Asian dust, which mainly consists of quartz, was found in volcanic loess on the island of Hawaii. The quartz grains, unknown in the basalts of the Hawaiian Islands, were characterized by X-ray diffraction of the bulk samples in combination with SEM-EDX of single mineral grains and X-ray mapping. Begét *et al.*[10] concluded that these quartz particles, from 1 to 10 μm in size, some up to 60 μm, must have been transported over a distance of 10 000 km by late Quaternary windstorms. Their contribution to the total loess deposit was estimated at 1–3%.

At MiTAC, EPXMA has been used now for several years for the characterization of individual North Sea aerosols.[11] Over a period of 4 years, more than 25 000 particles, sampled during successive campaigns on-board a research vessel over the North Sea and the English Channel, were characterized and classified based on their inorganic composition and size.[12] Hierarchical cluster analysis on the data revealed four different particle types in the North Sea samples: sea salt, S-rich particles, silicates and $CaSO_4$ particles. Meteorological conditions and sampling locations seem to influence the abundance of these different particle types. The differences between all samples, based on variations in abundance, was studied by principal component analysis (PCA). Three different components were found and apportioned to their sources. Marine-derived aerosol particles could be identified as the first component, which grows with increasing windspeed or for more remote locations. Anthropogenically derived $CaSO_4$ particles formed the second component. The third group was characterized by particles with a high content of Si and S. A second PCA on the latter group differentiated between two sources, namely a mixed marine/continental source and a pure continental one.

The difference in aerosol composition with height above the North Sea was studied by Rojas and Van Grieken.[13] The samples were collected on board an aircraft at six different altitudes and analyzed at MiTAC by EPXMA in combination with hierarchical cluster analysis. The analysis of 50 000 individual particles showed that, for continental air masses, the majority of particles could be classified into three types: aluminosilicates, $CaSO_4$ and Fe-rich particles. No compositional changes with altitude occurred in the main particle types from western and marine air masses due to the turbulent nature of the atmosphere. Non-hierarchical cluster analysis revealed that aluminosilicates, Fe-rich particles and sea salt enriched with lead and organic material could be identified as the major particle types in these air masses. Combustion or energy-generation processes seemed to be responsible for up to 60% of the analyzed particles. Variations in composition of air masses crossing the North Sea due to air–sea exchange processes in the lower troposphere were studied by De Bock *et al.*[14] Aerosol and rain water samples were collected on two research vessels positioned 200 km apart downwind from each other, in the central area of the North Sea. By combining automated EPXMA, cluster analysis and principal factor analysis (PFA), three to eight different particle types could be distinguished, which were apportioned to four major sources. When the air masses crossed the North Sea, a decrease in aluminosilicate particles appeared, associated with a relative increase for NaCl and sea-water crystallization products. The particle diameter remained constant. Manual EPXMA was performed on several samples to study the relations between particle composition, origin and shape. The characterization based on the particle shape was possible for most particle types. Variations in composition and diameter were found in the collected rainwater samples.

Xhoffer *et al.*[15] studied the composition of individual particles in the surface micro-layer and underlying seawater of the North Sea. A comparison was made with the atmospheric and riverine particle data.

Aerosol particles with diameters above 1 μm are classified as giant aerosols. Compared with the condensation mode particles, the amount of these particles in the lower troposphere is small, but their contribution to the atmospheric composition is of great importance.[16–18] The slow realization of the importance of these particles, together with sampling difficulties and measurement errors has ensured that the giant aerosol is still a demanding topic in the field of aerosol research. Giant aerosol particles, collected using an impactor rod on top of an aircraft above the Southern Bight of the North Sea, were analyzed by EPXMA and processed by multivariate techniques.[19] Four different aerosol sources could be distinguished by PFA: aluminosilicate dispersal, combustion processes, industrial activity and a marine source. Cluster analysis enabled the workers to classify the analyzed particles and revealed clear differences between marine and continental air masses. The size distributions of the main particle types could be well fitted by a log-normal distribution with an average diameter of 3 μm. A bimodal size distribution with average size maxima at 4 and 15 μm was only found in the case of aluminosilicate particles.

Coal fly ash particles emitted by a Hungarian power station[20] and background aerosols sampled in the middle of the Great Hungarian Plain[21] were both characterized by single-particle analysis using EPXMA. Two unexpected particle groups were detected in the power plant aerosol fraction below 2 μm: Ba-rich particles and As-rich gypsum particles. The first group is probably produced by the cleaning process with Ba-containing liquid used to reduce the sulphur content of added slag. The As coating on the second particle group results from the condensation in the cooled stack gas. The composition of the background Hungarian aerosol particles (0.3–20 μm) together with recorded air-back trajectories, refers to an anthropogenic origin.

During the Kuwait oil fire plumes in May 1991, aerosol samples were collected by an aircraft at different altitudes in the plume.[22] EM analysis (transmission and scanning) was performed to investigate the impact on the local and global environment. The increase of the small sulphate particle concentration found at higher levels and at larger distances from the fire source suggested the oxidation of SO_2 gas, followed by homogeneous nucleation. In those areas, large soot, salt and dust particles were converted into cloud condensation nuclei (CCNs) due to a S coating. These CCNs could play an important role in the formation of clouds, haze, smog and fog. Air trajectory studies showed that aerosols, especially black carbon particles which have the tendency in the absence of rain showers to remain airborne for a long time, could have reached China. Whether the severe rainfall in China at the end of May and the beginning of June is related to the fire plumes in Kuwait requires further research.

Concerning the urban aerosol composition, several studies have been focused on highly industrialized countries and only limited data are available from so-called developing countries. Aerosols from the city of Khartoum in the sub-Saharan region in Sudan were characterized using different bulk techniques and automated EPXMA for single-particle analysis.[23] Most of the Khartoum aerosol particles were identified as soil dust and differentiated into aluminosilicates and smaller amounts of quartz and $CaCO_3$. In comparison with literature data on urban aerosol composition, the concentrations of S, Cl, Zn, Br and Pb in the Khartoum dust particles are the lowest values ever published. The airborne levels of Br, Pb and crustal elements seemed to be controlled by traffic emissions.

The combination of bulk and single-particle analysis was also used by Cornille *et al.*[24] to study both the coarse (> 2 μm) and fine (< 2 μm) aerosol fraction collected in the Zabadani Valley near Damascus, Syria. The results obtained indicated that desert soil dispersion is the major particle source (90% of the total suspended particulate material) in this region, besides a minor anthropogenic input. Consequently the crustal element concentrations were comparable to those in urban and industrial areas and anthropogenic elements were clearly less abundant in this arid region. The single particle results revealed also that the soil dust component could be subdivided in two major components, namely one with a shale-like composition and the other with a limestone composition.

Aerosol sampling 4 km west of Santiago de Chile, followed by automated EPXMA revealed eight different particle types in both the fine and coarse aerosol mode.[25] The coarse mode was mainly dominated by soil dust particles while anthropogenic particles represented the fine particle mode. Particles rich in S could not be classified into one particle type but they are present in six out of eight particle types.

According to a recent publication by Katrinak *et al.*[26] on the indentification of individual particle types in the Phoenix aerosol (Arizona), the aerosol in this region consisted mainly of mineral-rich particles in the coarse fraction (crustal source), while the fine fraction was dominated by zero-count particles (elements lighter than Na) and to a lesser extent by mineral-rich particles. The zero-count particles can probably be classified as carbonaceous particles produced by anthropogenic sources such as the emissions of diesel motor vehicles. Compared with individual particle analysis data obtained 7–10 years ago, compositional variations appeared in the Phoenix aerosol. The contribution of S-bearing particles to the fine fraction declined from 30% in 1980 to 17% in 1989–1990, while the decrease in Pb concentration probably results from a reduction in the uses of leaded gasoline.

Due to the recent EEC legislation which controls the emission of Pb through car exhausts, the total particulate Pb concentration in Antwerp, Belgium also decreased from 110 ng m^{-3} in July 1986 to 74 ng m^{-3} in March 1987. Based on an EPXMA – particle-induced X-ray emission (PIXE) – laser microprobe mass spectro-metry (LMMS) study,[27] most of the Pb-containing particles collected near the city of Antwerp were identified in the fine fraction < 1 μm. Pb-containing particles could be classified into five main classes. The Pb sulphates and Pb halides produced by car exhausts accounted for up to 67% and 28% by mass of the total Pb-containing particles, respectively. The obtained results suggested also that the individual Pb-rich particles are not completely converted to pure Pb sulphate particles upon reaction with ammonium sulphate aerosols present in the urban atmosphere. Cl and Br were found to be completely removed from the lead sulphate particles.

Pb-bearing particles from the floor dust of 16 residences in the London borough of Richmond, England were studied by Hunt *et al.*[28] by SEM–EDX. The assignment of the analysed Pb-rich particles to different particle types (road dust, paint, etc.) was based on a classification scheme[29] obtained by the analysis of different types of Pb-source particles. In the size range 0–64 μm, paint, road dust and garden soil were identified as the major contributors of Pb-rich particles to floor dust. Pb-containing dust particles with diameters between 64 and 100 μm appeared to be paint. No relation seemed to exist between the age of the houses and the contribution of the major sources.

Concerning the characterization of S compounds in individual aerosol particles, Qian and Ishizaka reported[30] on the characterization of methane sulfonic acid using SEM, transmission electron microscopy and thin-film chemical tests in aerosols sampled over the Sakushima Island, Japan and a new method for the determination of the S-mass content in single aerosol particles using SEM was developed and described by Pardess *et al.*[31]

Due to the development of X-ray detectors with a removable or ultra-thin window, the detection of light elements such as O and C becomes possible. Applications in this field were only recently published by Fruhstorfer and Niessner[32] on the indentification and classification of airborne soot, by Hamilton *et al.*[33] on airborne carbonaceous particulate matter and by Zhang and McMurry[34] in a study on the mixing characteristics and water content of submicrometer aerosols. Bioaerosol particles with radii > 0.2 μm were examined by Maser and Jaenicke[35] by using SEM and optical light microscopy.

Micro-particle-induced X-ray emission

Scanning proton microprobe analysis (SPM) uses a high-energy proton beam of 1–3 MeV, provided by a cyclotron or nuclear electrostatic accelerator and focused to a diameter of 0.5–10 μm by magnetic quadrupoles and/or electrostatic lenses. Beam currents higher than 100 pA should be avoided during aerosol analysis to prevent sample damage. The beam position on the sample is controlled by a scanning system and collection of the different signals received from several detectors positioned around the sample is only possible with the help of a powerful computer system.

In micro-proton- or particle-induced X-ray emission (micro-PIXE), the produced X-rays are detected by a Si(Li) detector. This results in X-ray spectra with characteristic lines superimposed on a very low continuous background. Compared to EPXMA, the background in PIXE spectra in the region from $Z = 15$ onwards is 2–3 orders of magnitude lower because no continuum radiation is produced by the stopping of the projectile ions. As in EPXMA, the element detection is limited to elements heavier than sodium due to the presence of a thick Be window in front of the detector. To generate real-time X-ray elemental maps, the X-ray signal intensities are correlated with the beam position in the scanned area. The PIXE mappings are very similar to those obtained by EPXMA but show much better detection limits (1–10 p.p.m.) combined with an inferior spatial resolution (0.5–10 μm).

Applications

Micro-PIXE in combination with automated EPXMA and LMMS was used by Artaxo *et al.*[36,37] to characterize individual aerosol particles collected at the Brazilian Antarctic station and at several biomass burning sites in the Amazon basin. Compared to bulk analyses, their approach revealed a better source apportionment and clarified atmospheric processes in a unique way. The Antarctic samples were clearly dominated by sea-salt aerosols with NaCl and $CaSO_4$ as major compounds and Al, Si, P, K, Mn, Fe, Ni, Cu, Zn, Br, Sr and Pb as minor and trace elements. Soil dust particles, NaCl particles, $CaSO_4$ with Sr and finally Br-rich and Mg-rich particles were the four different components found by factor analysis on the elemental data set. The majority of particles identified in the Amazon Basin samples were biogenic with a high organic content and K, P, Ca, Mg, Zn and Si as predominant elements. Simultaneous measurement of C, O and N was done by Rutherford backscattering analysis (RBS).

Jakšic *et al.*[38] used SPM in a study to investigate the spatial trace element distribution in single coal fly ash particles. By combining micro-PIXE and RBS measurements, the minor and trace element composition as well as the indentification of the matrix components and thickness were obtained. Evidence for trace element enrichment at the particle surface was found in the recorded areal maps and radial line scans. The aluminosilicate fly ash particle analysis was complicated by the non-homogeneous character of the particles. Another micro-PIXE / RBS study on individual fly ash particles, collected at the inlet and outlet ports of the electrostatic precipitator of a coal-fired power station, was performed by Caridi *et al.*[39] Their investigation was focused on 1-μm particles, because, for this size of particle, the collection efficiency of the electrostatic precipitator is very poor. The importance of the chemical composition effect on the electrostatic precipitation is probably demonstrated by the difference in particle types, characterized at the inlet and outlet. In the future, a correlation between the chemical composition and the particle morphology is expected to be available by simultaneous collection of proton-induced secondary electron images. An evaluation of the effects of variations in areal density on the elemental intensity maps of individual particles obtained by micro-PIXE was acquired by comparison of theoretically produced X-ray yield maps of spherical particles with experimental micro-PIXE and scanning transmission ion microscopy (STIM) intensity maps of fly ash particles.[40] The fly ash particles were collected from electrostatic precipitators in Croatia and Greece. STIM was demonstrated to be a very useful technique which might prevent misunderstanding of elemental intensity images obtained by PIXE.

Using the SPM facilities of the Institute for Reference Materials and Measurements (IRMM) in Belgium and of the Lund Institute of Technology in Sweden, the major, minor and trace elements in individual giant North Sea aerosols were determined by micro-PIXE.[41,42] Ti, V, and Cr could be detected under the prevailing experimental conditions down to 50 fg. Three different aerosol types could be distinguished: sea salt particles, sea salt combined with a high content of S, K and Ca and particles rich in Ti, Cr, Fe, Ni. Via the elemental maps, the individual giant aerosol particles could be identified as agglomerates of several large particles.

Orlic *et al.*[43] reports on the methodology used at the National University of Singapore for the nuclear microscopic analysis of individual aerosol particles. Identification and characterization of the size and shape of the particles is performed by STIM. Determination of the matrix composition and effective thickness is acquired by RBS. PIXE reveals the minor and trace elements present in the particles. The optimal PIXE sensitivity requires that the collection medium is both very thin and clean; this could not be found in the different commercially available foils that were tested. However, thin pioloform films made in the laboratory appeared to be the most suitable. Minimum detection limits depend strongly on the particle's matrix and were observed to be between 50 and 150 mg l^{-1} for elements between Ca and Zn. Under the same experimental conditions the minimum detectable mass was as low as 2 fg.

Laser microprobe mass spectrometry

Laser microprobe mass spectrometry (LAMMS/LMMS) uses a high-power density-pulsed laser beam for the evaporation and ionization of a small area on the sample. Different mass spectrometers can be applied for the detection of the produced positive and negative elemental and molecular ions. Interpretation and classification of individual particle spectra can be obtained by pattern recognition and library search computer methods.

The time-of-flight (TOF) mass spectrometer provides, depending on the electric field polarity, separation of positive or negative ions with different mass-to-charge (m/z) ratios according to their flight times. The mass resolution achieved by commercially available TOF-LMMS instruments ranges from 850 in the low m/z range to 1 unit for m/z 500.

Applications

The composition of background aerosols collected at King George Island, Antarctica was studied by Wouters *et al.*[44] using LMMS. Due to the coastal environment, the majority of particles could be identified as sea salt and transformed sea salt. To a much lesser extent, sulphate-rich, aluminosilicate, Fe-rich, organic, K-rich and

Zn-rich particles were found. The sulphate particles detected in the size fraction 0.5–1 μm are suggested to be highly transformed sea salt in which little or no chloride was found. Earth crustal dust seemed to be responsible for the aluminosilicates and Fe-rich particles in the coarse size fraction (2–4 μm). A very low abundance (< 1%) was obtained for the K-rich and Zn-rich particles, which normally indicate local contamination events. Typical ions (ammonium, nitrate and some trace element ions), often identified in LMMS spectra of marine aerosol particles from less remote regions, were not present in the coastal Antarctic aerosols.

Combining EPXMA, LMMS and micro-PIXE, Artaxo *et al.*[8] characterized individual aerosol particles from the Amazon Basin. EPXMA revealed three major aerosol sources: sea salt particles, soil dust and a biogenic fraction. The LMMS study of the biogenic fraction showed two major particle types: K-rich and P-rich particles. Some LMMS spectra were too complex to interpret due to the superposition of many organic compounds.

Individual North Sea aerosol particles collected from an aircraft at six different heights were analysed by LMMS.[45] The different particle types previously distinguished by EPXMA were also found with LMMS but many particles seemed to appear as internal mixtures. The interpretation of the particle type abundances as a function of wind direction and particle size made it possible to apportion the different types to their source. Besides a decrease in relative sea salt concentration above the inversion layer, no clear differences were found in particle abundances as a function of height.

The LMMS results obtained from the EPXMA–LMMS–XRF study on aerosols collected in the city of Santiago de Chile[25] indicated that the sea spray particles which are transported into the city undergo several transformations and a S enrichment. Using the LMMS technique, carbon-rich particles, probably produced by fossil-fuel combustion, could be identified.

The specific harmfulness of coal mine dust to the health of coal workers has often been related to the quartz content in the respirable fraction of such materials. Because no consistent correlation was found between the experimental toxicity and the total quartz content determined by bulk analysis of coal mine dust, a single-particle approach was demanded. LMMS was used successfully by Tourmann and Kaufmann[46,47] to reveal the heterogeneous distribution of potentially toxic constituents such as silica or siderite. Three quartz-rich coal mine dusts, with significant differences in toxicity but no correlation with conventional data, have been investigated. The acquired analytical data seemed to be, in contrast to bulk analysis, in agreement with toxicity data.[46-48]

Fumes arising from iron and steel industries are considered to be the major source of airborne particles containing metal oxides which may be carcinogenic. The toxicity of these metals seems to be related to their chemical oxidation state. LMMS analysis on particles emitted as dust by the steel industry revealed a correlation between the Cr oxidation state and the particle size. Particles smaller than 1.1 μm were composed of P and Na matrices, whereas large particles (> 6 μm) consisted mainly of Ca. Chromium was found to be present in the hexavalent state for both size fractions. Trivalent Cr could only be detected in particles of intermediate size.[48,49]

Pb-containing aerosol particles, sampled on top of a 15-m-high building 5 km south of Antwerp, Belgium were characterized by LMMS, micro-PIXE and EPXMA.[27] LMMS was performed to detect elements with $Z < 11$, particularly ammonium compounds. Ammonium sulphate coatings were found to be present on nearly all Pb-containing particles.

Wonders *et al.*[50] reported on the LMMS analysis of Pb-containing aerosols collected both at the city Wageningen and at the downwind side of a highway at Ede, in The Netherlands. Most particles were identified as mixed salts of ammonium nitrate and ammonium sulphate and showed a variable content of metals, especially in the case of V and Pb.

Recently the *in situ* characterization of the size and chemical composition of individual particles became possible by performing on-line LMMS or so-called rapid single-particle mass spectrometry (RSMS). Using this technique, aerosol particles are immediately collected into the mass spectrometer. The scattered radiation obtained from the interaction of each individual aerosol particle with the He–Ne laser beam reveals information on the particle size and triggers a laser which vaporizes the particle and ionizes the fragments. For each single aerosol particle a complete mass spectrum is recorded with a TOF mass spectrometer. Reference is made to Prather *et al.*,[51] Carson *et al.*[52] and Jambers *et al.*[4] for a more detailed description of the instrument. Up to now on-line LMMS has only been used on artificial aerosols.[52-57]

A Fourier transform (FT) ion cyclotron resonance (ICR) mass spectrometer was recently coupled to the LMMS, providing a higher resolving power and mass accuracy.[58] Sample ionization can be achieved either inside the ICR cell or in an external source from which the produced ions are transferred to the cell for mass spectrometric detection. A detailed description of the FT–MS principles was published by Marshall and Verdun.[59] When performing routine FT–LMMS measurements, the mass resolution exceeds ~~106~~ below m/z 100 1
and ~~105~~ at m/z 1000 with an m/z accuracy around
10^5 1 p.p.m. Elemental ion detection can be obtained down
to ~~108~~ atoms and the minimum spatial resolution is
around 5 μm compared to 1 μm in TOF–LMMS. To

10^8

date no papers have been published on environmental particle studies using FT–LMMS.

Conclusion

At present, for a complete characterization of a sample, several, often complementary techniques must be implemented since each micro-analytical technique has its own draw-backs and the 'super instrument' revealing all information has not been developed. Performing different analytical techniques on the same particles implies, however, a suitable sample preparation which often differs according to the applied technique.

Possible problems concerning sample preparation, such as contamination of decomposition upon sample-surface interaction and loss of components due to vacuum conditions (e.g. SEM–EPXMA and SPM analysis), are being solved by on-line LMMS or RSMS. Since these techniques have only recently been developed, their applications are still being refined.

The necessity to understand, for example, the different formation processes of aerosol particles forces scientists to try to analyse smaller and smaller particles, requiring an improvement of the spatial resolution and detection limits of the instruments.

The analysis automation, leading to statistically relevant results in a very short time, which is up to now only available for SEM–EPXMA, can be considered as one of the demanding topics in the environmental field.

Acknowledgements

L.D.B. acknowledges financial support by the Instituut voor de Bevordering van het Wetenschappelijk-Technologisch Onderzoek in de Industrie (IWT). This study was partially prepared in the framework of the Impulse Programme in Marine Sciences, supported by the Belgian State – Prime Minister's Service – Services for Scientific, Technical and Cultural Affairs (contract MS/06/050) and by the Belgian Ministery of Public Health and the Environment.

References

1 M. Grasserbauer, *Mikrochim. Acta*, Part III, 1983, 415.

2 R. Van Grieken and C. Xhoffer, *J. Anal. At. Spectrom.*, 1992, **7**, 81.

3 C. Xhoffer, L. Wouters, P. Artaxo, A. Van Put and R. Van Grieken, *Environmental Particles*, ed. J. Buffle and H.P. Van Leeuwen, Lewis, Chelsea, MI, 1992, vol. 1, pp. 107–143.

4 W. Jambers, L. De Bock and R. Van Grieken, *Analyst*, 1995, **120**, 681.

5 P.C. Bernard, R.E. Van Grieken and D. Eisma, *Environ. Sci. Technol.*, 1986, **20**, 467.

6 P. Artaxo, M.L.C. Rabello, W. Maenhaut and R. Van Grieken, *Tellus*, 1992, **44B**, 318.

7 R.E. Van Grieken, P. Artaxo and C. Xhoffer, *Proceedings of the Fiftieth Annual Meeting by the Electron Microscopy Society of America*, eds. G.W. Bailey, J. Bentley and J.A. Small, San Francisco Press, San Francisco, 1992, pp. 1482–1483.

8 P. Artaxo, R. Van Grieken, F. Watt and M. Jakšic M., *Proceedings of the Second World Congress on Particle Technology, Society of Powder Technology*, Kyoto, 1990, pp. 421–426.

9 H. Van Malderen and R. Van Grieken, *Atmos. Oceanic. Opt.*, 1995, **7**, 622.

10 E.J. Begét, M. Keskinen and K. Severin, *Sediment. Geol.*, 1993, **84**, 189.

11 H. Van Malderen, L. De Bock, I. Injuk, C. Xhoffer and R. Van Grieken, *Progress in Belgian Oceanographic Research*, Royal Academy of Belgium, Brussels, 1993, pp. 119–135.

12 C. Xhoffer, P. Bernard, and R. Van Grieken, *Environ. Sci. Technology*, 1991, **25**, 1470.

13 C.M. Rojas and R. Van Grieken, *Atmos. Environ.*, 1992, **26A**, 1231.

14 L.A. De Bock, H. Van Malderen and R. Van Grieken, *Environ. Sci. Technol.*, 1994, **28**, 1513.

15 C. Xhoffer, L. Wouters and R. Van Grieken, *Environ. Sci. Technol.*, 1992, **26**, 2151.

16 R. Jaenicke, *Ann. N.Y. Acad. Sci.*, 1980, **338**, 317.

17 R. Jaenicke, *Chemistry of the Unpolluted and polluted Troposphere*, 1st edn., eds. W. Georgii and W. Jaeschke, D.Reidel Publishing Co., Dordrecht, The Netherlands, 1982, pp. 341–374.

18 H.L. Dedeurwaerder, Ph.D. Thesis, Free University of Brussels, Belgium, 1988.

19 H. Van Malderen, C. Rojas and R. Van Grieken, *Environ. Sci. Technol.*, 1992, **26**, 750.

20 S. Sándor, S. Török, C. Xhoffer and R. Van Grieken, *Proceedings of the Twelfth International Congress for Electron Microscopy*, eds. L.D. Peachy and S.B. Williams, San Francisco Press, San Francisco, 1990, pp. 245–255.

21 S. Török, S. Sándor, C. Xhoffer, R. Van Grieken, E. Mészáros and A. Molnar, *Idojaras*, 1993, **96**, 223.

22 F. Parungo, B. Kopcewicz, C. Nagamoto, R. Schnell, P. Sheridan, C. Zhu and J. Harris, *J. Geophys. Res.*, 1992, **97**, 15867.

23 M.A.H. Eltayeb, C.F. Xhoffer, P.J. Van Espen and R.E. Van Grieken, *Atmos. Environ.*, 1993, **27B**, 67.

24 P. Cornille, W. Maenhaut and J.M. Pacyna, *Atmos. Environ.*, 1990, **24A**, 1083.

25 C.M. Rojas, P. Artaxo and R. Van Grieken, *Atmos. Environ.*, 1990, **24B**, 227.

26 K.A. Katrinak, J.R. Anderson and P.R. Buseck, *Environ. Sci. Technol.*, 1995, **29**, 321.

27 W. Van Borm, L. Wouters, R. Van Grieken and F. Adams, *Sci. Total Environ.*, 1990, **90**, 55.

28 A. Hunt, D.L. Johnson, I. Thornton and J.M. Watt, *Sci. Total Environ.*, 1993, **138**, 183.

29 A. Hunt, D.L. Johnson, J.M. Watt and I. Thorton, *Environ. Sci. Technol.*, 1992, **26**, 1513.

30 G-W. Qian and Y. Ishizaka, *J. Geophys. Res. - Oceans*, 1993, **98**, 8459.

31 D. Pardess, Z. Levin and E. Ganor, *Atmos. Environ.*, 1992, **26A**, 675.

32 P. Fruhstorfer and R. Niessner, *Mikrochim. Acta*, 1994, **113**, 239.

33 R.S. Hamilton, P.R. Kershaw, F. Segarra, C.J. Spears and J.M. Watt, *Sci. Total Environ.*, 1994, **146/147**, 303.

34 X.Q. Zhang and P.H. McMurry, *Atmos. Environ.*, 1993, **27A**, 1593.

35 S. Matthias-Maser, R. Jaenicke, *J. Aerosol Sci.*, 1993, **24**, 539.

36 P. Artaxo, M.L.C. Rabello, F. Watt, G. Grime and E. Swietlicki, *Nucl. Instrum. Meth. B*, 1993, **75**, 521.

37 P. Artaxo, M.L.C. Rabello, F. Watt, G. Grime, E. Swietlicki, J. Knox and H-C. Hansson, *J. Aerosol Sci.*, 1992, **23**, 373.

38 M. Jakšic, F. Watt and G.W. Grime, *Nucl. Instrum. and Methods B*, 1991, **56/57**, 699.

39 A. Caridi, E. Cerede, G.W. Grime, M. Jakšic, G.M. Braga Marcazzan, V. Valkovic and F. Watt, *Nucl. Instrum. and Methods B*, 1993, **77**, 524.

40 I. Bogdanovic, S. Fazinic, M. Jakšic, G.W. Grime and V. Valkovic, *Nucl. Instrum. and Methods B*, 1994, **85**, 732.

41 J. Injuk, H. Van Malderen, R. Van Grieken, E. Swietlicki, J.M. Knox and R. Schofield, *X-ray Spectrometry*, 1993, **22**, 220.

42 J. Injuk, L. Breitenbach, R. Van Grieken and U. Wätjen, *Mikrochim. Acta*, 1994, **114/115**, 313.

43 I. Orlic, F. Watt, K.K. Loh and S.M. Tang, *Nucl. Instrum. and Methods B*, 1994, **85**, 840.

44 L. Wouters, P. Artaxo and R. Van Grieken, *Int. J. Environ. Anal. Chem.*, 1990, **38**, 427.

45 I. Dierck, D. Michaud, L. Wouters and R. Van Grieken, *Environ. Sci. Technol.*, 1992, **26**, 802.

46 J.L. Tourmann and R. Kaufmann, *Int. J. Environ. Anal. Chem.*, 1993, **52**, 215.

47 J.L. Tourmann and R. Kaufmann, *Analusis*, 1992, **20**, 65S.

48 E. Poitevin, G. Krier and J.F. Muller and R. Kaufmann, *Analusis*, 1992, **20**, M36.

49 A. Hachimi, E. Poitevin, G. Krier, J.F. Muller, J. Pironon and F. Klein, *Analusis*, 1993, **21**, 77.

50 J.H.A.M. Wonders, S. Houweling, F.A.J. De Bont, H.P. Van Leeuwen, S.E. Eeckhaoudt and R.E. Van Grieken, *Internat. J. Environ. Anal. Chem.*, ~~[in the press]~~

51 K.A. Prather, T. Nordmeyer and K. Salt, *Anal. Chem.*, 1994, **66**, 1403.

52 P.G. Carson, K.R. Neubauer, M.V. Johnston and A.S. Wexler, *J. Aerosol Sci.*, submitted.

53 P.J. McKeown, M.V. Johnston and D.M. Murphy, *Anal. Chem.*, 1991, **63**, 2069.

54 C-U. Ro, I.H. Musselman and R.W. Linton, *Anal. Chim. Acta*, 1991, **243**, 139.

55 T.W. Shattuck, M.S. Germani and P.R. Buseck, *Anal. Chem.*, 1991, **63**, 2646.

56 O. Kievit, J.C.M. Marijnissen, P.J.T. Verheijen and B. Scarlett, *J. Aerosol Sci.*, 1992, **23**, S301.

57 B.A. Mansoori, M.V. Johnston and A.S. Wexler, *Anal Chem*, submitted.

58 L. Van Vaeck, W. Van Roy, H. Struyf, F. Adams and P. Caravatti, *Rapid Commun. Mass Spectrom.*, 1993, **7**, 323.

59 A.G. Marshall and F.R. Verdun, *Fourier transform in NMR, optical and mass spectrometry*, Elsevier Science Publishers, Amsterdam, 1990, pp. 225–278.

SA 0254 73-205

Publication submitted to Analytica Chimica Acta, June 1996

Extraction of Environmental Information from Large Aerosol Data Sets through Combined Application of Cluster and Factor Analyses.

[a]L.A. De Bock*, [a]B. Treiger, [b]L. Van der Auwera and [a]R.E. Van Grieken

[a]University of Antwerp (UIA), Department of Chemistry,
Universiteitsplein 1,B-2610 Antwerp, Belgium

[b]Royal Meteorological Institute
Ringlaan 3, B-1180 Brussels, Belgium

Abstract

To reveal useful environmental information which is contained in large analytical data sets, an approach, based on the successive application of hierarchical cluster analysis and factor analysis, is proposed. Estimation criteria to determine the most suitable number of clusters and or factors, are discussed and the interpretation of the cluster and factor analyses results is performed using visual techniques. The data sets were obtained by scanning electron microscope-energy-dispersive X-ray analysis of individual North Sea aerosol particles.

Keywords: Aerosols; scanning electron microscope-energy-dispersive X-ray analysis*; Cluster analysis; Factor analysis; Chemometrics.*

1. Introduction

The availability of highly sophisticated computer equipment as well as fully automated analytical techniques led, in various disciplines, to the production of enormous data sets. The processing and interpretation of such large data sets requires the application of different statistical methods. Cluster analysis (CA) as well as principal factor analysis (PFA) belong to the most potent techniques in this field, e.g. for the processing of atmospheric aerosol composition data sets (1-3). Both techniques disclose complementary information.

In the field of aerosol microanalysis, CA is mainly performed to provide a classification of aerosol particles based on their composition. The acquired cluster groups can be identified as different particle types present in the sample. In general, CA techniques can be applied according to three main approaches: hierarchical, non-hierarchical and fuzzy clustering. Hierarchical cluster analysis (HCA), used for the data processing in this paper, is the most known one. Part of its popularity can be attributed to its relative computational simplicity but also to its ability of visually representing the results as a so-called dendrogram. The main disadvantage of this approach appears in the fact that, in any case, a hierarchical structure is being superimposed on the data set, even if no specific structure in the data set exists.

In contrast with CA, which seeks for the structure of the data set without reducing the dimensionality of the N-dimensional space, PFA tries to describe all variability in the data set with the help of a small number of hidden variables, factors. In this way, the dimensionality of the multidimensional space may be strongly reduced, the specific structure of the data set can be represented visually and the interrelationships between the variables (relative X-ray intensities of chemical elements) or between the objects (aerosol particles) can be investigated. In practice, PFA is performed whenever the real dimensionality of an N-dimensional space is much less than N, which often appears to be the case.

This paper reports on the successive application of CA and PFA on the data sets of 30 North Sea aerosol samples, acquired by single particle analysis on a scanning electron microscope with energy dispersive X-ray analysis attachment (SEM-EDX).

2. Brief outline of the theory

The following paragraphs summarise briefly the most important theoretical aspects of both statistical methods applied in this work. For more detailed descriptions on HCA and PFA, reference is made to the literature (4-8). The chemometric aspects of the IDAS Windows based software package, used for data processing, have been discussed and explained in a recent publication by Bondarenko et al.(9)

2.1. Hierarchical cluster analysis.

A hierarchical cluster analysis starts with M particles or clusters of which the most similar ones are joined successively into new clusters. The Euclidean distance was chosen to measure the similarity between two particles and Ward's strategy was followed to unite two clusters. In this way a maximum internal homogeneity into the separated groups (10) was achieved. However a feature of the Euclidean distance is that it is a weighted measurement; the higher the absolute value of the variable the higher will be its weight.

The initial results of the HCA are represented as a tree-like structure or dendrogram. To obtain meaningful information, the dendrogram has to be cut at a certain level, in order to reveal clusters of similar particles. To facilitate the choice of the most suitable number of clusters, stopping rules can be applied to indicate at what level the dendrogram should be cut. From the three stopping rules or clustering criteria, available in IDAS, the Consistent Akaike Information Criterion (CAIC) revealed the best results. The CAIC function reaches a minimum at the most suitable number of clusters and is represented by:

$$CAIC = MN(1+\ln(2\pi)) + \sum_{p=1}^{N_c} n_p \ln\left|S_p\right| + 2N_c N \ln M$$

where M and N represent the number of aerosol particles (objects) and chemical elements (variables) in the data matrix, respectively. N_c stands for the number of clusters with n_p being the number of particles in the *p-th* cluster. S_p can be defined as the maximum likelihood estimate of the variance- covariance matrix of this cluster p (11).

By absence of a clear minimum in the CAIC curve, the first sharpest decline was used as an indication for the most suitable number of clusters. However, when the dendrogram was cut too low, different groups were joined, based on experience, leading to a smaller, more suitable number of clusters. The Davies-Bouldin Index and the Sum of Distances Criterion, also available in IDAS, were excluded from this theoretical description since they did not reveal meaningful information. This can probably be attributed to their smaller application field, compared to CAIC, and to the sometimes complicated character of the experimental data sets.

The final HCA results for each of the North Sea aerosol data sets were visualised with the help of several graphs revealing: the average composition of the clusters, the distribution of the elements in each cluster and the percent abundance of the different clusters in the analysed sample. The graphical representations are illustrated in the section "Results and Discussion".

2.2. Principal Factor Analysis.

In IDAS, FA is performed as a two-step procedure. The first step is the principal factor analysis, uncovering the most suitable number of factors to take into account in the FA model. The next step is the meaningful interpretation of the results of PFA, with the help of either abstract factor rotation or target transformation.

The initial aim of PFA is to express each of the N original chemical elements (variables) in the data set as a linear combination of p ($p < N$) common factors, R, such that in matrix notation:

$$X_{MxN} = R_{Mxp} C_{pxN}$$

where R_{Mxp} and C_{pxN} are called the factor scores and factor loadings matrices, respectively. Since factors are in fact abstract variables, their loadings, showing the relative contribution of each factor into a variable, are of importance for the interpretation of the obtained results. Factor scores hold information about the position of the analysed particles (objects) in the factor space and can be used for interpretation as well.

The determination of p, the most suitable number of factors, is very difficult due to the presence of experimental error. The three most important types of error within FA are the real error (RE), imbedded error (IE) and the extracted error (XE). All of them are a function of the residual standard deviation (8). Various methods have been developed to solve this problem. In IDAS the following types of criteria are available to estimate p:

(1) Imbedded Error Function (IE): reveals a minimum for the most suitable number of factors. In practice, however, a clear minimum can not always be observed (8).

(2) *Factor Indicator Function* (*IND*): discovered by Malinowski (8), reportedly reaches a more pronounced minimum, even if no minimum could be distinguished in the *IE* function. *IND* is described as

$$IND = RE/(N-p)^2$$

(3) *Average Eigenvalue Criterion*: introduced by Kaiser (12) and known as "eigenvalue-one criterion", rejects all eigenvalues below an average eigenvalue. If the initial variables are normalised as to calculate correlation about the origin, the average eigenvalue is unity.

(4) *Cumulative Percent Variance :* calculated as

$$\sum_{j=1}^{p}\lambda_j \Big/ \sum_{j=1}^{N}\lambda_j$$

reflects the variance which is accumulated for by the particular eigenvalue (λ_j). Therefore it is called "percent variance in the eigenvalue".

(5) *Root-Mean-Square Error (RMS):*

$$RMS = \left[\sum_{j=p+1}^{N} \lambda_j \Big/ MN \right]^{1/2}$$

reveals the difference between the initial raw data and the FA reproduced data. Attention should be paid when applying this criterion, since the *RMS* vs. *p* graph sometimes overestimates the most suitable number of factors (8).

Besides these five criteria, IDAS also offers the possibility to calculate the maximal reasonable number p_{max} of eigenvectors:

$$p_{\max} \leq \frac{1}{2}\left(2N+1-(8N+1)^{1/2}\right)$$

According to PFA, the *p* first eigenvectors which make up the factor set are considered as primary eigenvectors and comprise all the information. The last *N-p* eigenvectors, or secondary eigenvalues, only reveal experimental error. One of the advantages of FA is that the reduction of the number of eigenvectors only to the primary eigenvectors, can lead to the improvement of the experimental data set.

To simplify the interpretation of the obtained p factors in each of the North Sea aerosol data sets, an abstract factor rotation was performed. This raw varimax rotation helped to clarify the unclear features of the PFA through changing the loadings of certain variables on certain factors. Comprehension of the acquired factor analysis information was moreover facilitated with the help of its visual representation (section Results and Discussion).

Based on the findings of Aitchison (13), special pre-processing of the aerosol compositional data was required for PFA in order not to reveal nonsense correlation. This pre-processing included a centred log-ratio transformation of the rows (objects) of the original data set to remove the existing correlation obtained by the compositional closure (sum of compositions equals unity).

3. Experimental

3.1. Sampling

A one week sampling campaign to characterise the composition of individual North Sea aerosol particles was organised for August 23-27, 1993. During this campaign aerosols were collected on the main deck of the research vessel R.V. Belgica, using a May impactor (14) positioned inside a wind tunnel (15). Using this type of impactor, aerosol particles are segregated in size, based on inertial characteristics, with theoretical cut-offs for stage 1 to 6 at 20, 8, 4, 2, 1 and 0.5 µm. Microscope slides covered with Apiezon coated Nuclepore filters (Nuclepore, Pleasanton, CA, USA) were used as impaction surface. The Apiezon coating reduces effects like “bounce off” and “re-entrainment”, which influence the collection efficiency and change the apparent size distribution. The use of a wind tunnel guarantees isokinetic sampling. For more details on the wind tunnel and the way of sampling reference is made to De Bock et al. (16).

The research vessel was also equipped for continuous monitoring of different meteorological parameters, providing information about the wind speed and direction, the relative humidity, the atmospheric pressure and temperature at any time during the sampling of atmospheric particles. Based on this information and the exact ship positions, it became possible to calculate “back-trajectories” which reveal the origin and the trajectory of the sampled air masses and this up to 48 hours back in time. The sampling campaign was characterised by wind speeds between 4.3 and 11.7 m/s with Northern wind directions.

3.2. Scanning electron microscope analysis

The set of 30 size-segregated North Sea aerosol samples was analysed using a JEOL JSM 6300 SEM (JEOL, Tokyo, Japan). The instrument is equipped with a PGT (Princeton Gamma Tech, Princeton, NJ, USA) energy dispersive X-ray detector. The PA6300 program was applied for the automated analysis of 300 individual particles per sample at an acceleration voltage of 20 kV and a beam current of 1 nA. The X-ray accumulation time was fixed at 20s. When the PA6300 program is run, the area of the sample to be analysed is subdivided in different fields and the particle analysis starts with the collection of a backscattered electron image of the field. Based on this image, the area, perimeter and diameter of the particles within the field are calculated and compared with a selection criterion. The X-ray spectrum is accumulated by rastering the electron beam on 40 points within the particles contour. Spectrum evaluation is performed by a tophat filter and storage on optical disk of images and spectra allows a re-evaluation of the acquired data.

In combination with multivariate techniques, SEM-EDX is considered to be a powerful method for discriminating different particle types and for source apportionment. Clear drawbacks of this technique are however the poor detection limits (about 0.1%) and the limitation to detect only elements with Z > 10, due to the presence of a Be window in front of the Si-Li detector. The X-rays of elements like C, O and N are too low in energy to penetrate this window. In SEM-EDX analysis, a particle group is classified as organic if no X-rays are collected or, in other words, when the sum of the characteristic X-ray peak intensities in the cluster is very low.

4. Results and discussion

Since consistent results were obtained for both HCA and PFA and no significant differences were found between the analysed samples, a representative sample N7i3I was selected. This aerosol sample was collected in the Southern bight of the North Sea at an average wind speed of 7.3 m/s and a wind direction of 271°. The corresponding back-trajectory, represented in Fig.1, indicates that the sampled air mass will be characterised not only by a marine influence but also by a terrestrial one (U.K.).

The different steps involved by the processing of the North Sea data, when performing successively HCA and PFA, will be illustrated for this representative sample in the following paragraphs.

4.1. Hierarchical cluster analysis results

The initial results of the HCA are represented by the dendrogram in Fig.2a. The *CAIC* function, used to determine the most suitable number of clusters, is illustrated by Fig.2b and reveals different minima. Meaningful results are obtained by taking exactly 5 clusters into account. If we prefer on the one hand to take only 3 cluster groups, indicated by the first sharp decline in the *CAIC* function, too much information will be lost. On the other hand, the pronounced minima at 8, 12 and 15 clusters will provide us with too many details. The average composition of the 5 clusters and their populations are represented by Figs.2c and 2d, respectively.

It is seen that 50% of the sample is represented by cluster #3 containing particles with Si, Al, Fe, K, Ca and S as major elements and Ti as minor one. This mineral particle type is classified as aluminosilicates and can be attributed to a continental influence (17). Aluminosilicates can occur as fly ash or soil dust particles. Only morphological differences exist between fly ash particles, emitted by high temperature combustion processes and soil dust particles, produced by soil erosion. The continental influence is also expressed in the presence of cluster #5 comprising Fe-rich particles, which contribute up to 10% to the total aerosol abundance. In Fe-rich particles analysed in other samples, also Si and or S were present in lower concentrations indicating clearly metallurgical industries as a possible origin of this particle type. Clusters #1 and #4 (27% and 8%, respectively) can be identified as a result of the marine influence. The sea salt particles found in cluster #4 are the result of sea spray ejected by the bubble-bursting mechanism after breaking waves at the sea surface (16). The fact that besides Na and Cl also S is present in these particles, indicates that the pure NaCl particles have been converted into aged sea salt by reaction with sulphuric acid or SO_2 from the continent. The particles in cluster #1 are sea water crystallisation products produced upon evaporation of sea water droplets (18).Finally the sample was also characterised by 5% of Na-rich particles (cluster #2). A further investigation of the low sum of peak intensities found for these Na-rich particles performed by spectrum fitting with AXIL (19), revealed that an organic nature could be associated with this particle type and that sometimes also Cl and S were present as minor elements. Similar results were obtained for the S-rich particles detected in other samples. Although pure S-rich organic particles were frequently found, also associations with K or Na were encountered. These organic particles can possibly be identified as derived from plant material. Enrichment of organic substances in the sea water surface layer is probably responsible for the presence of some organic material in sea water crystallisation particles.

The appearance of particle types in certain size fractions is mainly influenced by the wind direction and wind speed. Pure marine air masses are characterised by high abundances of sea salt and sea water crystallisation products on the different particle stages of the May impactor. Abundances of aluminosilicate particles, Fe-rich particles and organic material are suppressed and appear only at the small particle stages (<1 μm). However a change in wind direction, causing a more continental influence can clearly be identified by an increase of the latter particle types (aluminosilicates, Fe-rich particles and organic material) on all stages and by the disappearance of sea salt in the particle stages below 1 μm. According to Deleeuw (20) an increase in wind speed from 2 to 16 m/s at a sampling height of 11 m could increase the particle number concentration from 11 μm particles per particle diameter increment by up to a factor of 10, which confirms that the particle concentration is strongly influenced by the wind speed.

4.2. Principal factor analysis results

Although the communalities of the variables, which are defined as that part of the variable that is due to the common factors, are often used as an indication for the correctness of the factor model, they can not be applied in this context. It is stated that the more the chosen data set is suitable for factor analysis and the more correct the factor model is chosen, the more communality approaches the variance. The factor models acquired for the aerosol data sets revealed frequently communalities which were in great disparity of the variances. This was expected from the start, since several of the elements in the experimental data sets were considered not to be strongly correlated. These uncorrelated elements are represented as unique factors, which are not included in the PFA model. In spite of these facts we succeeded to apply PFA on aerosol data sets revealing interesting environmental information.

The determination of the most suitable number of factors, based on the calculated estimation criteria, appeared to be very difficult for the majority of samples. The criteria applied on the sample are represented in Figs. 3a-e. Considering the IE function (Fig.3a), realistic minima arise at 3 and 5 factors. The IND function (Fig.3b) reaches no substantial minimum but reveals very small values for the first factors. This function was applied by Malinowski for measurements which produced gradually changing values. Since this is not the case in aerosol data sets and the fact that the IND function is not fully understood at the present time, the IND function was not valid in our field. The comparison between the eigenvalues and the average eigenvalue is shown in Fig.3c. Application of the Average Eigenvalue Criterion results in the rejections of all eigenvalues below this average eigenvalue, indicating a PFA model with 6 factors. Fig.3d reflects the Cumulative Percent Variance and shows that the fraction of variance added to the total variance by factor 2 and

3 is most significant. The fraction becomes smaller for the subsequent factors and can be considered less important starting from factor 7, pointing out a possible solution with maximal 6 factors. The difference between the initial and the FA reproduced data is illustrated by the RMS vs. factor graph in Fig.3e. No pronounced minimum is found in this graph. The maximal reasonable number of factors, calculated by IDAS, appeared to be 6.

Since not all estimations provided the same number of factors that should be taken into account, in the FA model, the abstract factor rotation was performed for solutions with 6, 5, 4, 3 and 2 factors. Investigating the visual representations of the factor loadings and factor scores, for each case separately, the FA model including 3 factors was preferred. Taking more than 3 factors into account, correlation between different factors appeared in the scatter plots of the factor scores. The associated factor loadings and scores of the three factors are illustrated in Figs. 4a-4c.

Factor #1 (Fig. 4a) is characterised by high loadings for Si, Al, Fe and K, followed by lower values for Ca and Ti, indicating an aluminosilicate source. The presence of Na, Cl and S in "anti-correlation", meaning the increase in one particle source implies the decrease of the other source, refers to the continental origin of the aluminosilicate source. The presence of a marine source is more pronounced in factor #2 (Fig. 4b), with high loadings of K, Cl, Ca, S, and P, typically associated with marine crystallisation products (18). The appearance of the lower loading of Na in anti-correlation could be related to a minor source producing the 5% organic particle material that was identified as cluster #5 in the HCA results. Factor #3 (Fig.4c) represents probably the anthropogenic release of gypsum ($CaSO_4$) from flue gas in desulfurization processes, in view of its anti-correlation with Cl, K, Na and P.

Considering the scatter plots of the factor scores of factors #1 and #2, and factors #1 and #3 in Figs. 4d and 4e, respectively, it is obvious that there exists no correlation between these factors; they appear to be independent from each other. In Fig. 4f, we can detect some correlation between factors #2 and #3. This is in agreement with the factor loadings, which in both cases indicate the presence of a marine source. Based on these findings we could conclude to reduce the number of factors and take only two factors into account; their corresponding loadings are illustrated in Figs. 5a and 5b. Only small changes occur in the loadings of factor #1' (Fig. 5a), but in factor #2' (fig. 5b), which joins the original factors #2 and #3, no difference is made between Ca and S originating from a marine source and from a continental one. The scatter plot (Fig. 5c) of the factor scores of factors #1' and #2' reveals, as would be expected, an absolute independence between both factors. Apparently the solution with two factors should be rejected due to the loss of information and the PFA model with three factors should be preferred.

4.3. Comparison HCA-PFA

The significant difference between the obtained HCA and PFA results, besides their mathematical background, appears in the fact that, in the majority of samples (26/30), the number of particle types is always larger than the number of factors. In the remaining samples the corresponding numbers are equal. In this way PFA offers the possibility to investigate, whether several particle types are produced by a common source or belong to different origins.

Frequently Na and Cl are classified together with Ca, S , K and Mg as one factor, since both particle types represent the "marine factor". On the other hand, part of the Ca and S which is often associated with K, Cl and Na, and considered as one particle type in the HCA results, is identified by PFA to have, besides a marine source, also a possible pure anthropogenic origin. This is also the case for the N7i3i sample, as discussed above.

The anthropogenic Fe-rich particles with traces of other elements found by HCA as a separate particle type, appears in PFA frequently as part of the aluminosilicate factor. This indicates that the majority of Fe-rich particles occur as decomposition products of aluminosilicate particles or can be identified as Fe-rich aluminosilicates. In the N7i3i sample we can indeed observe that cluster #1 and #3 (Fig.4) are represented by one aluminosilicate factor, factor #1 in Fig. 11.

Organic clusters are hard to find as a single factor. They appear in anti-correlation with very low element loadings, which makes it only possible to identify them based on the knowledge acquired by the HCA.

Sometimes, also minor factors with e.g high loadings of Mg and or K were detected, which could not be identified with one of the particle types in the HCA results. This can only be explained by the fact that the Euclidean metrics used in HCA, actually dismisses the input of the minor elements.

5. Conclusion

The application of HCA in association with PFA for the processing of single aerosol particle data sets appeared to be a remarkable technique to uncover the real intrinsic structure of the data set, thus providing us with the valuable environmental information. The stability of the PFA procedure as well as the reproducibility of the sampling campaign was confirmed.

Concerning multivariate techniques, we can conclude that in the case of PFA not all estimation criteria provide the most suitable number of factors, often an overestimation of the number of factors is obtained. However the criteria used in PFA and HCA, should be applied as an indication for the most suitable number of factors and clusters, respectively, rather as a means to acquire the exact solution.

Acknowledgements

This work was partially financed by the Belgian State-Prime Minister's Services for Scientific, Technical and Cultural Affairs in the framework of the Impulse Programme on Marine Sciences (under Contract MS/06/050). L.D.B. acknowledges financial support by the Instituut voor de Bevordering van het Wetenschappelijk - Technologisch Onderzoek in de Industrie (IWT)

References

[1] K. Katrinak, J.R. Anderson and P.R. Buseck, Environ. Sci. Technol., 29 (1995) 321.

[2] B. Treiger, I. Bondarenko, H. Van Malderen and R. Van Grieken, Anal. Chim. Acta, 317 (1995) 33.

[3] I. Bondarenko, H. Van Malderen, B. Treiger, P. Van Espen and R. Van Grieken, Chemom. Intell. Lab. Syst., 22 (1994) 87.

[4] D.L. Massart and L. Kaufman, The Interpretation of Analytical Chemical Data by the Use of Cluster Analysis, Wiley, New York, 1983.

[5] M. Anderberg, Cluster Analysis for Applications, Academic Press, New York, 1973.

[6] B. Everitt, Cluster Analysis, Heinemann Educational Books Ltd., London, 1974.

[7] H.H. Harman, Modern Factor Analysis, University of Chicago Press, Chicago, 1970.

[8] E.R. Malinowski and D.G. Howery, Factor Analysis in Chemistry, Wiley, New York, 1980.

[9] I. Bondarenko, B. Treiger, R. Van Grieken and P. Van Espen, Spectrochim. Acta Electron., 51B (1996) 441.

[10] P.C. Bernard and R.E. Van Grieken, Anal. Chim. Acta, 267 (1992) 81.

[11] H. Bozdogan, Psychometrika, 52 (1987) 345.

[12] H.F. Kaiser, Educ. Psych. Meas., 20 (1960) 141.

[13] R.A. Reyment and K.G. Jöreskog, Applied Factor Analysis in the Natural Sciences, Cambridge University Press, Cambridge, 1993.

[14] K.R. May, J. Aerosol Sci., 6 (1975) 1.

[15] Y. Vawda, I. Colbeck, R.M. Harrison and K.W.J. Nicholson, J. Aerosol Sci., 20 (1989) 1155.

[16] L.A. De Bock, H. Van Malderen and R. Van Grieken, Environ. Sci. Technol., 28 (1994), 1513.

[17] C. Xhoffer, P. Bernard, and R. Van Grieken, Environ. Sci. Techmol., 25 (1991) 1470.

[18] H. Bochert, Chemical Oceanography, Academic Press, London, 1965.

[19] P. Van Espen, H. Nullens and F. Adams, Nucl. Instr. and Meth., 142 (1977) 243.

[20] G. Deleeuw, Tellus, 25 (1991) 1470.

Figure captions

Fig.1: Air mass back-trajectory for the N7i3i aerosol sample collected in the Southern bight of the North Sea during the August 1993 campaign.

Fig.2: HCA results of sample N7i3i.

a) Dendrogram showing the initial results of HCA.

b) Consistent Akaike information criterion.

c) Average composition of five clusters.

d) Pie chart of the cluster populations.

Fig.3: Criteria to estimate the most suitable number of factors for a data set of 17 variables and 300 particles (sample N7i3i), with arbitrary values in the Y-axis.

a) Imbedded error function criterion.

b) Factor indicator function.

c) Average eigenvalue criterion, with Av. Representing the average eigenvalue.

d) Cumulative percent variance criterion.

e) Root-mean-square error criterion.

Fig.4: PFA results of sample N7i3i, for a PFA model with three factors.

a) Factor loadings of factor #1.

b) Factor loadings of factor #2.

c) Factor loadings of factor #3.

d) Factor scores of factors #1 and #2.

e) Factor scores of factors #1 and #3.

f) Factor scores of factors #2 and #3.

Fig.5: PFA results of sample N7i3i, for a PFA model with two factors.

a) Factor loadings of factor #1'.

b) Factor loadings of factor #2'.

c) Factor scores of factors #1' and #2'.

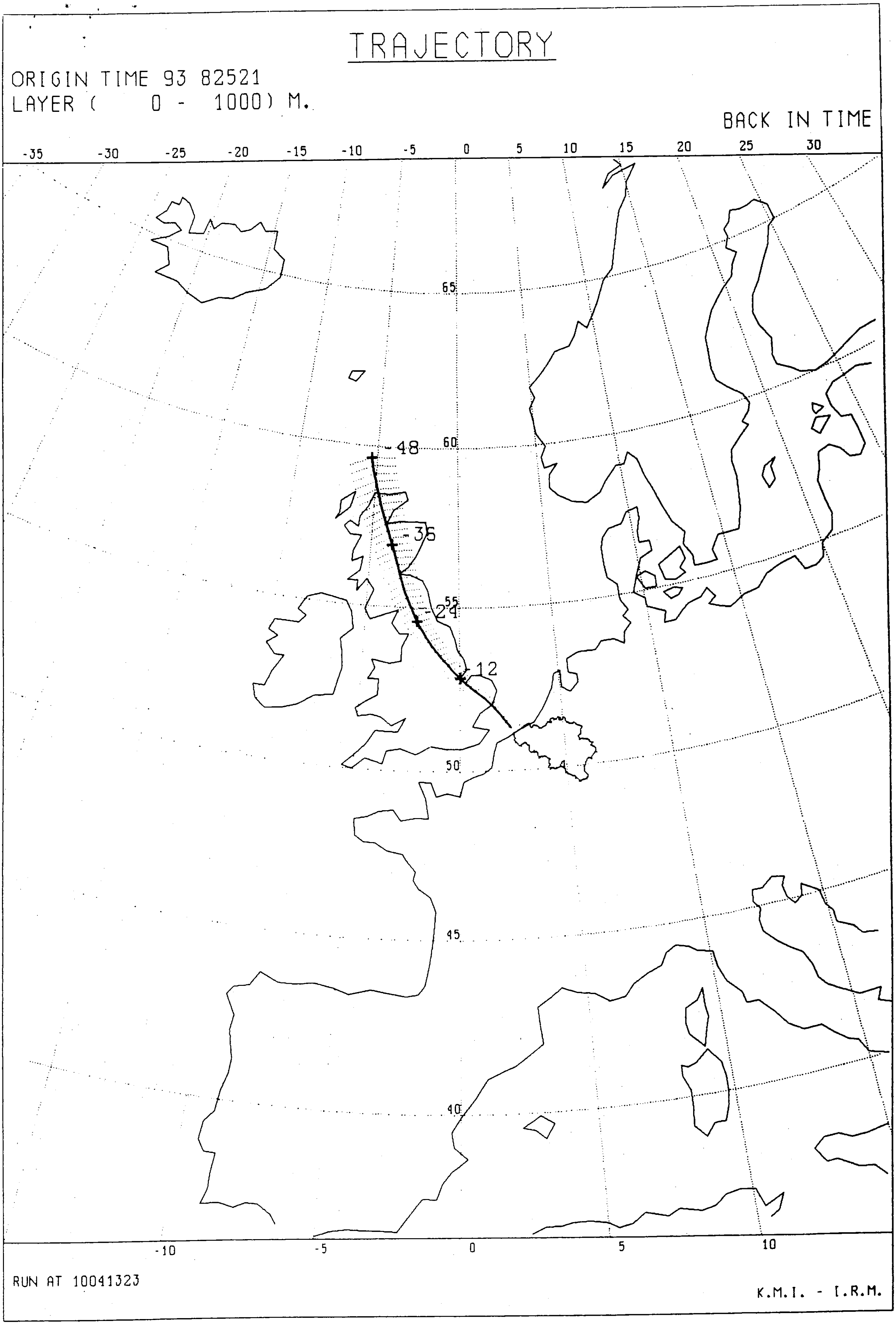
TRAJECTORY
ORIGIN TIME 93 82521
LAYER (0 - 1000) M.
BACK IN TIME
-35
-30
-25
-20
-15
-10
-5
0
5
10
15
20
25
30
65
60
55
50
45
40
30
25
20
15
-48
-36
-24
-12
-10
-5
0
5
10
RUN AT 10041323
K.M.I. - I.R.M.

Fig1

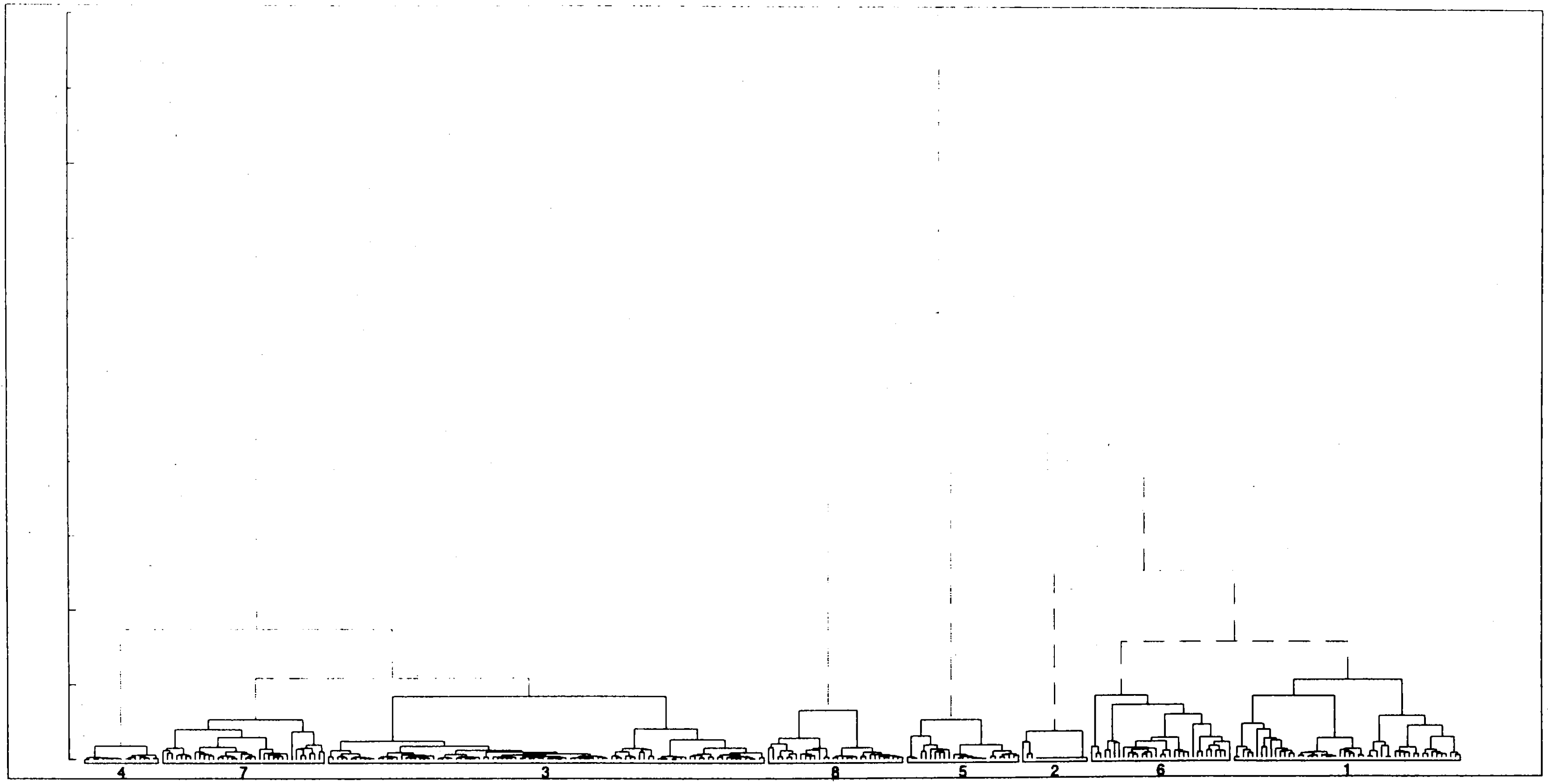

Fig.2a : Dendrogram showing the initial results of HCA.

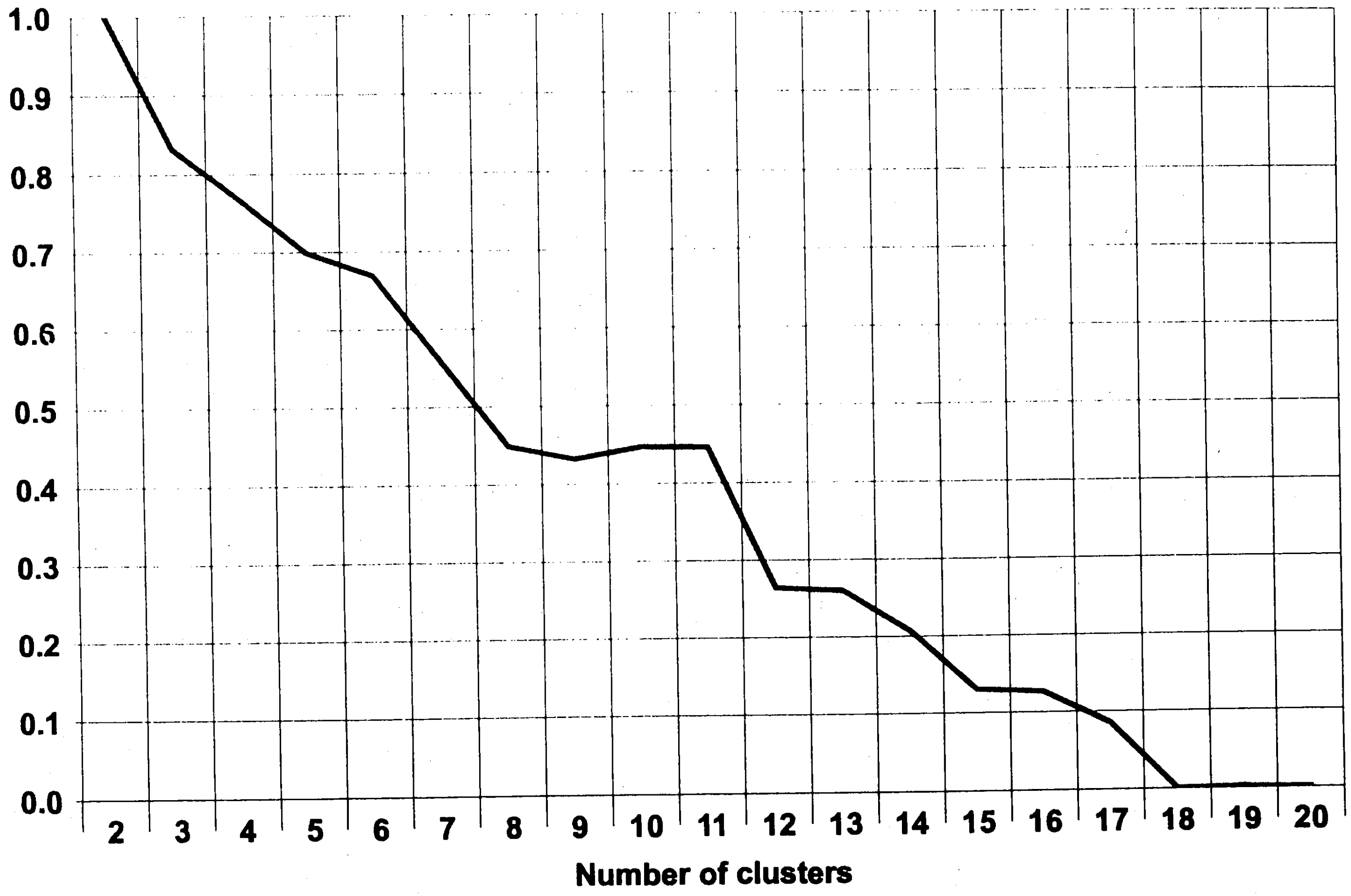

Fig.2b: Consistent Akaike information criterion.

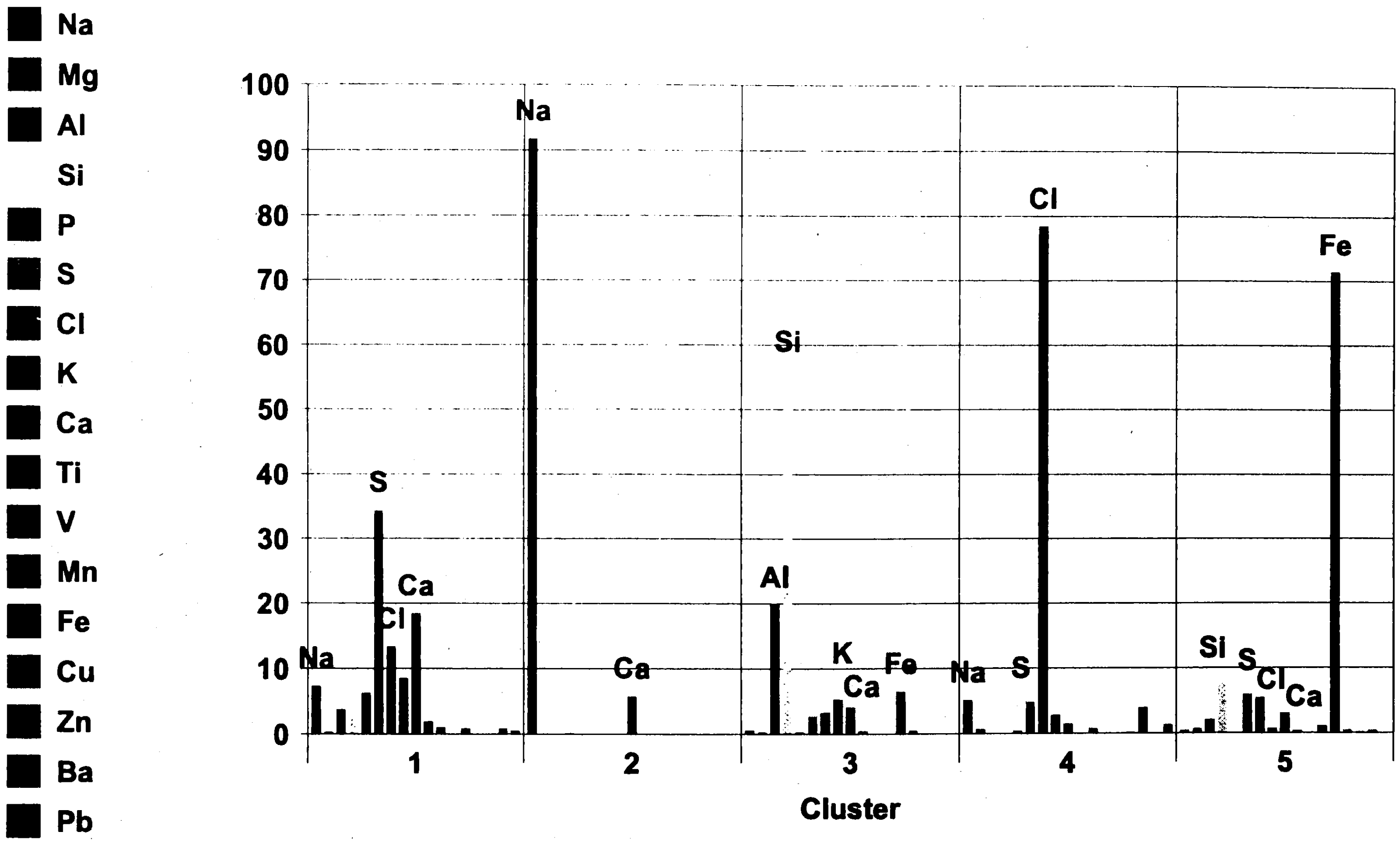

Fig.2c: Average composition of five clusters.

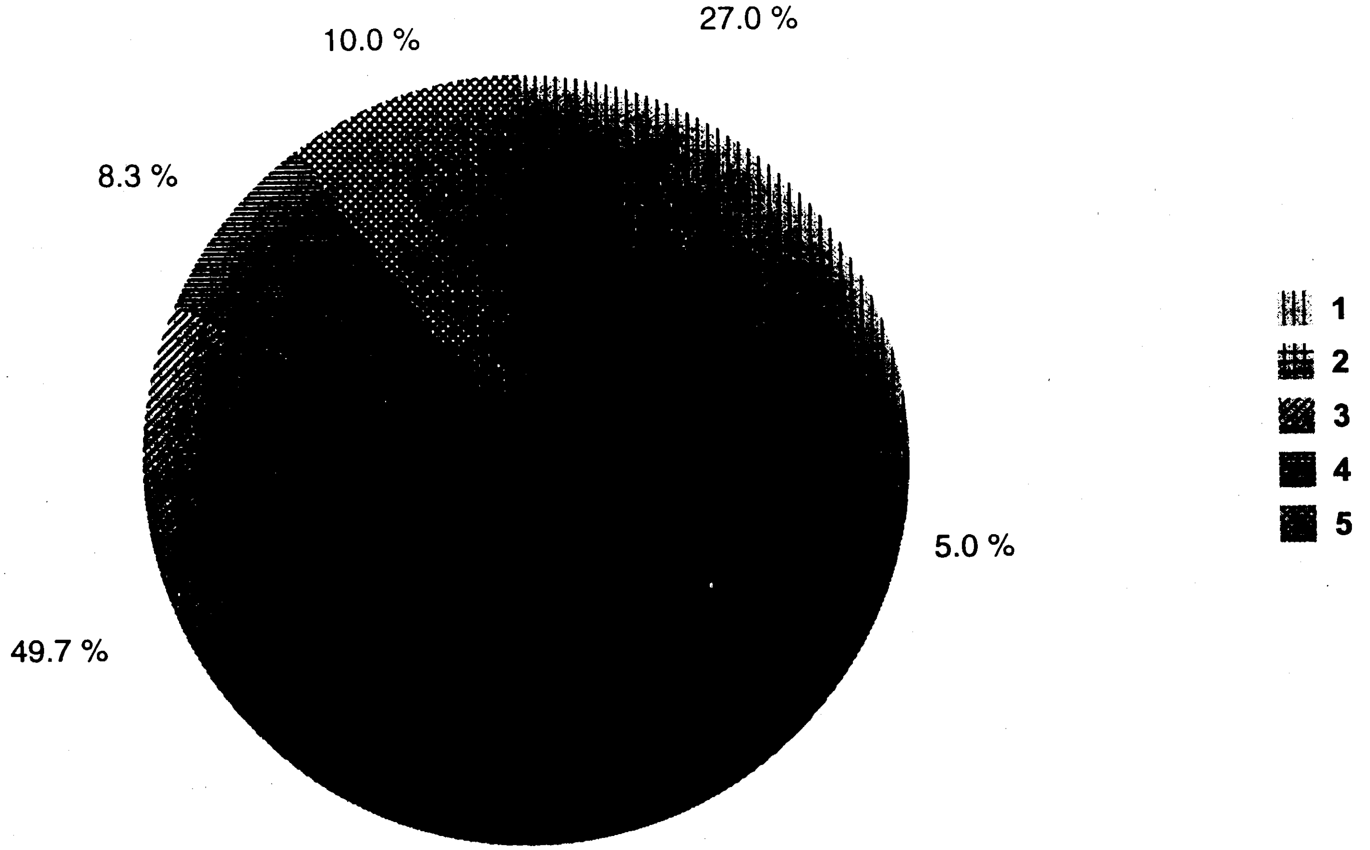

Fig.2d: Pie chart of the cluster populations.

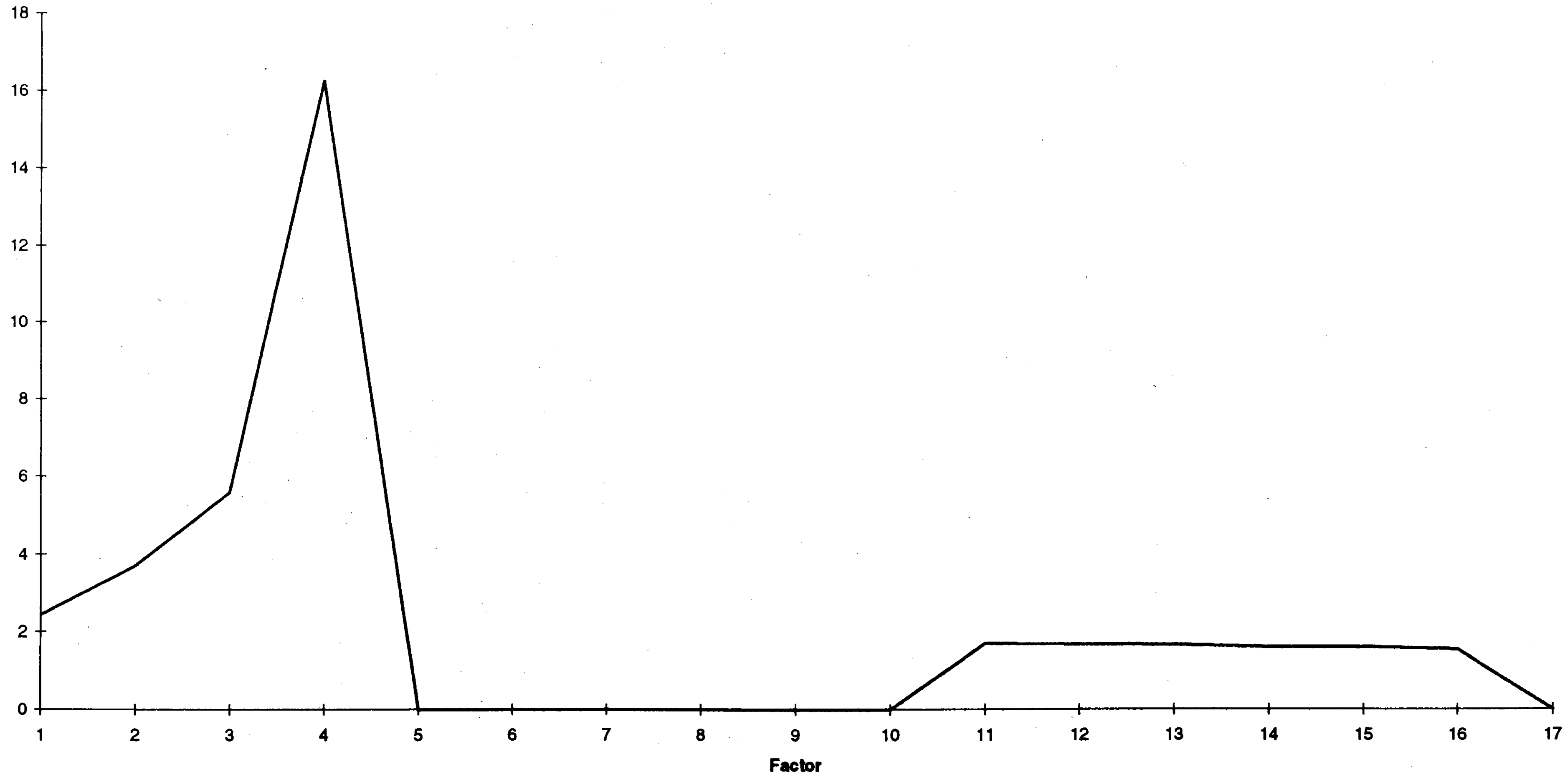

Fig 3a

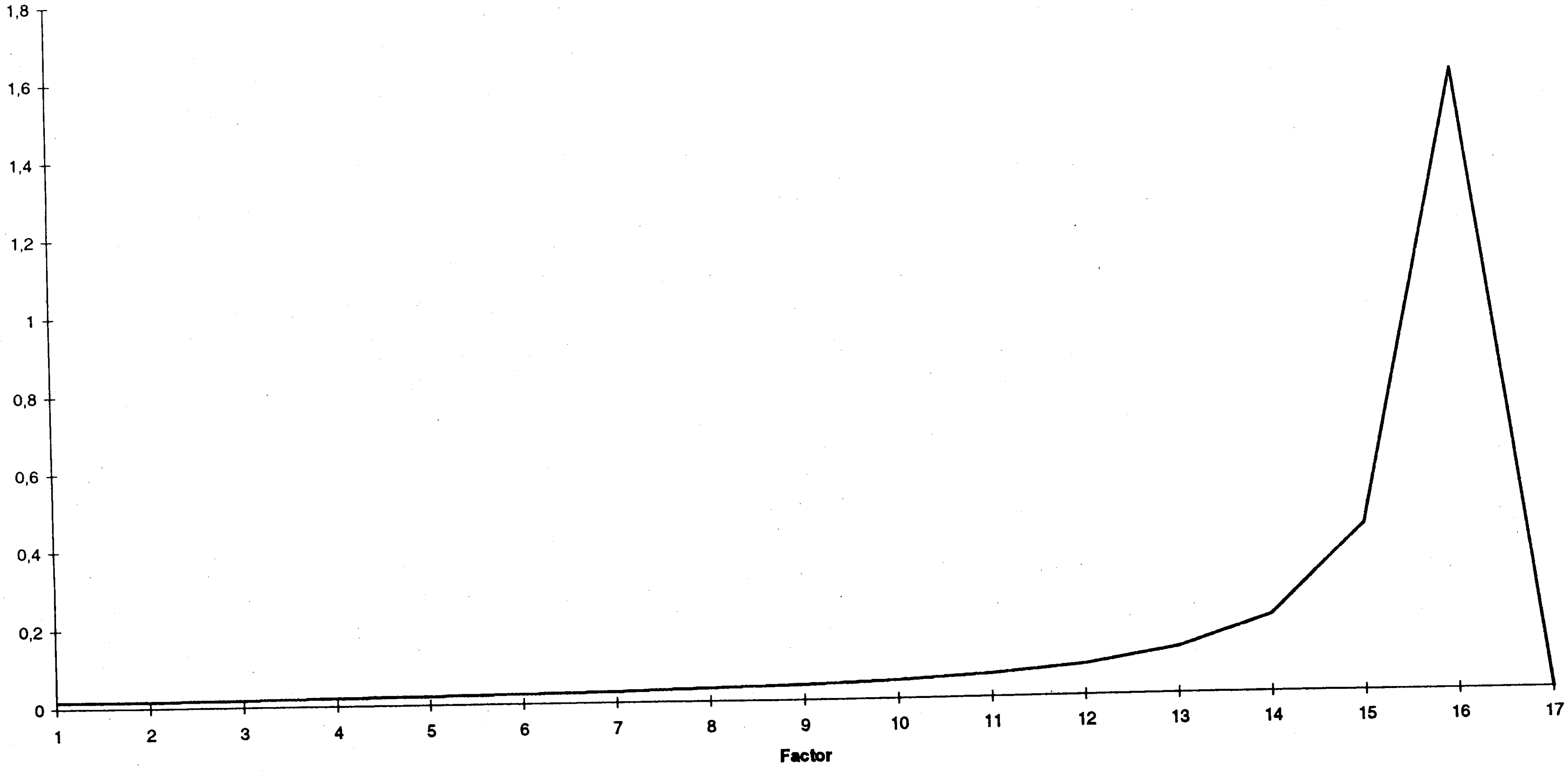

Fig. 3b

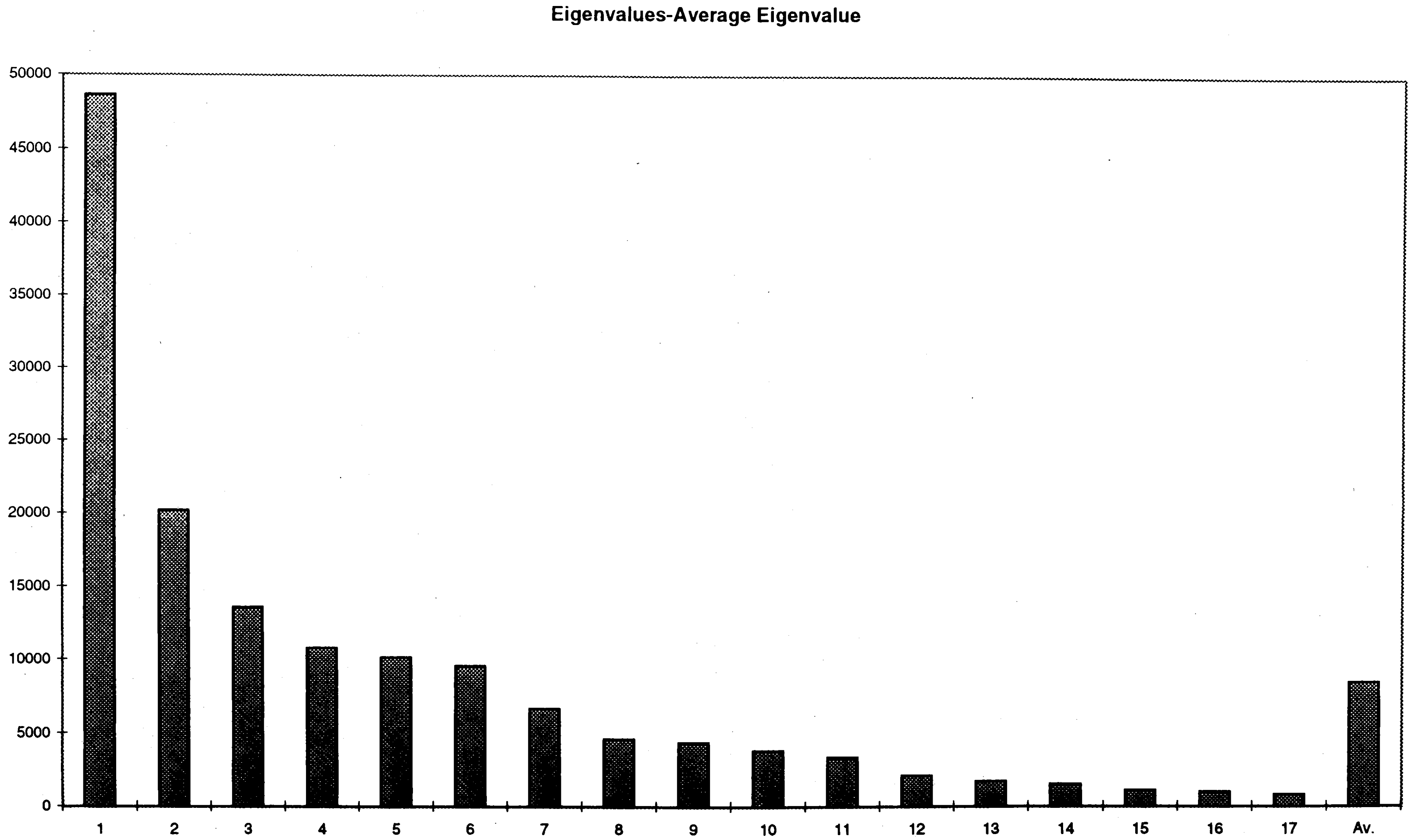
Eigenvalues-Average Eigenvalue
50000
45000
40000
35000
30000
25000
20000
15000
10000
5000
0
1
2
3
4
5
6
7
8
9
10
11
12
13
14
15
16
17
Av.

Fig. 3c

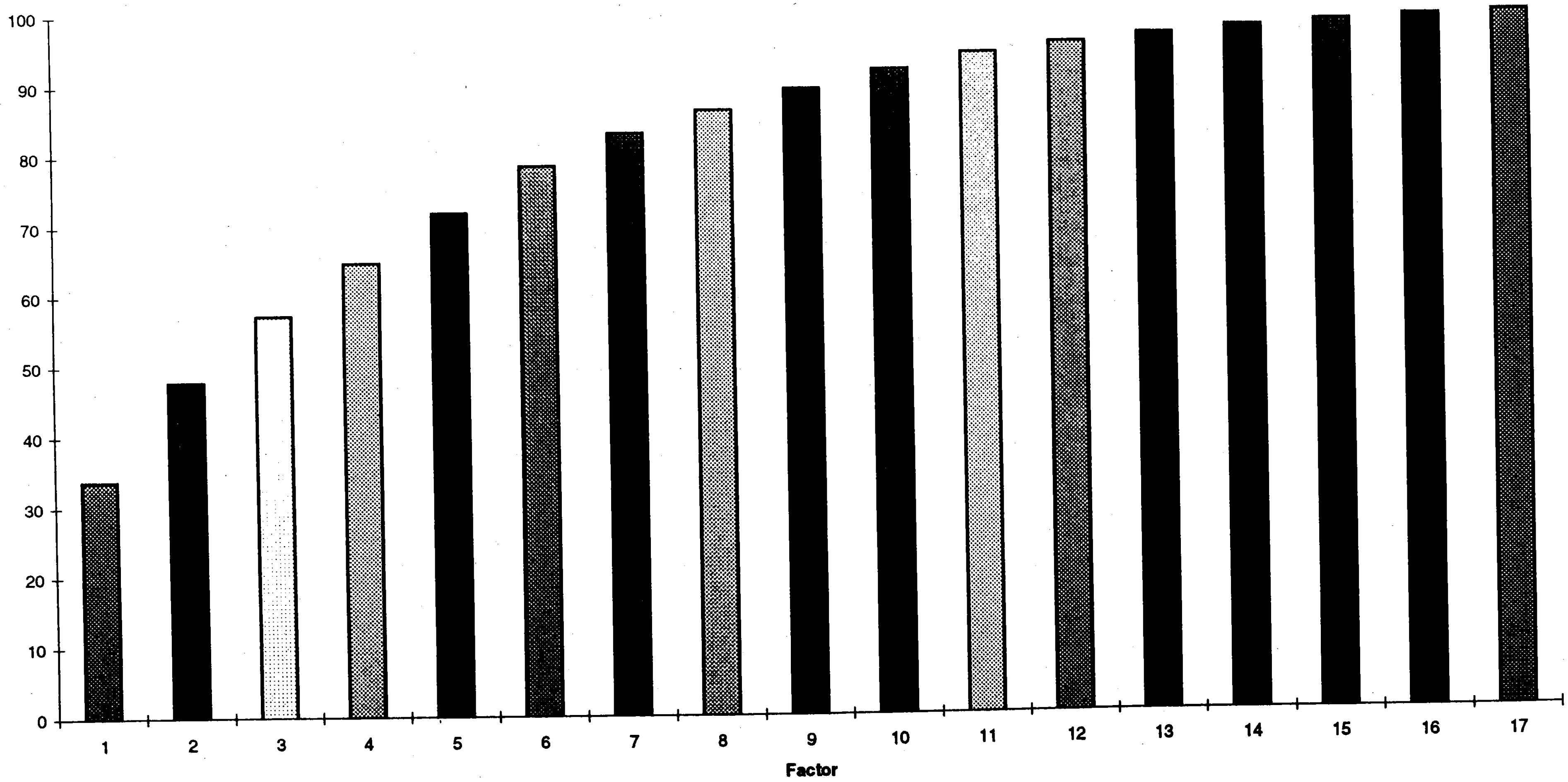
100
90
80
70
60
50
40
30
20
10
0
1
2
3
4
5
6
7
8
9
10
11
12
13
14
15
16
17
Factor

Fig. 3d

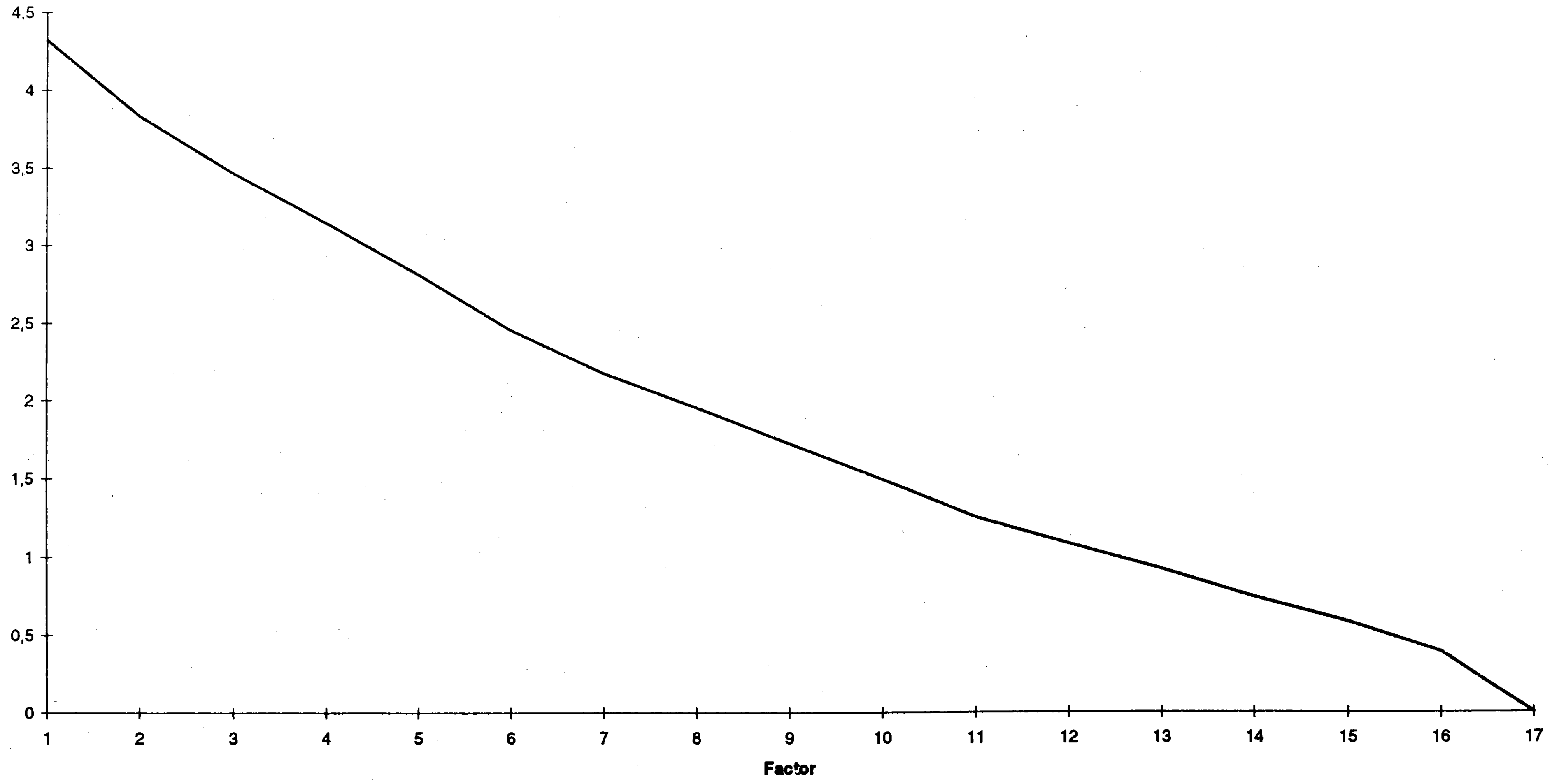

Fig. 3e

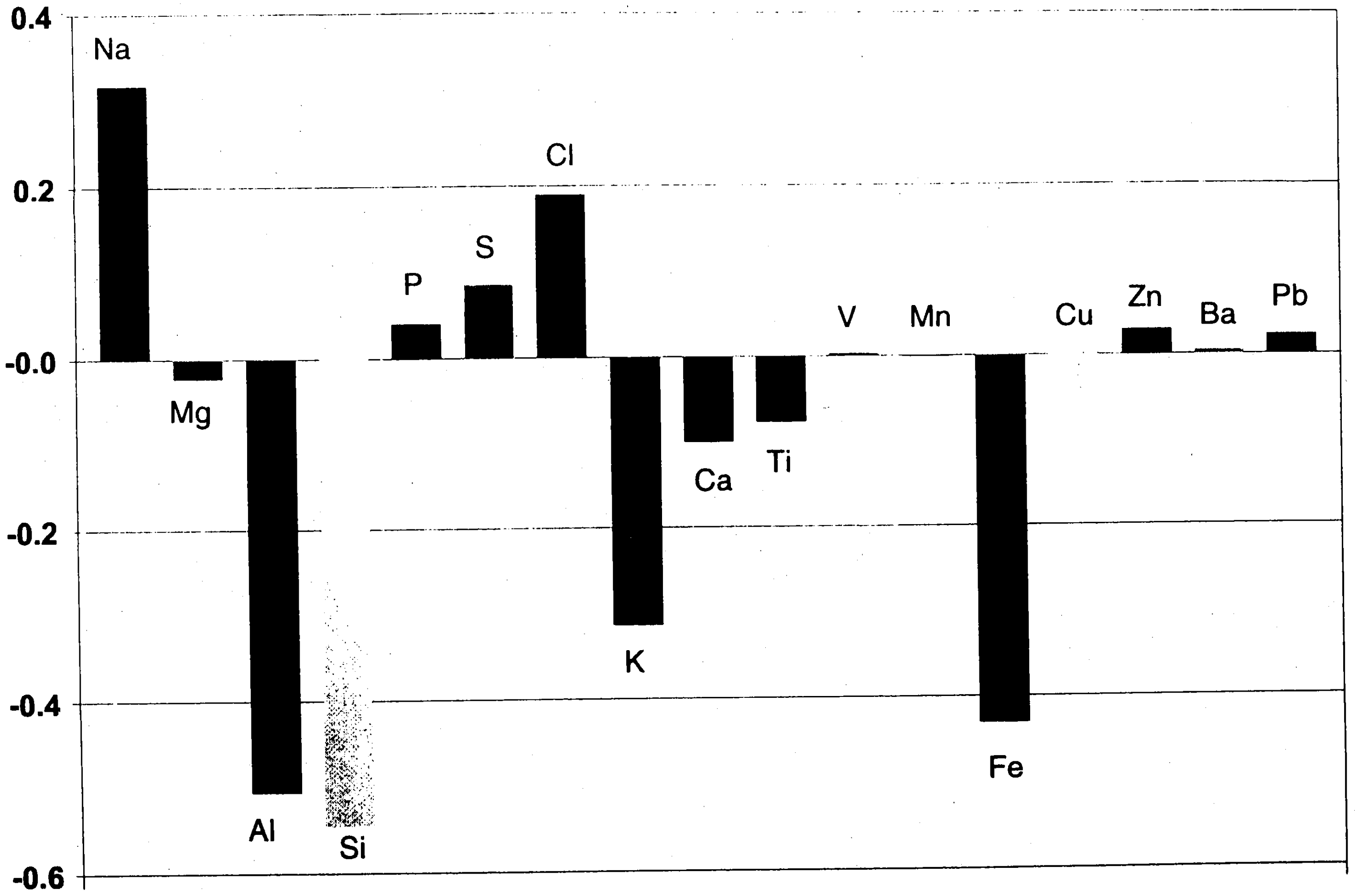

Fig.4a: Factor loadings of factor #1.

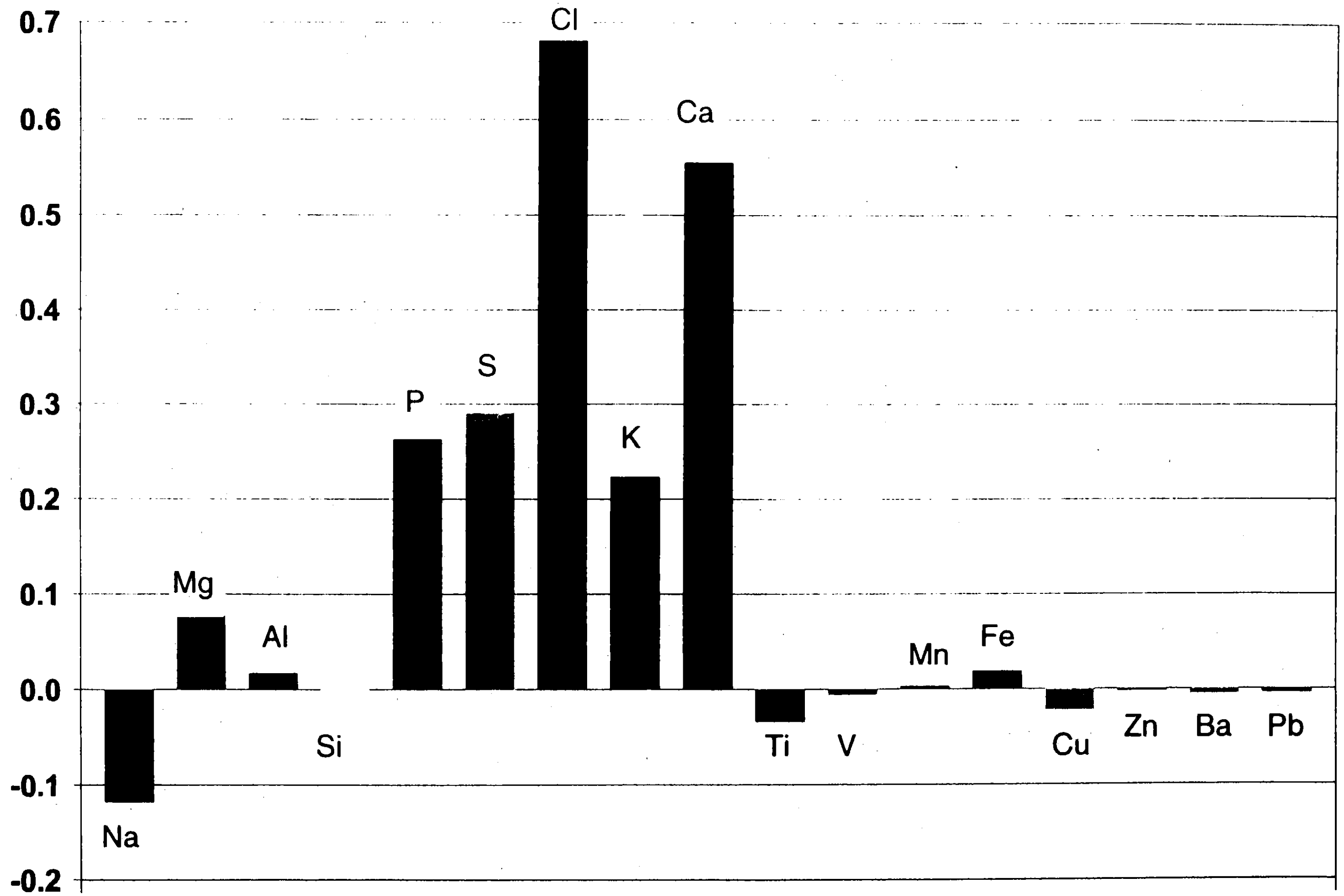

Fig.4b: Factor loadings of factor #2.

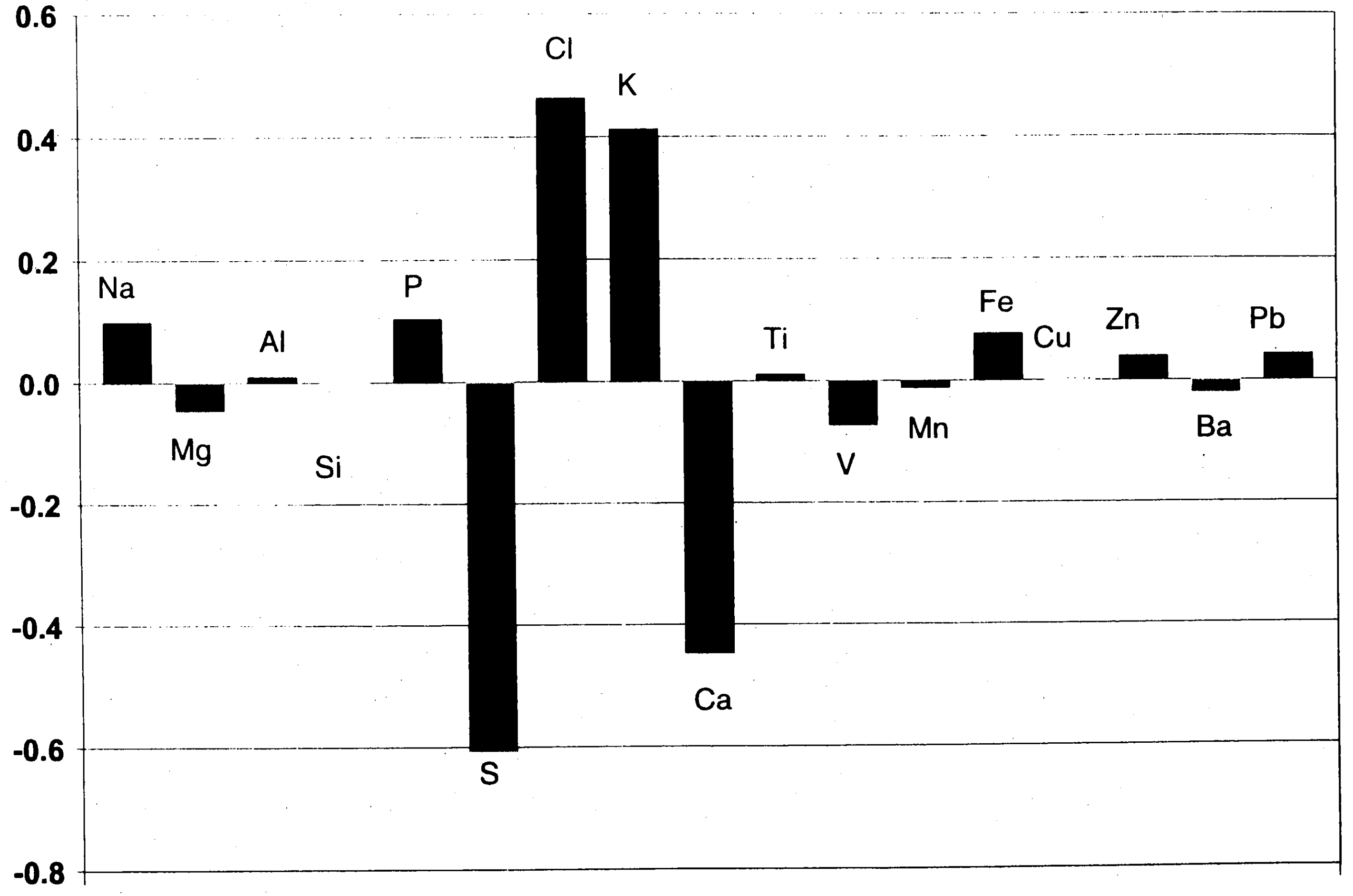

Fig.4c:Factor loadings of factor #3.

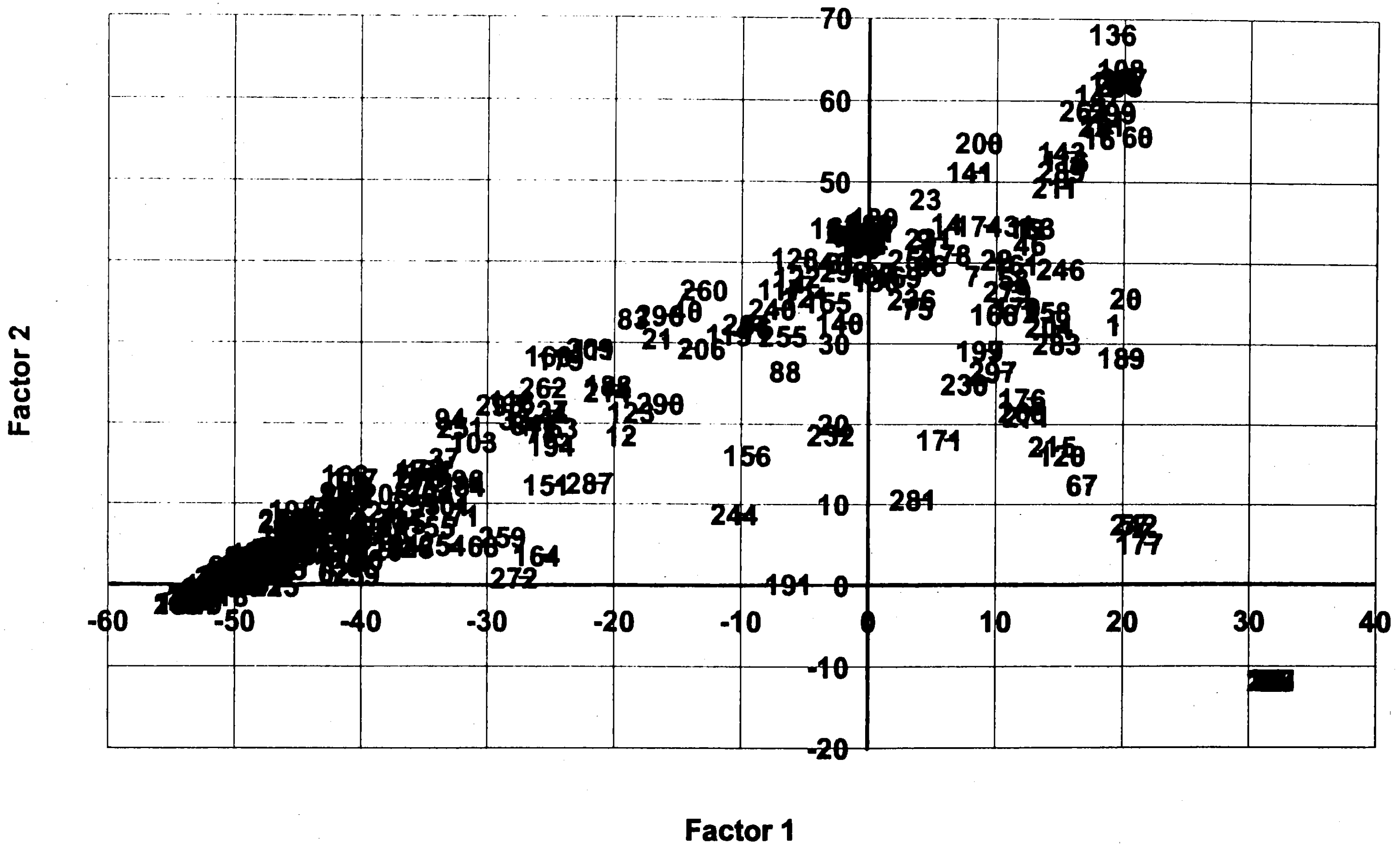

Fig.4d: Factor scores of factors #1 and #2.

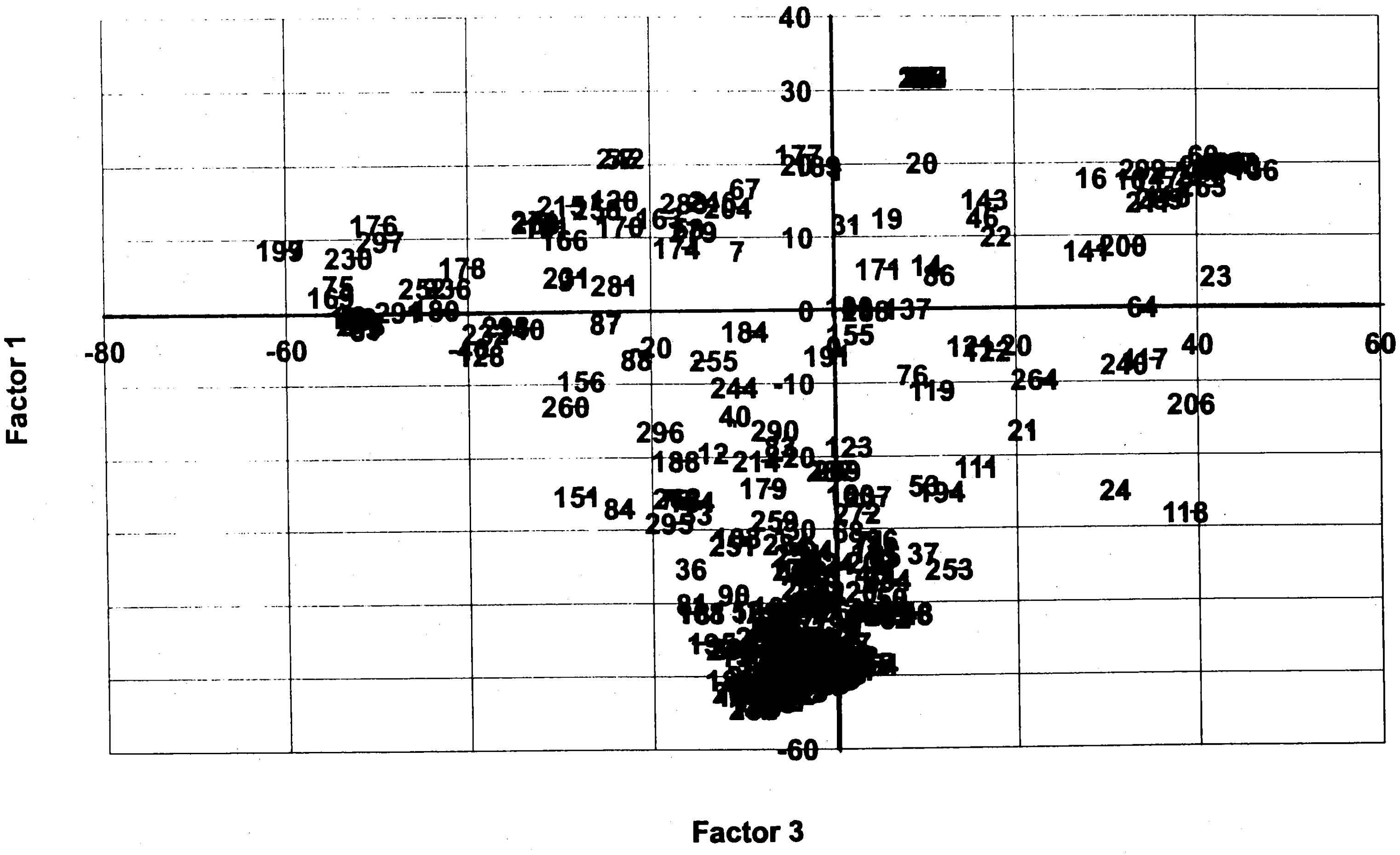

Fig.4e: Factor scores of factors #1 and #3.

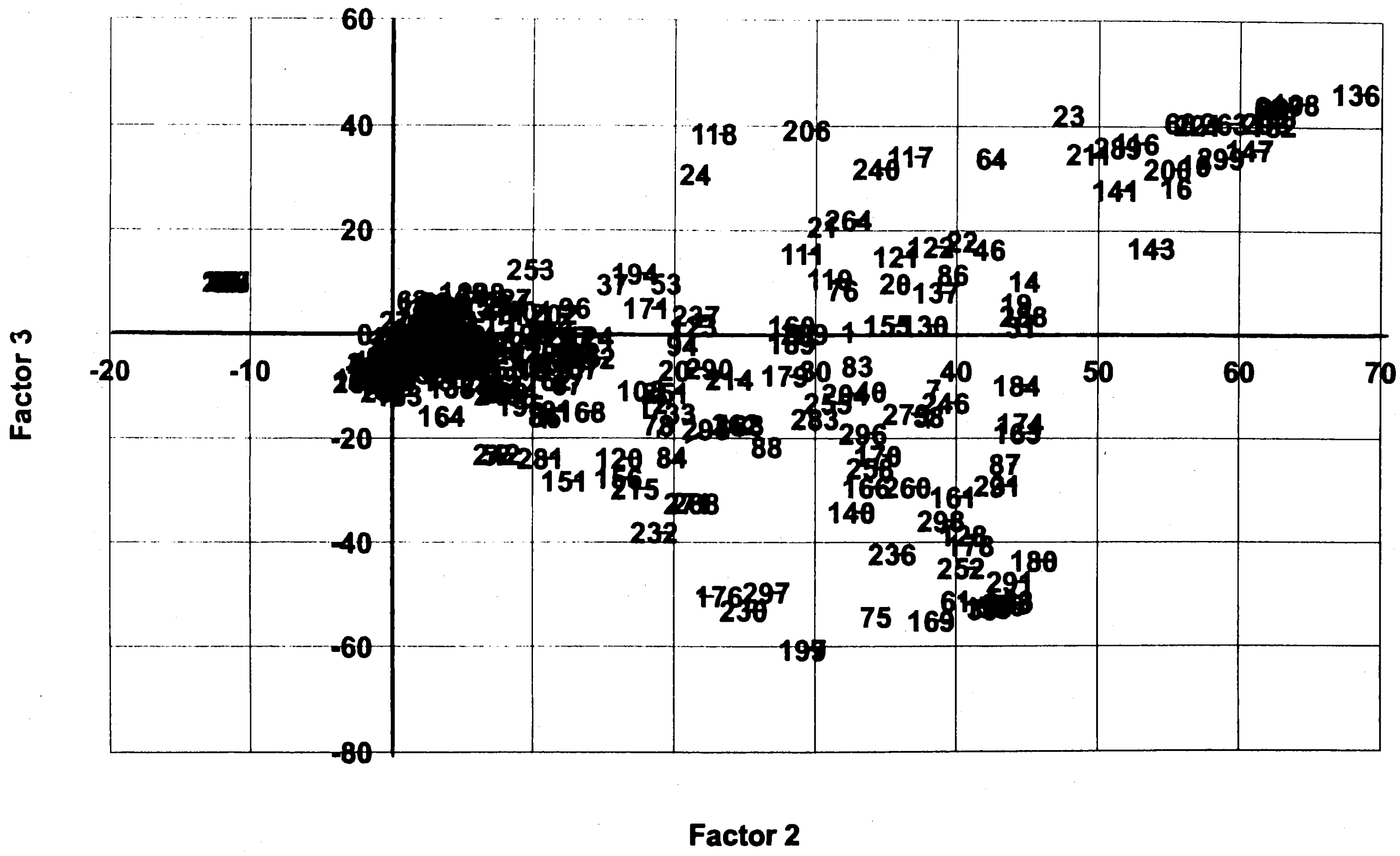

Fig.4f: Factor scores of factors #2 and #3.

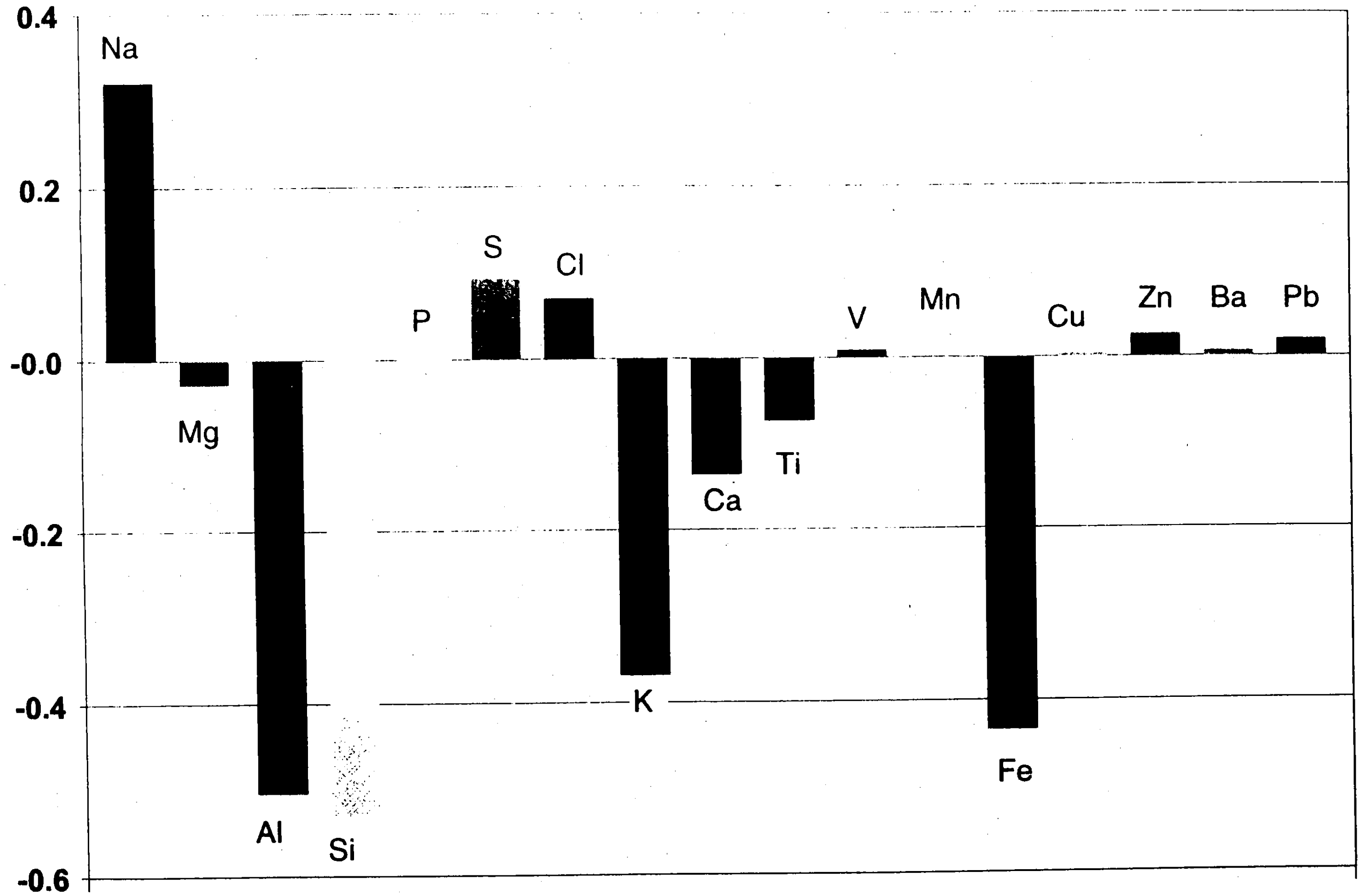

Fig.5a: Factor loadings of factor #1'.

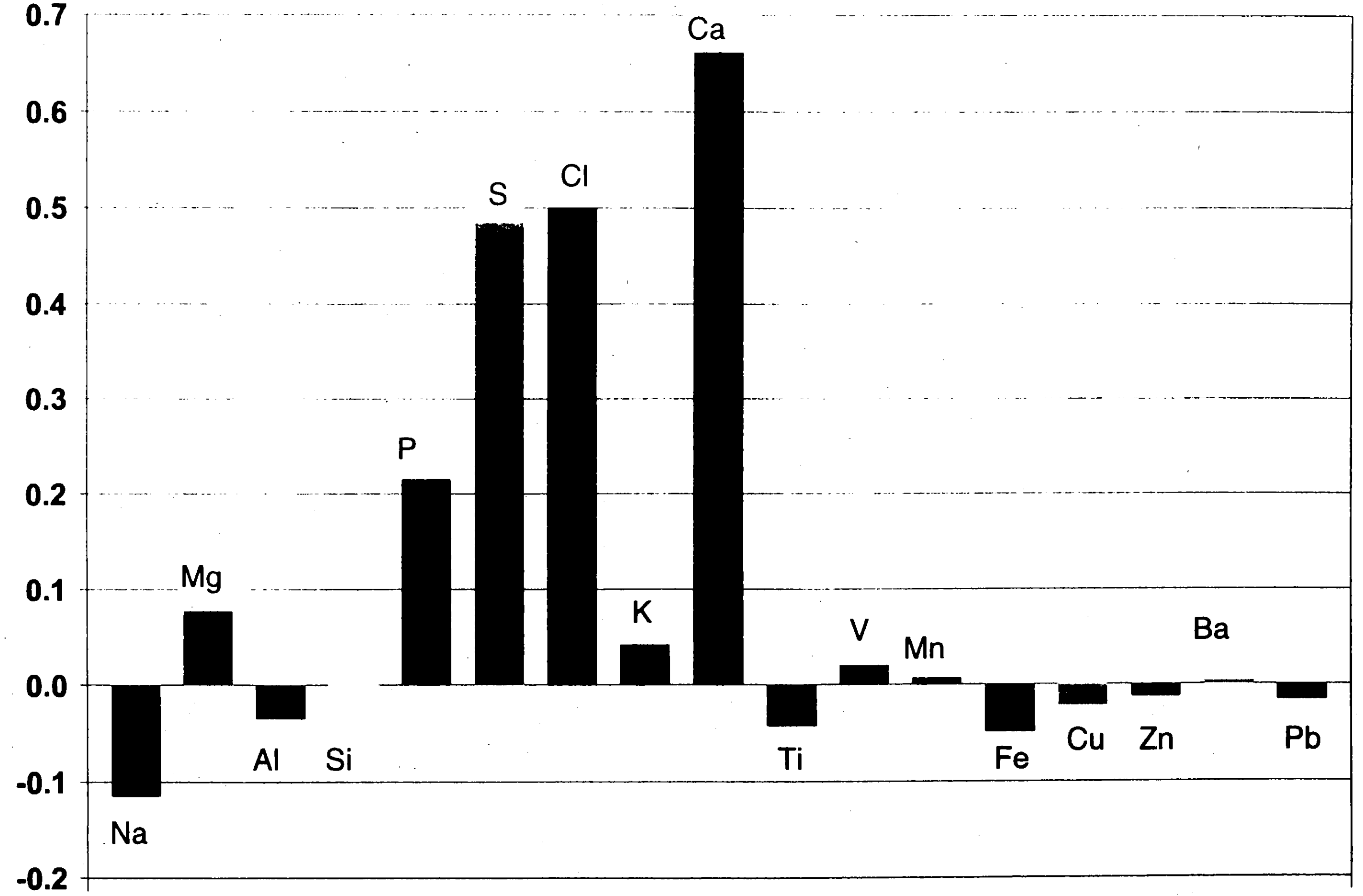

Fig.5b: Factor loadings of factor #2'.

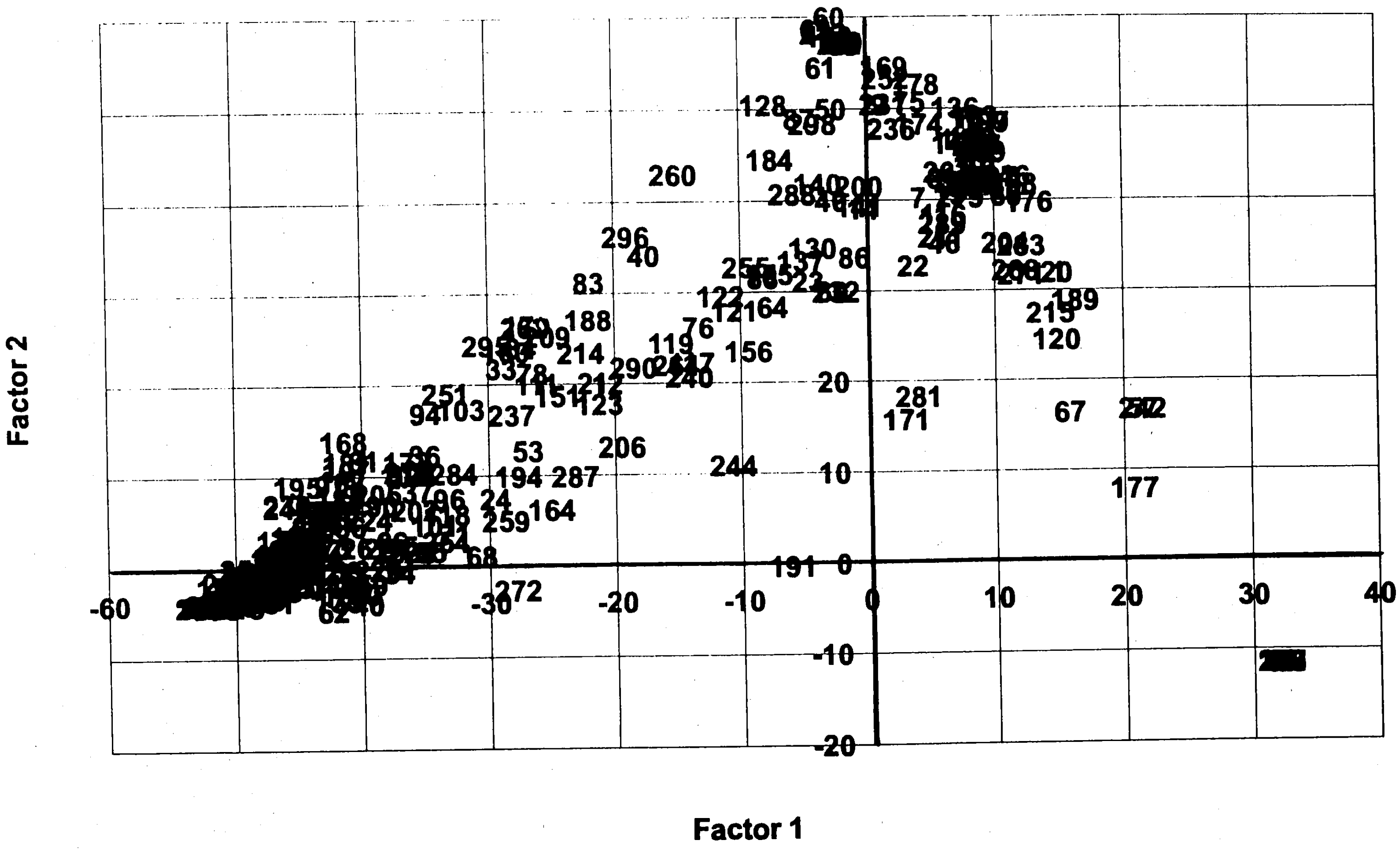

Fig.5c: Factor scores of factors #1' and #2'.

3.b

ENVIRONMENTAL PARTICLES: VOL IV
ATMOSPHERIC PARTICLES

Editors - Roy M. Harrison (University of Birmingham, U.K.) and Rene E. van Grieken (University of Antwerp)

CONTENTS

1. Atmospheric aerosol size distributions (R. Jaenicke, University of Mainz)
   A description of measurement methodology and published data on atmospheric particle size distributions and their interpretation.

2. Atmospheric aerosol sampling (J. Vincent, University of Minnesota)
   A review of particle behaviour and the means by which total or size-selective aerosol samples may be collected.

3. Inorganic composition of atmospheric aerosols (W. Maenhaut, University of Gent)
   A description of analytical techniques, and a review of measurements of bulk composition of inorganic aerosols.

4. Speciation techniques for inorganic aerosol (R. Tanner, Desert Research Institute)
   Methods for identification of specific chemical compounds and chemical associations with emphasis upon the bulk, rather than single particle methods.

5. Modelling the inorganic reaction chemistry of aerosols (A. Wexler, University of Delaware)
   Some reaction processes for inorganic atmospheric particles are well understood. Thermodynamic and kinetic approaches to modelling are reviewed.

6. Vapour/aerosol partitioning of semi-volatile organic compounds
   (R. Hites, University of Indiana)
   The factors which control the partitioning of semi-volatiles are now reasonably well understood. They are outlined, with examples.

7. Dioxins, dibenzofurans and PCBs in atmospheric aerosols
   (K. Jones, University of Lancaster)
   The ambient concentrations congener distributions and atmospheric behaviour are described.

8. Polynuclear aromatic hydrocarbons in atmospheric aerosols
   (R.M. Harrison and D.J.T. Smith, University of Birmingham)
   Ambient concentrations, speciation, atmospheric behaviour and source attribution are described.

9. Particulate elemental carbon in the atmosphere (H. Cachier, CNRS)
   "Black carbon" plays a number of important roles in the atmosphere. Its occurrences and behaviour are reviewed.

10. Source inventories for atmospheric trace metals (J. Pacyna, NILU)
    Rather refined inventories are available for many trace metals. The methodology by which inventories are constructed and the key features for important metals are described.

11. Dry deposition and resuspension processes (author to be agreed)
    A review of knowledge of factors controlling dry deposition and resuspension and the impact of chemical factors is given.

12. Wet processes affecting atmospheric aerosols (G. Jennings, University College, Galway)
    Wet processes include cloud condensation, and precipitation scavenging. These play a major role in the atmospheric cycle and chemistry of aerosols.

13. Influence of atmospheric aerosols upon the global radiation balance (author to be agreed)
Recognition of the importance of aerosol-mediated scattering and absorption processes in climate change has developed recently. The physico-chemical form of the aerosol is a key factor.

14. Measurement of aerosol heterogeneous chemical reaction rates
(D. Worsnop, Aerodyne Research)
The last five years have seen great advances in techniques for measuring the rates of heterogeneous atmospheric chemical reactions. The available techniques and data are reviewed.

15. Structural heterogeneity of airborne particles (R. van Grieken, University of Antwerp)
Methods of investigation (surface analytical methods; single particle analysis); environmental impact of particle surface (e.g. condensation scavenging; health effects).

16. Condensed water aerosols (J. Heintzenberg, Leipzig; abstract not yet received)
Fog and clouds; ice particles; sampling and analysis; surface properties; deposition of fog and cloud droplets.

17. Primary biological aerosol particles (S. Mathias-Maser, University of Mainz)

18. Formation of aerosol particles from biogenic precursors
(C.N. Hewitt, Lancaster University)

Structural heterogeneity within airborne particles

Jasna Injuk, Lieve de Bock and René Van Grieken
Department of Chemistry
University of Antwerp (U.I.A.)
B-2610 Antwerp, Belgium

Index (Key words):

Contents list:

1. INTRODUCTION

Particle characterization is of a great importance for a wide variety of fields related to technological progress and environmental pollution, and at the same time one of the most demanding issues of microbeam analysis. Through the availability of sophisticated image analysis systems and associated softwares, direct particulate measurements, at a microscopic scale, are nowadays becoming more and more important.

The number of studies of environmental particles has expanded rapidly during the last 20 years, as a result of technological advances in instrumentation and in improved knowledge of electron, proton and ion optics, and electronics.[1] Various micro-beam techniques like electron probe X-ray microanalysis (EPXMA), scanning electron microscopy (SEM-EDX), scanning proton microprobe (SPM), laser microprobe mass analysis (LAMMS), electron energy-loss spectroscopy (EELS), secondary ion mass spectrometry (SIMS) and Auger electron spectroscopy (AES) have proven their success in the field of aerosol research. Such microanalyses can reveal whether a specific element or compound is uniformly distributed over all the particles of a population or whether it is a component of only a specific group of particles. Even more, the elemental lateral and depth distribution within a particle can be inferred. However, each of the above techniques is limited by either poor resolution, or high detection limits, or poor low Z-elemental detection or lack of quantization.

The present Chapter is an attempt to present exclusively only the compositional heterogeneities within a single aerosol particle. Some examples of heterogeneity investigations from the literature and from recent research by the authors are given. Also, based on a literature study, the importance of particle surfaces with respect to toxicity and atmospheric reactions are outlined. The analysis of whole individual aerosol particles will not be treated since a chapter was addressed to it in a previous book of this series.[2] Rather, a brief overview will be given of the techniques, that have proven, so far, their success in studying the chemical heterogeneities within individual particles, in terms of quantification, elemental mapping, lateral and depth resolution and detection limits.

2. MICRO-ANALYSIS TECHNIQUES

2.1. Electron probe X-ray micro-analysis and scanning electron microscopy

In EPXMA as well as SEM, a nanometre sized electron probe generates various signals upon sample interaction. The detection of the emitted characteristic X-rays by wavelength- or energy-dispersive spectrometers (WDX and EDX, respectively) as well as the backscattered electron image provide compositional information on the sample. Morphological studies are based on the detection of backscattered and secondary electrons. The differences between EPXMA and SEM-EDX have been reduced over the years to only a slightly different instrumental set-up, so that both techniques are nowadays to some extent used for chemical as well as morphological studies.

In spite of their unfavourable detection limits (0.1%), EPXMA and SEM-EDX are considered to be the most popular non-destructive micro-analytical techniques. Part of this popularity can be attributed to the availability of statistically relevant information, since the automation of these techniques allows the analysis of several hundreds of particles in a few hours time with a relative accuracy of about 5% and a lateral resolution of 0.1-5 µm. The in-depth resolution of EPXMA/SEM-EDX is about 0.5-5 µm. Manual analysis, on the other hand, offers the possibility of detailed morphological studies and of element-mapping within individual (giant) aerosol particles.

A variety of programs have been developed over the years to solve the problem of quantisation with electron beam instruments. In the field of single particle analysis, the small dimensions of the particles, leading to uncertainties in the determination of the interaction volume, together with a lack of suitable standards still make the quantitative analysis rather difficult. However the recent CITZAF correction procedure package, proposed by Armstrong,[3] claims to provide reasonable quantitative results in the analysis of unconventional samples, such as individual unpolished particles.

Other specific problems are being solved by the new generation of scanning electron microscopes which permit probing down to low-Z elements, like C, N and O, analyse any sample wet or dry, insulating or conductive[4] and offer a higher lateral resolution while working with a high-magnification secondary electron image.[5] Moreover they provide much enhanced image analysis capabilities.

2.2. Electron energy loss spectroscopy

By combining electron spectroscopy and transmission electron microscopy, the analytical power of EELS is coupled with the ability to select, image and obtain diffraction patterns from small areas (<0.01 μm lateral resolution, 0.01-0.1 μm in-depth resolution). Apparatus for EELS has recently become commercially available and until now very few publications have dealt with individual particle analysis.[6-8]

The principle of EELS is based on the theory of electron-solid interactions. As the electrons of the beam (initial energy of E_0) interact with electrons of the atoms present in the sample, they can loose an amount of energy, ΔE, characteristic for these atoms. The initial electrons will leave the sample with reduced energy, $E_0 - \Delta E$. Thus the electron energy-loss spectrum represents the graphical display of the energy, ΔE, lost by the scattered electrons and its corresponding intensity. Accordingly, EELS detects directly the electron beam interaction with the atoms, which in turn, produces inner shell ionizations or the excitation of oscillations of the electrons in the valence band of a solid (plasmon oscillation). The transmission signal consists of electrons in an energy range from E_0 down to a loss of several thousand eV. After dispersion by an energy analyzer, electrons with the same energy loss are focused on the same point. By scanning this dispersion plane over a detector, the intensity I(E) of the transmitted signal can be plotted as a function of energy-loss. Various interaction processes can be related to the properties of the specimen by examining the features of a typical energy-loss spectrum.

Just as for X-ray spectroscopy, the characteristic absorption edges are of major importance for the microanalytical approach of EELS. The rapid increase in the spectrum intensity at the edge makes it fairly easy to distinguish among the elements. EELS can observe edges of all elements from Li to U (they have at least one edge in the energy loss range of 0 to 2000 eV that can be used for analysis). One complication in energy loss spectra is the variation in edge shapes that can be observed.

Quantitative analysis is simply conversion of the measured number of inner-shell excitation events to an atomic concentration. Quantification without the use of reference materials can be performed only for very thin samples of uniform thickness and homogeneous element distributions.

The technique has some advantages compared to X-ray analysis like: low-Z elements can be detected with a high sensitivity, the detectable mass is much lower and information about the electronic state and chemical bonding of the sample can be provided. EELS has been used to identify quantities of less than 10^{-20}g and concentrations of less than 100 ppm of elements such as P and Ca in an organic matrix. However, the accuracy of quantitative analysis is often no better than 20%. The main sources of error are in the background subtraction and inner shell cross section determination, in lens aberration and radiation damage problems.

2.3. Auger electron spectroscopy

AES is a surface sensitive technique in which the electrons, emitted by a radiationless transition from an excited state, produced upon impaction of an electron beam, are investigated. Since the energy of the Auger electrons is purely a function of the atomic energy levels and there exist no two elements with the same set of atomic binding energies, AES leads to direct element identification. The acquired Auger spectra reveal, besides the small Auger peaks, also other peaks due to elastic scattering, backscattering of primary electrons, etc., making the identification and location of the peaks of interest sometimes very difficult. To overcome this problem, the Auger spectra are usually smoothed, to reduce the noise in the spectrum as well as differentiated to remove the continuum. The AES technique is particularly useful to the detection of low Z-elements ($Z < 13$) because, for heavier elements, the emission of an X-ray photon or so called fluorescent decay, becomes the more significant relaxation process. The penetration depth is in the range of 2 - 10 atomic layers for the typical energies (50-2000 eV) used in AES. Elemental detection limits lie in the range of 0.1 to 1% atomic within the analytical volume, and the variation in sensitivity between the low-Z elements is less than a factor of 10. Sputter-cleaning of the specimen surface and in-depth profiling is achieved by an Ar^+ ion beam. Rastering of the electron beam over the sample surface becomes available in Scanning Auger Microscopy (SAM).

Although this technique appears to be very useful for investigating surface coatings on environmental particles, its low sensitivity to high Z-elements, its low detection power and the charging effects caused by non-conductive samples, are still major drawbacks for its frequent application in this field.

2.4. Laser microprobe mass spectrometry

LAMMS was originally designed for the analysis of biomedical samples, especially thin sections, with high lateral resolution and extreme detection sensitivity (10^{-18}-10^{-20} g). Since then, various instrumental set-ups were developed for different analytical purposes.

The principle of LAMMS is based on the excitation of a microvolume of the sample to an ionized state by a focused laser beam. The basic components of the instrument are a laser system, an optical instrument and a mass spectrometer. The ionized part of the evaporated material consists of positive and negative elemental and molecular ions. Usually a time-of-flight mass spectrometer separates the ions with different mass-to-charge ratios according to their flight times. The analytical information is derived from mass spectrometry of these ions.

Quantification by LAMMS is not yet straightforward. The way things stand now, since no theoretical model can predict the ion yield for a specific specimen as a function of target and laser beam parameters, quantification is based on the use of empirical procedures mostly involving standards. As it is very troublesome to determine the sampled mass, quantification must always rely on the use of either internal reference elements or standard samples which closely resemble the unknown one. Particle standards can be prepared by nebulization of aqueous solutions or by crushing material to micrometer size. Once suitable standards are available, quantification can be carried out with calibration curves or with relative sensitivity factors. The precision for quantitative particle analysis is at best 20-40% for elements of low ionization potential, with an accuracy of a factor of 2. For elements of high ionization potential, it worsens up to 80%. The best precision is obtained for thin samples: between 15-30% for all elements.

LAMMS is in principle capable of detecting all elements and organic compounds and of generating stoichiometric information. The spatial resolution of the analysis is 0.5-3 μm, the in-depth resolution is >1 μm and the detection limits are of a few ppm.

Since physicochemical properties of airborne particles have been stated to control different atmospheric processes, the necessity of analysing single airborne particles in their native state, i.e. by on-line analysis, evolved. Off-line analysis methods are often limited to the non-volatile part of the particle and, due to sample-surface interactions, chemical alterations of the sample can occur leading to a possible loss of valuable information. In situ characterization of the chemical composition and size of individual airborne particles becomes available by performing on-line laser microprobe mass spectrometry (on-line LAMMS) or rapid single-particle mass spectrometry (RSMS). Different experimental set-ups have been developed over the years[9-21], but all of them are based on the same principal of laser desorption/ionization and analysis using mass spectrometry. Applying this technique aerosol particles are collected immediately into the mass spectrometer. The scattered radiation obtained from the interaction of each individual aerosol particle with the He-Ne laser beam reveals information on the particle size and triggers the laser which vaporises the particle and ionises the fragments. For each single particle a complete mass spectrum is recorded with a time-of-flight mass spectrometer. Further research in this field will improve and optimize the different aspects of the on-line particle analysis. However recent developments by Prather et al.[15] revealed already the capability of characterizing simultaneously the size and chemical composition of individual aerosol particles down to 50-100 nm in real time. Reents et al.[20] reported even on the ability to detect particles as small as 20 nm using a different instrumental configuration. Moreover the simultaneous detection of positive and negative ions from the same airborne particle by real-time LAMMS was accomplished for the first time by Hinz et al.[21]

2.5. Secondary ion mass spectrometry

In SIMS, an ion beam (O_2^+, O^-, Ar^+, Cs^+, Ga^+, ...) or molecules generated in a duoplasmatron, with an energy between 1-20 keV, are used to bombard the surface of a solid sample. The primary ions set up a collision cascade and are implanted into the solid. The penetration depth (about 10 nm) is determined by the energy and mass of primary ion and the composition of the material. Due to the ion bombardment secondary particles such as ions, neutrals and clusters are emitted from the surface. This process is referred to as sputtering. The information depth (the depth where most of the secondary ions are emitted from) is of the order of one to several nanometres. The positive or negative secondary ions are extracted into a mass spectrometer (quadrupole, magnetic sector, time-of-flight) where they are separated according to their m/z ratio. After mass separation the ion current is recorded with a suitable detector. Different types of information can be obtained such as the surface composition, depth distribution and lateral distributions. A mass spectrometer provides elemental coverage from H to U, isotopic characterization, and detection limits of 10^{-15} to 10^{-19} g. Because of the continuous erosion of the sample surface by the ion bombardment, depth profiling of elements becomes possible. A depth resolution in the order of a few nanometres can be achieved. Most SIMS instruments are also capable of visualizing the lateral distribution (<1 μm) of the elements in the form of ion images. By the combination of ion images and depth profiling, a three-dimensional analysis of the sample surface becomes possible.

SIMS offers special capabilities for particle analysis. Compositional heterogeneities in the composition in single particles are frequently observed. SIMS, as a micro-analysis technique, is capable of obtaining signals from a minimum sample volume of 0.001 μm^3. Depth profiling can be successfully applied to individual particles, although irregular topography of particles can degrade the depth resolution. Quantification is possible by the use of relative elemental sensitivity factors estimated from analysing standard samples under conditions identical to the unknown sample. The detection limit is about 1 ppm, with an accuracy of 10%.

plannery lecture

2.6. Scanning proton microprobe

In SPM an intense radiation of MeV heavy ions is scanned across the sample to reveal microstructures in a wide range of materials. Heavy ions are attractive for single particle analysis since they penetrate deep into the material without being much deflected (the microbeam is almost free of scattered particles). Development of a focusing device for MeV ions did not create much interest in ´70s, but during the ´80s and ´90s nuclear microprobes have come into widespread use. One reason might be that commercial systems have become available.[22] It is only recently that SPM was applied in environmental science on a single particle level. A reason for this was the requirement of a micron or sub-micron stable beam for several hours of radiation, a bright and stable ion source and a fast and flexible data acquisition and analysis system. Today, there are only a few nuclear microprobes in the world which meet these requirements were the successful analyses of individual particles can be carried out.

Several analytical techniques could be implemented in the SPM, but µ-PIXE (micro-proton induced X-ray emission) is the most important one, due to its large reaction cross sections. SPM provides concentrations of 20-30 elements at ppm levels in small samples of a few µm in diameter and weighing only a pg or less. As a consequence, the absolute mass detectable by SPM is in the order of 10^{-17} to 10^{-18}g. This puts SPM in a very unique position of being able to provide trace element concentrations on a single particle level and at the same time retaining a high spatial resolution (from 0.5-10 µm). With its unique ability to simultaneously use several complementary nuclear analytical techniques like e.g. RBS (Rutherford backscattering spectrometry) and PIGE (particle induced gamma-ray emission), it can provide highly qualitative analytical data for almost all elements of periodic table. As the proton beam goes through the sample and is collected in a Faraday cup, quantification is relatively easy to perform, with an accuracy of 10-20%.

3. ELEMENTAL HETEROGENEITY INVESTIGATIONS WITHIN SINGLE AEROSOL PARTICLES

The recent recognition of aerosols and e.g. their capacity to affect the global climate, immediately initialised a great demand for a high quality data on fine aerosol concentrations from the entire world. Many micro- and trace analytical methods have already produced a very good data base on background aerosol concentration worldwide, but on the contrary, not much attention was focused on aerosols' internal heterogeneity studies. By focusing attention on exclusively one individual particle, detailed information can be achieved for aerosols with respect to: (a) their "life cycle" and evolution (b) their behaviour during physico-chemical interactions with the transporting medium (e.g. gas-to-particle conversion or coagulation processes), (c) the enrichments at the particle surface, (d) distribution of constituents with depth in the particle and (e) the particle size distribution. In the process of source identification, the analysis of single aerosol particle has an indispensable value and this is where single particle techniques can make a significant contribution.

3.1. Anthropogenic aerosols

Elements of anthropogenic origin are mainly released to the atmosphere in gaseous form as a result of fossil fuel combustion. Such elements (e.g. S, Cr, Pb, Br) are present in the submicrometer aerosol fractions and they usually form a thin film on larger particles of natural origin (e.g. Pb or Ti layer on a gypsum particle or S shell around a quartz particle). The bioavailability of such elements largely dependent on their concentration profile.

Anthropogenic aerosols, especially sulfates and soot particles, were found to be significant in the context of climate changes. The global increase of cloud reflectivity due to anthropogenic aerosols was estimated to be 2%.[23]

3.1.1. Fly-ash particles

Fly-ash particles have been one of the most widely studied types of airborne pollutant matter. It is well known, that these particles are of a complex structure and morphology and a broad size range; their surface layer is of special interest, since it contains certain toxic trace elements, often in a soluble form. Thus, fly-ash particles interacting with biological systems may produced, as it will be further discussed in more details, enhanced concentrations of toxic species at the point of direct contact.

Over the last 20 years the structure of fly-ash particles has been the subject of different studies involving various analytical techniques like in e.g. EPXMA, SEM-EDX, LAMMS, SIMS, SPM and AES.

About twenty years ago Linton et al.[24,25] demonstrated the elemental surface predominance in coal fly-ash particles of elements like, Li, Na, S, K, V, Cr, Mn, Fe, Tl and Pb. This was attributed to the condensation of species previously volatilized in the high temperature combustion zone of a particulate emission source. Potentially toxic elements like Pb and Tl were present at bulk concentrations of only 620 and 30 ppm respectively, while their surface concentrations were 4% and 4500 ppm, respectively. The predominant surface region for such elements was substantially soluble, thus being very likely accessible to the environment either by washout processes in the atmosphere or the ground water or by solubilization with biological systems. This problem was further investigated by Cox et al., [26] who also applied SIMS to characterize single fly-ash particles in terms of intra-particle concentration variations. A downward trend with depth for trace elements as Tl, Pb and U, as opposed to the flat profiles for Si and Ti, indicated that the observed profile shapes were not an artifact generated by loss of analytical volume or change in total yields.

In 1983, Vis et al.[27] scanned systematically, by a proton micro beam, fly-ash particles from the magnetic fraction, to find elemental distributions across their cross sections. In general, magnetic particles were characterized by high surface concentrations of K, Ti, V, Cr and S, while the Fe distribution showed a maximum at the centre of the particle. Experimental evidence on surface enrichments of toxic elements in the 10 μm and less size-fraction of fly-ash was reported by Jakšić et al.[28] in 1991. Based on elemental analysis, two main groups were recognised: alumino-silicate particles and Ca-rich or Fe-rich particles with a high level of Ti. Line scan across the particle diameter showed that for Ca- and Fe- rich particles, most of the elements appeared to have a homogeneous distribution; no significant surface or core enrichment was found. Contrary, the alumino-silicate fly-ash fraction was characterized by a compositional heterogeneity. Most of the analyzed particles formed an aggregate with usually one or a few larger spherical alumino-silicate particles surrounded by other submicron (usually Ca-rich) particles. An areal scan across one alumino-silicate particle, showing a complex surface structure is given in Fig 1. How an elemental composition affects the electrical properties of fly-ash particles was demonstrated by Cereda et al.[29] About two hundred particles, in the 1-5 μm size range, collected with high collection efficiency (99.8%) at the inlet and outlet of the electrostatic precipitator of a coal-fired power plant, were analyzed and compared. An increasing concentration trend of trace elements with decreasing particle size was clearly observed. Particularly in the case of S, enhanced concentrations, between 1600 to 2300 ppm, were found at the electrofilter outlet compared to the S "inlet values" of 500 to 1300 ppm. This result was accounted for by the condensation of sulfates on the particle surfaces when particles are passing through the electrofilter. The electrostatic precipitator acts selectively with the particle composition: particles with higher concentrations of minor and trace elements are more likely to escape the electrofilter. The analysis of particles from the inlet of the precipitators showed a non-uniform distribution of minor (P, Ca, Ti, Fe) and trace elements (S, Mn, Ni, Cu, Zn, Ga). These results reflected: a poor degree of coalescence upon combustion, in the case of minor elements, and surface segregation and evaporation-condensation mechanisms, in the case of the trace elements.

According to Van Malderen et al.,[30] fly-ash particles are one of the most abundant particle types in Siberian winter air-masses. Despite the presence of a major hydro-electrical plant at Novosibirsk, most of the electrical production in the region is based on coal burned power plants. The combined result of the burning of coal and the presence of a snow cover, which prevents soil to be blown into the air during the winter months, explains the enormous relative occurrence (up to 30% of the total abundance) of the fly-ash. Aerosol particles were analyzed by proton-micro beam, positioned first in the middle and then at the edges of a particle in order to check its homogeneity. In Fig 2. μ-PIXE and RBS spectra for three different points in a fly-ash particle are given. The RBS spectrum provides information on the lighter and some major elements of the investigated particle (so-called matrix composition), while its trace elemental composition is apparent from the μ-PIXE spectrum. Deconvolution of the RBS spectrum involves correction for the composition and thickness of the support layer (in this case: the Nuclepore filter, $C_{16}O_3H_{16}$). The corresponding composition of a "typical Siberian" fly-ash particle is given in Table 1. Complete thick target corrections for beam stopping, X-ray attenuation and X-ray fluorescence were implemented. Some compositional variabilities were shown, although not so drastical when compared to the above-mentioned studies.

Table 1. The main composition (wt%) of a giant "Siberian" fly-ash particle as determined by RBS and μ-PIXE at different position within the particle; (- not detected)

Fly-ash particle	C	O	Al	Si	Fe
Centre (RBS)	35	26	27	12	0.92
Centre (PIXE)	-	-	15	10	0.94
Side 1 (RBS)	65	19	3.6	12	0.75
Side 1 (PIXE)	-	-	11	25	0.92
Side 2 (RBS)	41	22	33	3.5	0.69
Side 2 (PIXE)	-	-	-	-	0.99

The majority of coal fly-ash particles seem to consist, as a result of the coal combustion process, of a mineral core containing a surface layer of volatile elements like S[31]. Evidence of the presence of S as a coating on individual coal fly-ash particles was recently demonstrated by plotting the S/Si X-ray intensity ratio, acquired by SEM-EDX analysis, as a function of the geometrical particle diameter.[32] These results showed the smallest coal fly-ash particles to contain the highest S-enrichments. Aerosol models developed by Biermann and Ondov[33] can be applied to determine the concentration of the thin surface layer deposited onto the solid core of the particle. On the other hand, in the fly-ash particles emitted by oil-fired power plants, three different particle modes could be distinghuised. Chemical and physical surface reactions taking place during and after combustion could be responsible for the S content in the coarse and large particle mode. These modes were composed of organic material and mineral elements, respectively. Based on the $BaCl_2$ microspot technique the small particle mode was identified as water soluble sulfates which occurs by nucleation and coagulation of sulfuric acid produced by burning S containing fuel.

A detailed AES study on the surface elemental composition of coal fly-ash particles was also performed by Linton et al.[25] Qualitative elemental depth profiles of Al, Ca , Fe, K, Na, S and Si revealed that only K, Na and S exhibited major surface enhancement although potentially toxic elements like Pb, Ti, Mn and Cr were also present. The obtained results were qualitatively in agreement with the SPM data suggesting that both techniques can be applied to investigate the actual elemental composition of the surface region. The overall results of this study suggest the elemental surface predominance to be a general phenomenon in particles produced by high temperature processes for which volatilization and subsequent condensation of elements likely occur. Similar research was performed by Hock and Lichtman[34] on nanometre surface coatings of individual coal fly-ash particles collected in-plume and in-stack.

Fly-ash particles formed by shells with different composition and structure are often observed.[35] In Fig 3. the Auger depth profile of the fy-ash particle is shown. The shell structure of this particle is clearly demonstrated. Three different shells can be observed. The topmost shell is mainly composed of alumino-silicates. Underneath this shell, an alumino-silicate and iron oxide shell are distinguished, while the inner shell is mainly composed of iron oxides.

In a study to investigate the potential effect of the Kuwait oil fire plumes, in May 1991, on the local and global environment, the $BaCl_2$ chemical spot test in combination with EM (transmission and scanning) was also performed to distinguish sulfate containing particles[36]. The aerosol samples, collected on board an aircraft at different altitudes in the plumes, were coated with $BaCl_2$ which formed particles < 50 nm on the background. Introducing the coated samples into a humid chamber for 2 hours provided the correct environment for the reaction of $BaCl_2$ with sulfate. Applying this method, which was first introduced by Bigg et al.,[37] sulfate containing particles were surrounded by a hollow ring and pure sulfate particles could be distinguished from sulfate coated particles based on the shape of the particles' centre core. The number of sulfate coated soot, salt and dust particles appeared to increase with the distance from the fire plumes and the thickness of the S coating increased with altitude. The presence of these particle types indicate a gas to particles conversion, by means of catalytic oxidation in combination with heterogeneous nucleation, during plume dispersion. The increase of small sulfate particle concentrations with height and distance from the plume can be attributed to the transformation of SO_2 gas into sulfate particles via oxidation followed by homogeneous nucleation. The majority of particles in the plume behaved as cloud condensation nuclei since their surface characteristics changed from hydrophobic to hydrophillic by the coating with sulfate. In this way these particles are able to initiate haze, smog, fog or cloud droplets. Air trajectory analysis suggested the existence of periods in which aerosols generated by the fires could have reached China and influenced the severe rainfall at the end of May and the beginning of June.

The characterisation of individual oil-soot particles on a Ta-substrate has been accomplished using SIMS by McHugh and Stevens.[38] On the average, high levels of O, V, C, Na, Ca and K could be identified; the total composition can vary strongly between different oil-soot particles since a wide variety exists in the inorganic trace elemental composition of crude oils and in the combustion conditions. Moreover the SIMS images of major elements present in the oil-soot particles showed that local differences in the elemental distribution within individual oil-soot aerosol particles were present for Na, K, Ca, Mg, Al, Si, Ti and B. A homogeneous distribution was usually found for V and C, the two major compounds.

Besides different on-line LAMMS studies on artificially generated aerosols,[11-16] a report was recently published on the possibilities of the LAMPAS system (laser mass analysis of particles in the airborne state), developed at the Institute of Laser Medicine, University of Düsseldorf, Germany, for the analysis of single atmospheric particles by on-line laser time-of-flight MS.[17] Using this set-up aerosol particles from ambient air could be detected with a high repetition rate, a superior mass resolution which remains constant over the entire mass range and a very high signal to noise ratio. The comparison between the on-line spectrum of an aerosol particle collected from the laboratory room air, showing the typical carbon cluster ion distributions of soot particles, and a candle soot particle analyzed by LAMMS, revealed the quality of the on-line spectrum to be as good as the LAMMS off-line spectrum. Both spectra appeared to be similar although additional information indicating the presence of an aqueous phase surrounding the soot particle could only be identified in the on-line spectrum. The capability of the instrument to distinguish dry and wet particles was previously demonstrated by analysis of aqueous salt droplets.[17,19]

3.1.2. Urban aerosols

Out-door aerosol particles in the urban areas stem to a great extent from anthropogenic emission. In many cases these particles contain higher concentrations of several potentially hazardous trace elements which are normally found in natural crustal dust, soil and sediment. These elements, like S, V, Cr, Mn, Co, Ni, Zn, Se, Cd, Sb, Tl and Pb, are preferentially associated with particle surfaces as a result of condensation from the vapour phase or adsorption from solution.

Fumes arising from iron and steel industries are considered to be the major source of airborne particles containing metal oxides which may be carcinogenic. The toxicity of these metals seemed to be related to their chemical oxidation state. LAMMS analysis on particles emitted as dust by the steel industry revealed a correlation between the Cr oxidation state and the particle size.[39] Particles smaller than 1.1 μm were composed of P- and Na-matrices, whereas large particles (> 6 μm) mainly consisted of Ca. Cr was found to be present in the hexavelant state for both size fractions. Trivalent Cr could only be detected in particles of intermediate size. For the verification of the Cr oxidation state and nature of the Cr-compounds present in particles the micro Raman technique is also desirable.

Airborne microparticles, collected from out-door air near the city of Karlsruhe, in the Rhine river valley, have a clear shell structure.[40] The majority of the particles was of respirable size with diameter < 2 μm. The core of the coarse particles (2-5 μm) contained geogenic material, which was covered by a double layer structure. The geogenic origin was confirmed by the presence of typical soil elements such as Na, K, Mg and Fe. The topmost layer of some 60 nm was of nitrate and ammonium sulfate, while a deeper layer of 400 nm primarily consisted of carbonate and organic carbon compounds. Moreover, Na and Mg (as carbonate and nitrate) were found in this surface region. Submicron particles (0.2-0.8 μm) contained a core dominated by graphitic or organic carbon, almost completely covered by a 15 nm thick layer of ammonium sulfate. These particles are basically originating from vehicle traffic. Ammonium sulfate is possibly directly formed from gaseous precursors at the surface of the soot (this reaction can even take place in the exhaust pipe of catalyst equipped cars) or agglomerates as fine particles onto the soot particles after emission. The observed layer structures are of importance for the removal of the soot from the atmosphere, since the conversion of the soot surface from originally hydrophobic into hydrophillic behaviour should ease wet precipitation. Another study[41] of large auto exhaust particles indicated surface enrichment (down to a few μm) by S, Cl, Br and Pb (with absence of Fe, although Fe was one of the major constituents). Also, the trace elements Cr, Ni and Tl were found to be highly surface enriched. This finding was attributed to the deposition of volatile Pb and S species (like PbBrCl and SO_2) onto the surfaces of refractory Fe-containing particles as the temperature decreases in the automobile exhaust system. The Fe-rich particles were derived from ablation of Fe from the exhaust system. The observed trace amounts of Cr, Ni and Tl have been introduced by impurities of Pb-gasoline additive or, in the case of Cr and Ni, by engine wear. The small particles (<1 μm) were found to be composed, almost exclusively, of Cl, Br and Pb (no Fe).

The overall composition and depth distributions of the components of combustion particles generated in household fires were investigated by Bentz et al.[42] The results showed that the combustion particles have a shell structure with organic halogen compounds and the PAH- content of about 1 ppm in a surface layer. Cl and HC were enriched in a surface region of some 100 nm thickness. This layer was of mainly aliphatic character. The concentration of HC decreased towards the core. Obviously, a condensation of low-volatiles HC with Cl-compounds or a surface reaction with gaseous Cl or HCl is responsible for the organic surface layer enriched with Cl.

In huge area of Siberia, there are many remote areas but also there are some regions where massive industrial complexes are located with a pollution levels several times higher than in any West European or North American country. Our recent sampling and research program, for some areas of Siberia, have provided a detailed characterization on the airborne particulate matter representative for this part of the world. Typical aerosol particles, resulting from emissions by the heavy metal industry, were found to be K- and Cl-rich particles containing significant amounts of heavy metals such as Cr, Ni, Zn, As and Pb in a concentration range of 0.2% (Ti) to 1.8% (Fe). Some elements like Cl, K, Ca and Fe were found to be homogeneously distributed over the particles, while Ti, Ni, Cu, As and Pb were dominantly concentrated at one edge of the particles. Frequently, particle agglomerates were also observed.[30]

Recently, the Singapore group has reported on the analysis of more than 300 urban aerosol particles by SPM.[43] Each particle was characterized by its size, thickness, total mass and concentration of up to 29 elements. Particles were characterised into several groups, according to their major components: marine and soil particles were found to be the most abundant, representing more than 86% of total mass, followed by Fe (3.6%), Pb (3.1%) and Ti (1.8%). "Exotic" particles with high concentrations of Sn, Sb and Ba were also found (2%), but their source was not identified. S, as one of major anthropogenic pollutants in urban areas, was found to be quite evenly distributed in all particles. This was expected, because S is released to the atmosphere in gaseous form which "condenses" on solid particles through reactions with water vapour and sunlight forming sulfuric acids. Also, it reacts with virtually "harmless" marine particles forming hydrochloric acids. Most of the S on Cl-rich particles was concentrated on the surface of larger particles. This was proven by "washing" one sample in a warm (40°C) solution of 5% HNO_3 for about 2 min, followed by rinsing in distilled water and proton irradiation once again. The result was quite surprising: most of the aerosol particles remained intact on pioloform substrate but PIXE spectra showed almost complete absence of marine components (Na, Mg, Cl) as well as a high depletion of S, Pb and Br. Such shell around particles limits the PIXE quantitative analysis; if e.g. S forms a shell around a Si-rich particle and matrix corrections are performed by a "classical approach", assuming a homogeneous distribution of all elements and a flat target, the obtained mass will be overestimated by a factor of two or even more, depending on the particle size and composition. Therefore, a precise concentration determination requires a more sophisticated approach.

Carbonaceous particles in the atmosphere contribute significantly to the total suspended particulate matter and can sometimes comprise more than 50% of the total submicron mass fraction. They exist mainly in the particle size range below 3 μm with the major amounts in the size range below 1 μm. Atmospheric carbonaceous material consists of different types of particulate carbon fractions, namely: carbonates, elemental carbon and organic carbon. Although observed in atmospheric particles, carbonates form a minor component in the fine fraction of aerosols, at least in polluted urban atmosphere. Mueller et al.[44] reported that the carbonate carbon present in aerosols from Pasadena, California, represent systematically less than 5% of the total carbon. Contrary, elemental carbon is a prominent constituent of atmospheric aerosols and is present in urban areas but also in remote environment, such as above tropical oceans and in the Arctic region. In urban areas, the elemental carbon fraction accounts for less than 40% of the total carbonaceous content in the atmosphere[45]. Elemental carbon is especially of interest since it is an extremely efficient absorber of visible light. Organic carbon aerosol present in the Los Angeles area was found to account for roughly 60% to 70% of the fine particulate carbonaceous aerosol.[46] Up to now, analysis of carbonaceous particles has mostly been limited to bulk analysis and only recently carbonaceous particles have been subjected to a single particle approach.[47] Carbonaceous particles in the Phoenix, Arizona, urban atmosphere have widely diverse origins and as a consequence, a considerable range in structures and morphologies. A significant coagulation between particles of anthropogenic and non-anthropogenic origin was found in ambient air samples. The graphitic structures were interpreted as a part of the primary soot spherules and the amorphous areas as hydrocarbons condensed during aggregation. Secondary transformation reactions of carbonaceous particles in the presence of SO_2/NO_2 mixtures were also observed. The coated aggregates have carbon structural variations similar to those in uncoated aggregates, suggesting both types of particles to form from similar pre-emission sources. The use of EELS has provided visual evidence of S and C coatings present on the surfaces of carbonaceous and quartz particles identified in the Phoenix environment.

A combination of a bulk-analytical technique, differential pulse anodic stripping voltametry (DPASV), and a micro-analytical technique, LAMMS, was applied to identify Pb in standard particles and natural aerosols.[48] The aerosol particles were collected both in the city of Wageningen and at the downwind side of a highway at Ede, in The Netherlands. Discrimination between Pb present as a coating or homogeneously distributed over the particle appeared to be possible for both techniques. LAMMS results revealed moreover that most of the particles could be identified as mixed salts of ammonium nitrate and ammonium sulfate with a variable content of metals, especially V and Pb.

3.2. Coal-mine dust particles

There are many reports of the inhibition of quartz toxicity in various quartz-containing dusts.[49] For many years, coal mine workers' pneumoconiosis has been related to the presence of quartz in the respirable coal dusts fraction. However, the experimental toxicity of coal mine dusts was usually found not to be consistently correlated with the gross quartz content as determined by bulk analysis. Such lack of distinct correlation can widely be ascribed to the heterogeneity of such materials. Mixed dusts, such as authentic coal mine dusts, represent rather heterogeneous mixtures of elements down to the individual particle level.[50] Comparative studies of the toxic potency of authentic coal mine dusts and artificial quartz-coal mixtures have suggested that quartz toxicity may be inhibited by protective impurities on the quartz surface.[51] This became more apparent after LAMMS studies of natural dusts and authentic coal mine dusts were performed.[52] These analyses revealed that only a minute fraction of "pure" quartz (about 1% of the total abundance) may be detected in coal mine dusts. Most of the quartz surface in such highly heterogeneous particulate matter appeared to be covered by alumino-silicates. LAMMS investigation has marked out that fibrogenicity of coal dust samples was not correlated with the incidence of the pure quartz particles but with the incidence of Fe, Mg(Ca)-containing particles. These particles seem to have a major role in harmfulness of coal mine dusts.

3.3. Marine aerosols

Andreae et al.[53] reported already in 1986 on the heterogeneous nature of remote marine aerosols collected during a cruise on the equatorial Pacific Ocean. Several thousand particles were subjected to automated EPXMA and imaging of silicon containing particles was performed by SEM. Beam focusing at high magnification revealed information on the individual components of composite particles and mineral standards were utilized to calibrate the acquired X-ray spectra. They concluded that the internal mixing with sea-salt, detected in a large fraction of the silicate mineral component, as well as the enrichment of excess sulfate on sea-salt particles could probably be attributed to processes occurring within clouds.

Individual North Sea aerosol particles collected from an aircraft at six different heights were analyzed by LAMMS.[54] The different particle types, earlier distinguished by EPXMA, were also found with LAMMS but many particles seemed to appear as internal mixtures. The interpretation of the particle type abundances as a function of wind direction and particle size made it possible to apportion the different types to their source. Besides a decrease in relative sea-salt concentration above the inversion layer, no clear differences were found in the particle abundances as a function of height.

SEM and TEM together with thin-film chemical tests were applied to study the nature, composition and morphology of methanesulfonic acid (MSA) particles, sampled over the Sakushima Island in Japan, near the Pacific Ocean.[55] MSA and SO_2 can be identified as the major reaction products obtained from the oxidation of marine dimethyl sulfate. At high relative humidity the coarse particle mode appeared to be dominated by mixed particles produced through heterogeneous nucleation reactions of gaseous MSA with sea-salt or soil particles. The fine particle mode was characterized by sulfate particles. Nitrate was present in both modes.

Concerning quantification, Pardess et al.[56] developed a new method, with a reasonable accuracy for the SEM-EDX determination of the sulfur mass content in single aerosol particles larger than 0.4 μm with a minimum of 10^{-13} g sulfur. Calibration was achieved by analysing particles of known composition and size. Moreover quantitative estimations can be acquired for the sulfur concentration inside heterogeneous aerosol particles.

Recent laboratory investigations by Cheng[57] revealed the existence of a shell structure composed of chlorides ($MgCl_2$ and KCl) on the surface of marine aerosol particles. Moreover the majority of sea water drops which evaporate and become salt-saturated during free fall in the air (RH < 60%) seemed to change phase to produce hollow sea-salt particles.[58] These results were obtained by close examination of the different stages in the evaporation process of an individual seawater droplet, using a polarizing microscope and a SEM. The shell structure is very valuable for the understanding of nucleation processes in the atmosphere, since the presence of a chloride film provides a highly hygroscopic surface, which already initiates the condensation of water vapour at a RH of 40%.

Direct evidence of the formation of nitrate on marine particles, which was already frequently stated by different scientists,[59-61] was provided by Mamane and Gottlieb.[62] They studied the heterogeneous reactions of NO_2 and HNO_3 on individual sea-salt and mineral particles, under controlled conditions inside a teflon reaction chamber, by bulk and individual particle analysis. Different particles did react with nitrogen oxides and HNO_3 to form nitrates. The formation of these nitrates seemed to depend on the presence of U.V. radiation. Under dark conditions, 0.1 to 8 mg NO_3^- g^{-1} aerosol was produced compared to 1.4-28 mg NO_3^- g^{-1} aerosol under U.V. radiation. Microscopic investigations associated with a specific microspot technique,[63] by which the particles after exposure to NO_2 or NO_3 are coated with Nitron, proved that in 50% of the studied soil dust particles, mixed nitrate particles were formed upon reaction with NO_2 and HNO_3 and that both gases reacted with 95% of all sea-salt particles to produce a surface coating of nitrates. Based on these results, the heterogeneous nitrate formation could be classified as an important removal process for NO_x under solar radiation in the ambient atmosphere.

On-line RSMS investigations performed by Carson et al.[18] on the behaviour of NaCl particles upon exposure to NH_3 and HNO_3 vapour prior to sampling into the MS provides also evidence for the formation of an NH_4NO_3 coating on the particles surface. Since no change in particle size distribution could be observed by an aerodynamic particle sizer, the coating thickness seemed to be less than 200 nm. RSMS was also performed for the speciation of semi-volatile and non-volatile sulfur compounds as well as for the measurement of isotopic ratios.[18]

The composition of giant North Sea aerosol particles was investigated by Injuk et al.,[64,65] using the SPM analytical facilities of the Institute of Reference Materials and Methods (IRMM) in Belgium and of the Lund Institute of Technology in Sweden. Together with other microanalytical research centres they offer the possibility of a total quantitative scanning analysis (TSQA), a new way of data acquisition and processing. Under these conditions, all the incoming data are recorded in the original time sequence of events or stored as sorted spectra in three-dimensional data sets, without any limitation on the amount of data taken up due to predefined energy regions. This mode allows to follow the complete experiment as it evolves in time and it is very valuable to investigate a possible instability of samples under microbeam irradiation or specimen damage. Storage of the energy spectra for each pixel can easily provide various cross-sections through the data set but restricts scanning frames to 64 x 64 pixels. Major, minor and trace elements with atomic number > 15 were identified by micro-PIXE and quantification of the acquired spectra revealed elemental compositions down to absolute masses of 50 fg in the case of Ti, V or Cr. Three different aerosol types could be distinguished: particles with a marine origin including pure sea-salt particles and sea-salt combined with high contents of S, K and Ca and anthropogenic particles rich in Ti, Cr, Fe and Ni. The lateral elemental distribution within different giant North Sea aerosol particles was characterized with a constant resolution of 3 μm throughout the depth of the particles. The elemental maps showed that these particles were heterogeneous and seemed to consist of agglomerated large particles

3.4. Remote aerosols

The recent interest in characteristics of the Antarctic atmosphere has resulted in a recognition of the need for long term background aerosol studies. The Antarctic continent is an ideal site to follow the trends in regional and global concentrations of trace elements in the atmosphere. Due to the surrounding ocean and the very low soil dust aerosol load, the Antarctic peninsula is also an ideal site to study properties of marine aerosol particles.[66]

A large diversity of particles of different origin was observed in the Antarctic troposphere; among them a significant number were heterogeneous.[67] NaCl and $MgCl_2$ particles contained small amounts of S, possibly indicating reactions of these particles with gaseous sulfur compounds. Internal mixtures of silicates and marine aerosols were observed too. Most of the S in particles larger than 0.1 μm was in the form of $CaSO_4$, and the abundance of these particles showed a seasonal variability with a maximum in summer. The S-containing particles are important because they could play a role in global climate change by influencing the radiation budget and the concentration of cloud condensation nuclei.[68]

3.5. In-door aerosols

In an effort to evaluate the possible effects of airborne particles on paintings, a combination of different analytical techniques, including EPXMA, SEM- and STEM-EDX and SPM, was successfully applied for the characterization of individual aerosol particles collected at the Correr museum in Venice[69]. Multivariate techniques performed on the EPXMA and SEM-EDX data revealed three different aerosol sources and six to eight different particle types. To study the spatial distribution of the elements inside individual Ca-rich giant aerosol particles (> 8 μm), the possibilities of a JEOL JSM 6300 SEM in the field of X-ray mapping were investigated. The optimal parameter adjustment was obtained by testing the variation of different instrumental parameters on the collection of an X-ray mapping. Processing of the collected X-ray mappings was performed by Image Math (Fig 4.), a program which enables mathematical operations on images. The X-ray mapping results demonstrated clearly the heterogeneous character of this particle type. They mainly contained of Ca and Si with small particles, identified as alumino-silicates, $CaSO_4$ particles or very small Fe-rich particles, adsorbed at their surface. Na and Cl were correlated as sea-salt crystals or found as a coating on the surface of the particles. The occurrence of these giant particles can probably be attributed to the coagulation of giant Ca-Si-rich particles, produced by decomposition of wall plaster and cement through ageing or introduced from the outside, with small particles present in the indoor environment. Verification of these results as well as information on the distribution and semi-quantisation of trace elements inside these individual giant aerosol particles was achieved by SPM measurements.

3.6. Artificially generated aerosols

Inorganic salts account for a 25-50 % of the fine aerosol mass in polluted urban environments; among them, $(NH_4)_2SO_4$ and NH_4NO_3 are the most common one. Hence, understanding mechanism of crystallization of different aerosol salts is crucial to the elucidation of the atmospheric processes affecting air quality, visibility degradation and climate change. But very few studies have been performed in this direction, due to limitations in available thermodynamic data and experimental methods. Based on thermodynamic analysis, the work of Ge et al.,[70] has shown that particles dried from multicomponent aqueous aerosols do not have a homogeneous chemical morphology except at the eutonic point. [When two salts, at a certain relative humidity, precipitate together they form a mixture of solid phases, and a corresponding aqueous phase composition is called the eutonic composition.] Rapid single-particle-Mass Spectrometry (RSMS) was used to examine the surface morphology and chemical composition of particles dried from KCl/NaCl, KCl/KI and $(NH_4)_2SO_4/NH_4NO_3$ mixed solutions at different mole ratios. For a simple salt mixture such as KCl/NaCl and KCl/KI, the surface composition of the dried particles is identical to the eutonic composition and is independent of the original solution mole fraction. Thermodynamic analysis showed that the composition of dried particles containing KCl/NaCl is not spatially homogeneous, but the surface composition of particles dried from solutions with different mole ratio of NaCl and KCl is the same. The same pattern was observed for particles containing KCl/KI mixtures. One consequence of this behavior is that the surface layer is enriched in the minor component. Particles dried from $(NH_4)_2SO_4/NH_4NO_3$ mixture solutions contained substantial amount of $(NH_4)_2SO_4$ at or near the surface. The surface composition of the particles is in general identical to each other, it is independent of the original solution composition and is most likely equal to that of the eutonic point.

4. CONCLUSIONS

In this chapter we have demonstrated how an increasing interest in the analysis of particle surfaces and the need for three-dimensional characterization of a single aerosol particle have led to the application of many micro- and trace analytical techniques. Microanalysis has been able, in many cases, to produce interesting and almost unique information on the intra-particle structure. Since no existing micro-analysis technique presently offers a panacea for all analytical demands, the most successful research programmes will be those in which several complementary techniques are to be used to provide relevant analytical information of environmental interest. As the structural information of a micro-particle is contained in its exterior boundary and interior texture, there are continued demands for higher resolutions and better sensitivities. Also, the power of computer-based image processing for a variety of applications has not been fully realized yet.

In this review, mostly off-line methods for particle characterization were described. These methods collect particles on substrates or filters for an extended period of time for later compositional analysis. In such a way, the informations on particle composition and possible sources are given, but the time information for each particle is missing. Additionally, a size selectivity as well as artifacts due to the sample preparation can be introduced. As a consequence, the particles from one or more events of interest are not readily distinguished from particles unassociated with the event. Also, particles smaller than roughly 0.08 µm do usually not contain sufficient mass for reliable compositional determination. At present there are only two methods described in the literature capable of single particle analysis in an on-line mode: atomic emission spectroscopy and mass spectrometry. With atomic emission spectroscopy, the particles are vaporized and ionized by either a laser spark or an inductively coupled plasma. The detection limits are element dependent and range from 100 to a few thousand ppm. The laser ionization mass spectroscopy offers new capabilities to the aerosol community like: highly efficient vaporization and ionization, general applicability generation of molecular and elemental information, ability to detect volatile species (particles spend less than 1 ms under vacuum conditions before ionization), possibility to study gas-phase reactions yielding solid products and etc. In contrast to filters or microscopic grids retained for analysis, each particle is sampled at a well defined time. Even in rapidly changing conditions, it is possible to go back and retroactively correlate the chemical composition with meteorological or other conditions. Particles of different sizes (0.02-10 µm) and composition like: $(NH_4)_2SO_4$, SiO_2, $RbNO_3$ and $CsNO_3$ could be detected and analyzed.[20]

The application of the X-ray photo electron spectroscopy (XPS or ESCA) in the environmental field is still limited to bulk analysis. XPS is, like AES, a surface analytical technique in which in this case the core-level electrons from the sample are ejected upon X-ray beam interaction. The energy analysis of the produced photoelectrons reveals information on the chemical bonding. XPS is not restricted to low Z-elemental analysis and the detection limits are comparable to AES. Up to now single particle analysis is only possible with the spatial resolution being in the order of 10 µm. Improvements in both the spatial resolution and the sensitivity are under investigation.

ACKNOWLEDGMENTS

Lieve De Bock acknowledges financial support by the Instituut voor de Bevordering van het Wetenschappelijk-Technologisch Onderzoek in de Industrie (IWT). This work was partially sponsored by the Belgian State Prime Minister's Service-Science Policy Office, in the framework of the Impulse Programme in Marine Sciences (Contract MS/06/050).

5. REFERENCES

1. Jambers, W., L. de Bock, L., and Van Grieken, R. (1996) Applications of Micro-Analysis to Individual Environmental Particles, *Fresenius'J. Anal. Chem.*, in press.

2. Xhoffer, C. and Van Grieken, R., Environmental Aerosol Characterization by Single Particle Analysis Techniques, in: Environmental Particles, Vol. 2. IUPAC Monography, J. Buffle and H. P. van Leeuwen Eds. (CRC Press, Inc., Florida, USA, Lewis Publishers, 1993).

3. Armstrong, T.J. (1995) CITZAF. A Package of Correction Programs for the Quantitative Electron Microbeam X-ray Analysis of Thick Polished Materials, Thin Films, and Particles, *Microbeam Analysis*, **4**, 177.

4. Danilatos, D.G. (1994) Environmental Scanning Electron Microscopy and Microanalysis, *Mikrochim. Acta,* **114/115**, 143.

5. Nockolds, C.E. (1994) Low-Voltage Electron Probe X-ray Microanalysis in an In-Lens Field Emission Gun SEM: An Evaluation, *Microbeam Analysis,* **3**, 185.

6. Katrinak, K., Rez, P. and Buseck, P.R. (1992) Structural Variations in Individual Carbonaceous Particles from the Urban Aerosol, *Envir. Sci. Technol.,* **26**, 1967.

7. Maynard, A.D. and Brown, L.M. (1992) Electron Energy Loss Spectroscopy of Ultrafine Aerosol Particles in Scanning Transmission Electron Microscopy, *J. Aerosol Sci.* **23**, S433.

8. Xhoffer, C., Jacob, W., Buseck, P.R. and Van Grieken, R. (1995) Problems in Quantitatively Analysing Individual Salt Aerosol Particles using Electron Energy Loss Spectroscopy, *Spectrochim. Acta*, **Part B 50**, 1281.

9. Shina, M.P. (1984) Laser-Induced Volatilization and Ionisation of Microparticles", *Rev. Sci. Instrum.*, **55**, 886.

10. Marijnissen, J., Scarlett, B. and Verheijen, P. (1988) Proposed On-Line Aerosol Analysis Combining Size Determination, Laser-Induced Fragmentation and Time-of-Flight Mass Spectroscopy, *J. Aerosol Sci.*, **19**, 1307.

11. McKeown, P.J., Johnston, M.V. and Murphy, D.M. (1991) On-Line Single-Particle Analysis by Laser Desortion Mass Spectrometry, *Anal. Chem.*, **63**, 2069.

12. Kievit, O., Marijnissen, J.C.M., Verheijen, P.J.T. and Scarlett, B. (1992) On-Line Measurements of Particle Size and Composition, *J. Aerosol Sci.*, **23**, 301.

13. Mansoori, B.A., Johnston, M.V. and Wexler, A.S. (1994) Quantitation of Ionic Species in Single Microdroplets by On-Line Laser Desorption/Ionisation, *Anal. Chem.*, **66**, 3681.

14. Murray, K.K. and Russel, D.H. (1994) Aerosol Matrix-Assisted Laser Desorption Ionization Mass Spectrometry, *J. Am. Soc. Mass Spectrom.*, **5**, 1.

15. Prather, K.A., Nordmeyer, T. and Salt, K. (1994) Real-time Characterization of Individual Aerosol Particles using Time-of-Flight Mass Spectrometry, *Anal. Chem.,* **66**, 1403.

16. Nordmeyer, and Prather, K.A. (1994) Real-time Measurement Capabilities using Aerosol Time-of-Flight Mass Spectrometry, *Anal. Chem.,* **66**, 3540.

17. Hinz, K.P, Kaufmann, R. and Spengler, B. (1994) Laser -Induced Mass Analysis of Single Particles in the Airborne State, *Anal. Chem.,* **66**, 2071.

18. Carson, P.G., Neubauer, K.R., Johnston, M.V. and Wexler, A.S. (1995) On-Line Chemical Analysis of Aerosols by Rapid Single-Particle Mass Spectrometry, *J. Aerosol Sci.,* **4**, 535.

19. Murphy, D.M. and Thomson, D.S. (1995) Laser Ionization Mass Spectroscopy of Single Aerosol Particles, *Aerosol Sci. Technol.,* **22**, 237.

20. Reents, W.D., Downey, S.W., Emerson, A.B., Mujsce, A.M., Muller, A.J., Siconolfi, D.J., Sinclair, J.D. and Swanson, A.G. (1995) Single Particle Characterization by Time-of-Flight Mass Spectrometry, *Aerosol Sci. Technol.,* **23**, 263.

21. Hinz, K-P, Kaufmann, R. and Spengler, B. Simultaneous Detection of Positive and Negative Ions from Single Airborne Paricles by Real-Time Laser Mass Spectrometry, *Aerosol Sci.Tecnol.,* in press.

22. Malmqvist, K.G. (1994) Ion Beam Analysis for the Environment, *Nucl. Instr. Methods in Physics Research*, **B 85**, 84.

23. Kondratyev, K.Y. and Binenko, V.I. Optical Properties of Dirty Clouds, in: Interactions between Energy Transformations and Atmospheric Phenomena, M. Beniston and R.A. Pielke, Eds. (Reidel, Dordrecht, 1987).

24. Linton, R.W., Loh, A., Natusch, D.F.S. and Williams, P. (1975) Surface Predominance of Trace Elements in Airborne Particles, *Science*, **191**, 853.

25. Linton, R.W., Williams, P., Evans, C.A. Jr and Natusch, D.F.S. (1977) Determination of the Surface Predominance of Toxic Elements in Airborne Particles by Ion Microprobe Mass Spectrometry and Auger Electron Spectrometry, *Anal. Chem.*, **49**, 1514.

26. Cox, X.B.III, Bryan, S.R., Linton, R.W. and Griffis, D.P. (1987) Microcharacterization of Trace Elemental Distributions within Coal Combustion Particles using Secondary Ion Mass Spectrometry and Digital Imaging, *Anal. Chem.*, **59**, 2018.

27. Vis, R.D., A.J.J. Boss, V. Valkovic and H. Verheul (1983) The Analysis of Fly-Ash Particles with a Proton Microbeam, *IEEA Trans. Nucl. Sci.*, **NS-30**, 1236.

28. Jakšić, M., Watt, F., Grime, G.W., Cereda, E., Marcazzan, G.M.B. and Valković, V. (1991) Proton Microprobe Analysis of Trace Element Distribution in Fly-Ash Particles, *Nucl. Instr. Methods in Physics Research*, **B 56/57**, 699.

29. Cereda, E., Marcazzan, G.M.B., Pedretti, M., Grime, G.W. and Baldacci, A. (1995) Nuclear Microscopy for the Study of Coal Combustion related Phenomena, *Nucl. Instr. Methods in Physics Research,* **B 99**, 414.

30. Van Malderen, H., Van Grieken, R., Bufetov, V. and Koutzenogii, K. (1996) Chemical Characterization of Individual Aerosol Particle Types in Central Siberia, *Environ. Sci. Technol.,* **30**, 312.

31. Natusch, D.F.S., Wallace, J.R. and Evans, C.A. (1974) Toxic Trace Elements: Preferential Concentrations in Respirable Particles, *Science,* **183**, 202.

32. Biermann, A.H. and Ondov, J.M. (1980) Application of Surface-Deposition Models to Size-Fractionated Coal Fly-Ash, *Atmos. Environ.*, **14**, 289.

33. Mamane Y., Miller, J.L. and Dzubay, T.G. (1986) Characterization of Individual Fly-Ash Particles Emitted from Coal- and Oil-Fired Power Plants, *Atmos. Environ.,* **11**, 2125.

34. Hock, J.L. and Lichtman, D. (1983) A Comparative Study of In-Plume and In-Stack Collected Individual Coal Fly-Ash Particles, *Atmos. Environ.,* **17**, 849.

35. Boni, C., Cereda, E., Braga Marcazzan, G.M. and Parmigiani, F. Bulk and Surface Studies of Fly-Ash Particles, in: Combustion Efficiency and Air Quality, Eds. I. Hargittai and T. Vidoczy (Plenum Press, New York, 1995).

36. Parungo, F., Kopcewicz, B., Nagamoto, C., Schnell, R., Sheridan, P., Zhu, C. and Harris, J. (1992) Aerosol Particles in the Kuwait Oil Fire Plumes: their Morphology, Size Distribution, Chemical Composition, Transport, and Potential Effect on Climate, *J. Geophys. Res.*, **97**, 15867.

37. Bigg, E.K., Ono, A. and Williams, Y.A. (1974) Chemical Tests for Individual Submicron Aerosol Particles", *Atmos. Environ.*, **8**, 1.

38. McHugh, J.A. and Stevens, J.F. (1972) Elemental Analysis of Single Micrometer-Size Airborne Particulates by Ion Microprobe Mass Spectrometry, *Anal. Chem.*, **44**, 2187.

39. Hachimi, A., Poitevin, E., Krier, G., Muller, J.F., Pironon, J. and Klein, F. (1993) Extensive Study of Oxidation States of Chromium in Particles by LAMMA and Raman Microprobes: Application to Industrial Hygiene, *Analusis*, **21**, 77.

40. Goschnik, J., Schuricht, J. and Ache, H.J. (1994) Depth-Structure of Airborne Microparticles Sampled Downwind from the City of Karlsruhe in the River Rhine Valley, *Fresenius' J. Anal. Chem.*, **350**, 426.

41. Keyser, T.R., Natusch, D.F.S., Evans, C.A.Jr. and Linton, R.W. (1978) Characterizing the Surfaces of Environmental Particles, *Envir. Sci. Technol.*, **12**, 768.

42. Bentz, J.W.G., Fichtner, M., Goschnick, J. and Ache, H.J. Depth-resolved Analysis of Microparticles Generated by a Household Fire, in: Abstracts from Fourth International Aerosol Conference, August 29-September 2, 1994, Los Angeles, California, R.C. Flagan, Ed. (American Association for Aerosol Research, Kemper Meadow Drive, Cincinnati, OH, USA, 1994).

43. Orlić, I., Watt, F., Loh, K.K. and Tang, S.M. (1994) Nuclear Microscopy of Single Aerosol Particles, *Nucl. Instr. Methods in Physics Research,* **B 85**, 840.

44. Mueller, P.K., Mosley, R.W. and Pierce, L.B. (1972) Carbonate and Non-carbonate Carbon Content in Photochemical Aerosols as a Function of Size, *J. Colloid Interface Sci.,* **39**, 235.

45. Appel, B.R., Hoffer, E.M., Kothny, E.L., Wall, S.M. and Haik, M. (1979) Analysis of Carbonaceous Material in Southern California Atmospheric Aerosols, *Environ. Sci. Technol.,* **13**, 98.

46. Turpin, B.J. and Huntzicker, J.J. (1991) Secondary Formation of Organic Aerosol in the Los Angeles Basin: a Descriptive Analysis of Organic and Elemental Carbon Concentrations," *Atmos. Environ.,* **25**, 207.

47. Katrinak, K., Rez, P. and Buseck, P.R. (1992) Structural Variations in Individual Carbonaceous Particles from an Urban Aerosol, *Environ. Sci. Technol.,* **26**, 1967.

48. Wonders, J.H.A.M., Houweling, S., De Bont, F.A.J. and Van Leeuwen, H.P. (1994) Characterization of Aerosol-Associated Lead by DPASV and LAMMA", *Intern. J. Environ. Anal. Chem.*, **56**, 193.

49. Walton, W.H., Dodgson, J., Hadden, G.G. and Jacobsen, M. The Effect of Quartz and Other Non-Coal Dusts in Coal Workers' Pneumoconiosis, in: Inhaled Particles 4, W.H. Walton, Ed. (Oxford Pergamon Press, 1977) pg. 669-690.

50. Tourmann, J.L. and Kaufmann, R. (1993) Laser Microprobe Mass Spectrometry (LAMMS) of Coal Mine Dusts: Single Particle Analysis and Toxicity Correlation, *Intern. J. Environ. Anal. Chem.*, **52**, 215.

51. Le Bouffant, L., Daniel, H., Martin, J.C., Bruyère, S. (1982) Effect of Impurities and Associated Minerals on Quartz Toxicity, *Ann Occup. Hyg.*, **26**, 625.

52. Tourmann, J.L. and Kaufmann, R. (1994) Laser Microprobe Mass Spectrometric (LAMMS) study of Quartz-Related and Non-Quartz Related Factors of the Specific Harmfulness of Coal Mine Dusts, *Ann. Occup. Hyg.*, **38**, 455.

53. Andreae, M.O., Charlson, R.J., Bruynseels, F., Storms, H., Van Grieken, R. and Maenhaut, W. (1986) Internal Mixture of Sea-Salt, Silicates and Excess Sulfate in Marine Aerosols", *Science,* **232**, 1620.

54. Dierck, I., Michaud, D., Wouters, L. and Van Grieken, R. (1992) Laser Microprobe Mass Analysis of Individual North Sea Aerosol Particles, *Environ. Sci. Technol.,* **26**, 802.

55. Qian, G.W. and Ishizaka, Y.J. (1993) Electron Microscope Studies of Methane Sulfonic Acid in Individual Aerosol Particles", *J. Geophys. Res. Oceans,* **98**, 8459.

56. Pardess, D., Levin, Z. and Ganor, E. (1992) A New Method for Measuring the Mass of Sulfur in Single Aerosol Particles, *Atmos. Environ.,* **4**, 675.

57. Cheng, R.J. Shell Structured Marine Aerosol: a Laboratory Observation, Proc. of the Twelfth Annual Meeting of the American Association for Aerosol Research, held at Oak Brook, Illinois, October 11-15, (1993).

58. Cheng, R.J., Blanchard, D.C. and Cipriano, R.J. (1988) The Formation of Hollow Sea Salt Particles from the Evaporation of Drops of Seawater, *Atmos. Environ.,* **22**, 15.

59. Bruynseels, F., Storms, H., and Van Grieken, R. (1988) Characterisation of North Sea Aerosols by Individual Particle Analysis", *Atmos. Environ.*, **11**, 2593.

60. Ottley, C.J. and Harrison, R.M. (1992) The Spatial Distribution and Particle Size of some Inorganic Nitrogen, Sulphur and Chlorine Species over the North Sea, *Atmos. Environ.,* **9**, 1689.

61. Otten, Ph., Bruynseels, F. and Van Grieken, R. (1986) Nitric acid interaction with marine aerosols sampled by impaction", *Bull. Soc. Chim. Belg.,* **95**, 447.

62. Mamane, Y. and Gottlieb, J. (1992) Nitrate Formation on Sea-Salt and Mineral Particles-A Single Particle Approach, *Atmos. Environ.,* **9**, 1763.

63. Mamane, Y. and Pueschel, R.F. (1980) A Method for the Detection of Individual Nitrate Particles", *Atmos. Environ.*, **14**, 629.

64. Injuk, J., Van Malderen, H., Van Grieken, R., Swietlicki, E., Knox, J.M. and Schofield, R. (1993) EDXRF Study of Aerosol Composition Variations in Air Masses Crossing the North Sea," *X-Ray Spectrom.,* **22**, 220.

65. Injuk, J., Breitenbach, L., Van Grieken, R. and Wätjen, U. (1994) Performance of a Nuclear Microprobe to Study Giant Marine Aerosol Particles, *Mikrochim. Acta.*, **144/155**, 313.

66. Fitzgerald, J. (1991) Marine Aerosols: A Review, *Atmos. Environ.*, **25A**, 533.

67. Artaxo, P., Rabello, M.L.C., Maenhaut, W. and Van Grieken, R. (1992) Trace Elements and Individual Particle Analysis of Atmospheric Aerosols from the Antarctic Peninsula, *Tellus,* **44B**, 318.

68. Götz, G. Aerosols and Climate, in: Atmospheric Particles and Nuclei, Eds. G. Götz, E. Mészàros and G. Vali (Akademiai Kiaido, Budapest, 1991).

69. De Bock, L.A., Van Grieken, R.E. and Camuffo, D. Micro-Analysis of Museum Aerosols to Elucidate the Soiling of Paintings: Case of the Correr Museum, Venice, Italy, *Environ. Sci. Technol.,* submitted.

70. Ge, Z., Wexler, A.S. and Johnston, M.V. (1996) Multicomponent aerosol crystallization, *J. Coll. Int. Sci.,* submitted

Figure captions:

Fig 1. Results of line scans on an alumino-silicate fly-ash particle. (Reprinted from Jakšić et al., Nucl. Instr. Meth. B56/57:699-703 (1991), with permission of Elsevier)

Fig 2. The PIXE (left) and proton backscattered spectra (right) of the Siberian fly-ash particle, taken at the three different positions: a) centre, b) upper and c) bottom side of the particle

Fig 3. Auger depth profile of the fly-ash particle; sputtering rate 25 Å min^{-1} (Reprinted from Boni et al., in: Combustion Efficiency and Air Quality, pp. 213-240, I. Hargittai and T. Vidoczy, Eds., with permission of Plenum Press).

Fig 4.

a) X-ray elemental mappings by SEM-EDX on an indoor aerosol particle collected in the Correr museum in Venice, Italy

b) Application of the Image Math program on the elemental X-ray mappings. Ca and Si are clearly associated and 3 alumino-silicate particles as well as a few NaCl particles and an Fe-rich particle appear to be adsorbed at the surface of the particle.

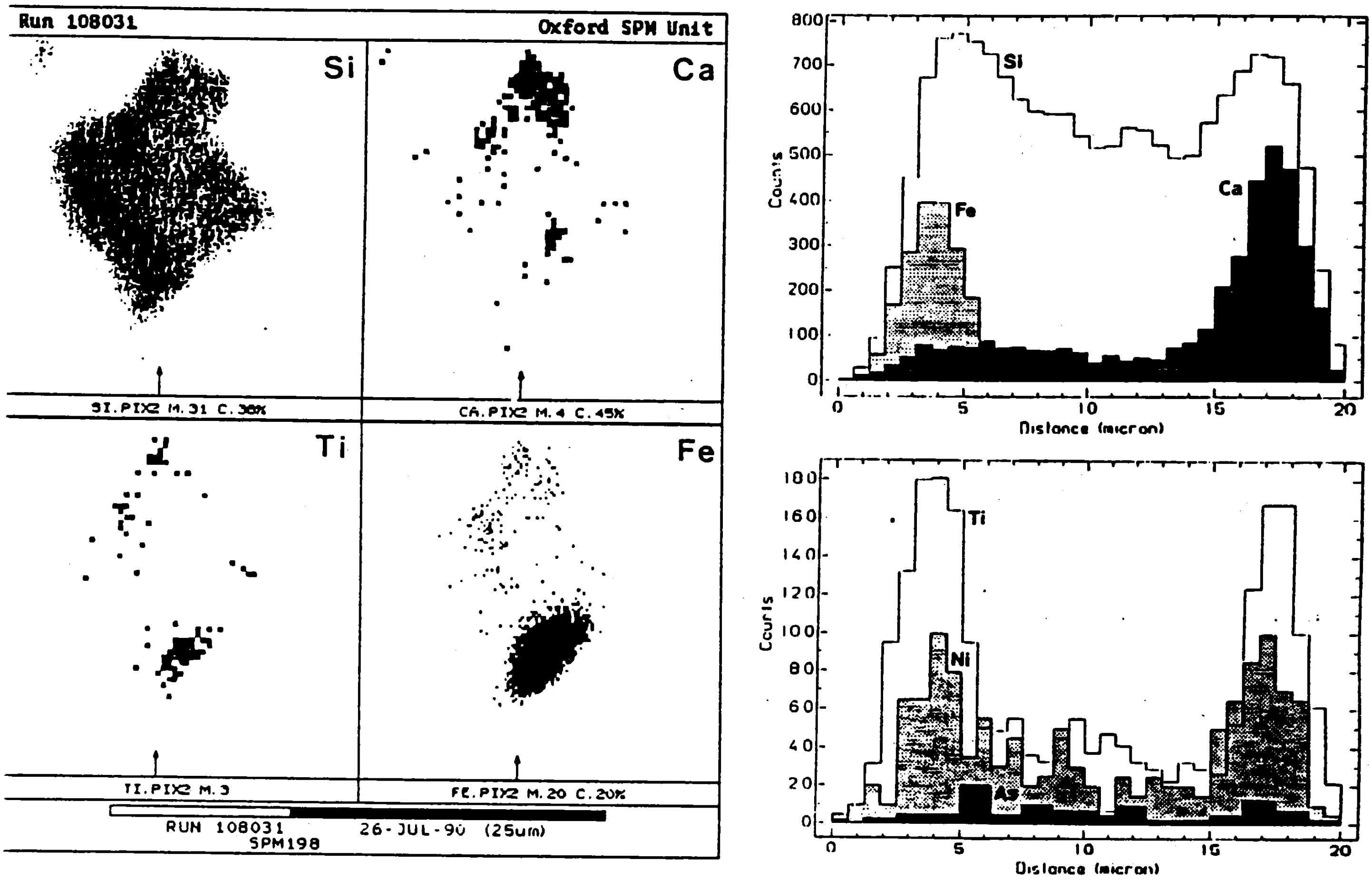
Run 108031
Oxford SPM Unit
Si
Ca
SI.PIX2 M.31 C.38%
CA.PIX2 M.4 C.45%
Ti
Fe
TI.PIX2 M.3
FE.PIX2 M.20 C.20%
RUN 108031
26-JUL-90 (25um)
SPM198
800
700
600
500
400
300
200
100
0
Counts
Si
Fe
Ca
0
5
10
15
20
Distance (micron)
180
160
140
120
100
80
60
40
20
0
Counts
Ti
Ni
As
0
5
10
15
20
Distance (micron)

FIG 1,

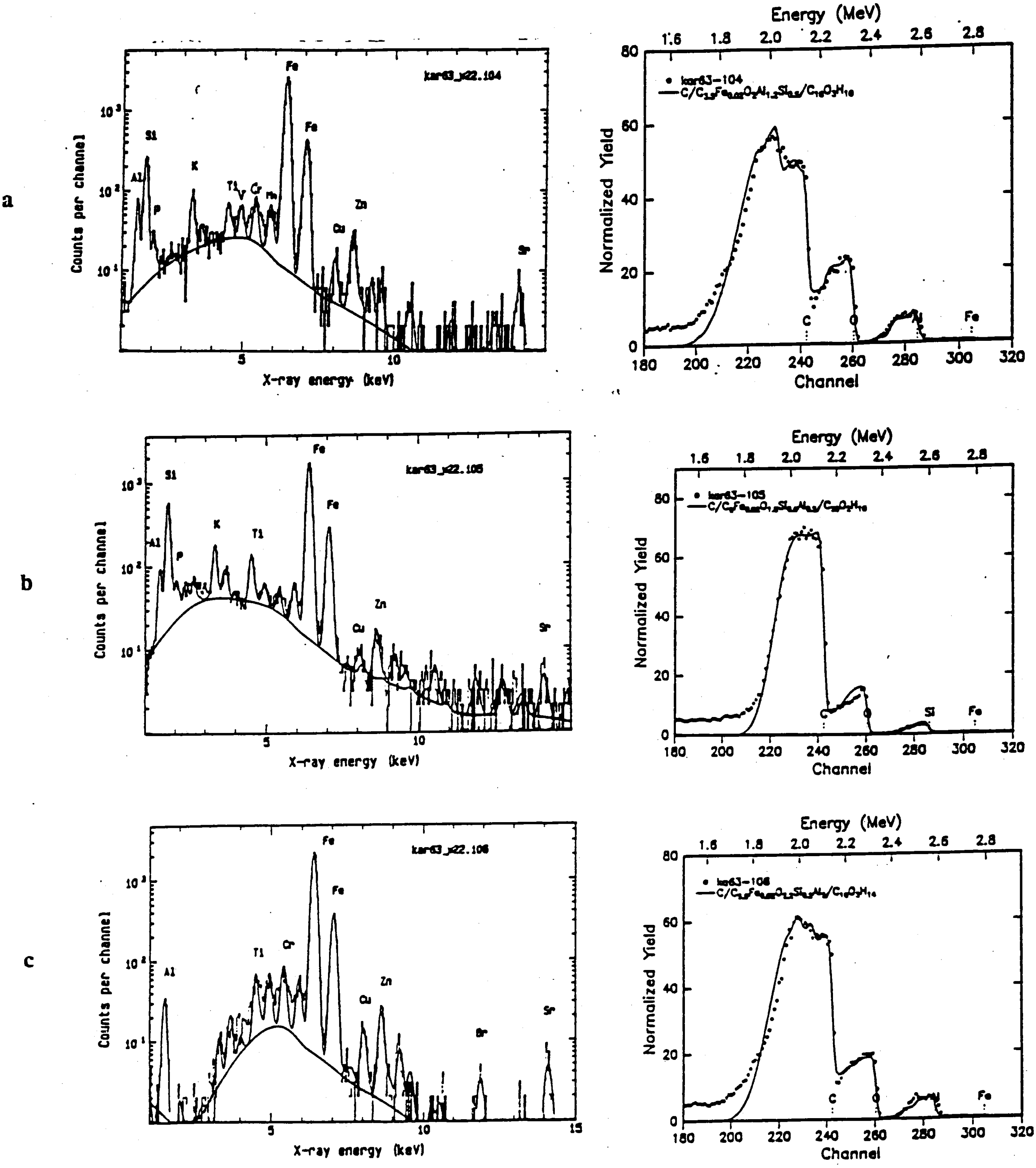
a
kar63_x22.104
Counts per channel
X-ray energy (keV)
Al
Si
P
K
Ti
V
Cr
Mn
Fe
Fe
Cu
Zn
Sr
Energy (MeV)
1.6 1.8 2.0 2.2 2.4 2.6 2.8
• kar63-104
— C/C1.5Fe0.02O2Al1.2Si0.5/C16O3H10
Normalized Yield
Channel
C
O
Fe
b
kar63_x22.105
Counts per channel
X-ray energy (keV)
Al
Si
P
K
Ti
Fe
Fe
Cu
Zn
Sr
Energy (MeV)
• kar63-105
— C/C2Fe0.02O1.5Si0.5Al0.5/C20O2H10
Normalized Yield
Channel
C
O
Si
Fe
c
kar63_x22.106
Counts per channel
X-ray energy (keV)
Al
Ti
Cr
Fe
Fe
Cu
Zn
Br
Sr
Energy (MeV)
• ka63-106
— C/C1.5Fe0.02O2.2Si0.5Al1/C16O3H14
Normalized Yield
Channel
C
O
Fe

FIG 2.

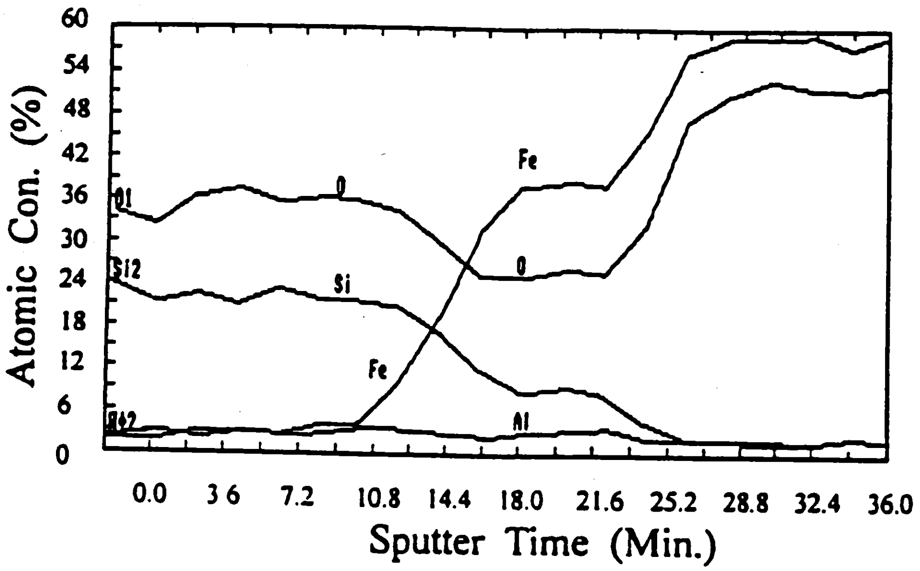
60
54
48
42
36
30
24
18
12
6
0
Atomic Con. (%)
01
O
Fe
O
Si2
Si
Fe
Al2
Al
0.0
3 6
7.2
10.8
14.4
18.0
21.6
25.2
28.8
32.4
36.0
Sputter Time (Min.)

Fig 3.

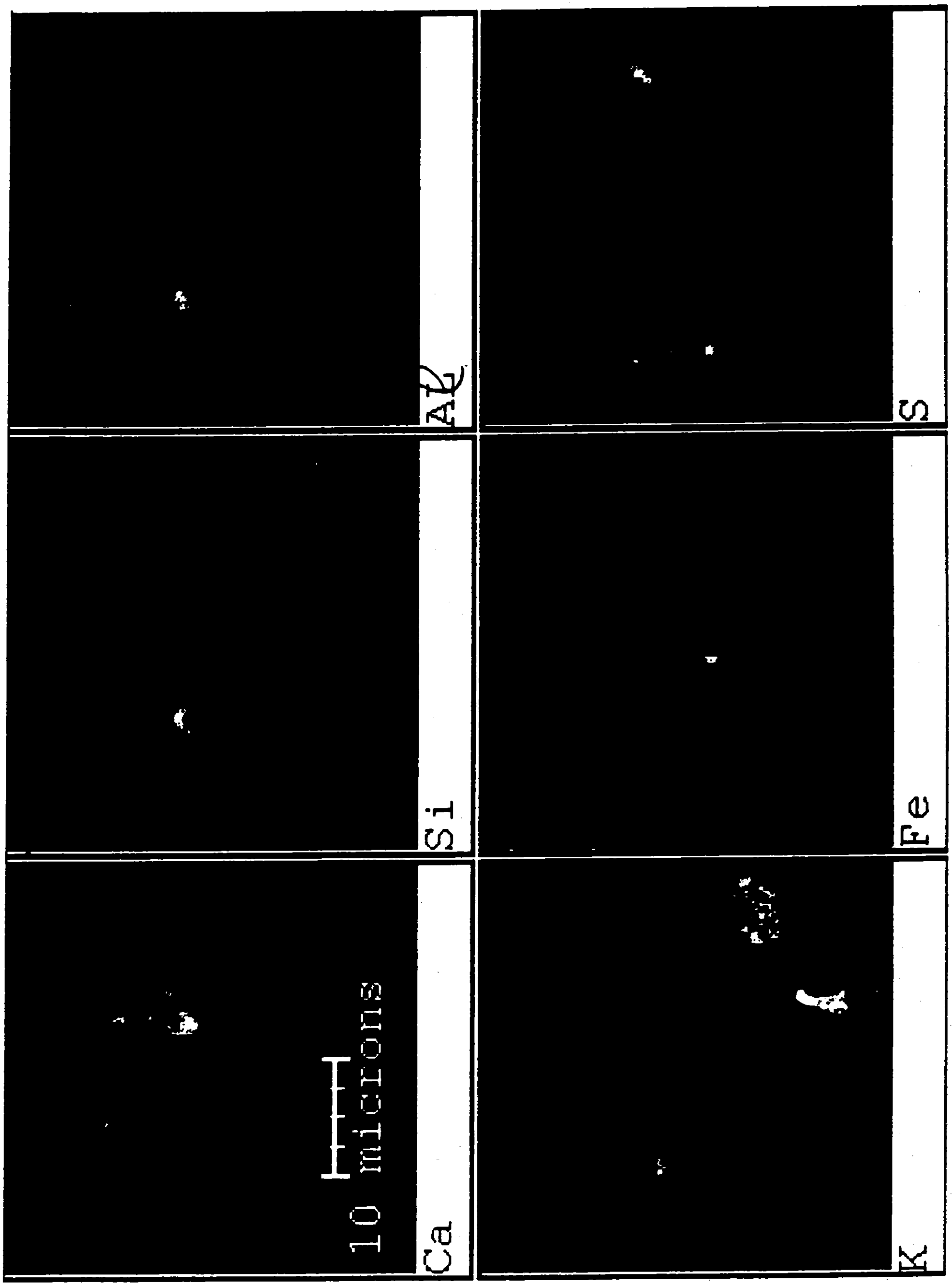

4U

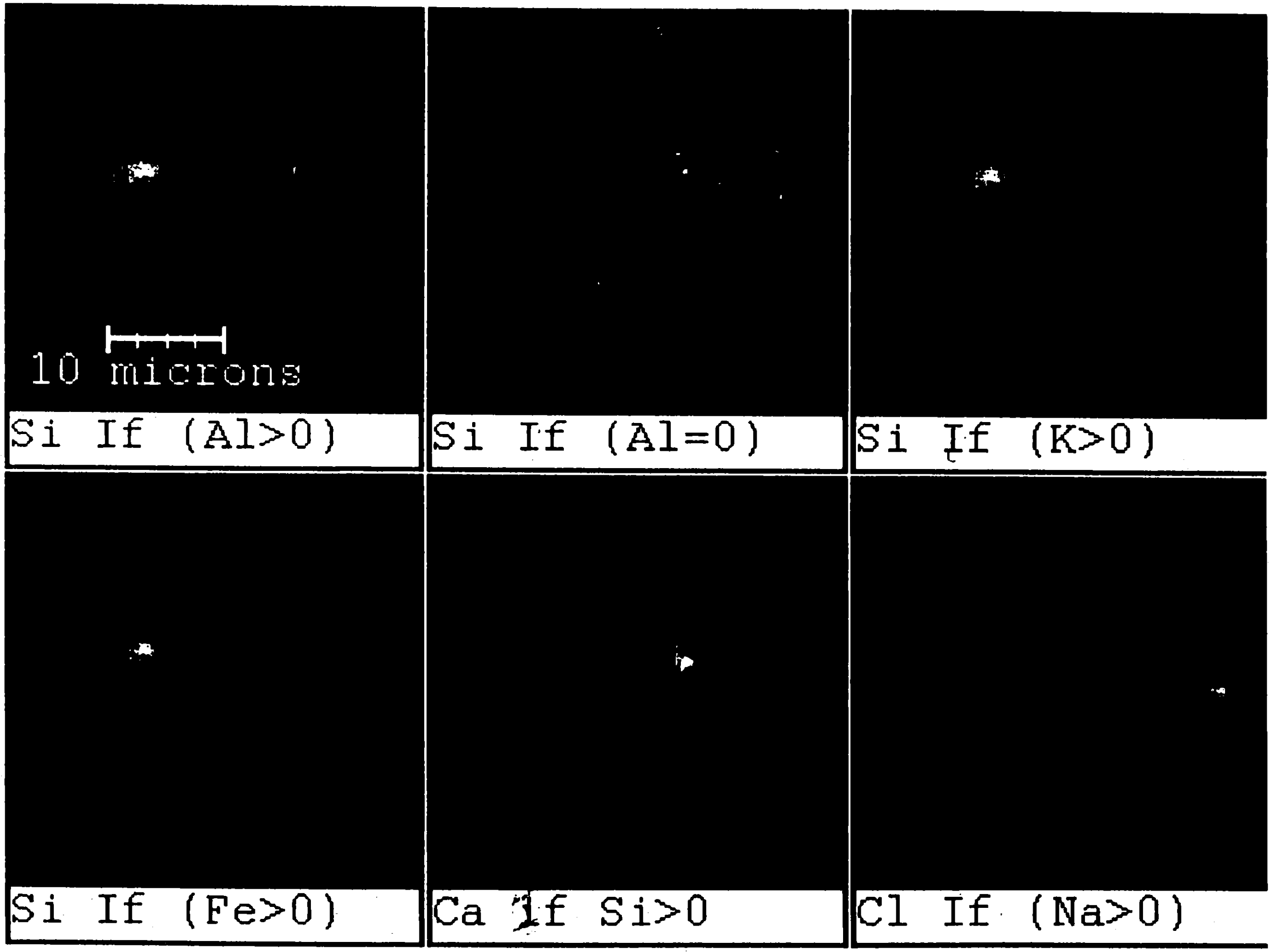
10 microns
Si If (Al>0)
Si If (Al=0)
Si If (K>0)
Si If (Fe>0)
Ca If Si>0
Cl If (Na>0)

4.b

Submitted to Atmos. Environm

Deposition of atmospheric trace elements into the North Sea: coastal, ship, platform measurements and model predictions

Jasna Injuk and René Van Grieken
Department of Chemistry, University of Antwerp (UIA), B-2610 Antwerp, Belgium

Gerrit de Leeuw
TNO Physics and Electronics Laboratory, P.O. Box 96864,
NL-2509 JG The Hague, The Netherlands

ABSTRACT

The atmospheric input of up to 16 heavy metals and other elements into the North Sea is further assessed from aerosol concentrations measured at a coastal station in Belgium, on ships during two cruises, and on a platform, in the years 1992-1994. The Slinn and Slinn model is used to calculate the deposition from the measured aerosol concentrations. The total (dry and wet) deposition into the North Sea environment is estimated to be (in tonnes per year): 560 for V, 1300 for Cr, 650 for Ni, 690 for Cu, 3500 for Zn and 1970 for Pb. The "giant" particles dominate the fluxes. The atmospheric contribution to the total input into the North Sea, including riverine inputs and direct discharges, are estimated to be 28% for Cu, 29% for Zn and 57% for Pb. The inputs estimated from the experimental data are compared with results from a model applied for the same area and period. The experimental and model results agree within 56%, which is considered as "satisfactory" in view of both the experimental and the model uncertainties.

Key words: aerosols, heavy metals, deposition fluxes, North Sea

INTRODUCTION

Budget calculations, based on inputs by rivers, direct discharges, incineration and industrial waste, suggest that atmospheric inputs of metals and nutrients to the world's oceans are significant (Jickells, 1995). This view is supported by measurements at sea that clearly demonstrate not only the importance of the atmospheric input in mass terms but also the nature of the atmosphere/ocean interaction.

In this paper we report on deposition fluxes based on size-segregated airborne concentrations that were obtained by applying the total-reflection X-ray fluorescence (TXRF) analysis technique to impactor samples collected in the North Sea area. Dry deposition velocities were calculated from these concentrations with the Slinn and Slinn (1980) model. Wet deposition fluxes are derived from the mean aerosol concentrations, rainfall intensity and theoretical scavenging rates. In comparison with previous work (Rojas et al., 1993; Baeyens et al., 1990; Ottley and Harrison, 1991; Ottley and Harrison, 1993; Otten et al., 1994), here we combine measurements at a coastal station, on ships and on a platform to assess the atmospheric inputs to the North Sea, and we compare the results with model calculations for the same area and period of time.

In addition, the use of TXRF as an appropriate analytical method for atmospheric studies is confirmed; it allows a short sampling time of, e.g., half an hour, virtually no sample preparation and simultaneous determination of 17 and more elements with detection limits down to 0.2 ng.m^{-3}.

EXPERIMENTAL

Sampling Strategy. The dry and wet deposition fluxes, reported here for the southern and central North Sea area, are derived from airborne concentrations measured over the North Sea in the period between September 1992 and May 1994. A huge data set of more than 1000 mass-segregated samples was collected during research cruises aboard the R/V Belgica (August 21-27, 1993) and Hr. Ms. Tydeman (MAPTIP experiment, October 11 to November 5, 1993 (De Leeuw et al., 1994), on the research platform "Nordsee" (FPN: 54° 42'N, 7° 10'E; NOSE Experiment'92, September 2-21, 1992) and at a station located approximately 100 m from the Belgian coastal line in Blankenberge (from October 1992 to May 1994). The samples on R/V Belgica were taken during a cruise along the east coast of England, starting in Ipswich (52° 3'N, 1° 9'E); the end of cruise was at 54° 27'N, 0° 30'E. The MAPTIP experiment was centred around the Dutch research tower Meetpost Noordwijk (MPN: 52° 16'N, 4° 17'E, 9 km from the Dutch coast). Hr. Ms. Tydeman was used to study lateral homogeneity in this part of the North Sea along tracks of up to 150-200 km from MPN. The sampling locations are indicated in Figure 1.

Size-segregated samples were collected utilizing a 7-stage Battelle cascade-impactor with cut-off diameters of 0.25, 0.5, 1, 2, 4, 8 and 16 µm at a flow-rate of 1.2 $\mathrm{l.min^{-1}}$. The impactor was mounted inside a wind tunnel (Vawda et al., 1992) where a forced air flow was maintained to avoid problems associated with non-isokinetic sampling of large particles (from 4 µm in diameter) with a cut-off that varies with wind direction and wind speed. The tunnel is directed into the wind by means of a light wind vane. A ventilator produces a constant forced air stream inside the tunnel to adjust the linear velocity of the particles in the air exactly to the intake velocity in the sampling device. The aerosol was impacted on polished quartz discs (30 mm diameter, 3 mm thickness) that were also used as target in the TXRF analysis. The discs were cut in a special way to allow for appropriate mounting above the stage orifice. A steel spring presses them firmly against the three disc holders.

Sample Preparation and Analysis. The use of the reflector holders of TXRF as a sample support for the direct impaction of size-segregated airborne material is a rather new method that has not been widely attempted thus far (Schneider, 1989; Salvá et al., 1993; Injuk and Van Grieken, 1995a). Prior to the collection, the quartz discs were coated with silicone to reduce both blow-off and bounce-off effects. This was achieved by dispersing a 5 µl drop of silicone solution (SERVA, Polylab). After sample collection, a Ga solution aliquot was added as an internal standard. Subsequently the samples were dried in an exsiccator under reduced pressure, and analyzed.

All samples were analyzed by TXRF. The prototype TXRF module, used in this study, was developed in the Atominstitut in Vienna (Wobrauschek and Aiginger, 1975). The equipment consists of a 2 kW Mo tube (Philips), TXRF unit and a Kevex Si(Li) detector, with a resolution of 165 eV at the Mn-Kα line. The detector was positioned with the Be-window looking upward, at a distance of about 4 mm from the sample on the reflector. The equipment is designed as a mechanically stable unit; once the adjustments were completed, a series of measurements could be analyzed without any instrumental problems. It generally allows for absolute detection limits down to a few 100 pg. All samples were irradiated for 500 s at 20 mA and 45 kV. X-ray spectra were evaluated with the computer programme AXIL (Van Espen et al., 1986).

RESULTS ANS DISCUSSION

Atmospheric inputs of trace elements into the North Sea were determined from the concentrations of the elements in each of the size-segregated aerosol fractions. Size-dependent deposition velocities were used to calculate the dry deposition fluxes. The meteorological conditions (wind speed, relative humidity) were taken into account for these calculations. For the interpretation the wind direction is also an important factor. Therefore, meteorological parameters were recorded as part of the data sets. In addition the dry deposition fluxes, also the contribution of wet deposition was estimated. Below, the used procedures are described and the resulting fluxes are discussed.

Atmospheric concentrations. The relatively large data set from the 19-month monitoring period at the coastal station in Blankenberge has made it possible to calculate the long-term average atmospheric concentrations of S, Cl, K, Ca, Ti, V, Cr, Mn, Fe, Ni, Cu, Zn, As, Se, Br, Sr and Pb and to separate the data for the summer and winter seasons. The results are reported in Table 1. The average values from the research cruises with the R/V Belgica and with Hr. Ms. Tydeman are presented in Table 2. Finally, the atmospheric concentrations measured at the FPN are given in Table 3. The data in Tables 1 to 3 are arithmetic mean values calculated from the total concentrations in each sample, i.e. the sum of the concentrations measured in each of the seven size classes.

The results are comparable to previously published values for trace element concentrations in the North Sea atmosphere (Injuk and Van Grieken, 1995b). Some differences are observed, which can be attributed to the effect of the air mass history on the aerosol concentrations. In their analysis of aerosol particle size distributions measured at MPN, Van Eijk and De Leeuw (1992) devided their data set in eight sectors based on geographical considerations. For each sector, the concentrations of the aerosol and their wind speed dependence were different and the various source regions could clearly be identified. Obviously, for the analysis of the chemical composition, a similar partitioning of the data will be of crucial importance to explain differences observed between the various sampling sites. In Tables 3 and 4, we have made a crude classification, based on wind direction, of the data measured on the FPN and aboard R/V Belgica. The differences between the concentrations in the indicated wind sectors are obvious. During the whole sampling campaign with the R/V Belgica (Table 4), the wind direction was from the north, except on the first day when the wind was west. As a result, the anthropogenic elements (Ti, Ni, Cu, Zn) have higher concentrations when the wind is from land, i.e. from the source regions (west on R/V Belgica; south-east on MPN) and when the wind is from the open ocean the concentrations are low. Since the concentrations decrease with travel time over the sea (fetch!) a N-S gradient is expected when the wind is from land, and with no source to the North.

This analysis clearly indicates that for the assessment of the total atmospheric input into the North Sea, the climatology is a very important factor with which the emissions in the various source regions must be weighted. Furthermore, thorough consideration should be given to the influence of factors such as the travel time from the source region, precipitation scavenging during advection, and other meteorological conditions that affect the concentration levels. During the MAPTIP experiment, part of the ship time of Hr. Ms. Tydeman was designated to address lateral homogeneity (De Leeuw et al., 1994). The aim was to measure aerosol particle size distributions and meteorological parameters simultaneously at the MPN and on Hr. Ms. Tydeman, during long tracks of the ship up- or downwind from MPN. The preliminary results from the comparison of the data collected simultaneously aboard the ship and on MPN clearly show the effect of meteorological parameters such as wind speed and air temperature on the transport of the air mass over a large water mass and on the aerosol size distributions (De Leeuw et al., to be published). As regards the chemical composition, a similar analysis cannot be made because only one impactor/wind tunnel combination was available. Since this sampler was mounted on the ship, only a comparison can be made between samples near the MPN and at a large distance from the tower (the end points of the trajectories shown in Figure 1), which were consecutively collected. An initial analysis of the impactor samples was presented in (Van Eijk et al., 1995). This analysis was limited to only four elements that are representative for aerosols from anthropogenic sources (Cu, Zn, Pb and Se) and three elements that are characteristic for marine aerosols (Ca, Sr and Cl). In the easterly winds encountered during the larger part of the MAPTIP experiment, the end points of all tracks were downwind from MPN. Hence the concentrations of the anthropogenic elements were expected to decrease along the track, whereas the concentrations of the marine elements were expected to increase as a consequence of the larger fetch, and thus generation over a larger surface. As discussed by Van Eijk et al. (1995), for the marine elements Ca, Sr and Cl, indeed the concentrations were observed to increase with longer fetch, but for the anthropogenic elements, the expected decrease was observed in only 50% of the cases. At present we have no sound explanation for those cases where the concentrations of the anthropogenic elements did not decrease. The MAPTIP data set on chemical composition is too small for a more detailed analysis.

A further complication is the drastic change in meteorological conditions during the MAPTIP experiments, which further limits the use of the data for a more systematic analysis. This change in meteorological conditions resulted in the occurrence of heavy fog, whereas prior to this event the visibility was generally good. Obviously, the aerosol properties had changed, both in a physical sense, as evidenced by the formation of fog, and chemically as shown in Table 5. In Table 5 the concentrations of the selected elements before (samples A and B) and after (samples C, D and E) the change in the meteorological conditions are compared. The general decrease in the concentrations of the marine elements and the increase of the concentrations in the anthropogenic contribution can only qualitatively be understood. The wind speed is the driving factor for most of the exchange processes of aerosols between air and sea. The wind speed during the earlier part of the MAPTIP experiment varied between 5 and 20 m.s^{-1} with wave heights of 0.5-1.5 m, whereas later the wind speed did not exceed 10 m.s^{-1} and wave heights were typically 0.4 m. Most likely the decrease in wind speed resulted in less surface generation and thus smaller concentrations of the marine components. The anthropogenic contribution, for which there are no sources over sea, can only become smaller due to dispersion, deposition at the surface and entrainment at the top of the mixed layer. The wind speed is a governing factor because both the dispersion and the deposition velocity are wind speed dependent. By Van Eijk and De Leeuw (1992), the wind speed dependence of the smaller particles was explained by this effect.

The data obtained with the Battelle cascade impactor consist of the elemental masses on each impaction stage, i.e the mass distribution for a large number of elements. For the assessment of the deposition velocities, which vary strongly with particle mass, it is essential to accurately analyze cascade impactor data. In Figures 2 and 3 the mass distributions for S, Cl, K, Ca, Ti, V, Cr, Mn, Fe, Ni, Cu, Zn, Se, Br, Sr, Zr, Mo and Pb are given. The masses are obviously not log-normally distributed as is they would be for an aerosol from a single source. Obviously the North Sea aerosol originates from multiple sources. Therefore their size distributions are multi-modal and a description in terms of a single log-normal distribution is not appropriate. Elements like K, S, V, Mn, Pb, Ni, Cu, Zn, Se are mostly associated with the small particle range below 1 µm diameter, while elements like Cl, Ca, Sr are found mostly in the larger size range, above 4 µm diameter. Figures 2 and 3 clearly confirm that the smaller aerosol is predominantly of anthropogenic origin, whereas the larger aerosol is of marine origin. This observation justifies our approach to treat the aerosol over the North Sea as a mixture of smaller aerosol of continental origin and a larger aerosol of marine origin (Injuk et al., 1994). Similar approaches have been followed since over a decade to describe the physical properties of the marine aerosol, e.g. by Gathman (1983, 1989).

Dry deposition fluxes. The dry deposition flux, F_d ($ng.m^{-2}.s^{-1}$) of material to the water surface was calculated from the product of atmospheric concentrations, C_a ($ng.m^{-3}$), and the dry deposition velocity, V_d ($m.s^{-1}$). The dry deposition velocity of aerosols is strongly dependent on particle size and meteorological factors, primarily wind speed and humidity. The dry deposition model of Slinn and Slinn allows for taking into account the response of the size of small particles to changes in relative humidity, as well as for impaction and interception mechanisms of deposition. We have used the assumption that the relative humidity at the air-sea interface is 98.3%, and that hygroscopic particles (all elements except Fe-rich particles) instantly reach their equilibrium size [cf. response times calculated by Andreas (1990)]. During our sampling campaign in Blankenberge, the average wind speed was 4.6 $m.s^{-1}$, while during the R/V Belgica cruise and on the "Nordsee" platform, the average wind speed varied from 5 to 10 $m.s^{-1}$. During the MAPTIP experiment the wind speed was from 5 $m.s^{-1}$ to 15 $m.s^{-1}$. The current wind speeds were used to calculate the deposition velocities.

To take into account the mass dependence of the dry deposition velocities, it is necessary to normalize aerosol mass and particle size for the calculation of the total flux. The mass-weighted dry deposition velocities were derived using the following expression:

$$\text{mass-weighted } v_{di} = \sum \frac{v_{di} C_i}{C_i}$$

where V_{di} is the deposition velocity of size fraction i and C_i the mass of a certain element in size fraction i. The mass-weighted dry deposition velocity was calculated for each element in the individual each cascade impactor samples. The arithmetic mean values for the mass-weighted deposition velocities together with the standard deviations are given in Table 6.

For the calculation of the dry fluxes to the sea, the total concentration of an element in each cascade impactor sample was multiplied by the corresponding mass-weighted deposition velocity. The average dry deposition rates and the standard deviations, based on calculations from the different sampling campaigns in '92, '93 and '94 are given in Table 7.

The values for the dry deposition fluxes determined in this work are generally smaller than previously published data (Injuk and Van Grieken, 1995b). These lower values may be the result of using a spatial distribution of measurements, whereas earlier estimates were obtained from extrapolation of point measurements over the whole North Sea. Furthermore, the lower levels, especially for the heavy metals, may also reflect the effect of the many voluntary and enforced emission controls implemented in recent years.

The uncertainty in the dry deposition flux strongly depends on the accuracy of the aerosol size distribution, especially the large size fraction. Numerous workers, (e.g. Dulac et al., 1989; Slinn, 1983; Steiger et al., 1989; Ottley and Harrison, 1993) have shown the dominant contribution of the large particle fraction to the overall dry deposition flux, even if this would contribute only a small fraction to the total mass. This is due to the large deposition velocities associated with the greater particles. The same pattern was also observed in this work. In Figure 4, the dry deposition flux and atmospheric mass are given for each size fraction as a percentage of the total atmospheric mass and dry deposition flux for Cr, Ni, Cu and Zn. The results compare favourably with those presented in earlier publications where the dominance of the largest particle on the overall dry deposition flux was demonstrated.

Based on the average dry deposition rates given in Table 7, the total dry deposition fluxes, in tonnes.y^{-1}, for the whole area of the North Sea have been calculated. The results are presented in Table 8.

Wet deposition fluxes. Wet deposition fluxes (Table 9) were calculated using the scavenging factors recommended by GESAMP (1989): 1500 (S, K, Ca, Br), 1000 (Ti, Fe, Sr), 500 (V, Cr, Mn, Ni, Cu, Zn, Pb) and 200 (As, Se). An annual rainfall above the North Sea of 677 mm.y^{-1} and the average elemental atmospheric concentrations of the whole data set were used in the calculations. In Table 10 average wet deposition fluxes, calculated from the values given in Table 9, are given together with the total amount of wet deposited material in tonnes.y^{-1}. The data presented in Table 10 suggest that on average wet deposition fluxes are approximately a factor of 3 larger than the dry deposition fluxes, for all elements of interest.

Total deposition fluxes. In Table 11, the estimates for the total (dry and wet) atmospheric inputs to the North Sea are presented together with the most recently published values given by OSPARCOM (1993). Unfortunately, from OSPARCOM compiled data are available for only few elements. For Ni, Cu, Zn, As and Pb, the total deposition fluxes obtained in this study are of similar order of magnitude as those reported by OSPARCOM.

Table 12 summarizes information on riverine, direct and atmospheric inputs to the North Sea together with the disposal at sea for some heavy metals. It is clear that substantial amounts of metals are introduced into the marine environment through the rivers and the atmosphere. The atmospheric deposition contributes 28% (Cu), 29% (Zn) and 57% (Pb). The impact of smaller point sources can, however, be highly significant and should not be ignored. In order to reduce inputs via the atmosphere, reduction of emissions at the source will usually prove to be the most effective method.

The atmospheric input data, presented here, must be used with great care: the method of extrapolating measurements at a coastal station (although in this study we used also data from two ships, platform and from an off-shore tower) is crude and can result in an overestimate of inputs to the open sea. Furthermore, the accuracy is dependent on the accuracy of our concentration measurements (20%) and deposition calculations (50%) and also on the accuracy of the estimate of the other input routes (30%).

Comparison with model calculations. The indirect deposition calculations were compared with the results obtained from a model, calculated for the same area and period. The model used was the so-called EUTREND model developed at the Dutch National Institute of Public Health and Environmental Protection (Van Jaarsveld et al., 1986). It is a statistical long-range version of the Gaussian plume model, i.e. the dispersion from a source is assumed to follow the prevailing wind direction and wind speed within a sector of 30% in the horizontal plane. Atmospheric processes included in the model are: emission, dispersion, advection, chemical conversion and wet and dry deposition. The model describes the behaviour of pollutants attached to particles as a function of particle size. The emission is considered to be distributed over five size classes: < 0.95, 0.95 - 4, 4 - 10, 10 - 20, >20 µm. The model calculations are performed for each of the size classes separately, with specific deposition properties for each class. Chemical reaction rates used in the model are independent of concentration levels. The model is applied here using a fixed receptor grid over the North Sea area with a 0.5° long. x 0.25° lat. resolution. Emission factors for heavy metals were taken from the PARCOM-ATMOS emission factor manual (Van der Most and Veldt, 1992).

In Table 13 the calculated annually averaged concentrations of Ni, Cu, Zn and Pb are compared with 'experimental' values, for the North Sea and for the Belgium coast. On average the measured and calculated values agree within a variation of 44 - 100%. The average discrepancy between the indirectly calculated deposition rates and the modelled ones is within a factor of ca. 2 (Table 14). We note here that the total uncertainty of the results is a consequence of uncertainties introduced by the model concept, in compound specific parameters and in the emission estimates. The range of uncertainty in the emissions is wide and ranges from a factor of 2 to 3.5. This range must be considered as a maximum margin (Baart et al., 1995). Also, there is a large uncertainty in the experimental values. Taking into account all these uncertainties, we can conclude that the agreement between the atmospheric inputs estimated from our measurements and those calculated with the model is quite satisfactory.

CONCLUSIONS

In the period from 1992 to 1994, an extensive research program has been carried out for the North Sea environment, aiming to assess more quantitatively the total (dry and wet) atmospheric deposition fluxes. The fluxes were calculated from a large set of *in situ* measured particle size distributions and their elemental concentrations, using the model of Slinn and Slinn. Comparison of the results with those from a model for the same area and period shows that they reasonably agree and the observed differences are acceptable.

A rather new approach was used for the determination by TXRF of trace element concentrations in size-segregated aerosol deposits. The aerosol particles were deposited directly on the quartz discs which also served as sample supports for the TXRF analysis.

The determined total (dry + wet) deposition fluxes for 16 elements (S, K, Ca, Ti, V, Cr, Mn, Fe, Ni, Cu, Zn, As, Se, Br, Sr and Rb) have pointed out the importance of the atmosphere as a pathway for deposition of pollutants into the North Sea.

ACKMOWLEDGEMENTS

This work was supported by the Belgian State-Prime Minister's Service-office for Scientific, Technical and Cultural Affairs, in the framework of the Impulse Programme in Marine Sciences (Contract MS/06/050) and in the framework of EUROTRAC Programme (Contract EU 7/08), and by the Belgian Ministry of Public Health and the Environment, Department of Protection against Ionizing Radiation. The MAPTIP experiments were supported by the Netherlands Ministry of Defence (A91-KM-615), the US Office of Naval Research (Grant N00014-91-J-1948) and NATO (Grants 6056 and 6092). The measurements aboard Hr. Ms. Tydeman were made by Dr. F.P. Neele. Computational support and detailed model calculations presented in this paper were made by Arthur Baart from the TNO Institute of Environmental Sciences, Energy Research and Process Innovation, in the framework of EC DG XII project EV5V-CT93-0313.

REFERENCES

Andreas, E.L. (1990) Time constants for the evolution of sea spray droplets. Tellus. **B 42**, 481-497.

Baeyens, W., Dehairs, F. and Dedeurwaerder, H. (1990) Wet and dry deposition fluxes above the North Sea. Atmos. Environ. **24A,** 7, 1693-1703.

Baart, A.C., Berdowski, J.J.M., van Jaarsveld, J.A. (1995) Calculation of atmospheric deposition of contaminants on the North Sea. TNO Institute of Environmental Sciences, Delft, The Netherlands, Report No. TNO-MW-R95/138.

De Leeuw, G., Van Eijk, A.M.J., Jensen, D.R. (1994) MAPTIP experiment, Marine Aerosol Properties and Thermal Imager Performance: An overview. TNO Physics and Electronics Laboratory, Report FEL-94-A140.

De Leeuw, G., Moerman, M., Van Eijk, A.M.J. to be published

Dulac, F., Buat-Menard, P., Ezat, U., Melki, S. and Bergametti, G. (1989) Atmospheric input of trace metals to the Western Mediterranean: uncertainties in modelling dry deposition from cascade impactor data. Tellus. **41B,** 362-378.

Gathman, S.G. (1983) Optical properties of the marine aerosol as predicted by the Navy aerosol model. Opt. Eng. **22**, 57-62.

Gathman, S.G. (1989) A preliminary description of NOVAM, the Navy Oceanic Vertical Aerosol Model. Naval Research Laboratory, Washington D.C., U.S.A., NRL Report 9200.

GESAMP-IMO/FAO/UNESCO/WMO/WHO/IAEA/UN/UNEP Joint Group of Experts on the Scientific Aspects of Marine Pollution. The Atmospheric Input of Trace Species to the World Ocean. Rep. Stud. GESAMP (38) 1989.

Injuk, J., Breitenbach, L., Van Grieken, R., and Wätjen, U. (1994) Perfomance of nuclear microprobe to study giant marine aerosol particles. Mikrochim. Acta. **114/115,** 313-321.

Injuk, J. and Van Grieken, R. (1995a) Optimisation of total-reflection X-ray fluorescence spectrometry for aerosol analysis. Spectrochim. Acta. **B 50**, 1787-1803.

Injuk, J. and Van Grieken, R. (1995b) Atmospheric concentrations and deposition of heavy metals over the North Sea: a literature review. J. Atmos. Chem. **20,** 179-212.

Jickells, T. (1995) Atmospheric inputs of metals and nutrients to the oceans: their magnitude and effects. Mar. Chem. **48**, 199-214.

OSPARCOM (1993) North Sea Assessment Report 2b. North Sea Task Force. Oslo and Paris Commissions, London. Olsen and Olsen, Fredensburg, Denmark.

Otten, Ph., Injuk, J. and Van Grieken, R. (1994) Elemental concentrations in atmospheric particulate matter sampled on the North Sea and the English Channel. Sci. Total Environ. **155**, 131-149.

Ottley, C.J. and Harrison, R.M. (1991) The atmospheric input flux of trace metals to the North Sea: a review and recommendations for research. Sci. Total Environ. **100**, 301-318.

Ottley, C.J. and Harrison, R.M. (1993) Atmospheric dry deposition flux of metallic species to the North Sea. Atmos. Environ. **27A**, 685-695.

Rojas, C.M., Injuk, J., Van Grieken, R. and Laane, R.M. (1993) Dry and wet deposition fluxes of Cd, Cu, Pb and Zn into the Southern Bight of the North Sea. Atmos. Environ. **27A**, 251-259.

Salvá, A., von Bohlen, A., Klockenkämper, R. and Klockow, D. (1993) Multielement analysis of airborne particulate matter by total reflection X-ray fluorescence. Quimica Analitica. **12**, 57-62.

Schneider, B. (1989) The determination of atmospheric trace metal concentrations by collection of aerosol particles on sample holders for total-reflection X-ray fluorescence. Spectrochim. Acta. **44B**, 519-523.

Slinn, S.A. and Slinn, W.G.N. (1980) Predictions for particle deposition on natural waters. Atmos. Environ. **14**, 1013-1016.

Slinn, W.G.N. (1983) Air to sea transfer of particles. In: Air-Sea Exchange of Gases and Particles. Liss, P.S. and Slinn, W.G.N. (eds.), D. Reidel Publishing, Dordrecht, Holland, p. 299.

Steiger, M., Schulz, M., Schwikowski, M., Naumann, K. and Dannecker, W. (1989) Variability of aerosol size distribution above the North Sea and its implication to the dry deposition estimates. J. Aerosol Sci. **20**, 1229-1232.

Van der Most, P.F.J. and Veldt, C. Emission factors manual PARCOM-ATMOS. Emission factors for air pollutants 1992. TNO Report 92-235, Apeldoorn, The Netherlands.

Van Eijk, A.M.J. and De Leeuw, G. (1992) Modelling aerosol particle size distributions over the North Sea. J. Geophys. Res. **97** (Vol. C9), 14417-14429.

Van Eijk, A.M.J., Bastin, F.H., Neele, F.P., De Leeuw, G., Injuk, J. (1995) Characterisation of atmospheric properties during MAPTIP. In: "Propagation assessment in coastal environments", Advisory Group for Aerospace Research and Development (AGARD-CP 567, NATO), pp. 19-1 to 19-8.

Van Espen, P., Janssens, K. and Nobels, J. (1986) Axil-PC, Software for the analyses of complex X-ray spectra. Chemometrics Intelligent Lab. Syst. **1**, 109-114.

Van Jaarsveld, J.A.; van Aalst, R.M.; Onderdelinden, D. Deposition of metals from the atmosphere into the North Sea: Model calculations. RIVM, Bilthoven, Report No. 842015002, **1986**.

Vawda, Y., Colbeck, I., Harrison, R.M., and Nicholson, K.W. (1992) Assessment of the performance of a tunnel sampler and cascade impactor system for ambient air sampling. J. Aerosol Sci. **23**, 233-243.

Wobrauschek, P. and Aiginger, H. (1975) Total-reflection X-ray fluorescence spectrometric determination of elements in nanogram amounts. Anal. Chem. **47**, 852-855.

Figure Captions

Figure 1. The North Sea map with the sampling locations (Belgian coastal station-Blankenberge, "Nordsee" platform-FPN, MPN platform) and cruise tracks of R/V Belgica and Hr. Ms. Tydeman.

Figure 2. Average mass distributions for K, Br, S, Cu, Zn, Se, V, Mn, Pb and Ni in aerosol samples collected over the North Sea.

Figure 3. Average mass distributions for Ca, Sr, Cl, Ti, Mo, Cr, Zr and Fe in aerosol samples collected over the North Sea.

Figure 4. Relative contributions of each size fraction to the atmospheric mass and dry deposition fluxes for Cr, Ni, Cu and Zn.

Figure 5. Concentration maps of Ni, Cu, Zn and Pb in the North Sea area - modelled values

Figure 6. Deposition maps of Ni, Cu, Zn and Pb in the North Sea area - modelled values

Table 1. Atmospheric concentrations determined at the Belgian coastal station in Blankenberge in the period October '92 - May '94; arithmetic mean, standard deviation and range (all in ng.m^{-3}), ND=below detection limit

Element	Blankenberge - summer				Blankenberge - winter			
	Arith. mean	St. dev.	Min.	Max.	Arith. mean	St. dev.	Min.	Max.
S	1240	590	642	2392	490	270	176	949
Cl	1140	830	70	2731	1260	1070	66	2035
K	130	70	47	295	110	60	30	141
Ca	180	120	34	405	130	120	33	335
Ti	13.9	10.5	4.1	37.8	5.5	3.7	1.9	13.1
V	5.4	3.8	1.9	12.9	3.6	2.3	0.2	6.7
Cr	6.7	8.9	0.5	32.1	3.5	2.7	0.3	6.4
Mn	13.6	8.6	3.1	22.1	4.6	2.6	0.4	8.6
Fe	310	190	85	551	130	100	32	262
Ni	4.1	5.1	0.9	19.1	2.1	1.2	0.2	3.1
Cu	3.9	2.7	0.5	6.3	3.2	2.8	0.2	12.7
Zn	22.5	19.5	3.9	68	21.8	18.2	4.1	62.3
As	2.3	1.8	0.4	6.1	0.28	0.66	ND	2.24
Se	0.5	0.2	0.4	0.7	ND	ND	ND	ND
Br	17.8	13.3	2.2	38.9	16.1	14.5	2.1	20.7
Sr	6.4	4.3	0.7	15.2	4.1	4.2	ND	6.9
Pb	14.3	3.2	1.6	10.1	12.1	15.2	ND	52.7

Table 2. Atmospheric concentrations determined during research cruises aboard R/V Belgica and Hr. Ms. Tydeman in '93; arithmetic mean, standard deviation and range (all in ng.m^{-3}), ND=below detection limit

Element	North Sea cruises Hr. Ms. Tydeman				North Sea cruises R/V Belgica			
	Arith. mean	St. dev.	Min.	Max.	Arith. mean	St. dev.	Min.	Max.
S	1650	1110	179	2886	320	190	103	380
Cl	430	580	24	1515	620	450	107	1459
K	67	10	58	79	62	18	48	93
Ca	89	59	31	151	68	20	43	92
Ti	5.2	0.5	ND	5.7	4.6	2.9	1.8	9.7
V	2.3	1.5	0.6	5.1	0.7	0.3	ND	0.9
Cr	2.9	2.6	0.3	7.2	1.5	0.4	0.4	7.2
Mn	3.3	1.2	1.2	5.3	3.1	1.5	2.6	3.4
Fe	100	30	51	122	80	70	31	217
Ni	4.4	4.6	1.4	13.5	1.7	1.2	0.5	3.3
Cu	4.2	3.3	0.7	9.4	1.9	1.0	1.5	2.3
Zn	20.5	14.7	3.1	42.2	6.2	4.2	1.1	13.2
As	ND	ND	ND	ND	ND	ND	ND	ND
Se	1.4	0.8	0.07	1.9	ND	ND	ND	ND
Br	3.9	2.9	1.9	9.7	3.6	3.9	1.6	10.7
Sr	0.9	0.6	0.2	1.9	1.1	0.6	0.4	1.6
Pb	17.4	13.1	1.6	37.4	ND	ND	ND	ND

Table 3. Average airborne concentrations and associated standard deviations (ng.m^{-3}) as a function of wind direction, measured on the "Nordsee" platform in '92

Element	Northwest -north	Southwest -west	Southeast -east	All sectors (weighted)
S	180±40	250±50	400±180	270±50
Cl	700±50	440±40	210±100	260±30
Cr	0.4±0.5	0.5±0.24	7.9±6.3	1.7±0.5
Mn	1.2±0.2	18.4±0.4	22.7±1.9	14.4±0.5
Fe	29±1	76±1	400±7	140±2
Ni	0.8±0.5	2.2±0.3	3.5±0.7	1.4±0.3
Cu	1.1±0.2	3.4±0.2	6.7±0.7	3.5±0.2
Se	0.5±0.2	1.1±0.2	1.2±0.7	0.9±0.2
Br	10.7±0.3	10.8±0.4	7.9±0.8	10.1±0.3
Sr	4.5±0.2	6.3±0.3	7.4±0.8	6.0±0.2
Pb	10.8±0.8	12.6±0.5	24.9±2.1	15.1±1.1

Table 4. Elemental concentrations in aerosols (ng.m^{-3}) measured aboard R/V Belgica in October '93 as a function of wind direction

	Sample I (east)	Samples II+III+IV+V - mean value (north)
Cl	107	660
Ti	9.7	3.3
Ni	3.3	1.3
Cu	2.3	1.2
Zn	13.6	4.5

Table 5. Elemental aerosol concentrations (ng.m^{-3}) during MAPTIP'93

	A+B	C+D+E
Cl	1020	32
Ca	113	74
Sr	1.34	0.61
Cu	1.0	6.3
Zn	4.0	31
Pb	4.7	26
Se	0.08	1.52

Table 6. Mass-weighted deposition velocities V_d (cm.s^{-1}), together with st. dev., for different aerosol size distributions as outlined in the text. The average wind speed during each sampling campaign is indicated.

	Blankenberge - summer	Blankenberge - winter	"Nordsee"-platform	R/V Belgica	Hr. Ms. Tydeman	
	5.0 m s^{-1}	5.0 m s^{-1}	7.8 m s^{-1}	8.2 m s^{-1}	5.0 m s^{-1}	15.0 m s^{-1}
S	0.33 (0.14)	0.18 (0.09)	-	0.50 (0.18)	0.08 (0.01)	0.90 (0.25)
K	0.43 (0.13)	0.45 (0.15)	-	0.61 (0.20)	0.22 (0.04)	1.16 (0.25)
Ca	0.50 (0.12)	0.58 (0.17)	-	0.62 (0.19)	0.55 (0.03)	1.70 (0.17)
Ti	0.42 (0.16)	0.42 (0.12)	-	0.27 (0.16)	0.57 (0.07)	1.27 (0.90)
V	0.24 (0.16)	0.14 (0.08)	-	0.24 (0.18)	0.27 (0.07)	0.64 (0.15)
Cr	0.46 (0.26)	0.71 (0.34)	0.42 (0.21)	0.80 (0.21)	0.42 (0.08)	1.41 (0.38)
Mn	0.42 (0.21)	0.53 (0.19)	0.36 (0.18)	0.26 (0.09)	0.21 (0.09)	1.10 (0.27)
Fe	0.44 (0.14)	0.55 (0.18)	0.34 (0.10)	0.49 (0.10)	0.32 (0.06)	1.34 (0.05)
Ni	0.19 (0.08)	0.61 (0.31)	0.23 (0.09)	0.15 (0.08)	0.27 (0.03)	0.78 (0.25)
Cu	0.32 (0.07)	0.50 (0.13)	0.26 (0.10)	0.21 (0.07)	0.45 (0.34)	1.26 (0.37)
Zn	0.32 (0.17)	0.29 (0.14)	-	0.40 (0.12)	0.20 (0.08)	0.90 (0.14)
As	0.35 (0.24)	0.30 (0.19)	-	-	-	-
Se	0.63 (0.29)	-	-	-	0.07 (0.02)	0.69 (0.05)
Br	0.51 (0.24)	0.39 (0.23)	-	0.43 (0.12)	0.20 (0.02)	1.89 (0.08)
Sr	0.62 (0.15)	0.49 (0.18)	-	0.48 (0.24)	0.71 (0.33)	1.86 (0.05)
Pb	0.07 (0.06)	0.11 (0.09)	0.15 (0.11)	-	0.08 (0.004)	0.79 (0.71)

Table 7. Dry deposition fluxes into the North Sea ($kg.km^{-2}.y^{-1}$) together with the standard deviations.

	Blankenberge - winter	Blankenberge - summer	"Nordsee" - platform	R/V Belgica	Hr. Ms. Tydeman
S	108 (77)	28 (15)	-	570 (560)	75 (23)
K	18 (13)	16 (9)	-	13 (12)	13 (12)
Ca	29 (22)	25 (23)	-	13 (10)	33 (30)
Ti	1.54 (1.39)	0.74 (0.49)	-	0.36 (0.18)	0.96 (1.56)
V	0.31 (0.29)	0.17 (0.07)	-	0.05 (0.03)	0.21 (0.06)
Cr	1.34 (2.11)	0.26 (0.18)	0.64 (0.17)	1.39 (0.92)	1.64 (2.09)
Mn	1.53 (1.35)	0.78 (0.44)	1.47 (0.13)	0.25 (0.14)	0.40 (0.17)
Fe	36 (29)	24 (18)	18 (3)	13 (10)	22 (16)
Ni	0.16 (0.14)	0.42 (0.23)	0.51 (0.09)	0.08 (0.09)	0.48 (0.51)
Cu	0.34 (0.25)	0.49 (0.62)	0.29 (0.04)	0.13 (0.09)	0.83 (0.97)
Zn	1.55 (1.49)	1.99 (1.66)	-	0.79 (0.87)	1.57 (0.58)
As	0.25 (0.22)	0.003 (0.006)	-	-	-
Se	0.09 (0.07)	-	-	-	0.03 (0.004)
Br	4.52 (5.36)	1.67 (1.49)	-	4.87 (0.74)	1.76 (2.54)
Sr	1.58 (1.35)	0.53 (0.54)	-	1.58 (0.74)	0.52 (0.46)
Pb	0.20 (0.25)	0.44 (0.56)	0.71 (0.13)	ND	0.59 (0.29)

Table 8. Calculated dry deposition fluxes to the North Sea

Element	Average dry flux and st.dev. (kg km^{-2} y^{-1})	Total dry flux to the North Sea (tonnes y^{-1})
S	196 (220)	103,600
K	15 (2)	8,000
Ca	25 (7)	13,300
Ti	0.91 (0.42)	490
V	0.17 (0.10)	90
Cr	1.10 (0.52)	560
Mn	0.89 (0.53)	470
Fe	22 (8)	11,900
Ni	0.33 (0.17)	180
Cu	0.42 (0.23)	220
Zn	1.47 (0.43)	790
As	0.13 (0.13)	70
Se	0.06 (0.03)	30
Br	3 (1)	1,700
Sr	1.05 (0.53)	560
Pb	0.49 (0.20)	60

Table 9. Wet deposition fluxes (kg km^{-2} y^{-1}) into the North Sea and standard deviations, calculated for different sampling campaigns

	Blankenberge-summer	Blankenberge-winter	"Nordsee"-platform	R/V Belgica	Hr.Ms. Tydeman
S	1050 (500)	410 (230)	-	270 (160)	1390 (940)
K	110 (62)	60 (51)	-	55 (15)	57 (8)
Ca	150 (100)	120 (110)	-	58 (17)	75 (50)
Ti	7.8 (5.9)	3.1 (2.1)	-	2.6 (1.6)	2.9 (0.3)
V	1.5 (1.1)	1.1 (0.65)	-	0.2 (0.1)	0.7 (0.4)
Cr	1.9 (2.5)	1.0 (0.8)	1.2 (0.2)	1.6 (0.3)	0.8 (0.7)
Mn	3.8 (2.4)	1.3 (0.7)	4.1 (0.8)	0.9 (0.4)	0.9 (0.3)
Fe	180 (110)	76 (58)	79 (2)	45 (39)	57 (15)
Ni	1.2 (1.4)	0.6 (0.3)	1.7 (0.5)	0.5 (0.4)	1.2 (1.3)
Cu	1.1 (0.8)	0.6 (0.8)	1.0 (0.2)	0.6 (0.3)	1.2 (0.9)
Zn	6.4 (5.5)	6.2 (5.1)	-	1.7 (1.2)	5.8 (4.2)
As	0.2 (0.2)	0.03 (0.07)	-	-	-
Se	0.06 (0.02)	-	-	-	0.2 (0.1)
Br	15.1 (11.2)	13.6 (3.8)	-	3.0 (2.8)	3.3 (2.5)
Sr	3.6 (2.4)	2.3 (2.4)	-	0.6 (0.4)	0.5 (0.3)
Pb	1.3 (0.9)	3.4 (4.3)	4.3 (0.4)	-	4.9 (6.7)

Table 10. Wet deposition fluxes to the North Sea

Element	Average wet flux and st.dev. (kg km^{-2} y^{-1})	Total wet flux to the North Sea (tonnes y^{-1})
S	780 (459)	417,600
K	71 (23)	37,700
Ca	103 (38)	54,800
Ti	4.1 (2.2)	2,200
V	0.88 (0.48)	470
Cr	1.33 (0.44)	710
Mn	1.73 (1.21)	920
Fe	89 (52)	47,400
Ni	0.88 (0.33)	470
Cu	0.88 (0.28)	470
Zn	5.03 (1.93)	2,700
As	0.12 (0.09)	62
Se	0.13 (0.07)	70
Br	8.75 (5.63)	4,700
Sr	2.03 (1.48)	1,100
Pb	3.20 (1.47)	1,700

Table 11. Total (dry + wet) deposition fluxes to the North Sea and comparison with the literature values

Element	Total flux - this work (tonnes y^{-1})	Total flux - OSPARCOM (1993) (tonnes.y^{-1})
S	521,000	-
K	45,700	-
Ca	68,100	-
Ti	2,700	-
V	560	-
Cr	1,300	-
Mn	1,400	-
Fe	59,300	-
Ni	650	180 - 400
Cu	690	320 - 740
Zn	3,500	2,700 - 5,500
As	130	95 - 220
Se	100	-
Br	6,400	-
Sr	1,600	-
Pb	1,970	1,960 - 1,700

Table 12. Estimates of inputs (tonnes.y^{-1}) to the North Sea via various pathways (OSPARCOM, 1993)

Pathway	**Cu**	**Zn**	**Pb**
Riverine inputs*	1,200	6,400	1,000
Direct inputs**	290	1,300	160
Atmosphere (this work)	690	3,500	2,000
Incineration	4.6	5.7	4.9
Industrial waste***	180	440	220
Sewage sludge	76	160	77

* here it must be recognized that for some rivers, such as those in northeast and southeast England, inputs of metals such as Cu, Zn, Pb are largely derived from natural ores

** sewage effluents, sewage sludge, industrial effluents, polder effluents

*** chemical waste, slurries, fly-ash, minestones and colliery tailings

Table 13. Comparison of measured and calculated concentrations of Ni, Cu, Zn and Pb for the North Sea area (ng.m^{-3})

	The North Sea		Belgian coast	
	Model	Measurements	Model	Measurements
Ni	< 3	2.5	3-5	3.1
Cu	3-5	3.2	5-7	3.6
Zn	< 30	13	30-60	22
Pb	< 30	11	30-60	13

Table 14. Comparison of total deposition fluxes to the North Sea determined indirectly (measurements & Slinn and Slinn model) with modelled values ($kg.km^2.y^{-2}$)

	Ni	Cu	Zn	Pb
Measurements & Slinn and Slinn model	1.21	1.30	6.5	3.7
Model	0.25-0.5	0.25-0.5	2.5-5	2.5-5

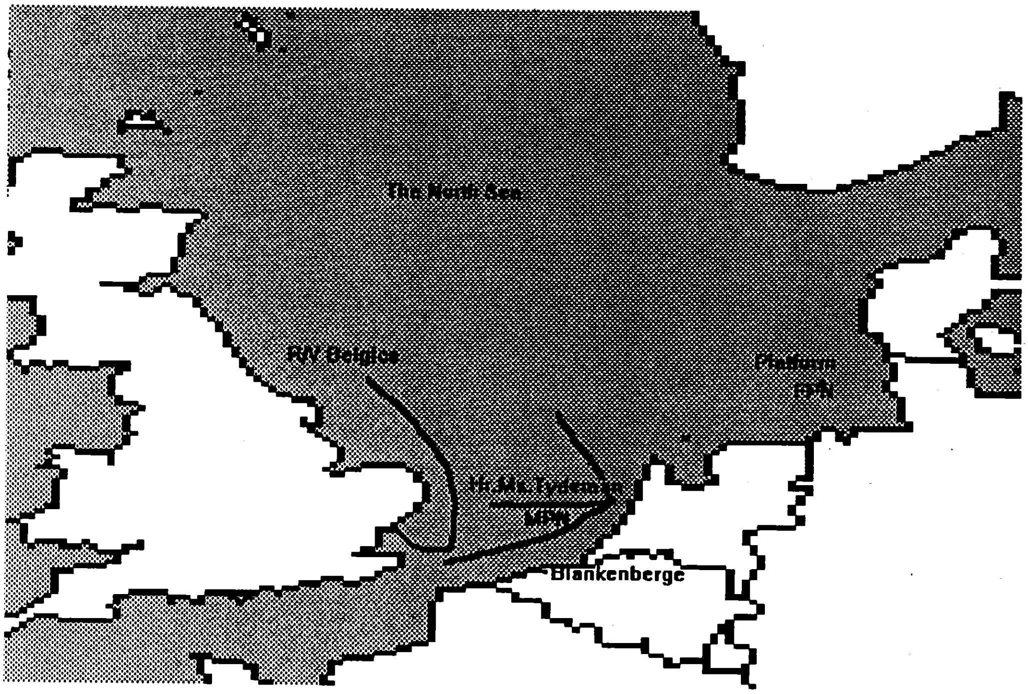
The North Sea
R/V Belgica
Platform
FPN
Hr.Ms.Tydeman
MSN
Blankenberge

FIG. 1,

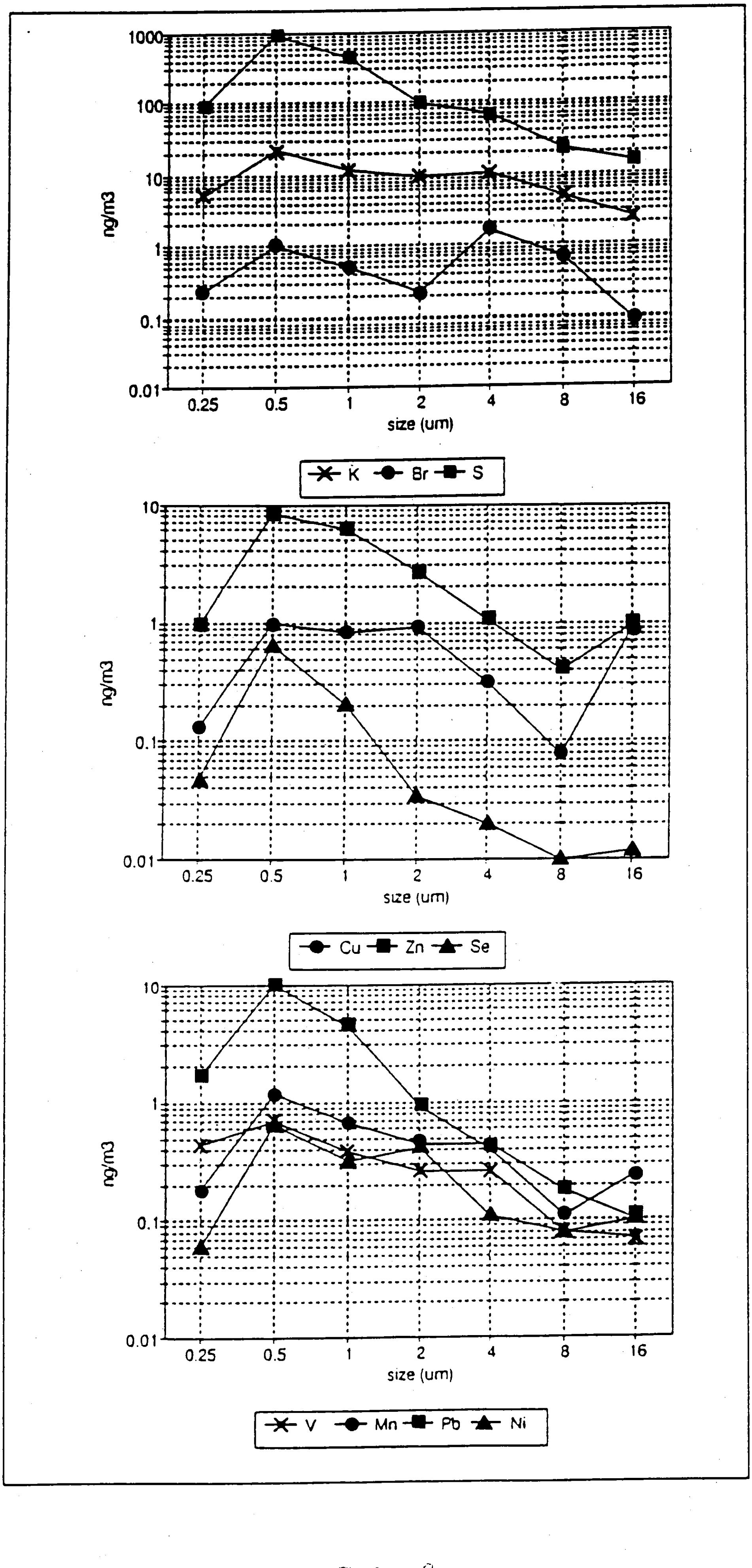
1000
100
10
1
0.1
0.01
ng/m3
0.25
0.5
1
2
4
8
16
size (um)
K
Br
S
10
1
0.1
0.01
ng/m3
0.25
0.5
1
2
4
8
16
size (um)
Cu
Zn
Se
10
1
0.1
0.01
ng/m3
0.25
0.5
1
2
4
8
16
size (um)
V
Mn
Pb
Ni

FIG. 6.

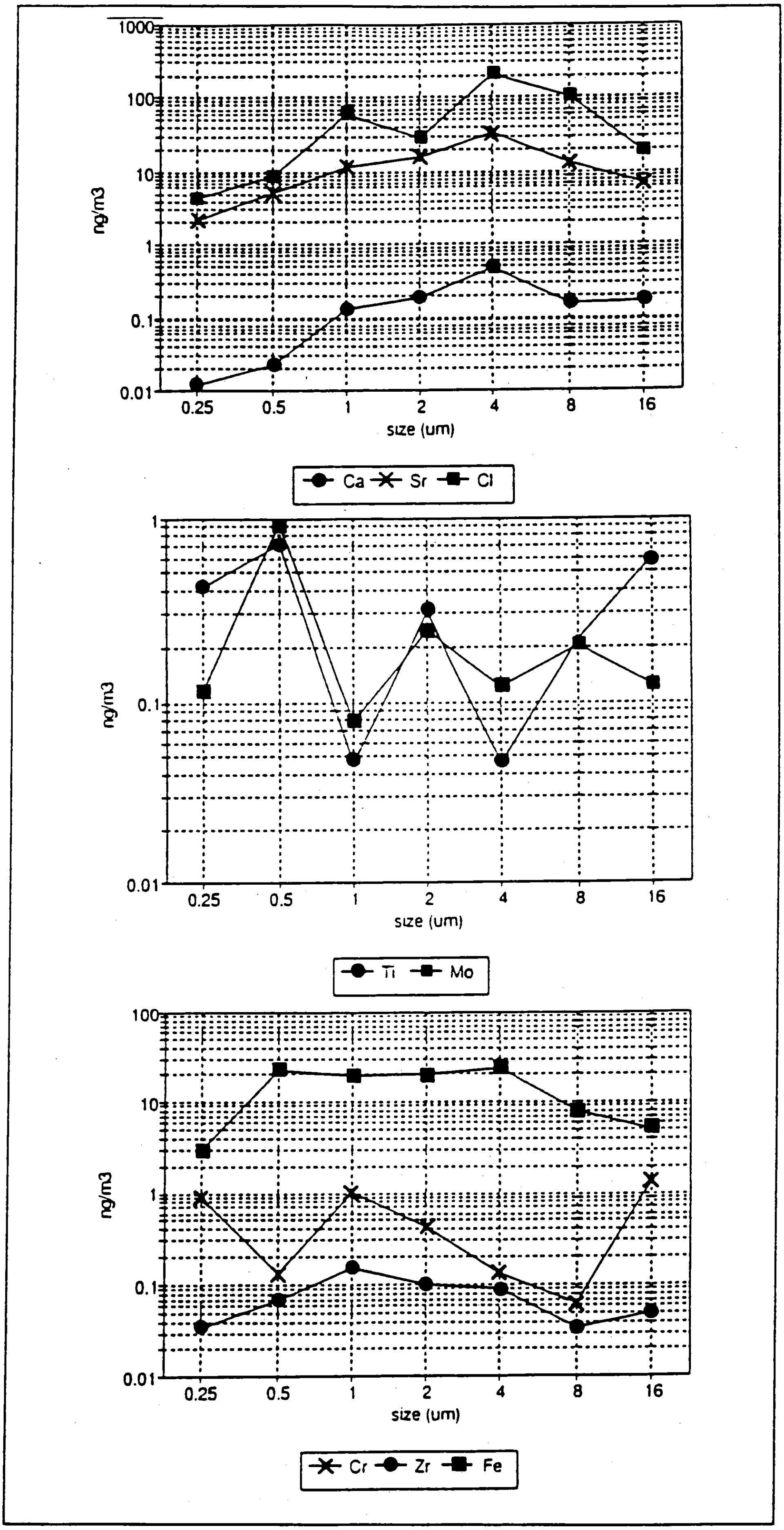
1000
100
10
1
0.1
0.01
ng/m3
0.25
0.5
1
2
4
8
16
size (um)
Ca
Sr
Cl
1
0.1
0.01
ng/m3
0.25
0.5
1
2
4
8
16
size (um)
Ti
Mo
100
10
1
0.1
0.01
ng/m3
0.25
0.5
1
2
4
8
16
size (um)
Cr
Zr
Fe

FIG. 3.

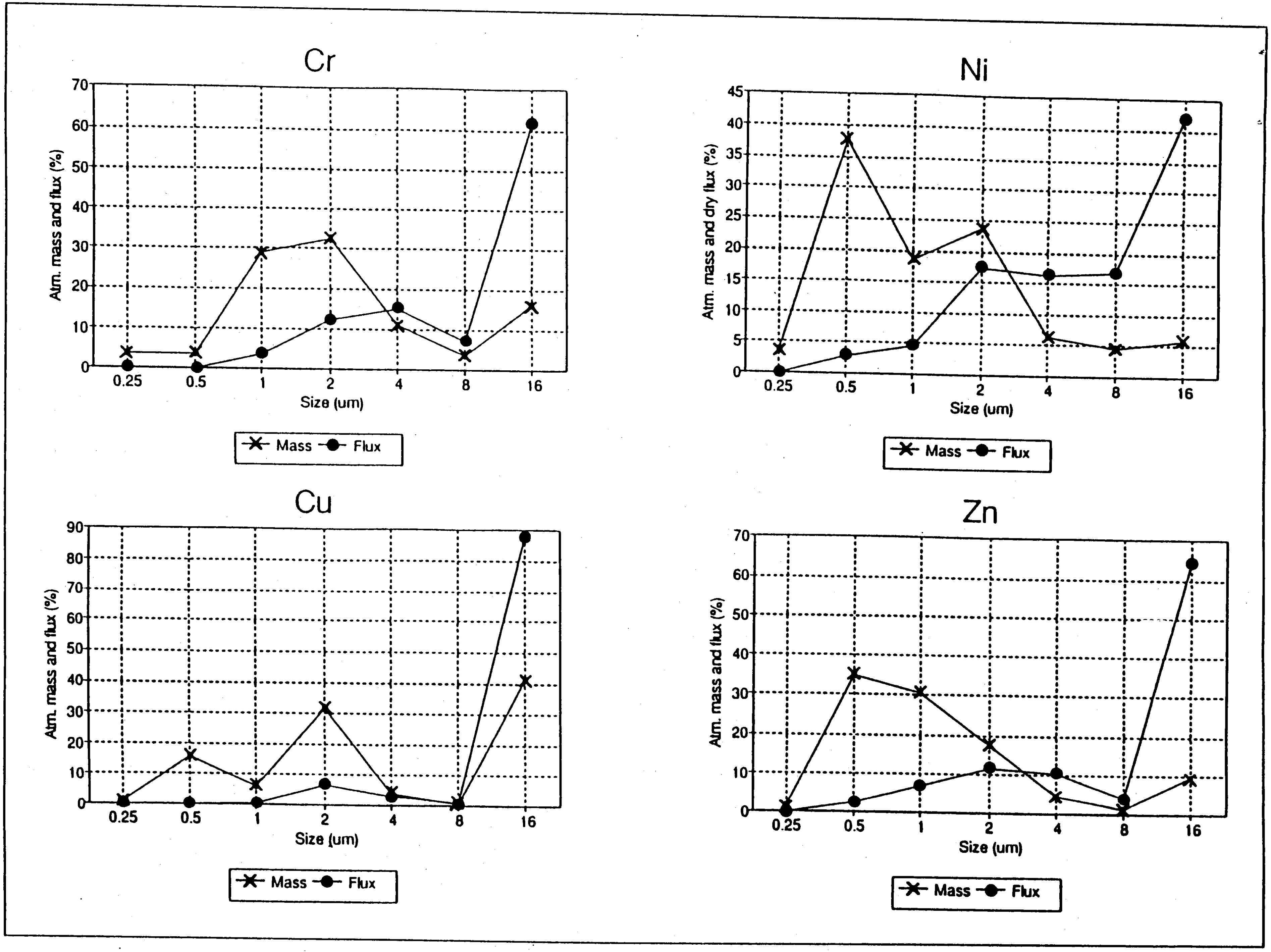
Cr
Atm. mass and flux (%)
0
10
20
30
40
50
60
70
0.25
0.5
1
2
4
8
16
Size (um)
Mass
Flux
Ni
Atm. mass and dry flux (%)
0
5
10
15
20
25
30
35
40
45
0.25
0.5
1
2
4
8
16
Size (um)
Mass
Flux
Cu
Atm. mass and flux (%)
0
10
20
30
40
50
60
70
80
90
0.25
0.5
1
2
4
8
16
Size (um)
Mass
Flux
Zn
Atm. mass and flux (%)
0
10
20
30
40
50
60
70
0.25
0.5
1
2
4
8
16
Size (um)
Mass
Flux

FIG 4.

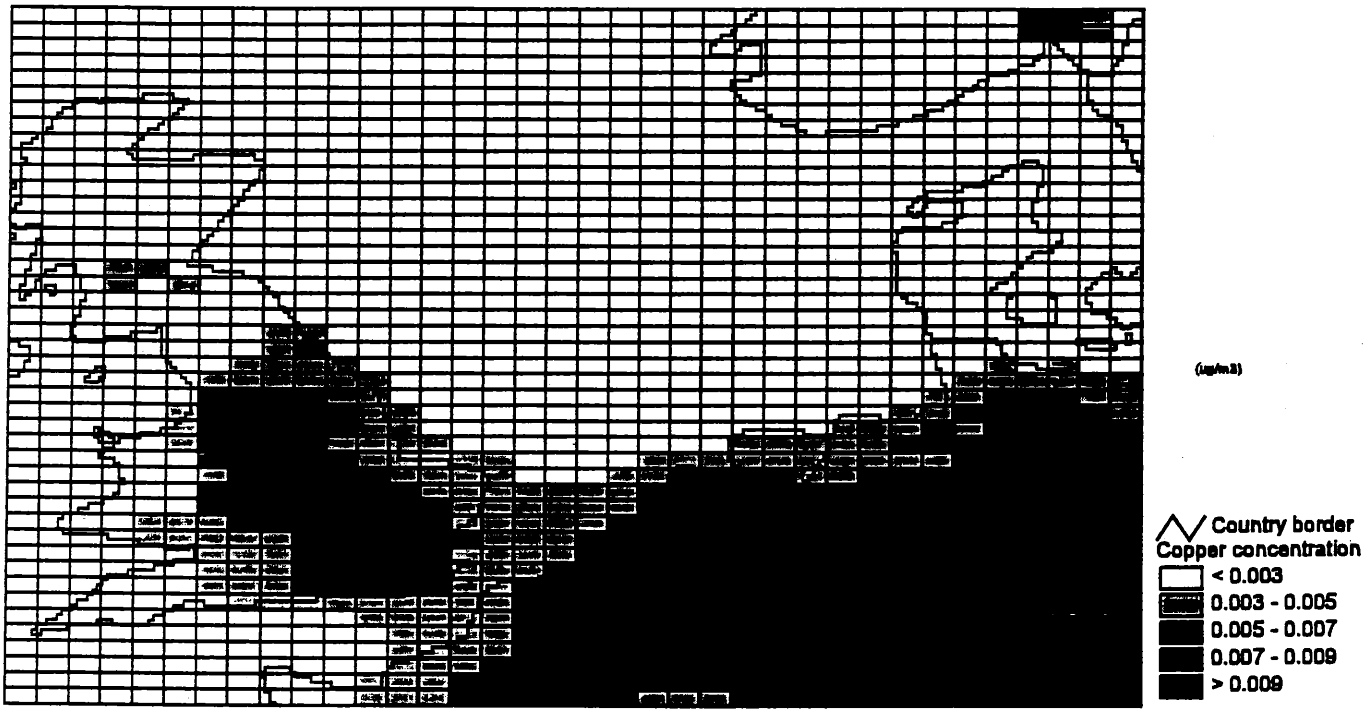
(ug/m3)
Country border
Copper concentration
< 0.003
0.003 - 0.005
0.005 - 0.007
0.007 - 0.009
> 0.009

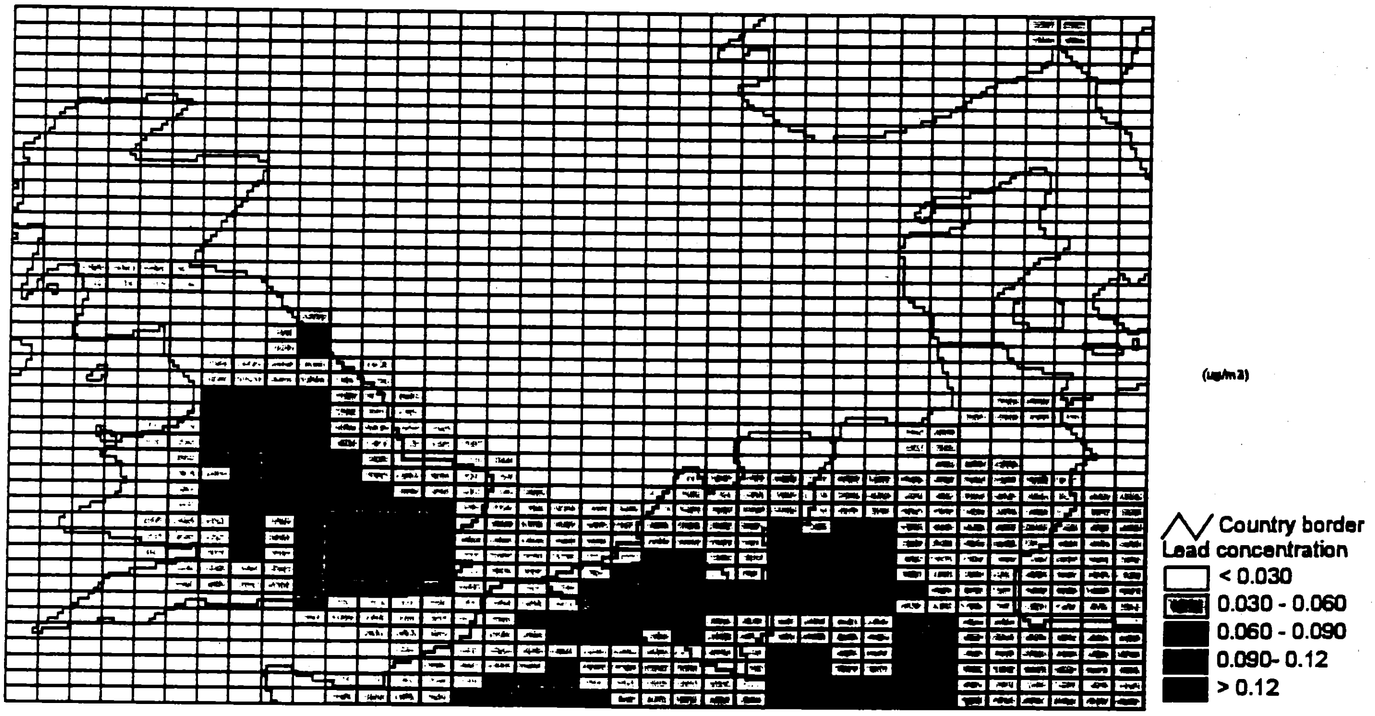
(ug/m3)
Country border
Lead concentration
< 0.030
0.030 - 0.060
0.060 - 0.090
0.090- 0.12
> 0.12

FIG. 5.

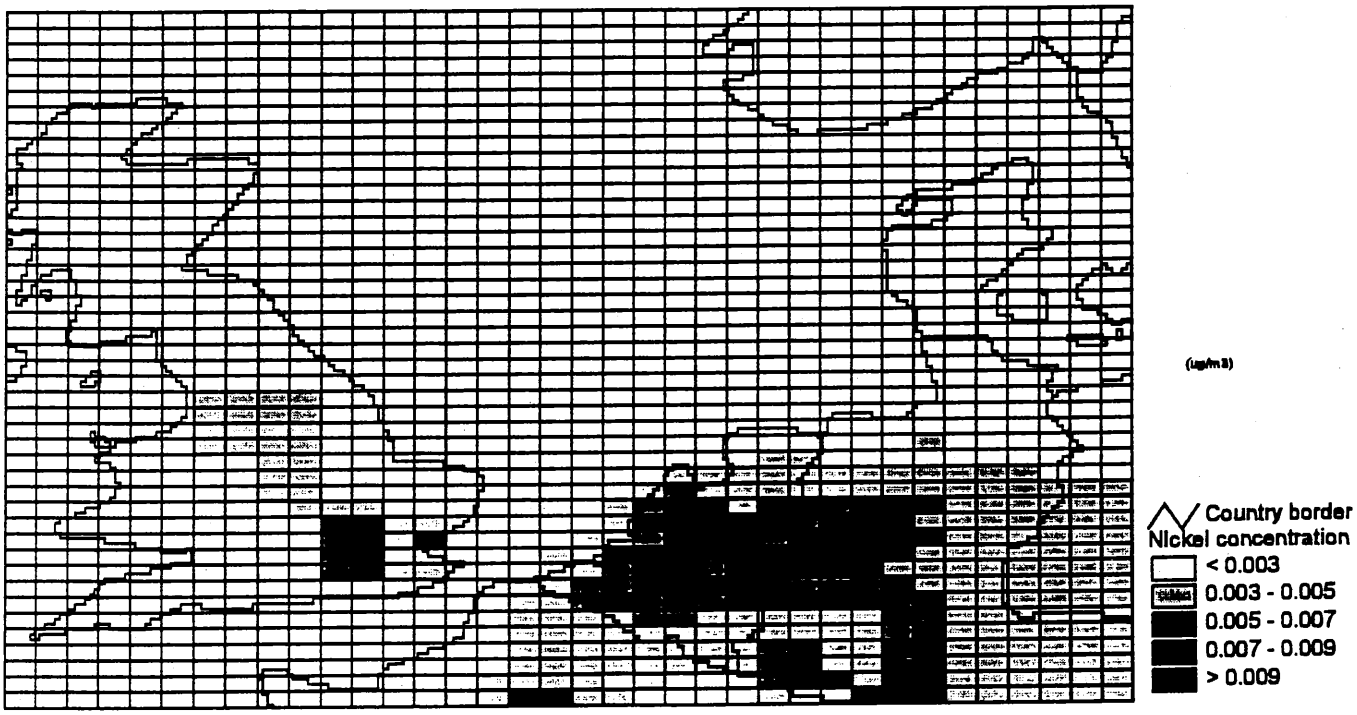
(ug/m3)
Country border
Nickel concentration
< 0.003
0.003 - 0.005
0.005 - 0.007
0.007 - 0.009
> 0.009

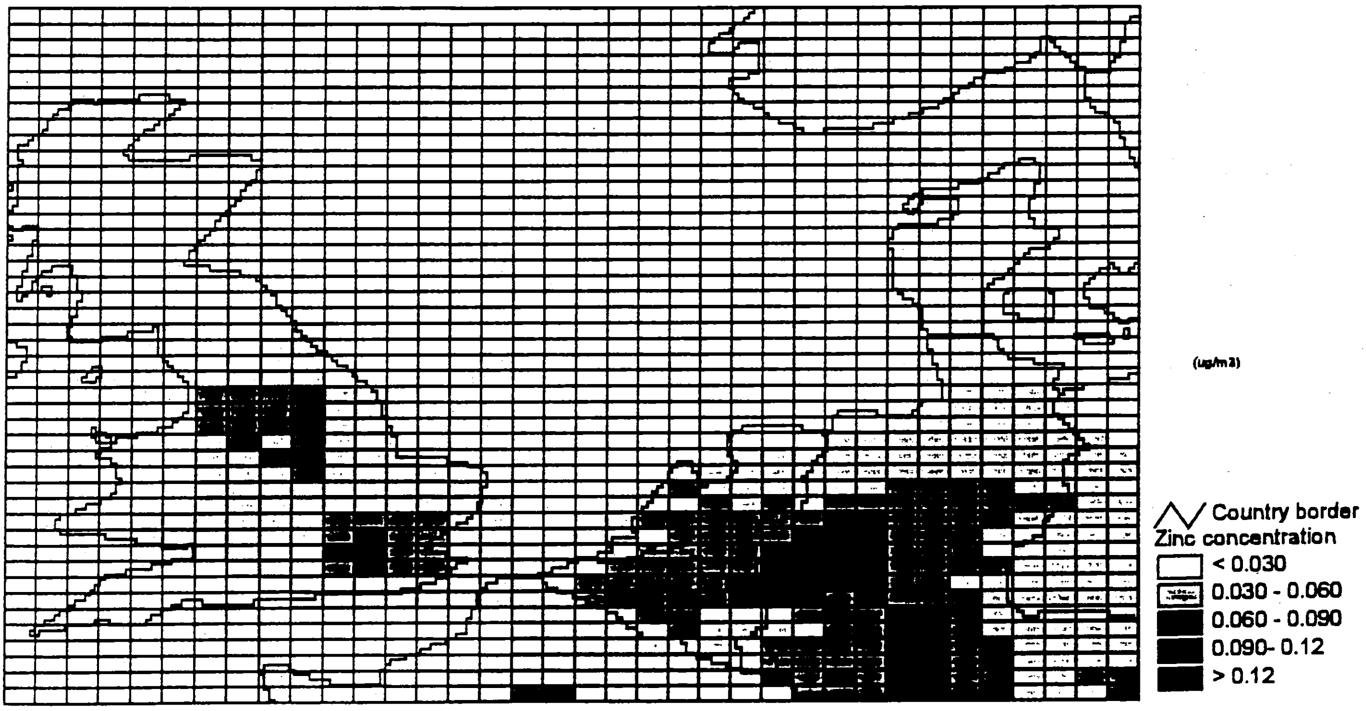
(ug/m3)
Country border
Zinc concentration
< 0.030
0.030 - 0.060
0.060 - 0.090
0.090- 0.12
> 0.12

FIG. 5i

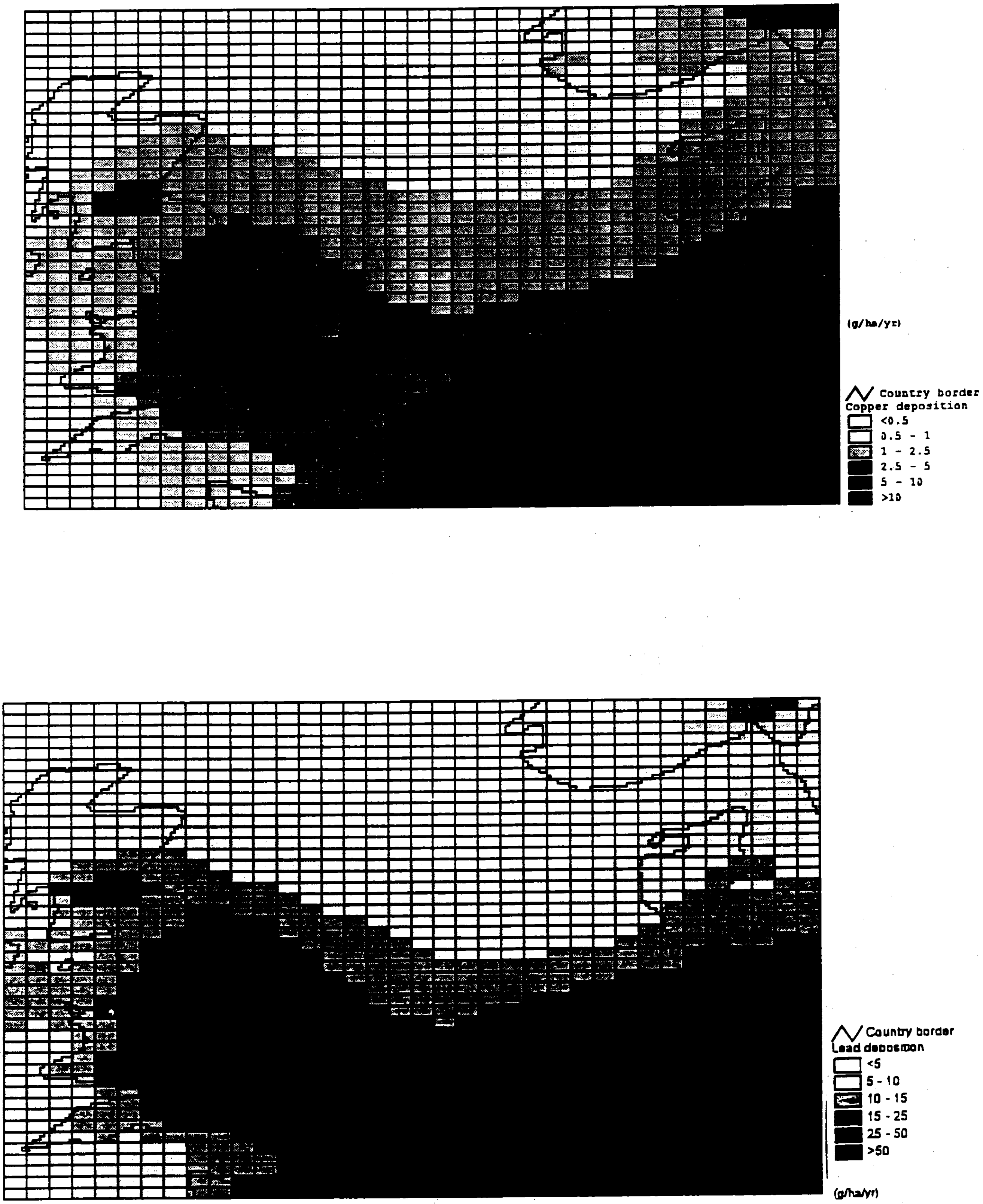
(g/ha/yr)
Country border
Copper deposition
<0.5
0.5 - 1
1 - 2.5
2.5 - 5
5 - 10
>10
Country border
Lead deposition
<5
5 - 10
10 - 15
15 - 25
25 - 50
>50
(g/ha/yr)

FIG. 6.

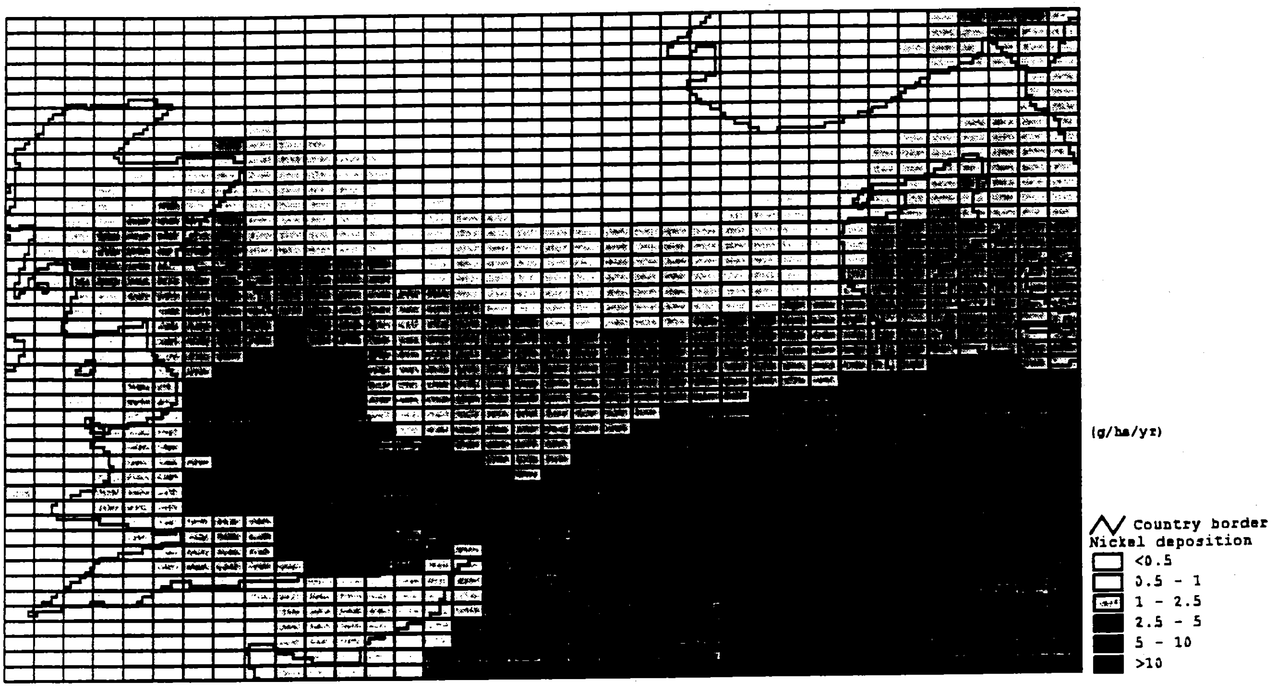
(g/ha/yr)
Country border
Nickel deposition
<0.5
0.5 - 1
1 - 2.5
2.5 - 5
5 - 10
>10

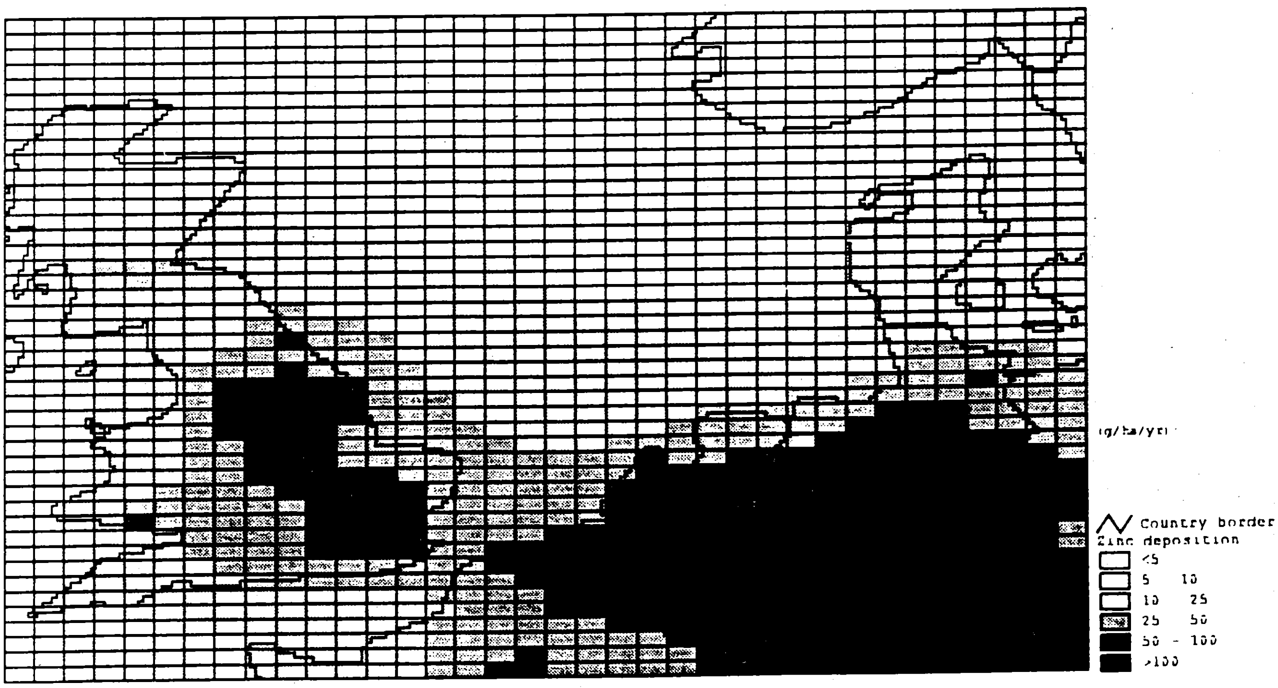
(g/ha/yr)
Country border
Zinc deposition
<5
5 - 10
10 - 25
25 - 50
50 - 100
>100

FIG.6,

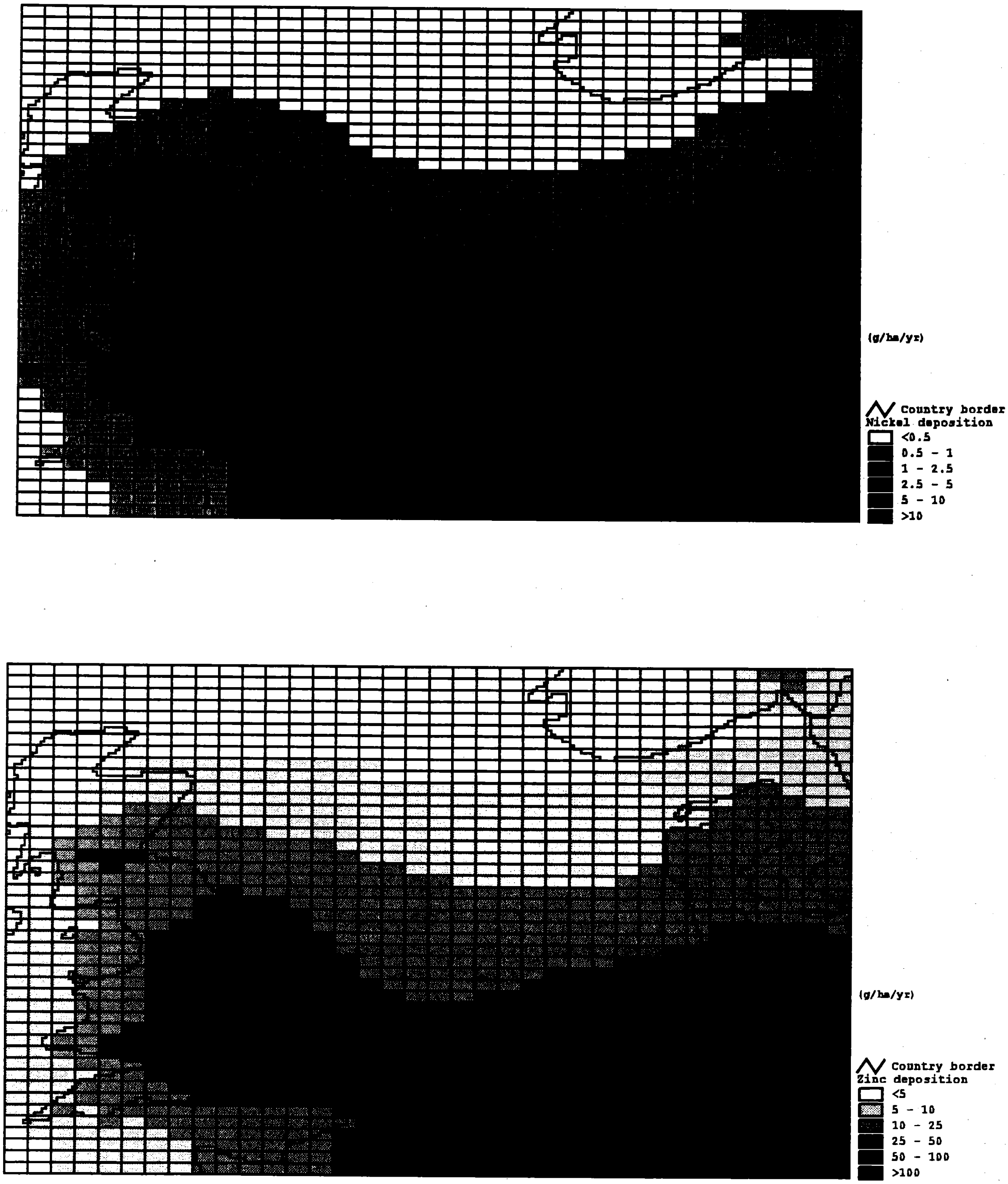
(g/ha/yr)
Country border
Nickel deposition
<0.5
0.5 - 1
1 - 2.5
2.5 - 5
5 - 10
>10
(g/ha/yr)
Country border
Zinc deposition
<5
5 - 10
10 - 25
25 - 50
50 - 100
>100

FIG. 6.

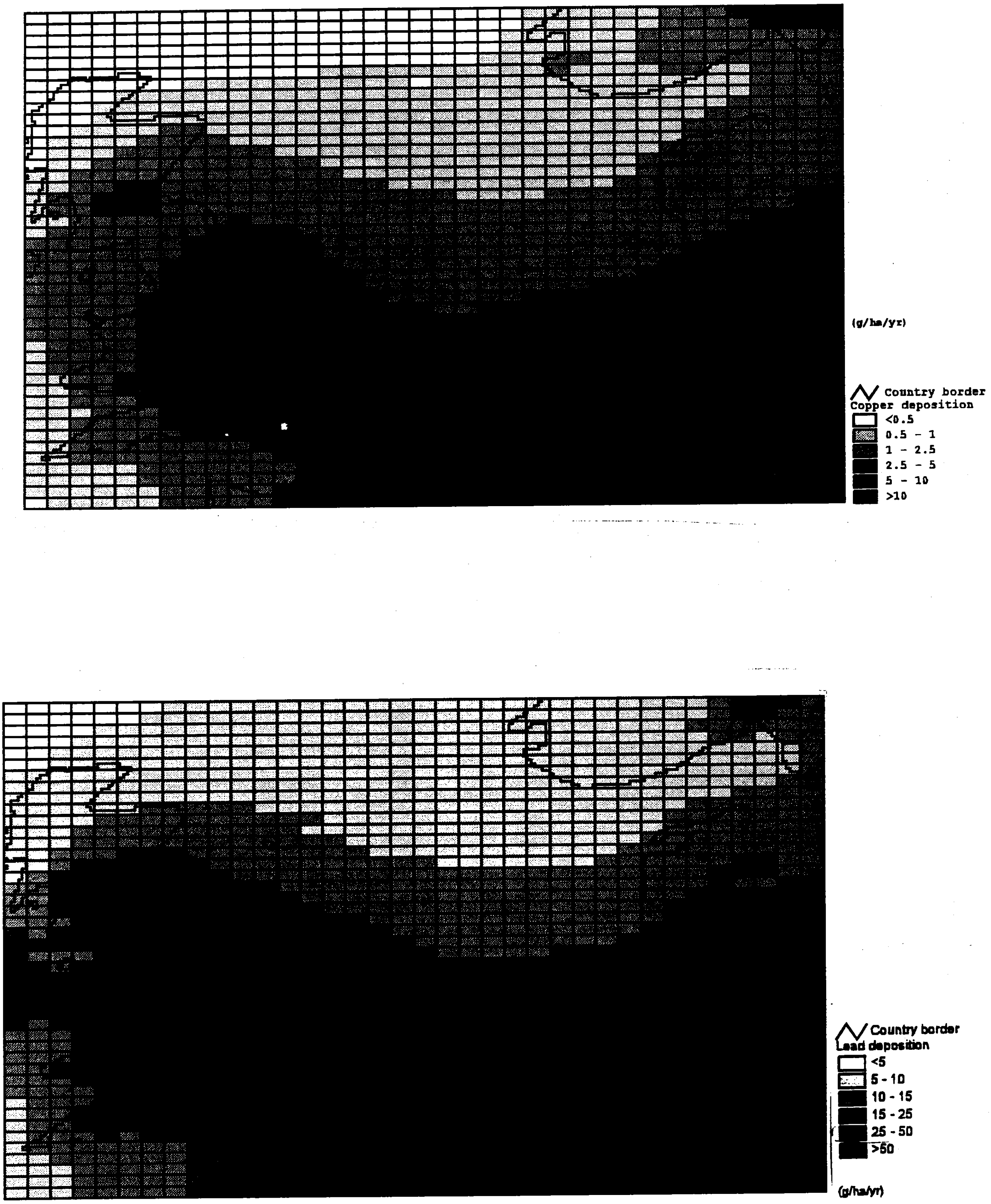
(g/ha/yr)
Country border
Copper deposition
<0.5
0.5 - 1
1 - 2.5
2.5 - 5
5 - 10
>10
Country border
Lead deposition
<5
5 - 10
10 - 15
15 - 25
25 - 50
>50
(g/ha/yr)

FIG 6.

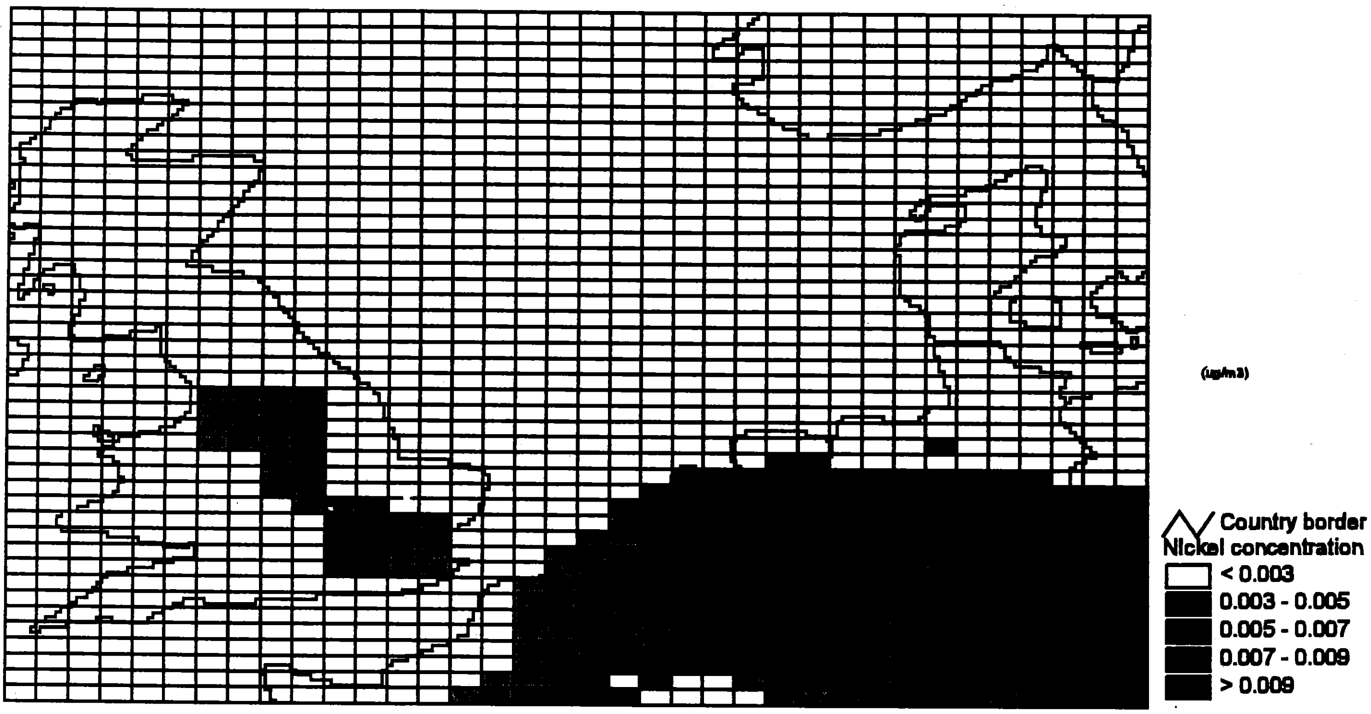
(ug/m3)
Country border
Nickel concentration
☐ < 0.003
■ 0.003 - 0.005
■ 0.005 - 0.007
■ 0.007 - 0.009
■ > 0.009

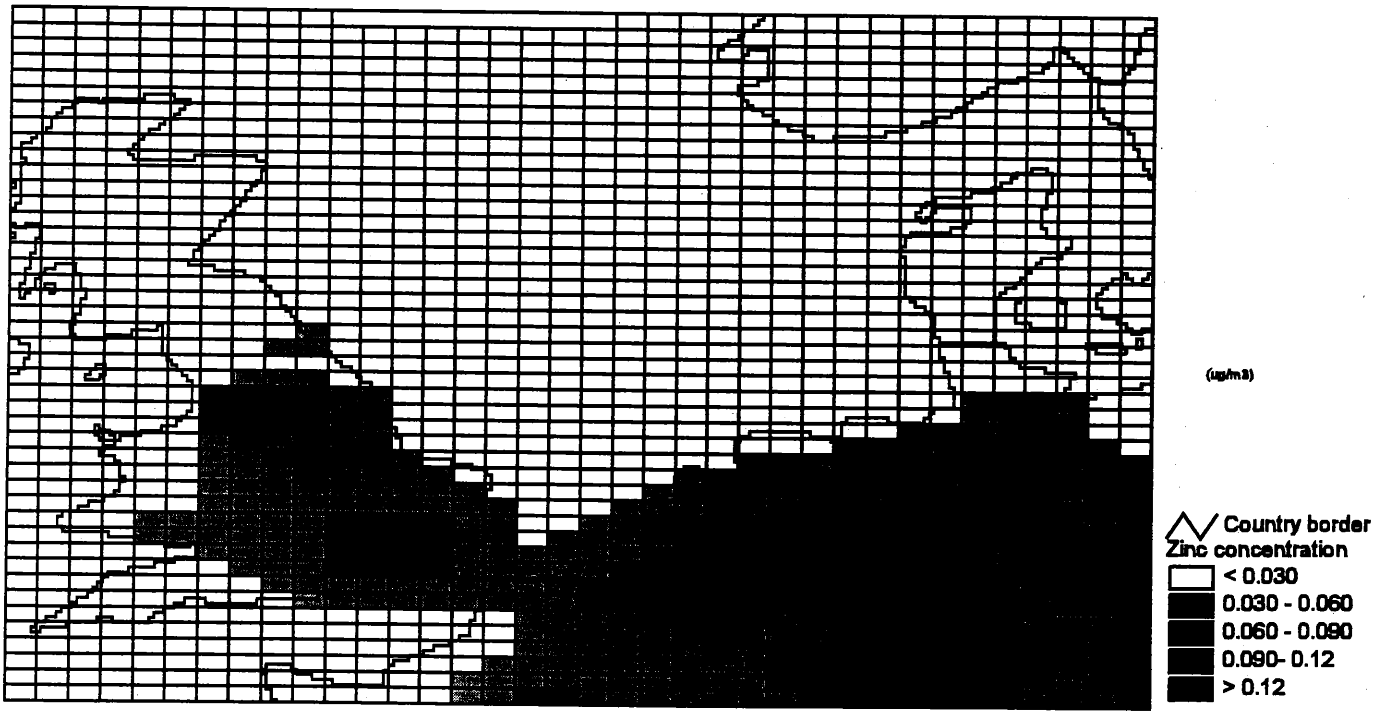
(ug/m3)
Country border
Zinc concentration
☐ < 0.030
■ 0.030 - 0.060
■ 0.060 - 0.090
■ 0.090- 0.12
■ > 0.12

FIG. 5

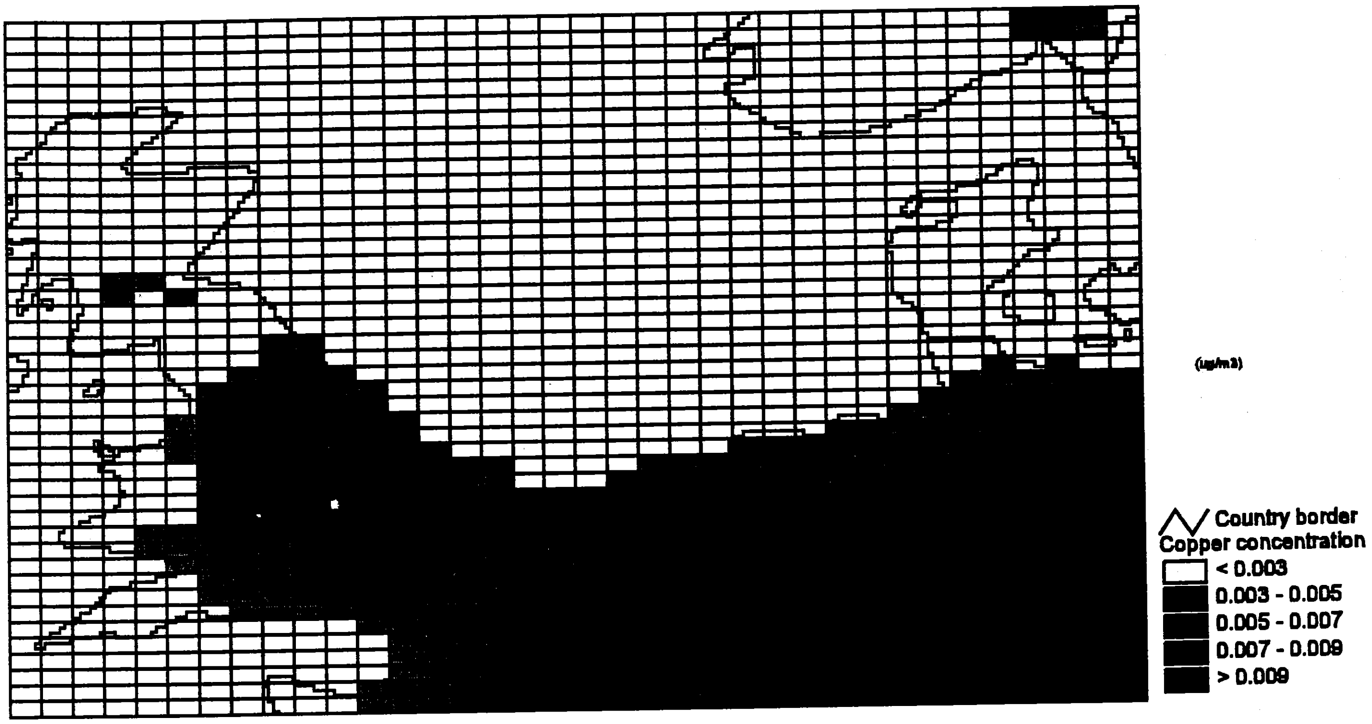
(ug/m3)
Country border
Copper concentration
□ < 0.003
■ 0.003 - 0.005
■ 0.005 - 0.007
■ 0.007 - 0.009
■ > 0.009

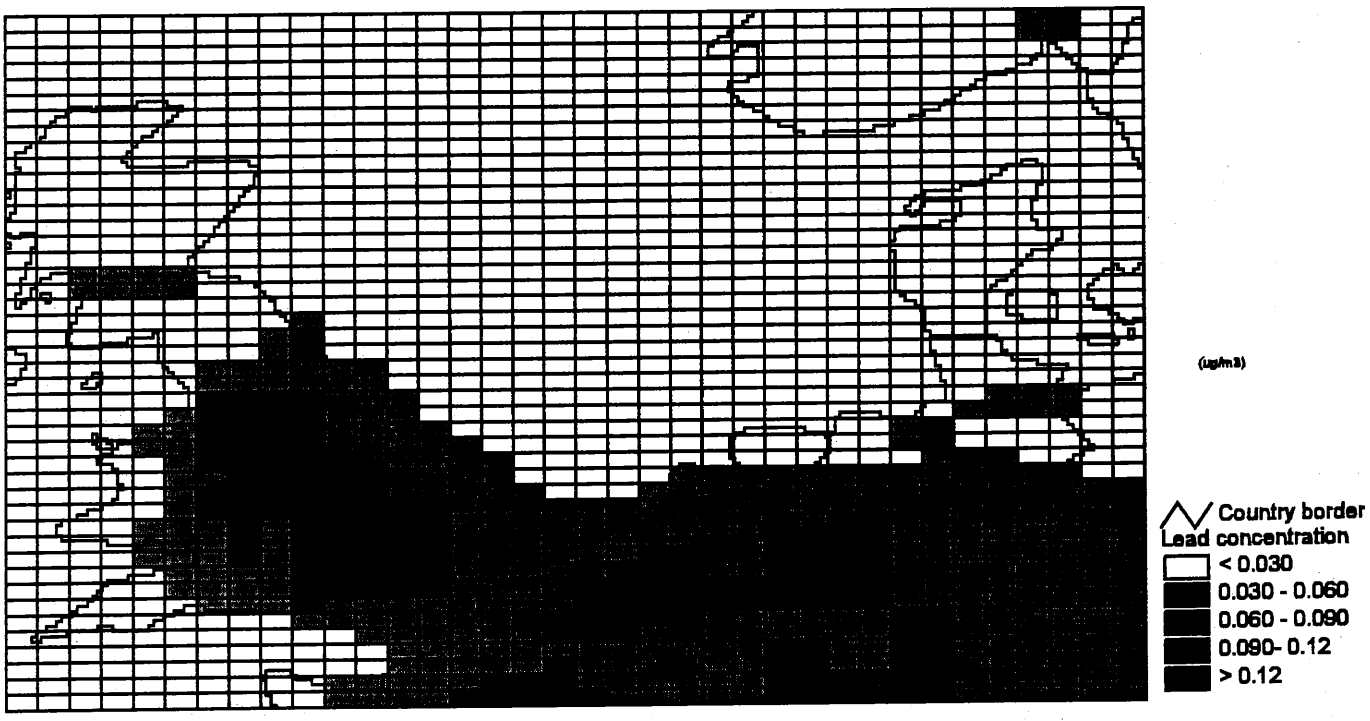
(ug/m3)
Country border
Lead concentration
□ < 0.030
■ 0.030 - 0.060
■ 0.060 - 0.090
■ 0.090- 0.12
■ > 0.12

FIG 5

Trend analysis of the published concentrations of heavy metals in aerosols above the North Sea and The Channel for the period 1971-1994

Stefaan Hoornaert, Boris Treiger and René Van Grieken
University of Antwerp (UIA), Department of Chemistry,
Universiteitsplein 1, B-2610 Antwerpen-Wilrijk, Belgium

Remi Laane
Institute for Coastal and Marine Management (RIKZ), Rijkswaterstaat,
Kortenaerkade 1, 2500 EX The Hague, The Netherlands

Summary

A literature review is given of atmospheric trace metal concentrations in aerosols above the North Sea and the English Channel over the period 1971-1994. All literature data have been gathered and intercompared to look for possible trends. Six trace metals are considered: Cd, Cu, Pb, Zn, Ni and Cr. A distinction is made between measurements in different regions of the North Sea, and between coastal and marine areas.
The majority of the data deals with the Southern Bight, providing the most reliable trends. Strong decreasing trends are observed for the Pb and Zn concentrations above the North Sea during the years 1971-1994. A remarkably consistent correlation is found between the concentration patterns of both elements in most parts of the North Sea. For Cd, Cu, Ni and Cr, much less data are available in the literature. Despite this, also for Cd a decreasing trend is present. Cr, Ni and Cu concentrations are fluctuating, mostly without a certain pattern.

Introduction

Apart from other pollutants significant amounts of trace metals are released into the atmosphere mainly due to the volatility of the corresponding elements at the high temperatures. Nriagu and Pacyna (1988), who made an inventory of global emissions of trace metals, found that the anthropogenic emissions of Cd, Cu, Ni and Zn exceed the inputs of these elements from natural sources by about two-fold or more and in the case of Pb even by a factor 17. The main sources of anthropogenically emitted trace metals are the non-ferrous metal and steel manufacturing, oil and coal combustion and refuse incineration. The airborne pollutants are a threat to human health, directly through inhalation and also indirectly since they are deposited, after transport in the atmosphere, on the soil and in the surface waters and oceans. Several studies on the deposition of airborne particulate matter have shown that the atmospheric input is a significant route of trace metals to the ocean. It can even exceed the other inputs like rivers and direct discharges, especially in the case of open seas, where the influence of rivers is minimal (GESAMP 1989).

The North Sea, being only a shallow sea, is characterised by a high biological production which is overexploited by intensive fishing activities. However, the North Sea ecosystem is also under stress because it is surrounded by some very industrialised and populated areas (mainly situated around the southern part, the so-called Southern Bight) and she is exposed to heavy ship traffic which together cause a serious threat to the health of this very sensitive ecosystem.

In the sea the deposited trace metals can initiate changes in natural biochemical processes. Perhaps even more important is the fact that they are also accumulated in the food chain, thereby causing negative effects on biologically important species and a threat on the health of man. As a result of the growing concern about these hazardous effects of the increased dispersion of trace metals in the environment, scientists have tried to evaluate the atmospheric deposition of heavy metals into the sea (NAS, 1978; GESAMP, 1980; GESAMP, 1989; Duce, 1991). Much attention has been paid to the case of the North Sea because of the proximity of the industrial areas. Beside model calculations, during several sampling campaigns on, above and around the North Sea, scientists have tried to assess trace metal concentrations and size-distributions of North Sea aerosols. This has produced quite a lot of individual data sets which, up till now, have not really been intercompared.

The aim of this work therefore is to gather all these data, to compare them and to look for possible trends in the concentrations as a function of time. Those can be generated by, for example, reduced emissions as the result of the development of new and cleaner production techniques like the use of stack emission filter mechanisms or the use of unleaded gasoline which should result in a decrease of the atmospheric Pb level. However differences in reported concentrations might sometimes also be caused by the use of different analysis techniques.

Experimental

The statistical analysis is done on all available published data for the period 1971-1994. Six trace metals are considered: Cd, Cu, Pb, Zn, Ni and Cr.
We have separated the North Sea and the Channel into four different regions (Fig. 1): the Channel itself (below 51°N), the Southern Bight (between 51°N and 54°N), the central North Sea (between 54°N and 57°30'N) and the northern North Sea (between 57°30'N and 61°N). This distinction is not done on a geographical basis but it is based on the results and is meaningful in the following sense:

- Concentrations above the Channel are expected to be lower than for the other regions because of the influx of relatively clean air from the Southwest and because of the smaller number of emission sources in this sector of Europe.

- The Southern Bight is only a narrow area, very close to the major sources. As reported by Pacyna (1984 a), the major western European emissions of Cd, Cu, Zn and Cr are situated around the Southern Bight, more precisely in the Benelux region, the neighbouring German Ruhr area and in the south-eastern part of the UK. So it is obvious that the highest trace metal concentrations should be found in this region. It is therefore not surprising that the major part of the available data deals with this part of the North Sea.

- Above 54°N, the North Sea is much wider. Lower concentrations are expected for this region due to the increased distance to the aerosols major source areas and the lower emissions in this region. A further subdivision of this part of the North Sea is made into central and northern North Sea. The central part is still influenced to some extent by the high emissions around the Southern Bight while the northern part usually experiences the flow of clean air from above the Atlantic Ocean.

A second distinction is made, for each of the four regions, between coastal measurements (these are measurements performed at land but close to the sea) - for which higher concentrations should be expected - and measurements on or above the sea (cruises, flights, lightships and platforms)

For each region all data were ordered chronologically. If more data were present for a specific year, all available data were averaged. Only yearly averages were taken into account when data were present for different time periods, to minimise possible effects of seasonal changes on the concentration patterns.

Results and discussion

* *English Channel*

Data on atmospheric trace metal concentrations above the English Channel are rather scarce. For both the marine and coastal part of the Channel, values in the literature are only present for a few periods of time between 1981 and 1988 (Dedeurwaerder, 1988; Flament et al., 1987; Otten et al., 1994; Rädlein and Heumann, 1992). Therefore it is hardly possible to speak about possible trends in the concentration profiles.

* *Southern Bight*

- Marine area of the Southern Bight

The Southern Bight is surrounded at the east side by the Netherlands and Belgium, and by the UK at the west side. It is the most investigated region of the North Sea. This is not surprising since it is also the most endangered part. Measurements in the marine area include sampling on ships (cruises), on the lightship Westhinder, on a gas platform and during airplane flights (between sea level and the inversion layer) above the North Sea (Fig. 1).

The complete set of data for the marine part of the Southern Bight is given in Table 1 and represented in Fig. 2. In the table, and in all subsequent ones, only the name of the first author is mentioned. As mentioned previously the data, published by different authors for one and the same year, have been averaged (the individual data are not shown in the table) and only yearly averages were taken into account if data were present for different time periods, to minimise the effect of seasonal changes on the concentration patterns. Additional data can be found in Baeyens and Dedeurwaerder (1991) and Dedeurwaerder (1988) but were not taken into account in the trend analysis since for the same periods yearly averages were reported by other authors. As mentioned previously only yearly averages were taken into account when data were present for different time periods, to minimise possible effects of seasonal changes on the concentration patterns.

Only one sampling campaign has been organised in the seventies. All other campaigns have been done between 1980 and 1993. The trace metal concentrations between 1980 and 1983 were measured on the lightship Westhinder. Data are not available for individual years but for overlapping periods of several successive years. However, since all data originate from the same sampling campaign, we are able to observe certain trends in the concentrations. Pb and Zn are highly intercorrelated: their average concentrations show a sharp drop from about 180 ng/m³ in 1980 to 80 ng/m³ for the period 1980-1981. Since the high concentrations observed in 1980 are also included in the values for the period 1980-1981, the concentrations in 1981 should be even lower than 80 ng/m³. From 1981 on, both concentrations start to increase again. Cu concentrations show a similar behaviour. Data for the other elements are lacking.

The picture becomes more clear if one also considers the data from measurements during cruises on the Southern Bight between 1984 and 1993 as well as airplane measurements in 1988-1989. Similar to the case of the Westhinder site, the Pb and Zn concentration patterns are very alike. Between 1984 and 1988 they are subjected to heavy fluctuations with very high values in 1986 (up to 245 ng/m³ for Zn and 124 ng/m³ for Pb). The fluctuations can be explained by the fact that for the period 1984-1988, only very few and possibly not representative samples have been analysed during rather short sampling campaigns. Concentrations therefore are subjected to seasonal changes and other time dependent factors such as wind direction. From 1989 to 1993, the Pb and Zn concentrations are much lower (below 60 ng/m³), so despite the fluctuations there seems to be an overall decreasing trend. The Ni concentrations above the Southern Bight have increased by a factor of two between 1984 and 1986, from 6 ng/m³ to a level of 12 ng/m³. From 1986 on, its concentration varies between 2 ± 1 and 6 ± 3 ng/m³ but without a certain pattern. The Cu concentrations have dropped from 21 ng/m³ in the early seventies to less than 10 ng/m³ in the eighties and nineties, except for 1986 when higher values, up to 19 ng/m³, were found. If one does not consider the high values of 1986, the Cu concentrations are fluctuating since 1980 between 3 and 10 ng/m³ without a consistent pattern. For Cr and Cd too few data are present so that no trends can be observed. The heavy fluctuations in the period 1985 - 1987 cannot be due to the use of different sampling equipment of analysis techniques. All these data were obtained by the same people (Otten et al., 1994) using exactly the same instrumentation. Since the same fluctuation pattern is observed for most of the elements, the effect of seasonal changes and other time dependent factors is most likely responsible for the observed fluctuations. Also during these sampling campaigns only a few samples have been analysed, which might explain the observed fluctuations.

- Coastal area of the Southern Bight

Measurements have been done at coastal sites on both sides of the Southern Bight in the period 1972-1994: in the Netherlands, Belgium, Germany and the UK (Fig. 1). All data on coastal measurements around the Southern Bight, which is the largest dataset of the whole North Sea region, are summarised in Table 2. The trace metal concentration patterns for the whole coastal region are represented in Fig. 3. Values for Hamburg have not been considered in the graphs since the concentrations at this highly industrialised site are rather high and would therefore interfere with data from other places. Additional data can be found in Peirson et al. (1973), Kretzschmar and Cosemans (1979) and Steiger (1991).

Measurements at Leiston and Styrrup in the UK have been done in the framework of an extensive sampling campaign in the whole area of the UK between 1972 and 1976 to estimate the amount of trace metals in the atmosphere. The values for both sites have been averaged in Fig. 3. Since all values are yearly averages seasonal effects can be excluded. Also the interference by other factors such as the use of different sampling and analysis procedures is not present because during the whole period 1972-1976 the same sampling and analysis devices have been used. For 1973 the data were averaged with additional data, measured at Petten in the Netherlands. The average airborne Zn level is decreasing continuously from more than 300 ng/m³ in 1972 to about 150 ng/m³ in 1976. The Pb concentrations show a sharp drop of about 50 ng/m³ between 1973 and 1974 and then remain stable until 1976. Cr behaves quite similarly. The values found in 1974 till 1976 are only half of the ones observed before 1974 (7 ng/m³ instead of 15 ng/m³). High Cd concentrations (around 30 ng/m³) are found for the period 1972-1973. From 1973 on, Cd concentrations decrease to a low value of 3 ng/m³ in 1976. The Cu pattern shows a decreasing trend in the period 1972-1974 (from 26 ng/m³ to 8 ng/m³) but increases again from 1974 till 1976 when even a higher Cu concentration is found than in 1972 (38 ng/m³). Ni remains quite stable with a slightly higher value in 1973.

The values, reported for the period 1977-1987, are the results of measurements at the Belgian coast (Oostende and The Blankaert) and in the Netherlands (Schiermonnikoog, Petten, Rijnmond, Haamstede and five different locations in the province of South Holland). All concentrations are fluctuating heavily without any systematic pattern. The observed fluctuations could be explained to some extent by the fact that, during the different sampling campaigns, different sampling devices have been used (Whatman filters, glass fibre filters and siliconised quartz discs).The values reported for 1981 are geometric mean values contrary to all other values which are arithmetic means.

Trends become more clear if the data for both periods are combined and complemented with additional, more recent values from single campaigns at some new sites in the UK (Hemsby, Mannington and Spurnhead) and the Belgian coast (Blankenberge). Despite the heavy fluctuations, there is a very strong decreasing trend in the average Pb and Zn concentrations: Pb concentrations have dropped from 270 ng/m³ in 1972 to 8 ± 8 ng/m³ in 1992-1994, Zn from 306 ng/m³ to 22 ± 13 ng/m³. The fluctuating trend in the average Cu concentrations which was found earlier is confirmed in this graph. However the values in the 80's and 90's remain below the values found in the seventies. Cd concentrations are decreasing; the strongest decrease is observed between 1973 and 1976. From 1986 on Cd concentrations remains below 1 ng/m³. Ni concentrations were quite stable till 1976. For the period 1976-1985 higher, but also stable values are observed. Since 1985, Ni concentrations are decreasing again to reach its lowest level ever in 1992-1994. The airborne Cr level does not show a regular pattern.

* *Central North Sea*

- Marine area of the Central North Sea

In contrast to the Southern Bight almost no data are available for the marine area of the central North Sea. Concentrations are only reported in two publications, for three different sampling campaigns (Injuk et al., 1993; Otten et al., 1994)

- Coastal area of the Central North Sea

The coastal area around the central North Sea includes the eastern part of the UK, Denmark and the upper north-western part of Germany. Measurements of concentrations of airborne trace elements have been performed at the following sampling sites (Fig. 1): Aberdeen (UK), Tange (DK), Keldsnor (DK), Westerheversand (D), Pellworm (D), Helgoland (D) and the research platform "Nordsee" (FPN) (D). The last three locations are not real coastal sites: Pellworm and Helgoland are islands while the FPN site is a research platform. However in our discussion we consider them as coastal because they are located not in the open sea but rather close to the coast.

The complete set of coastal data for the central part of the North Sea is summarised in Table 3. All measurements are represented chronologically in Fig. 4. The Aberdeen values are not considered: the concentrations reported for this location are very high in comparison to all other data and hence they are considered as outliers. Also values which span a period of several years are not considered in the graphs if values are present for the different years separately. Additional data can be found in Schneider (1987), Stössel (1987), Kersten et al. (1988), Dannecker et al. (1994) and Spokes (1991).

If one compares Figures 2, 3 and 4, one can clearly see that the absolute trace metal concentrations above the central North Sea are lower than those found for the Southern Bight, especially in the case of Pb, Zn and also for Ni.
As can be seen from Fig. 4, the Pb concentrations are fluctuating between 22 and 55 ng/m³ until 1985 but from 1985 on they are decreasing to 13 ng/m³ (except for a negligible increase in 1992). The big difference in Pb concentrations between 1984 and 1985 could possibly be explained by the fact that these values, in contrast to the other values, are not yearly averages and hence subjected to seasonal changes. The airborne Zn level, although it is fluctuating, seems to increase from about 30 ng/m³ to 50 ng/m³; so contrary to the other North Sea regions Pb and Zn do not behave in the same way. Ni concentrations are increasing slightly in the period 1986 - 1992. Cu concentrations vary only between 2.5 and 4 ng/m³. They are slightly decreasing since 1986 to a level of 2.5 ng/m3 in 1990 but in 1992 a higher value of 3.5 ± 0.2 ng/m³ is observed again. However the overall higher values that are observed in 1992 could be the result of other factors like the use of a different analysis technique: the results from 1985 till 1990 have been obtained by ICP-AES, those of 1992 by TXRF. Because of the lack of data for Cd and Cr nothing can be concluded for these elements.

** Northern North Sea*

- Marine and coastal area

The northern part of the North Sea is surrounded at the east side by the southern part of Norway and at the Southwest side only by a small part of the United Kingdom. Almost no sampling campaigns, dealing with trace metals, have been done on this part of the North Sea, so we combined the few data available on the marine area with the coastal data. This seems to be justified since there is no significant difference between the marine and coastal data. Coastal measurements have been done more frequently but only at a limited number of places. In southern Norway trace metal concentrations have been determined at two locations: most of them at Birkenes and only two in Vasser (Fig. 1).

The complete set of data which has been used for the marine and the coastal area of the northern North Sea is summarised in Table 4. Concentrations are represented graphically in Fig. 5. The only two series of data for the Vasser site (1974 and 1975) are not considered since for these periods values are also present for the Birkenes site but mainly because there seems to be a significant difference between these two sites. Concentrations measured at Vasser are systematically higher than those from Birkenes probably due to the influence of local sources in urban areas along the Oslofjord. Additional data can be found in Pacyna et al. (1984c) and Bartnicki (1994).

Comparing Fig. 5 with the previous ones again clearly shows the difference between this region and the other regions of the North Sea. The observed concentrations for the northern North Sea are the lowest of all, as we expected.
Fig. 5 shows that for the northern part of the North Sea the average Pb concentrations are decreasing continuously from about 18 ng/m³ in the seventies to only 1 ng/m³ in 1989. Also Zn is decreasing to small values (2 ng/m³) but not as smoothly as Pb unless one only looks at Birkenes and does not consider the value for the marine area in 1985. However fluctuations can also be caused by seasonal differences since most of the sampling campaigns only span a rather short period of time. From the literature it is also clear that several different analysis techniques have been used during the different sampling campaigns which also might have its effect on the atmospheric concentrations. Average Ni and Cu concentrations are fluctuating without a certain pattern. However the maximum Cu levels detected during the eighties are only about half of these measured at the end of the seventies (3.6 ng/m³ instead of 7 ng/m³). The Cr level shows an enormous increase between 1985-1986 and 1988 but it is impossible to speak about a certain trend with the small amount of data available. The average Cd level was rather stable between 1974 and 1979 (2 ng/m³). More recent information about Cd concentrations is only available for 1985-1986 when only 0.08 ng/m³ of Cd is found.

* *Comparison with atmospheric trace metal concentrations in remote areas*

From the discussion in the previous sections it is clear that some strong decreasing trends can be observed. Of course the interesting question now is whether the observed concentrations already reach the natural background concentrations. In Table 5 airborne trace metal concentrations, collected in some remote areas and hence are supposed to represent the natural background concentrations, are shown. For this comparison the most recent reported concentrations (in most cases also the lowest), for the different marine parts of the North Sea, are also given in Table 5. If concentrations were lacking, the data were supplemented with data from earlier sampling campaigns.
As can be seen from both tables, all concentrations found above the North Sea are still higher than those in the remote areas. However the differences are getting smaller. For Pb and Zn a clear south to north decreasing trend can be observed.

Conclusions

All literature data on trace metal concentrations in aerosols above the North Sea have been gathered and intercompared to look for possible trends. Six trace metals are considered: Cd, Cu, Pb, Zn, Ni and Cr. A distinction is made between measurements in different regions of the North Sea: the Southern Bight, the central and northern North Sea and the Channel. A second distinction is made between coastal and marine areas.

The majority of the data on trace metals in the literature deals with the Southern Bight. So the trends observed for this part of the North Sea are the most reliable. More data are needed to confirm the concentration patterns found for the other regions.

Despite some heavy fluctuations a strong decreasing trend is observed for the Pb and Zn concentrations above the North Sea. A remarkably consistent correlation is found between the concentration patterns of both elements in most parts of the North Sea. This similar behaviour between Pb and Zn, which has also been reported by Schneider (1987), is most clearly seen for the Southern Bight. Only in the coastal area of the central North Sea a different behaviour is found. Here Zn concentrations are increasing and Pb and Zn are anti-correlated. Although Pb- and Zn-containing particles originate from different sources (Pb mainly from cars and Zn from various combustion processes in industry, in addition to metallurgy emissions for both), their correlation probably reflects the fact that the changes in these fields have the same trend. This assumption is further confirmed by the observation that the temporal changes of the Pb and Zn concentrations are the same for such different regions as the Channel, the Southern Bight and the northern part of the North Sea.

For Cd, Cu, Ni and Cr, much less data are available in the literature. Despite this, also for Cd a decreasing trend is present, however not so strong as for Pb and Zn. Cr and Ni concentrations are fluctuating, mostly without a certain pattern so with the small amount of data it is hard to recognise a particular trend. Airborne Cu levels, also subjected to heavy fluctuations, in most cases do not show a consistent behaviour.

Not enough data are available in the literature to assess trends of heavy metal concentrations with wind directions or with particle size.

Acknowledgement

Stefaan Hoornaert is supported by the Belgian National Science Foundation (NFWO).
This study was carried out on behalf of the Institute for Coastal and Marine Management (RIKZ), Rijkswaterstaat, Den Haag, the Netherlands. It was also partially supported via the Impulse Programme Marine Sciences (contract MS06/050) of the Belgian State, Prime Minister's Service, Services for Scientific, Technical and Cultural Affairs

References

Amundsen, C.E., Hanssen, J.E., Semb, A. & Steinnes E. (1992). Long-range transport of trace elements to southern Norway. Atmos. Environ., 26A, 1309-1324.

Baeyens, W. & Dedeurwaerder H. (1991). Particulate trace metals above the Southern Bight of the north sea - I. Analytical procedures and average aerosol concentrations. Atmos. Environ., 25A, 293-304.

Bartnicki, J. (1994). An eulerian model for atmospheric transport of heavy metals over Europe: model description and preliminary results. Water, Air and Soil Pollution, 75, 227-263.

Cambray, R.S., Jefferies, D.F. & Topping G. (1975). An estimate of the input of atmospheric trace elements into the North Sea and the Clyde Sea (1972-3). AERE Report R 7733, Harwell.

Cawse, P.A. (1974). A survey of atmospheric trace elements in the UK (1972-73). AERE Report R 7669, Harwell.

Cawse, P.A. (1975). A survey of atmospheric trace elements in the UK: results for 1974. AERE Report R 8038, Harwell.

Cawse, P.A. (1976). A survey of atmospheric trace elements in the UK: results for 1975. AERE Report R 8398, Harwell.

Cawse, P.A. (1977). A survey of atmospheric trace elements in the UK: results for 1976. AERE Report R 8869, Harwell.

Chester, R. & Bradshaw, G.F. (1991). Source control on the distribution of particulate trace metals in the North Sea atmosphere. Marine Pollution Bulletin, 22, 1, 30-36.

Dannecker, W., Hinzpeter, H., Kirzel, H.J., Luthardt, H., Kriews, M., Naumann, K., Schulz, M., Schwikowski, M., Steiger, M. & Terzenbach, U. (1994). Atmospheric transport of contaminants, their ambient concentration and input into the North Sea. In: Circulation and Contaminant Fluxes in the North Sea. (Sündermann, ed.), pp. 138-189. Springer-Verlag, Berlin.

DCMR (19--). Quarterly and yearly reports, DCMR, Schiedam, the Netherlands.

Dedeurwaerder, H.L., Dehairs, F.A., Decadt, G.G. & Baeyens, W.F. (1983). Estimates of dry and wet deposition and resuspension fluxes of several trace metals in the Southern Bight of the North Sea. In: Precipitation Scavenging, Dry Deposition and Resuspension (Pruppacher, ed.), vol. 2. Elsevier, New York.

Dedeurwaerder, H.L. (1988). Study of the dynamic transport and of the fall-out of some ecotoxicological heavy metals in the troposphere of the Southern Bight of the North Sea. Ph. D. Thesis, University of Brussels (VUB), Belgium.

Dehairs, F., Dedeurwaerder, H., Dejonghe, M., Decadt, G., Gillain, G., Baeyens, W. & Elskens, I. (1982). Boundary conditions for heavy metals at the air-sea interface. In: Hydrodynamic and dispersion models. Boundary fluxes and boundary conditions (Nihoul & Wollast, eds.)

Diederen, H.S.M.A. & Guicherit, R. (1981). Source recognition of aerosols by concentration measurements of elements in ambient air. IMG-TNO Report G 799, IMG-TNO, Delft, the Netherlands.

Ducastel, G. (1994). Het atmosferisch aerosol in zuidelijk Noorwegen en het Arctisch gebied: chemische samenstelling, deeltjesgrootte, bronnen en brongebieden. Ph. D. Thesis, University of Gent (RUG), Belgium.

Duce, R.A., Liss, P.S., Merrill, J.T., Atlas, E.L., Buat-Menard, P., Hicks, B.B., Miller, J.M., Prospero, J.M., Arimoto, R., Church, T.M., Ellis, W., Galloway, J.M., Hansen, L., Jickells, T.D., Knap, A.H., Reinhardt, K.H., Schneider, B., Soudine, A., Tokos, J.J., Tsunogai, S., Wollast, R. & Zhou M. (1991). The atmospheric input of trace species to the world ocean. Global Biogeochem. Cycles, 5, 193-259.

Elskens, Y., Decadt, G., Dedeurwaerder, H., Dehairs, F. & Dejonghe, M. (1981). Study of the immission values and the transport of heavy metals above the North Sea. National Scientific and Development Report on Air. Scientific End Report 1978-1981.

Flament, P., Leprêtre, A. & Noel S. (1987). Coastal aerosols in Northern Channel. Oceanol. Acta, 10, 1, 49-61.

GESAMP (1980). Joint Group of Experts on the Scientific Aspects of Marine Pollution. Interchange of pollutants between the atmosphere and ocean. Reports and Studies No. 13.

GESAMP (1989). IMO/FAO/UNESCO/WMO/WHO/IAEA/UN/UNEP Joint Group of Experts on the Scientific Aspects of Marine Pollution. The atmospheric input of trace species to the world ocean. Reports and Studies No. 38.

Injuk, J., Otten, Ph., Laane, R., Maenhaut, W. & Van Grieken, R. (1992). Atmospheric concentrations and size distributions of aircraft-sampled Cd, Cu, Pb and Zn over the Southern Bight of the North Sea. Atmos. Environ., 26A, 14, 2499-2508.

Injuk, J., Van Malderen, H., Van Grieken, R., Swietlicki, E., Knox, J.M. & Schofield, R. (1993). EDXRS study of aerosol composition variations in air masses crossing the North Sea. X-Ray Spectrometry, 22, 220-228.

Injuk, J. (1995). Assessment of atmospheric pollutant fluxes to the North Sea by X-ray emission analysis. Ph. D. Thesis, University of Antwerp (UIA), Belgium.

Kane, M.M., Rendell, A.R. & Jickells, T.D. (1994). Atmospheric scavenging processes over the North Sea. Atmos. Environ., 28, 15, 2523-2530.

Kemp, K. (1984). Multivariate analysis of elements and SO_2 measured at the Danish EMEP stations. National Agency of Environmental Protection, MST Report LUFT-A88, Roskilde, Denmark.

Kersten, M., Dicke, M., Kriews, M., Naumann, K., Schmidt, D., Schulz, M., Schwikowski, M. & Steiger, M. (1988). Distribution and fate of heavy metals in the North Sea. In: Pollution of the North Sea (W. Salomons, ed.), pp. 303-347.

Kersten, M., Kriews, M. & Förstner, U. (1991). Partitioning of trace metals released from polluted marine aerosols in coastal seawater. Marine Chemistry, 36, 165-182.

Krell, U. & Roeckner, E. (1988). Model simulation of the atmospheric input of lead and cadmium into the North Sea. Atmos. Environ., 22, 375-381.

Kretzschmar, J.G. & Cosemans, G. (1979). A five year survey of some heavy metal levels in air at the Belgian North Sea coast. Atmos. Environ., 13, 267-277.

Kriews, M. (1992). Charakterisierung mariner Aerosole in der Deutschen Bucht sowie Prozessstudien zum Verhalten von Spurenmetallen beim Übergang Atmosphäre/Meerwasser. Ph. D.Thesis, University of Hamburg, Germany.

Laane, R. (1992) Background concentrations of natural compounds in rivers, sea water, atmosphere and mussels. Summary of the group reports written during the International Workshop on Background Concentrations of Natural Compounds, The Hague, April 6-10. Report DGW-92.033.

NAS (1978). The tropospheric transport of pollutants and other substances to the oceans. National Academy of Sciences Press, Washington, D.C.

Nriagu, J.O. & Pacyna, J.M. (1988). Quantitative assessment of worldwide contamination of air, water and soils by trace metals. Nature, 333, 134-139.

Otten, Ph., Injuk, J. & Van Grieken R. (1994). Elemental concentrations in atmospheric particulate matter sampled on the North Sea and the English Channel. Sci. Total Environ., 155, 131-149.

Ottley, C.J. & Harrison, R.M. (1993). Atmospheric dry deposition flux of metallic species to the North Sea. Atmos. Environ., 27A, 685-695.

Pacyna, J.M. (1984a). Estimation of the atmospheric emissions of trace elements from anthropogenic sources in Europe. Atmos. Environ., 18, 41-50.

Pacyna, J.M., Semb, A. & Hanssen, J.E. (1984b). Emission and long-range transport of trace elements in Europe. Tellus, 36B, 163-178.

Pacyna, J.M., Ottar, B., Hanssen, J.E. & Kemp, K. (1984c). The chemical composition of aerosols measured in southern Scandinavia. OR 66/84, Norwegian Institute for Air Research, Lillestrøm, Norway.

Peirson, D.H., Cawse, P.A., Salmon, L. & Cambray, R.S. (1973). Trace elements in the atmospheric environment. Nature, 241, 252-256.

Peirson, D.H., Cawse, P.A. & Cambray, R.S. (1974). Chemical uniformity of airborne particulate material and a maritime effect. Nature, 251, 675-679.

Rädlein, N. & Heumann, K.G. (1992). Trace analysis of heavy metals in aerosols over the Atlantic Ocean from Antarctica to Europe. Intern. J. Anal. Chem., 48, 127-150.

Schneider, B. (1987). Source characterisation for atmospheric trace metals over Kiel Bight. Atmos. Environ., 21, 1275-1283.

Schulz, M. (1993). Räumliche und zeitliche Verteilung atmosphärischer Einträge von Spurenelementen in die Nordsee. Ph. D. Thesis, University of Hamburg, Germany.

Slanina, J. & Asman, W.A.H. (1981). Analytical chemical research on precipitation in the Netherlands. Energiespectrum, 81, 292.

Spokes, L. J. (1991). In: Eurotrac air sea exchange experiment North Sea, 14-27 September 1991 (T.D. Jickells & L.J. Spokes, eds.).

Steiger, M. (1991). Die Anthropogenen und natürlichen Quellen urbaner und mariner Aerosole charakterisiert und quantifiziert durch Multielementanalyse und chemische Receptormodelle. Ph. D. Thesis, University of Hamburg, Germany.

Stössel, R.P. (1987). Untersuchungen zur Nass- und Trockendeposition von Schwermetallen auf der Insel Pellworm. Ph. D. Thesis, University of Hamburg, Germany.

Thrane, K.E. (1978). Background levels in air of lead, cadmium, mercury and some chlorinated hydrocarbons measured in south Norway. Atmos. Environ., 12, 1155-1161.

Van Daalen, J. (1991). Air quality and deposition of trace elements in the province of South-Holland. Atmos. Environ., 25A, 691-698.

Wiersma, G.B. & Davidson, C.I. (1986). Trace metals in the atmosphere of remote areas. In: Toxic Metals in the Atmosphere (J.O. Nriagu & C.I. Davidson, eds.). Wiley Series in Advances in Environmental Science and Technology, vol. 17, pp. 201-266. John Wiley and Sons, New York.

Yaaqub, R.R., Davies, T.D., Jickells, T.D. & Miller, J.M. (1991). Trace elements in daily collected aerosols at a site in Southeast England. Atmos. Environ., 25A, 5/6, 985-996.

Figure and table captions :

Figure 1	The North Sea and the Channel with the different subregions and location of the sampling sites (cruises and flights are not indicated)
Figure 2	Average airborne trace metal concentrations (ng/m^3) for the marine area of the Southern Bight.
Figure 3	Average airborne trace metal concentrations (ng/m^3) for the coastal area of the Southern Bight
Figure 4	Average airborne trace metal concentrations (ng/m^3) for the coastal area of the central North Sea
Figure 5	Average airborne trace metal concentrations (ng/m^3) for the marine and coastal area of the northern North Sea
Table 1	Trace metal concentrations (ng/m^3) for all sampling campaigns in the marine area of the Southern Bight (Values marked with § are indirectly cited values since we were unable to get the original reports; Values marked with † are averaged values (different authors, sampling campaigns, locations))
Table 2	Trace metal concentrations (ng/m^3) for all sampling campaigns in the coastal area of the Southern Bight (Values marked with § are indirectly cited values since we were unable to get the original reports; Values marked with † are averaged values (different authors, sampling campaigns, locations))
Table 3	Trace metal concentrations (ng/m^3) for all sampling campaigns in the coastal area of the central North Sea (Values marked with § are indirectly cited values since we were unable to get the original reports; Values marked with † are averaged values (different authors, sampling campaigns, locations))
Table 4	Trace metal concentrations (ng/m^3) for all sampling campaigns in the marine and coastal area of the northern North Sea (Values marked with § are indirectly cited values since we were unable to get the original reports; Values marked with † are averaged values (different authors, sampling campaigns, locations))
Table 5	Airborne trace metal concentrations (ng/m^3) in some remote areas as reported by Laane (1992), Rädlein and Heumann (1992) and Wiersma and Davidson (1986) compared with the most recent airborne trace metal concentrations reported in literature for the different marine parts of the North Sea.

Figure 1

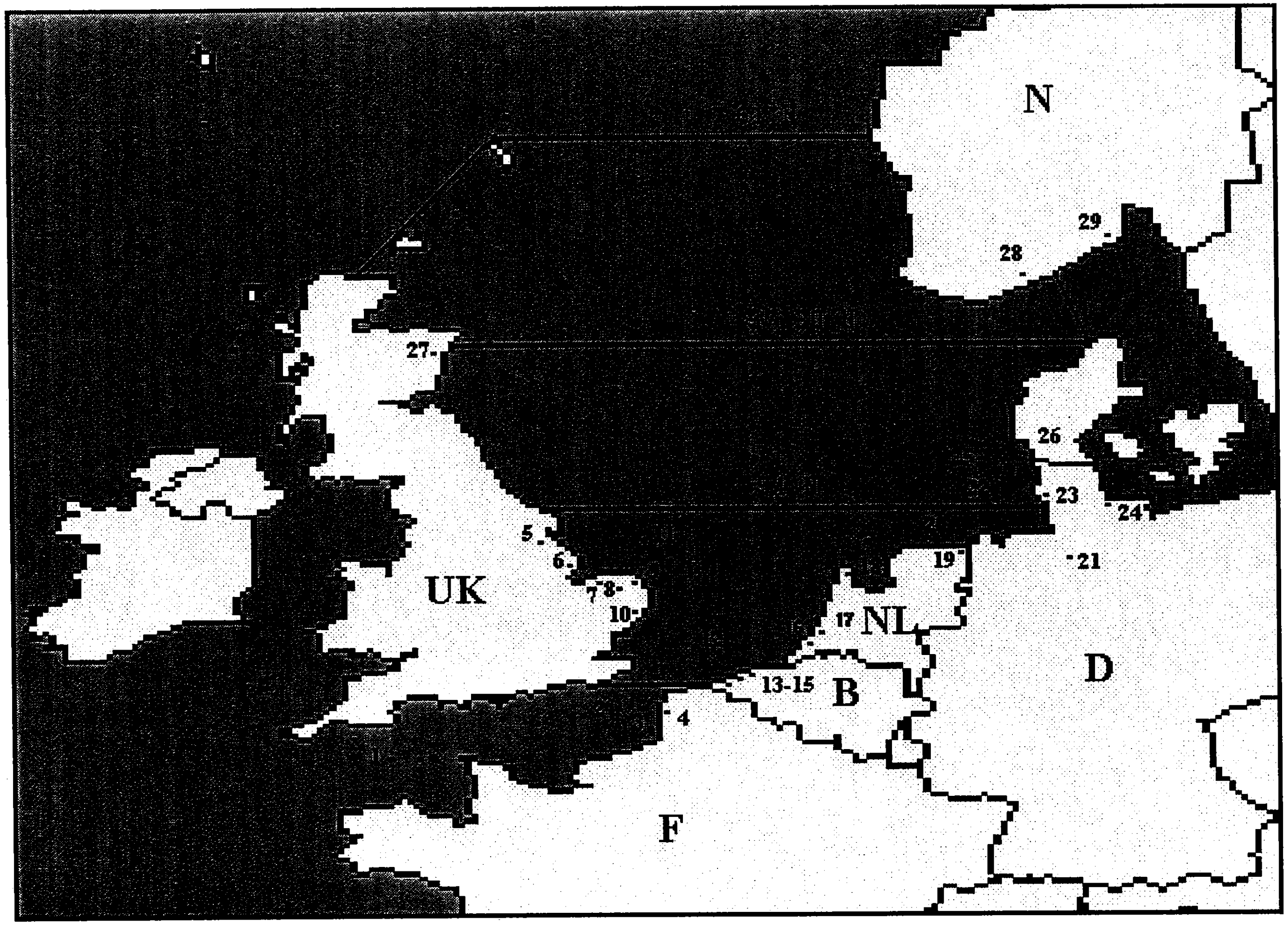

Legend of Figure 1

Channel

1 Atlantic station
2 Bassurelle
3 Baie d'Ambleteuse
4 Wimereux

Southern Bight

5 Styrrup
6 Spurn Head
7 Gresham
8 Mannington
9 Hemsby
10 Leiston
11 Gasplatform
12 Westhinder
13 Blankaert
14 Oostende
15 Blankenberge
16 Haamstede
17 Rijnmond
18 Petten
19 Hage
20 Schiermonnikoog
21 Hamburg

Central North Sea

22 Helgoland
23 Westerheversand
24 Kiel
25 FPN
26 Pellworm
27 Aberdeen

Northern North Sea

28 Birkenes
29 Vasser

Figure 2

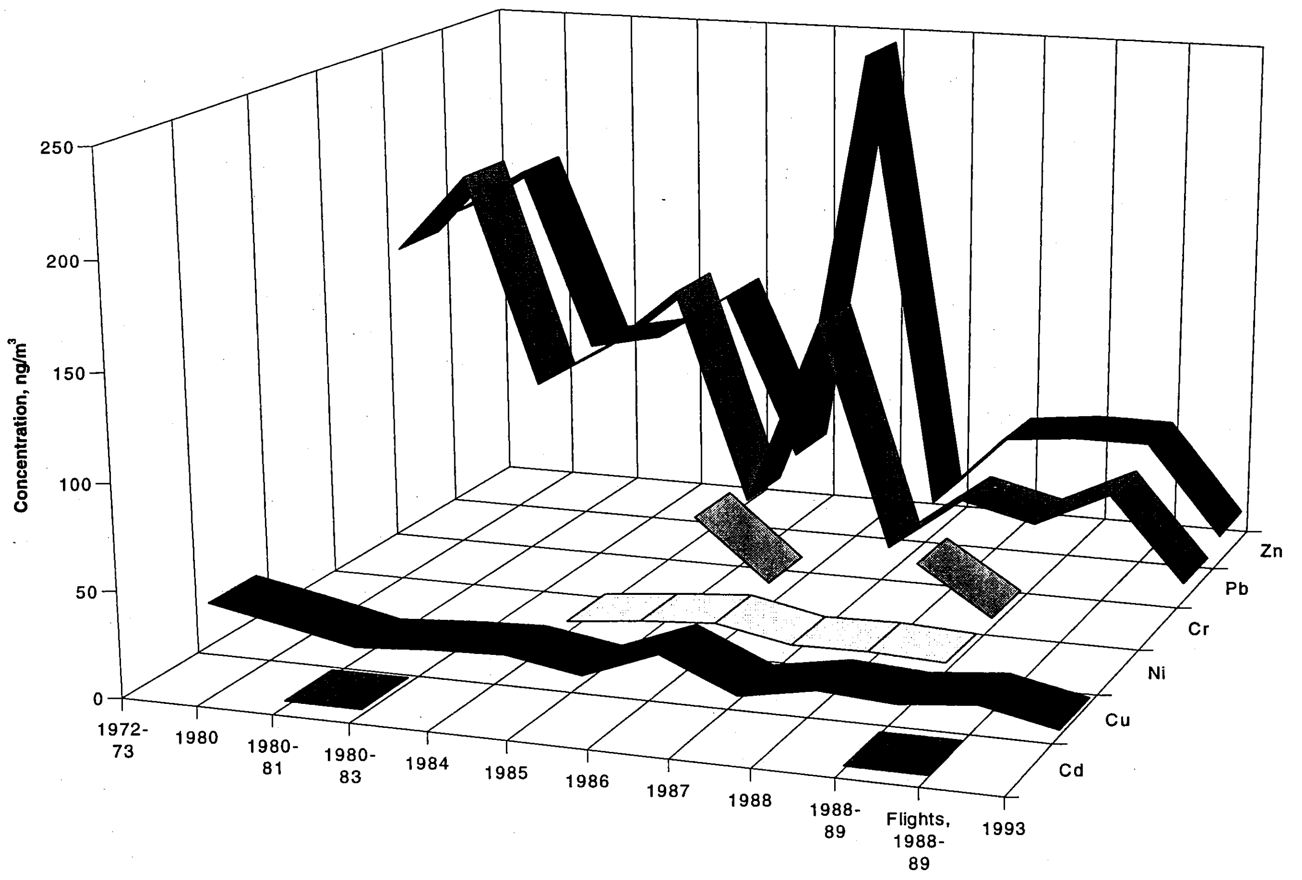
Concentration, ng/m³
250
200
150
100
50
0
1972-73
1980
1980-81
1980-83
1984
1985
1986
1987
1988
1988-89
Flights, 1988-89
1993
Zn
Pb
Cr
Ni
Cu
Cd

Figure 3

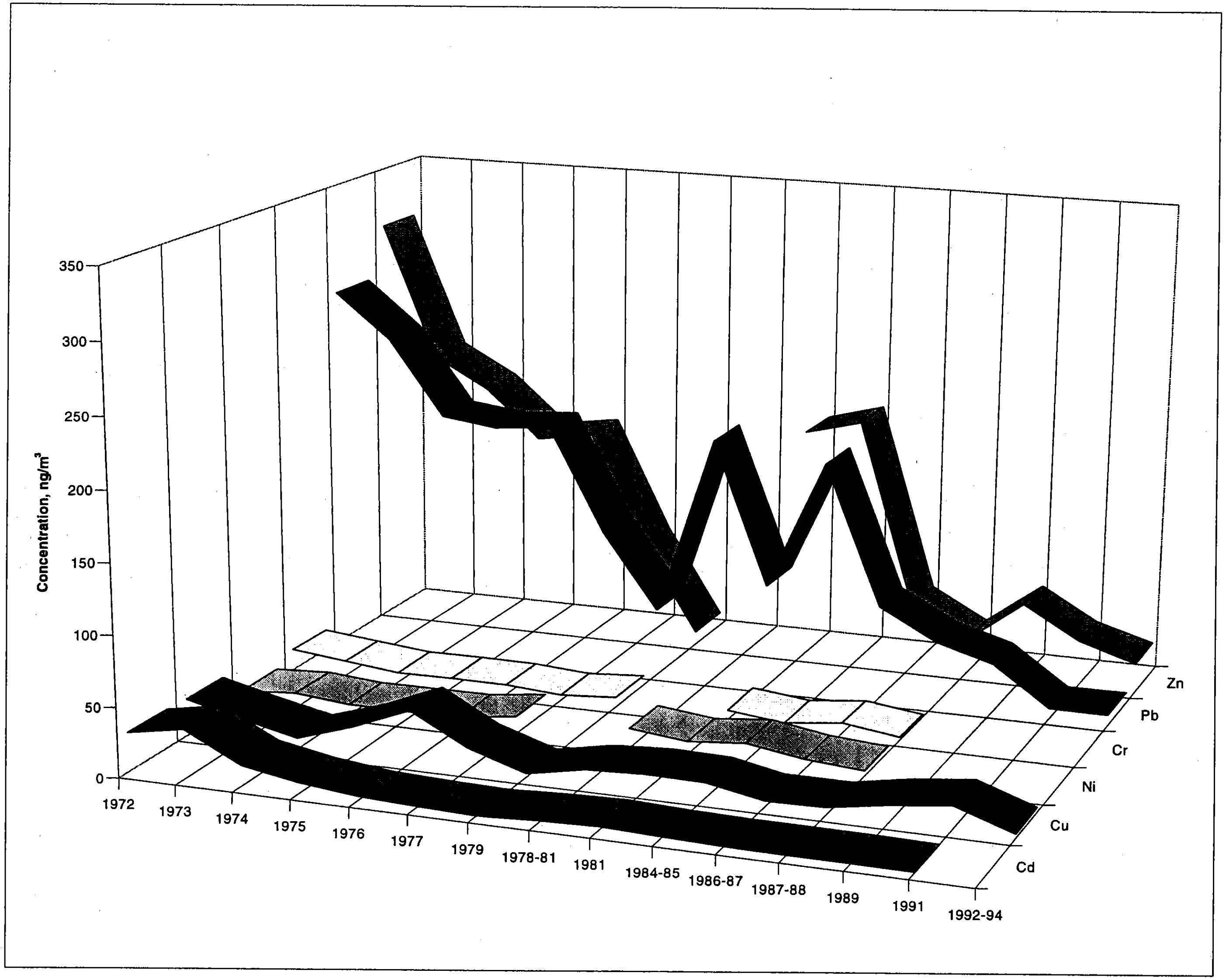
Concentration, ng/m³
350
300
250
200
150
100
50
0
1972
1973
1974
1975
1976
1977
1979
1978-81
1981
1984-85
1986-87
1987-88
1989
1991
1992-94
Zn
Pb
Cr
Ni
Cu
Cd

Figure 4

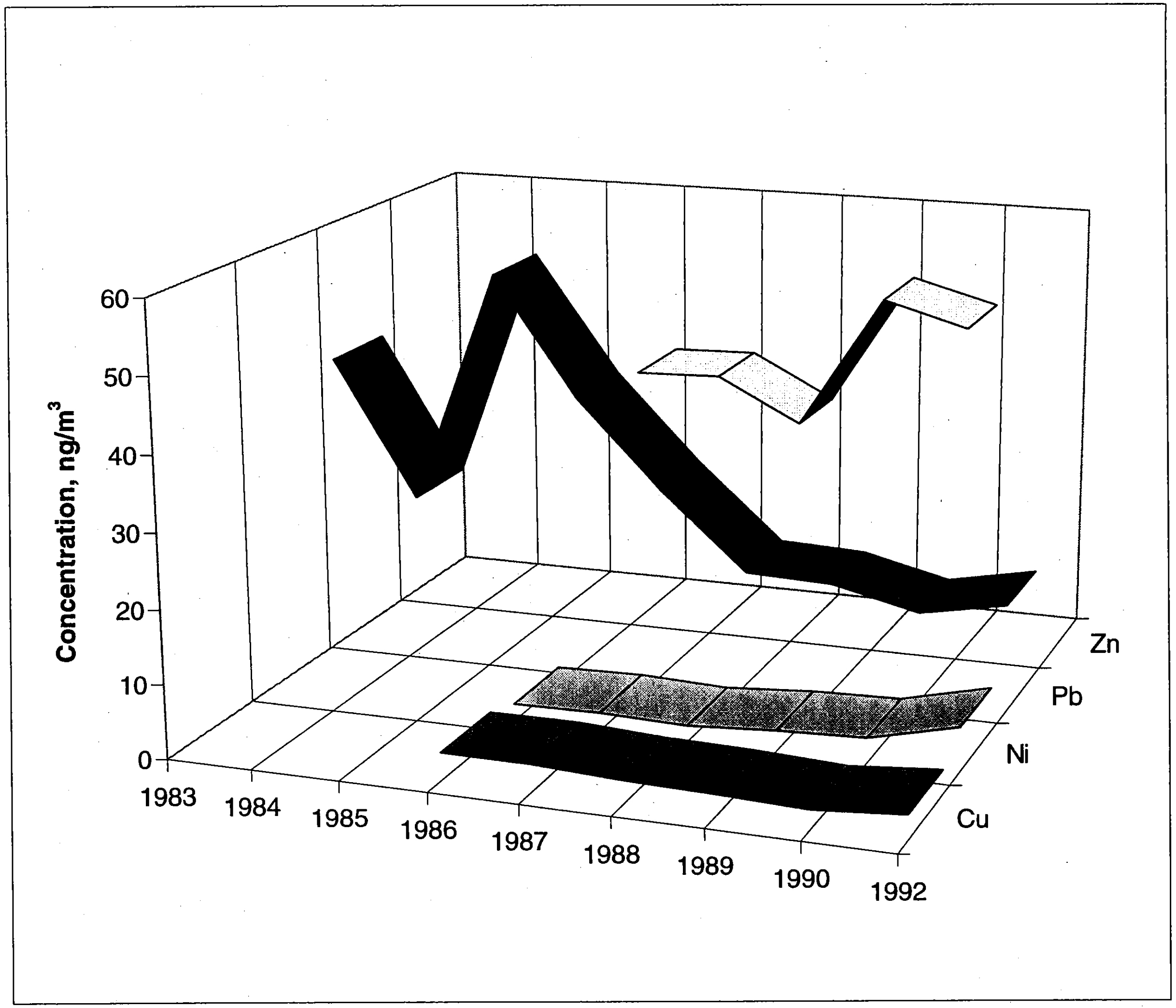
Concentration, ng/m^3
60
50
40
30
20
10
0
1983
1984
1985
1986
1987
1988
1989
1990
1992
Zn
Pb
Ni
Cu

Figure 5

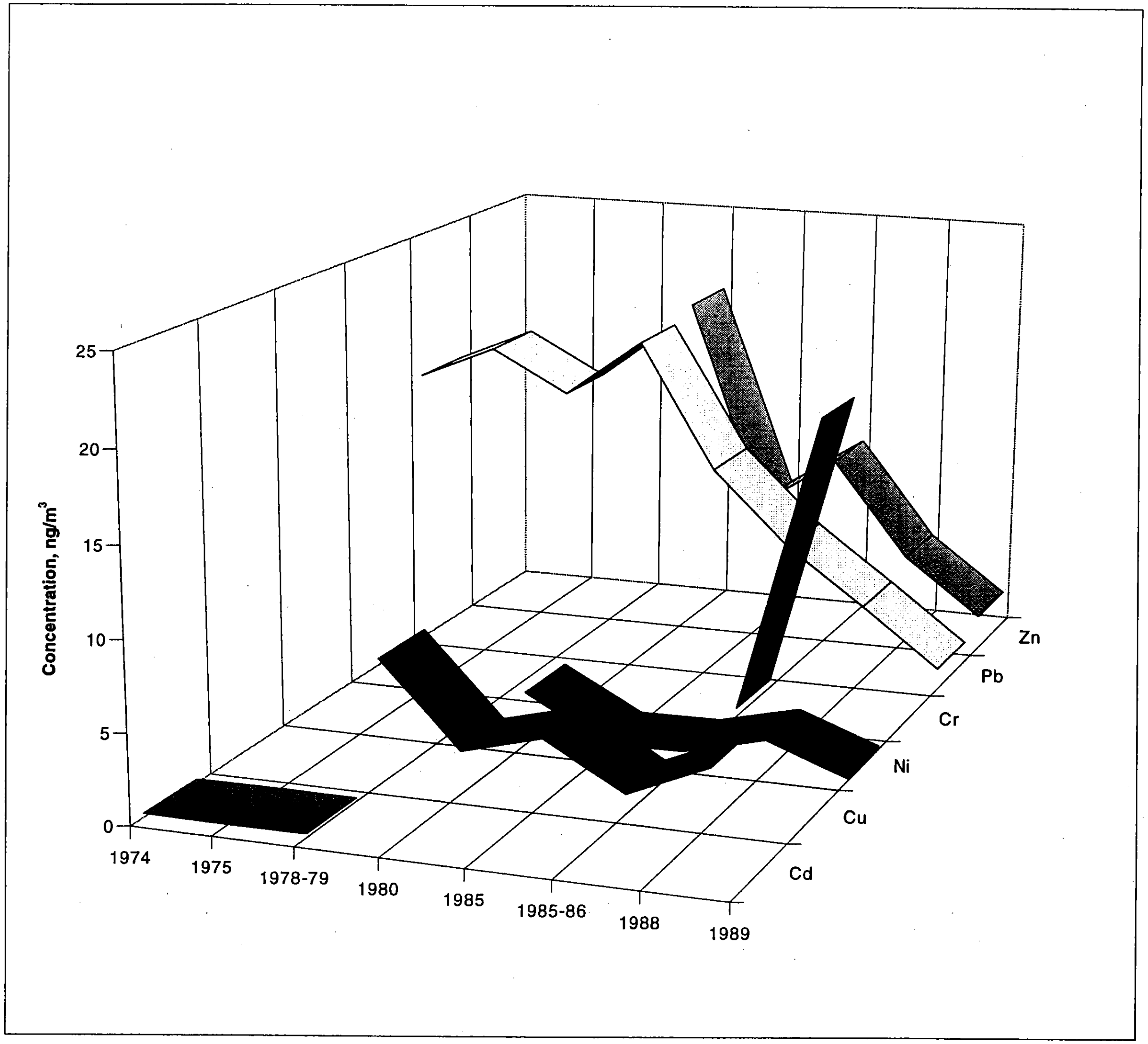
Concentration, ng/m³
0
5
10
15
20
25
1974
1975
1978-79
1980
1985
1985-86
1988
1989
Zn
Pb
Cr
Ni
Cu
Cd

Table 1

Period	1972-1973	1980	1980-1981	1980-1983	1984	1985	1986	1987	1988	1988-1989 †	1988-1989	1993 †
Location	gas platform	Westhinder	Westhinder	Westhinder	Cruise	Cruise	Cruise	Cruise	Cruise	Cruise	Flights	Cruise
	arithm. mean			geom. mean	arithm. mean	arithm. mean	arithm. mean	arithm. mean	arithm. mean	arithm. mean	mean	arithm. mean
Cd	-	-	2.7	2.9 ± 1.8	-	-	-	-	-	1.25	1.4 ± 1.0	-
Cu	20.8	14	6.5	9.0 ± 3.0	10 ± 16	4.5 ± 2.8	19 ± 9	2.6 ± 1.1	8.9 ± 4.5	6.6	10 ± 10	3.1
Pb	147	186	82.6	104 ± 2.3	135 ± 70	31 ± 21	124 ± 75	13 ± 10	41 ± 44	32	50 ± 14	17
Zn	153	176	86.6	94 ± 3.1	118 ± 74	37 ± 32	245 ± 223	18 ± 2	54 ± 48	58	58 ± 16	13
Ni	10.1	-	-	-	5.8 ± 6.9	9.4 ± 9.4	12 ± 7	5.0 ± 3.9	5.5 ± 2.9	3.8	-	3.0
Cr	4.5	-	-	-	-	41 ± 33	11 ± 9	-	28 ± 12	4.7	-	2.2
Reference	Peirson 1974 Cambray 1975	Elskens 1981 §	Dehairs 1982 §	Dedeur-waerder 1983	Otten 1994	Otten 1994	Otten 1994	Otten 1994	Otten 1994	Chester 1991 Ottley 1993	Injuk 1992	Injuk 1995

Table 2

Period	1972 †	1973 †	1974 †	1975 †	1976 †	1977 †	1979	1978-1981
Location	Styrrup Leiston	Styrrup Leiston	Styrrup Leiston	Styrrup Leiston	Styrrup Leiston	Schiermonnikoog Haamstede	Petten	Rijnmond
	arithm. mean	arithm. mean	arithm. mean	arithm. mean	arithm. mean			
Cd	28	35	15	7.8	3.1	1.5	0.4	2.5
Cu	26	17	8.0	21	38	17	3	10.5
Pb	270	238	183	178	181	105	50	183
Zn	307	208	186	151	158	75	10	-
Ni	7.9	11	7.3	7.5	7.7	14	-	14
Cr	15	11	6.9	7.4	7.2	4.2	7	-
Reference	Peirson 1974 Cawse 1974	Peirson 1974 Cawse 1974 Cambray 1975	Cawse 1975	Cawse 1976	Cawse 1977	Diederen 1981 §	Slanina 1981 §	DCMR 19-- §

Table 2 (continued)

Period	1981	1984-1985 †	1986-1987 †	1987-1988 †	1989	1991 †	1992-1994 †
Location	De Blankaert	South-Holland	South-Holland	Hemsby South-Holland	Mannington	Hemsby Spurn Head	Blankenberge
	geom. mean	arithm. mean	arithm. mean	arithm. mean	arithm. mean	arithm. mean	arithm. mean
Cd	3.4 ± 2.0	1.9	0.9	0.5	0.7 ± 0.9	0.3	-
Cu	13 ± 3	12	4.1	4.8	12 ± 22	17	3.1
Pb	77 ± 2	173	70	48	36 ± 33	8.0	8.2
Zn	174 ± 3	186	49	26	58 ± 70	35	22
Ni	9.5 ± 4.3	14	7.0	4.1	-	-	3.1
Cr	7.4 ± 4.3	2.7	7.4	2.1	-	-	5.1
Reference	Dedeurwaerder 1983	Van Daalen 1991	Van Daalen 1991	Yaaqub 1991 Van Daalen 1991	Kane 1994	Spokes 1991	Injuk 1995

Table 3

Period	1983	1984 †	1985 †	1986 †	1987 †	1988	1989	1990	1992
Location	Tange	Tange Keldsnor Pellworm	Tange Keldsnor Pellworm	Helgoland	Helgoland FPN German Bight	Helgoland	Helgoland	Helgoland	FPN
		arithm. mean	arithm. mean	arithm. mean	arithm. mean	arithm. mean	arithm. mean	arithm. mean	arithm. mean
Cd	0.6	-	-	1.9	0.95	-	-	-	-
Cu	3.0	-	-	3.9	3.8	3.3	3	2.5	3.5 ± 0.2
Pb	41	22.1	54	38	26.2	16	16	13	15 ± 1
Zn	30	-	-	36	37	31	50	46	-
Ni	3.0	-	-	2.3	2.6	2.2	3	3.4	6.2 ± 0.3
Cr	1.6	-	-	1.9	-	-	-	-	4.1 ± 0.5
Reference	Kemp 1984 §	Krell 1988	Krell 1988	Kersten 1991 Kriews 1992	Kriews 1992 Steiger 1991 Schulz 1993	Kriews 1992	Kriews 1992	Kriews 1992	Injuk 1995

Table 4

Period	1974	1975	1978-1979 †	1980	1985	1985-1986	1988 †	1989
Location	Birkenes	Birkenes	Birkenes	Birkenes	Cruise	Birkenes	Birkenes Cruise	Birkenes
	arithm. mean	arithm. mean			arithm. mean	median		median
Cd	0.2 ± 0.2	0.2 ± 0.4	0.2	-	-	0.1	-	-
Cu	-	-	7	2.4	3.6 ± 5.0	1.1	3	-
Pb	16 ± 22	18 ± 26	16	19	12 ± 5	7.8	4.6	1.2
Zn	-	-	-	20	8.0 ± 12	11	5.4	2.1
Ni	-	-	-	3	0.6 ± 0.3	0.7	1.8	0.2
Cr	-	-	0.9	-	-	0.5	18	-
Reference	Thrane 1978	Thrane 1978	Amundsen 1992 Pacyna 1984 b	Pacyna 1984 c §	Otten 1994	Amundsen 1992	Ducastel 1994 Otten 1994	Ducastel 1994

Table 5

	Alaska	Canadian Arctic	Greenland	East Atlantic Ocean	Bermuda	Hawaii
Cd	0.37				0.4	0.022
Cu		0.3	0.31	0.9	2.0	0.3
Pb		1.0	0.15 - 8.0	7	7	1.2
Zn	15	1.0	0.18 - 2.8	5	6	0.8
Ni			0.08 - 0.13			
Cr			0.09 - 0.2	0.2	0.5	0.2

Table 6

	North Sea subregion			
	Channel	Southern Bight	Central	Northern
	1987	1993	1991	1988
Cd	3 (1982-84)	1.4 (1988-89)		0.3
Cu	2.1	3.1	1.5	4.5
Pb	36	17	18 (1985)	12 (1985)
Zn	30	13	6.5	2.8
Ni	2.3	3.0	2.0	2.4
Cr	3.1 (1986)	2.2	3.5	18
	Otten 1994	Injuk 1995	Injuk 1993	Otten 1994

Submitted to Environmental Science and Technology

SINGLE PARTICLE CHARACTERISATION OF INORGANIC AND ORGANIC NORTH SEA SUSPENSION

Wendy Jambers and René Van Grieken*
Department of Chemistry, University of Antwerp (UIA), Universiteitsplein 1, B-2610 Antwerpen, Belgium.

ABSTRACT

Automated electron probe X-ray micro-analysis was used to characterise the chemical composition of individual suspended particles, collected in the Southern Bight of the North Sea. By staining the samples with RuO_4, extra information about the organic content of the particles could be obtained. Because at least small amounts of organic matter were detected in all samples, the presence of an organic coating on particles in natural waters was confirmed. Also the organic complexation of metals and the high affinity of fine-grained organic particles for heavy metal adsorption could be proven directly by the high amount of organic material detected in all Mn-, Cr-, Zn- and Ni-rich particles. By comparing the calculated total suspended matter concentration of the Ru-stained and unstained samples, it was confirmed that the amount of organic material in the southern part of the North Sea is low in winter and high, but also very variable, during primary production peaks in spring. Only very close to the Westerschelde estuary, the amount of suspended matter was relatively constant in time.

KEYWORDS

Suspension, EPXMA, Ru-staining, Single particle, North Sea

INTRODUCTION

Particles are of great importance in the aquatic environment, because they are responsible for the majority of material transport and because they act as adsorbance media for different, mostly toxic, heavy metals. Because single particle analysis can give more detailed information about the origin, formation, transport reactions and transformation reactions, it is a valuable complement to environmental bulk analysis. Unfortunately hardly any research has been done on the characterisation of single particles in aqueous suspension and in sediments. (1-3).

Most applications have been done using electron probe X-ray micro analysis (EPXMA) or scanning electron microscopy combined with energy dispersive X-ray detection (SEM-EDX), which is comparable to EPXMA. The greatest advantage of these techniques is the possibility for automation, based on recognizing particles on a filter backing via the backscatter electron

---

* fax: +32-3-820 23 76, e-mail: vgrieken@uia.ua.ac.be

signal. This automation improves the accuracy of the analysis by allowing characterisation of large amounts of particles in a reasonable time. However, automated analysis of organic particles is difficult, because low Z-elements only give backscatter electron images with low contrast. These difficulties can be overcome by staining of the samples with a strong oxidizer like ruthenium tetroxide (4).

This article will discuss the results of EPXMA measurements of suspended matter samples collected during three different seasons at ten locations and three depth in the Southern Bight of the North Sea. To enable comparison, each samples was prepared twice, once using the more conventional method of carbon-coating and once by heavy metal staining with ruthenium tetroxide.

Not many data are available on single particle analysis of North Sea suspension. Xhoffer et al. (5) were the only ones to publish results of EPXMA and laser micro-probe mass analysis (LMMS) on suspension of the North Sea surface boundary layer and the underlying bulk water and to compare these results with those of aerosols collected above the North Sea. Bulk analyses of the inorganic and organic suspended North Sea material have been performed by e.g. Eisma and Kalf (6-7). They have found that the southern North Sea could be characterised by a high suspended matter concentration (for January on average 5 mg/l in the centre and 12 mg/l for the coastal regions), but the amount of organic matter is relatively low (lower than 20% for the coastal regions). This can partly be explained by the large contribution of resuspended bottom material (in the order of several million tons per year). Large parts of the Southern Bight only have a shallow depth (water depth less than 30 m) and bottom material can thus easily be suspended by large waves and swell. This resuspended material has a low organic matter content, because a large fraction of the organic matter (at least 75%) is lost, presumably through consumption by bottom organisms, during and/or after deposition of the suspended matter. This low organic content also explains the smaller average diameter of the micro-flocs in the suspension of the southern part in comparison with the northern part of the North Sea. Organic matter acts as a glue between the mineral particles of the micro-flocs, but because the amount of organic material is smaller in the souther part, micro-flocs cannot grow to such a large size as in regions with less resuspension. The amount of suspended matter is also dependant on the season. Due to stronger winds and more intensive wave actions, the concentration is higher during autumn and winter (7). However during summer, much higher and variable concentrations of organic matter were detected, because of the presence of variable primary production.

EXPERIMENTAL

Sampling

During cruises with the R/V Belgica in February and November 1994 and in May 1995, 30 samples were collected in the Southern Bight of the North Sea. At the 10 locations, shown in Figure 1, collections were performed near the surface, near the bottom and at intermediate depth. Sampling was performed using a 10 l PTFE Niskin bottle and sub-samples were collected in 1 l acid cleaned PE bottles. For the analysis of organic material, samples should normally be collected and handled in glassware, while for inorganic material plastics are recommended (8,9). Because both organic and inorganic material was analyzed, it was preferred to work with acid cleaned plastic.

The suspension is filtered immediately after collection to prevent interaction between the dissolved and particulate phases in the storage bottles. Filtration is performed on 47 mm aerosol-grade Nuclepore (Pleasanton, CA, USA) filters with 0.4 µm pore-size, using a polycarbonate

Sartorius (Göttingen, Germany) filter holder. To enhance the homogenity of the particle distribution on the thin Nuclepore filter, a Whatman (Maidstone, England) filter was placed underneath during filtration. An suitable particle loading for single particle analysis was obtained by filtering 10 ml for the two sampling sites close to the coast (i.e. location I and VIII in Figure 1) and 100 ml for the other sites. To remove crystallised salts, the filters were three times rinsed with de-ionized water. Further, the filters were put in petri dishes, air dried and stored in a deep-freezer until preparation for EPXMA. During this preparation, part of the filter was cut with stainless steel scissors and mounted with double sided tape on a 25 mm plastic plate which fits into the EPXMA sample holder. For every sample two pieces were cut and put on a plate. One was coated with 50 nm of carbon, while the other was stained with ruthenium tetroxide.

At the end of the November campaign a blank samples was collected by filtering 100 ml of di-ionised water.

Ru-staining

Ruthenium tetroxide was used as a 0.5% stabilized aqueous solution (Polysciences, Eppelheim, Germany). This solutions is a strong oxidizer, but it is also toxic and the same safety precautions as for OsO_4 should be taken. Approximately 5 ml of RuO_4 was put in a 50 mm glass petri dish to completely cover the bottom. The plastic plate with part of the filter was mounted with double sided tape to the cover of the petri dish. Subsequently, the filter was exposed for 15 min to the RuO_4 vapours by putting the cover over the petri dish. This results in a charcoal-grey sample which is conductive and which can, without further preparations, be used for EPXMA measurements.

Instrumentation

All measurements were performed using a JEOL (Tokyo, Japan) JXA-733 Superprobe which was coupled with a Tracor Northern (Middelton, WI, USA) TN-2000 X-ray analysis system and a 486 personal computer. The system was automated with the home made 733 Particle Recognition and Characterisation program. In this procedure, successive horizontal scanning of the backscatter image of a preset area is used to locate the individual particles. The scanning stops when all contour points of a particles are resolved and an energy-dispersive X-ray spectrum is recorded during a 20 s star scan over the particle. Subsequently, the horizontal scanning recommences for the localisation of the next particle. Immediatly after recordering the spectra are deconvoluted using the fast filter algorithm (FFA) and the peak intensities are stored in a large data matrix. This data matrix also contains the sum of the peak intensities and the spherical diameter and shape factor of the particle, which can be calculated using the information of the recorded contour points.

Per sample, 500 particles with a diameter larger than 0.4 μm were characterised using an acceleration voltage of 25 kV, a beam current of 1 nA and a magnification of 1 000. After analysis, the predominant elements (i.e. elements present in more than 1% of the particles) were selected for data treatment.

Extra information concerning the shape and homogeneity of the particles was obtained by manual EPXMA measurements. Spectra were collected during 60 s in either spot or selected area mode. Deconvolution was also performed using FFA and the peak intensities were normalized.

Data treatment

For interpretation of the results, it is necessary to reduce the dimension of the data matrix. By using hierarchical clustering, this can be done with a minimum loss of information. For environmental studies, a hierarchical clustering is usually performed in the Euclidian dimension using the Ward's error sum classification. This method allows to describe a large data set with a minimum number of groups which contain a maximum of geochemically relevant information and, at the same time, it avoids fusion of geochemical important groups (10). As a stopping rule the consistent Akaike information criterion (CAIC) (11,12) was used, because this generally produces the most reliable results.

All cluster analyses have been performed using the Windows-based integrated data analysis system (IDAS), developed at the University of Antwerp (12). For the unstained samples all predominant elements were selected and the X-ray peak intensities were normalized before clustering. For the stained samples, the Ru-peaks were rejected from the data matrices and clustering was performed as described above. However, these results only give information on the pure organic particles (i.e. particles which only have a Ru-peak) and can not be used to determine the amount of organic material coagulated with or coated on inorganic particles. A clustering in which the Ru-peak are included was thus necessary. However, the Ru peak was present in all particles and when it was included in the clustering, the division was based on the Ru-content of the particles and other geochemical information was lost. For this reason a second clustering was performed including the normalized Ru-peak intensities in the cluster results, but still rejecting them for the actual clustering. This was possible because, when elements are rejected from clustering during the preprocessing in the IDAS program, they will still be used to calculate the average composition of the resulting groups. When elements were rejected from both clustering and results, this was done before entering the IDAS program. To ensure comparison of the unstained and stained samples, it was necessary to cluster them under the same conditions. This implied an extra normalisation for the clustering of the stained samples which include Ru, resulting in a clustering with normalised elements excluding Ru and a representation of the results with normalised elements including Ru. As a last comment on these cluster analyses, it should be mentioned that although more information is obtained from the clustering of the stained samples which include Ru, the clustering excluding Ru was still performed, because the results of this last clustering give the same particle types as for the unstained samples and thus simplify the identification of the particle groups.

RESULTS AND DISCUSSION

Particle types

The particle types found in these samples are comparable with those found by Xhoffer et al. (5) and their sources will thus only be discussed briefly.

The **aluminosilicates** particle type is characterised by high relative X-ray intensities for Al, Si, Fe, K and sometimes Ca or Ti. It dominates most samples and according to their composition, they have been subdivided into 6 classes: pure aluminosilicates which only contain Al and Si, aluminosilicates with small amounts of K, Fe and/or Ca, and Ca-rich, K-rich, Fe-rich and Ti-rich aluminosilicates with high abundances for the respective elements. The main source for these particles is erosion of rocks consisting of clay minerals and micas. The Fe-rich aluminosilicates can generally be characterised by chlorite and Fe-smectite, but because clay minerals are known to adsorb trace metals (13); these particles can also be clay minerals which have adsorbed large amounts of Fe. No mineral is known which corresponds to the Ti-rich aluminosilicate subgroup (14-15) and these particles are most likely natural aggregates of rutile in granite, gneiss and mica schist (15).

Si-rich particles are characterised by a relative peak intensity of Si which is higher than 70% and an Al peak intensity which is lower than 5%. These particles have two main sources: mineral quartz and biogenic opal. These biogenic particles are mostly silicon skeletons of diatoms, but also silicoflagellates and parts of sponges can contribute (13, 16). Since mineral and biogenic particles have a comparable spectrum, they can only be distinguished by their shape and are thus during automated analysis classified in the same group.

Ca-rich particles also have a mineral and biogenic source and are characterised by a Ca-relative peak intensity which is higher than 70%. These particles can be calcite or aragonite or can be skeletons of coccolithophores, foraminefera or pteropods (13, 16).

Fe-rich particles contain Fe as the predominant element (relative peak intensity higher than 50%) and sometimes also small amounts of Si or Ca. The main source are minerals like hematite, goethite and siderite, but Fe-rich particles are also produced during metallurgy processes. However, these anthropogenic Fe-particles mostly have a spherical shape and because only small abundances of these spherical Fe-rich particles were detected during manual analysis of the samples, their contribution to this particle group must be limited. This particle type was detected in the majority of the samples, but the abundances found were much lower (on average 3%) than those of the former groups.

Ti-rich particles originate from the mineral rutile or from anthropogenic sources like asphalt production and paint. The low abundances found in all samples (about 1%) are comparable with those found in the air above the North Sea (5). However, Ti-rich particles are detected in most natural waters and a mineral source cannot be excluded (13).

The **S-containing particles** are subdivided in S-rich, Fe-S-rich, Ba-S-rich and Ca-S-rich particles. The S-rich particles were only detected in 14 samples (7 stained and 7 unstained) and are characterised by a relative peak intensity for S which is higher than 70%. The are most likely of biogenic origin. Low abundances of Fe-S-rich particles were also detected in some of the samples. These particles can be pyrite or marcasite, but because these minerals are not very stable in oxic environments, it is more likely that these are biogenically produced pyrite framboids. The Ba-S-rich particles were only detected in one unstained sample and can be characterised as barite ($BaSO_4$) which is frequently found in oceanic suspended matter and has a biogenic origin (13,17-18). The Ca-S-rich particles could be gypsum which is present in dissolved form in most natural waters, but the samples have been desalted by rinsing with di-ionized water and the soluble gypsum is thus removed from the filters. However, these Ca-S-rich particles are only detected in small abundances in 7 Ru-stained samples and are thus most likely organic particles which contain Ca and S.

Small amounts of **Al-rich particles** were detected in 3 samples. They are characterised by particles which only contain Al and are thus most likely aluminium oxides. The most probable source is corundum (Al_2O_3) which has been reported to be associated with diatoms (4, 19).

Heavy metal rich particles were detected in small abundances in 50% of the samples. They are characterised by relative peak intensities for Mn, Cr, Zn or Ni which are higher than 50%. These particles are detected in small abundances in most marine systems, but for the North Sea, additional heavy metal input from various anthropogenic sources will certainly contribute to these particle types (20). The importance of the anthropogenic heavy metal input to the North Sea is confirmed by the relatively large amounts of Cr- and Zn-rich particles which were detected in aerosols collected above the North Sea (21,22). These particles are especially important in the samples collected in May. During this campaign, they were present in relatively large abundances (up to 13%) in the majority of the samples, which could point to a correlation between these particles and the large organic fraction present in these samples. This correlation was confirmed during principal factor analysis.

In the unstained samples, **organic particles** are characterised as particles with a total peak intensity which is lower than 1 000 counts, while in the Ru-stained samples they only contain a Ru-peak. The majority of these particles are biogenically produced, but because organic material is also discharged by human activities, an anthropogenic source cannot be excluded. The higher primary production during spring and summer is clearly visible in the higher, but also more variable, abundances detected in May (2 to 82 % with an average of 16%) compared to those found in winter (on average 3%). Part of the organic particles were also detected in the unstained samples, but these are only the more dense particles which are not representative for the total organic fraction

Organic content

In the Ru-stained samples the organic content of a particles can be estimated using the relative peak intensity of the Ru-X-ray peak. Because Ru was detected in all particles, it can be concluded that all at least contained a small amount of organic matter. This observation could confirm the presence an organic coating on all particles in natural waters (13,23). By performing manual spectrum collections on small particles and on filter material next to the particles, it was seen that the Ru-peak of the particles was always higher than for the filter material. This excludes artefacts due to the filter material.

The amount of organic material coagulated with the particles seems to vary with the season. In winter (i.e. for the samples collected in November and February), only S-rich, Ca-S-rich and Mn- and Cr-rich particles contain large amounts of organic material (relative peak intensity of Ru > 30%). Because the source of S- and S-Ca-rich particles is organic, large quantities of organic material were expected in these particles. The large amounts of organic material in the heavy metal rich particles confirm the organic complexation of the metals (5, 24, 25) and the high affiliation of the fine-grained organic fraction for the adsorption of heavy metals (13).

In summer, not only high amounts of pure organic material were detected (up to 50% of the particles were organic), but also large quantities of organic matter were associated with other particle types. This was again true for the S-containing and heavy metal rich particle types, but also for the Fe-rich particle type. For the Si- and Ca-rich particle types only part of particles had a high organic content, which confirms the presence of both mineral and biogenic particles. To illustrate the difference between both, the spectra of a quartz particle and a diatom skeleton are shown in Figure 2. The pure aluminosilicate and Ca-rich aluminosilicate particle type also contained a large amount of organic material, while the other aluminosilicate sub-types seemed to be less sensitive to coagulation with or coating of organic material.

Depth profiles

The area of the filter on which the 500 particles have been detected can be used to calculate the amount of particles per filter and, when the diameter of the detected particles are included, also the volume of particles per filter. The total suspended matter can be obtained by dividing the volume of the particles by the filtered volume of water. However, this calculation will only give a rough estimation of the total suspended matter, because only the particles which are detected during automated analysis, i.e. particles larger than 0.4 µm with a high enough backscatter signal, are included and, more importantly, a homogeneous loading of the filter is presumed. In spite of these restrictions, this calculated total suspended matter content is very useful to evaluate the fluctuation as a fuction of place, time and depth.

When the Ru-stained and unstained samples are compared it can be seen that the volumes are higher in the stained samples. This enlargement is small in winter (i.e. February and November) and is larger, but also more variable, for the samples collected in May. As an example, the depth profiles at location IX in February and May are given in Figure 4. At this location and at location III, the enlargement is more pronounced in the surface waters, while for the other locations there, is an increase at all depths. This is again another proof for the small amount of organic material present in the Southern Bight of the North Sea during winter and its variable increase during intense primary production periods (7).

For the evaluation of the total suspended matter with time, the depth profiles of the Ru-stained samples at the locations VI, VIII, IX and X are given in Figure 5. Both Ru-stained and unstained samples revealed the same tendency of the lowest amount in November, an intermediate, but also more variable, concentration in May and the largest amount of total suspended matter in February. This increase is comparable with that found in earlier studies (7) and can be explained by the higher wind and increased wave action in autumn and winter and the variable primary production during spring and summer (7). Also the small increase of suspended matter during winter at location VIII, i.e. off the Westerschelde, is in agreement with the chances found by Eisma and Kalf (7).

ACKNOWLEDGEMENTS

This work was prepared in framework of the Impulse Programme in Marine Sciences, supported by the Belgian State - Prime Minister's Service - Services for Scientific, Technical and Cultural Affairs (contract MS/06/050). Special thanks are due to the captain and the crew of the R/V Belgica.

REFERENCES

(1) Van Grieken, R.; Xhoffer C. *J. Anal. Atomic Spectrom.* **1992**, 7, 81-88.

(2) Jambers, W.; De Bock, L.; Van Grieken, R. *Analyst* **1995**, 120, 681-692.

(3) Jambers, W.; De Bock, L.; Van Grieken, R. *Fresenius* **1996**, 355, 521-527.

(4) Lavoie, D.M. *Deep-Sea Research* **1992**, 39, 1655-1668.

(5) Xhoffer, C.; Wouters, L.; Van Grieken, R. *Environ. Sci. Technol.* **1992**, 26, 2151-2162.

(6) Eisma, D.; Kalf, J. *Neth. J. Sea Research* **1987**, 21, 265-285.

(7) Eisma, D.; Kalf J. *Neth. J. Sea Research* **1979**, 13, 298-324.

(8) Topping, G.; Wells, D.E.; Griepink, B. *Quality Assurance of Information in Marine Environmental Monitoring Programmes in Europe (QUASIMEME): Guidelines on Quality Assurance for Marine Measurements*, Bureau of Community Reference, EC, Brussels, 1993, Chapter 13.

(9) Benoliel, M.J. *Intern. J. Environ. Anal. Chem.* **1994**, 57, 197-206.

(10) Bernard, P.C.; Van Grieken, R.E.; Eisma, D. *Environ. Sci. Technol.* **1986**, 20, 467-473.

(11) Bondarenko, I.; Van Malderen, H.; Treiger, B.; Van Espen, P.; Van Grieken, R. *Chemom. Intell. Lab. Syst.* **1994**, 22, 87-95.

(12) Bondarenko, I.; Treiger, B.; Van Grieken, R.; Van Espen, P. *Spectrochim. Acta Electronica* **1996**, 51B, 441-456.

(13) Eisma, D. *Suspended Matter in the Aquatic Environment*, Spinger-Verlag, Berlin, 1992.

(14) Hurlbut, C.S. *Dana's Manual of Mineralogy 18th ed.*; J. Wiley and Sons: New York, 1971.

(15) Betekhtin, A. *A Course of Mineralogy*; Peace Publishers, Moscow, 1965.

(16) Friedrich, H. *Marine Biology: An Introduction to its Problems and Results*, Sidgwick & Jackson, London, 1969.

(17) Dehairs, F.; Chesselet, R.; Jedwab J. *Earth Planet. Sci. Lett.* **1980**, 49, 528-550.

(18) Stroobants, N.; Dehairs, F.; Goeyens, L.; Vanderheijden, N.; Van Grieken, R. *Marine Chem.* **1991**, 35, 411-421.

(19) Vinogradov, A.P. *The Elemental Chemical Composition of Marine Organisms*, Yale University Press, Princeton, NJ, 1953.

(20) Everaarts, J.M.; Fischer, C.V. *Neth. J. Sea Research* **1992**, 29, 323-331.

(21) Van Malderen, H.; Hoornaert, S.; Van Grieken, R. *Environ. Sci. Technol.* **1996**, 30, 489-498.

(22) Injuk, J.; Van Grieken, R. *J. Atmos. Chem.* **1995**, 20, 179-212.

(23) Neihof, R.A.; Loeb, G.I. *J. Mar. Res.* **1974**, 32, 5-12.

(24) Hood, D.W. *Environ. Sci. Technol.* **1967**, 1, 303-305.

(25) Kersten, M.; Dicke, M.; Kriews, M.; Naumann, K.; Schmidt, D.; Schultz, M.; Schwikowski, M.; Steiger, M. In *Pollution of the North Sea: An Assessment*; Salomons, W., Bayne, B.L., Duursma, E.K., Förstner, U., Eds.; Springer-Verlag: Berlin, 1988, pp. 300-347.

FIGURE CAPTIONS

Figure 1	Map with the ten different sampling locations. The dashed lines indicate the borders of the territorial waters of Belgium, The Netherlands, England and France.
Figure 2	Secondary electron image and spectrum of a quartz particle.
Figure 3	Secondary electron image and spectrum of a diatom skeleton.
Figure 4	Comparison of the total suspended matter calculated for both Ru-stained and unstained samples at location IX in (a) February and in (b) May.
Figure 5	Comparison in time of the total suspended matter calculated for the Ru-stained samples collected at the locations (a) VI, (b) VIII, (c) IX and (d) X.

Fig 1

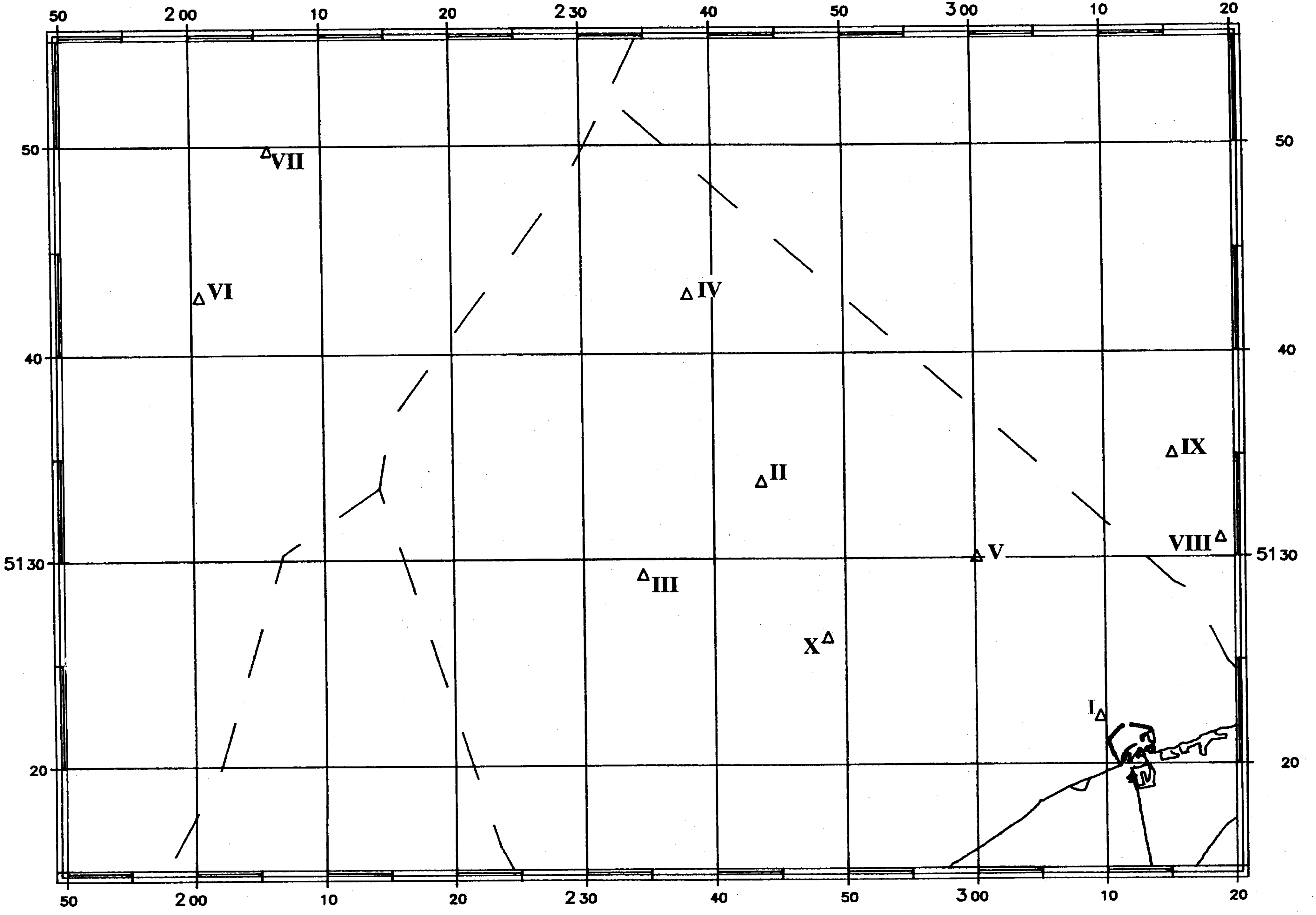
50
2 00
10
20
2 30
40
50
3 00
10
20
50
40
51 30
20
VII
VI
IV
II
IX
VIII
V
III
X
I
IV

Fig 2

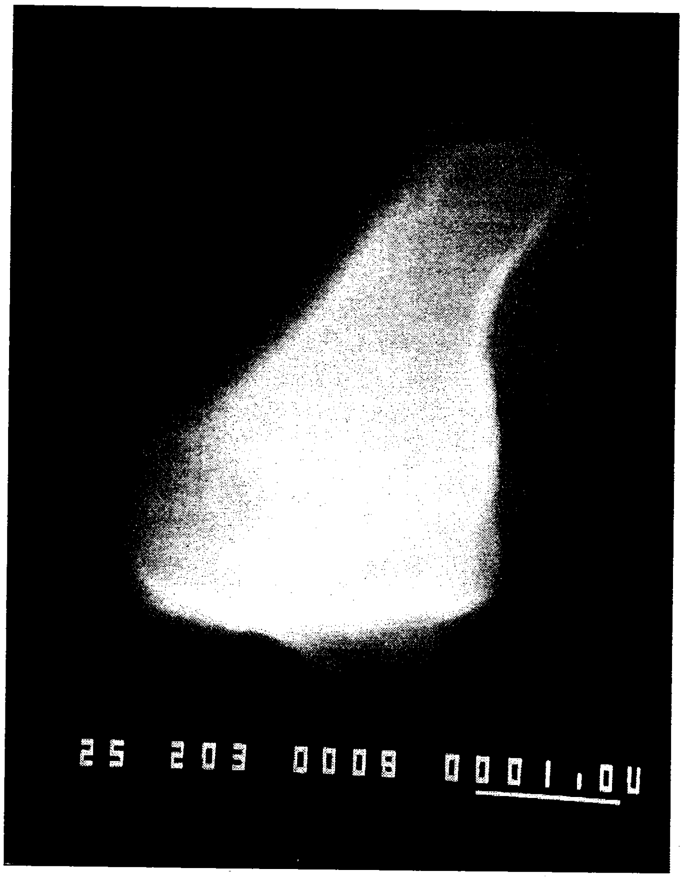

Fig 2

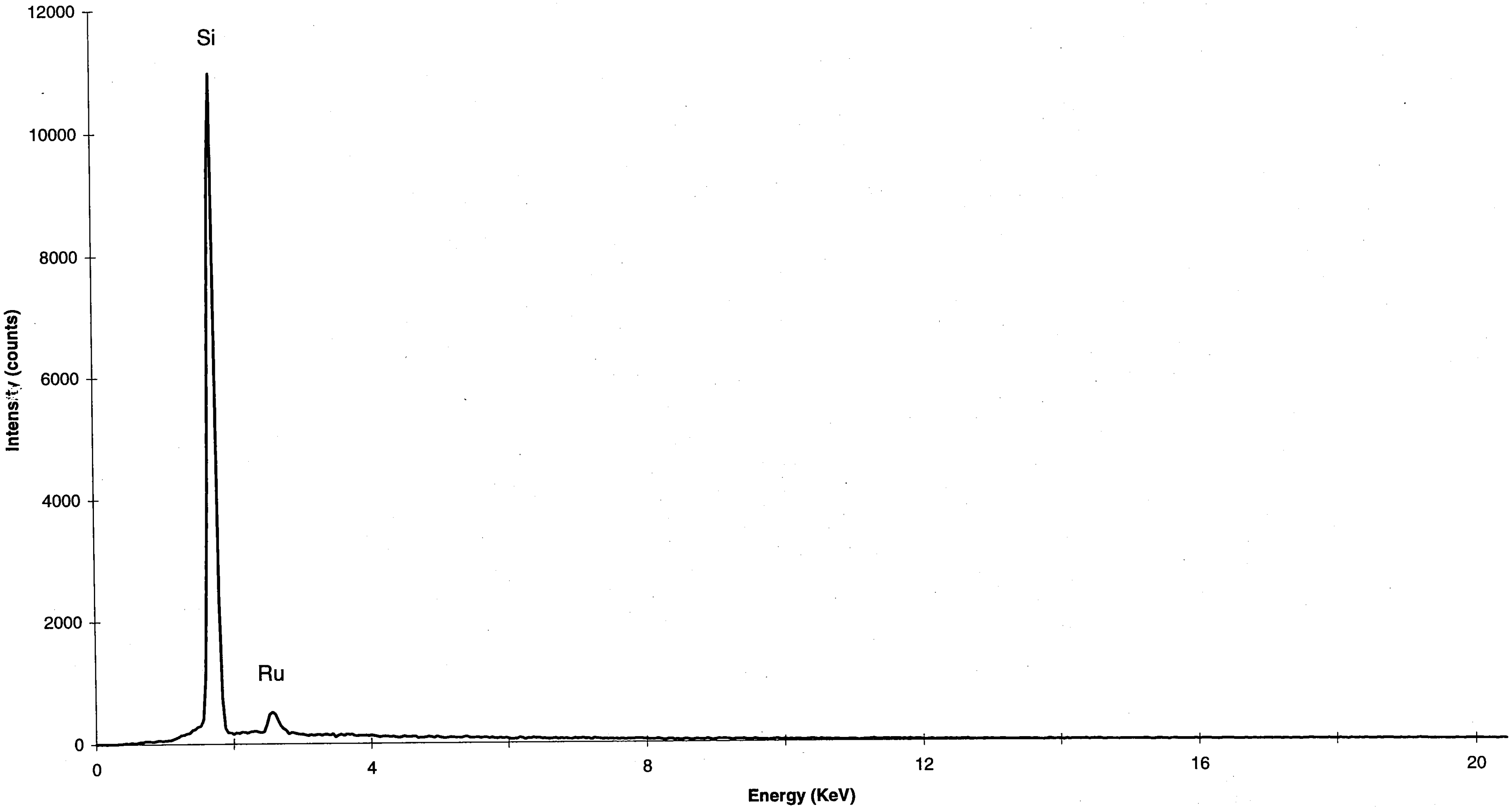
Si
Ru
Intensity (counts)
0
2000
4000
6000
8000
10000
12000
0
4
8
12
16
20
Energy (KeV)

fig 3

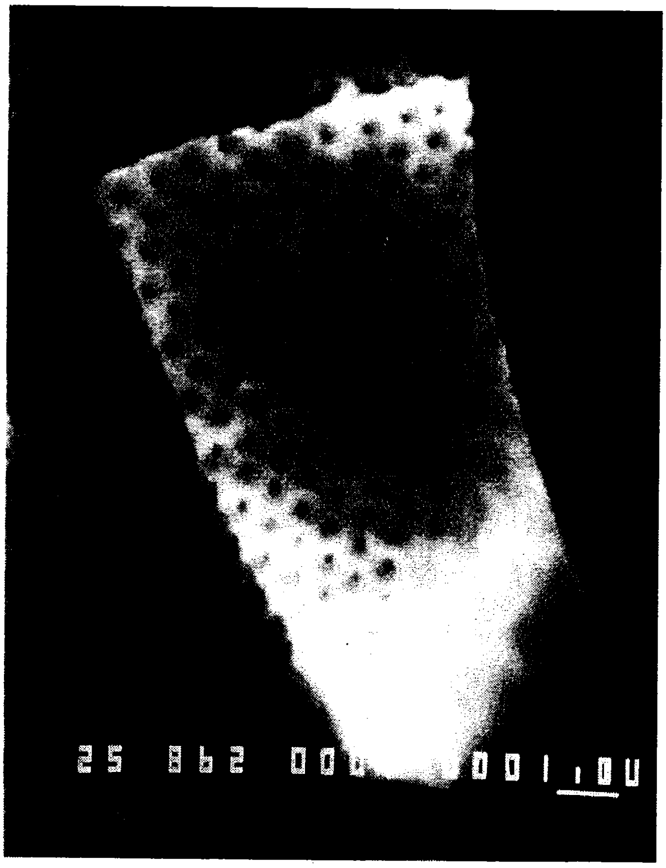

Fig 3

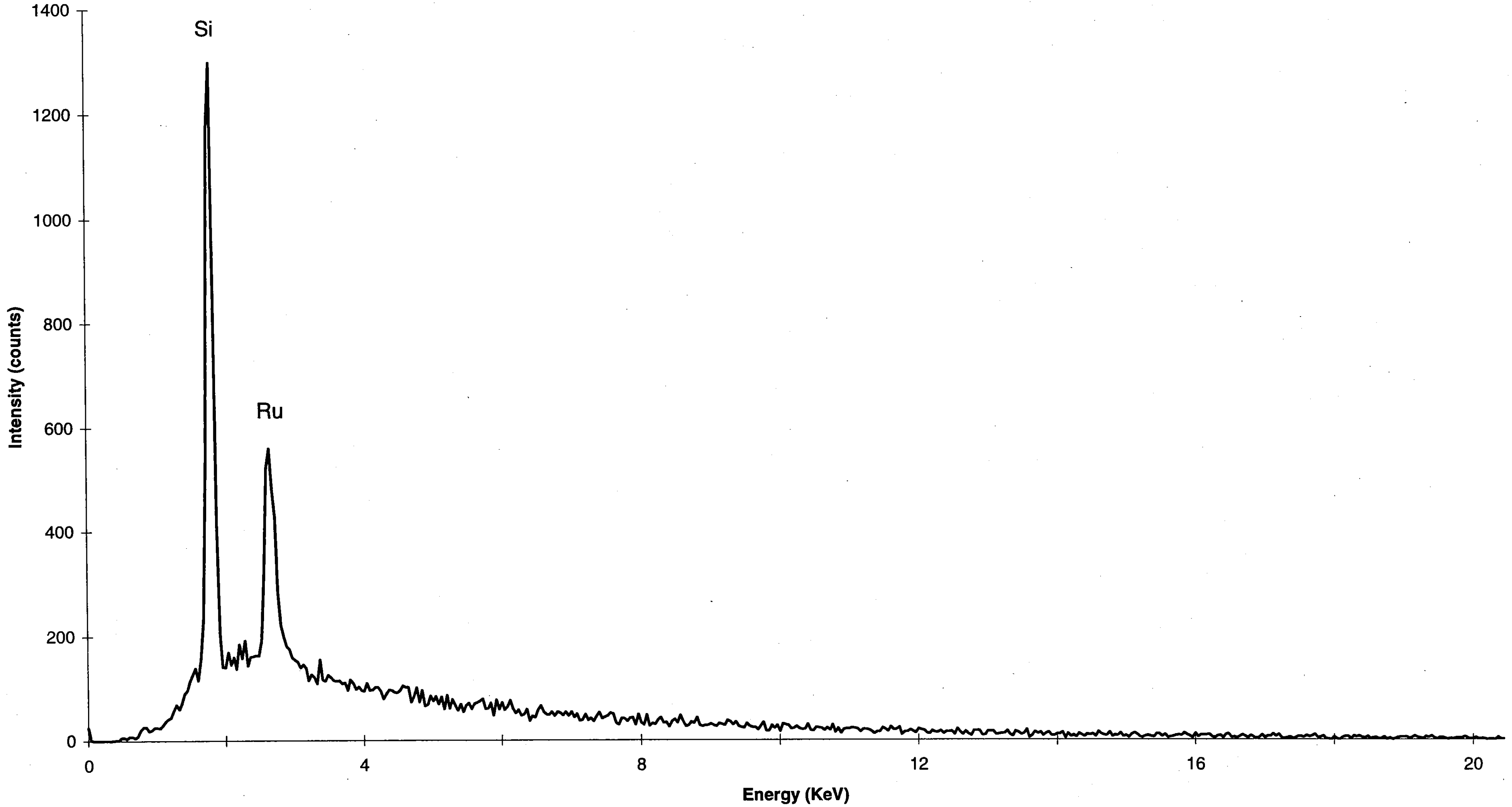
1400
1200
1000
800
600
400
200
0
Intensity (counts)
Si
Ru
0
4
8
12
16
20
Energy (KeV)

fig 4

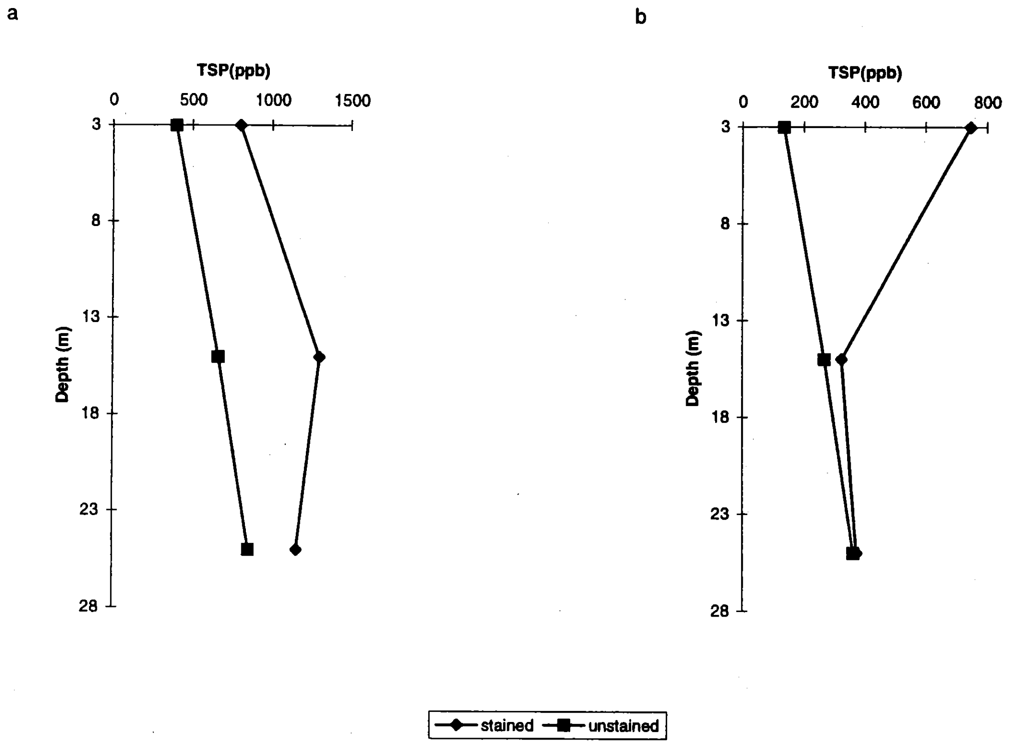
a
TSP(ppb)
0
500
1000
1500
Depth (m)
3
8
13
18
23
28
b
TSP(ppb)
0
200
400
600
800
Depth (m)
3
8
13
18
23
28
stained
unstained

fig 5

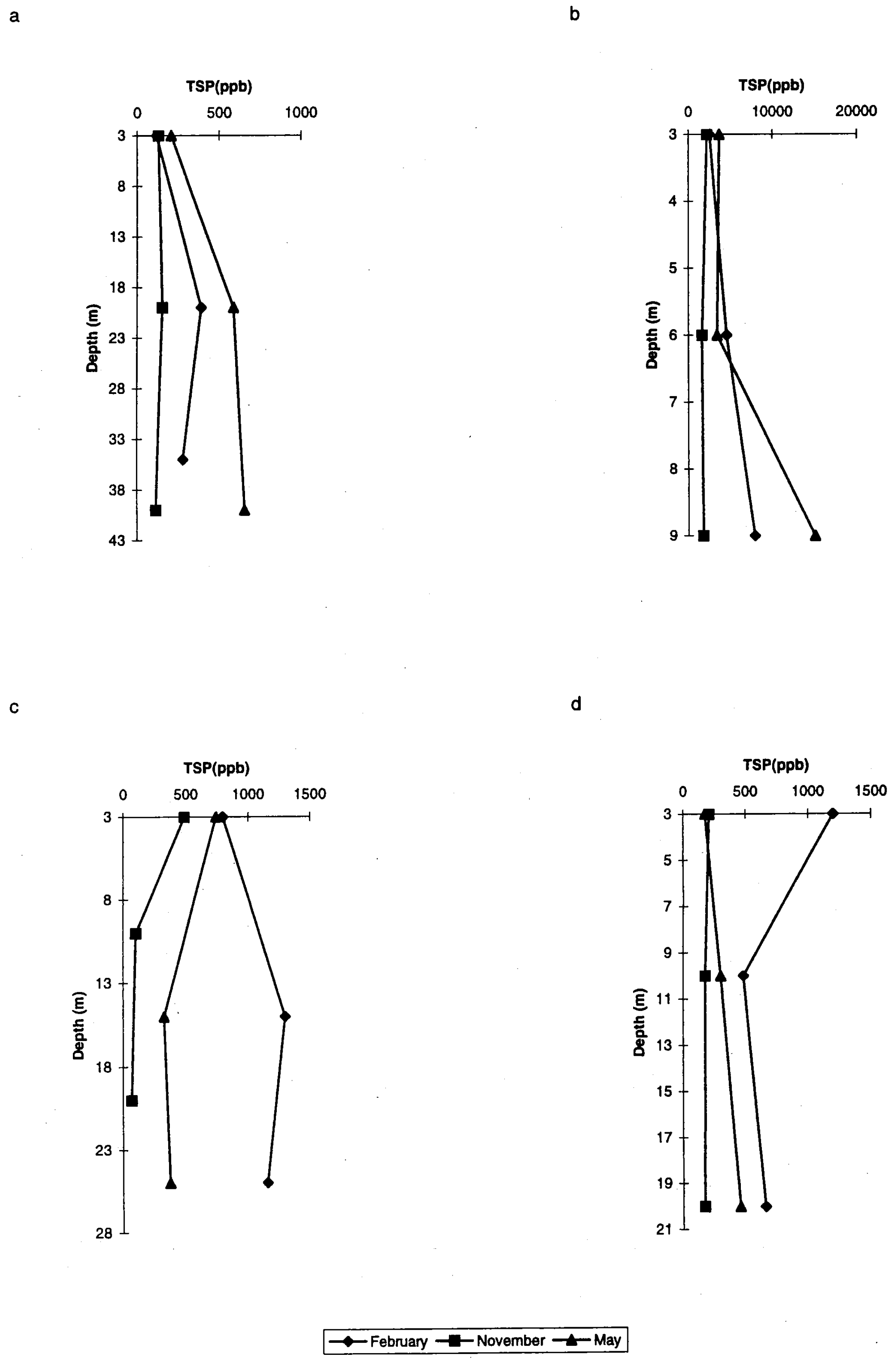
a
TSP(ppb)
0
500
1000
Depth (m)
3
8
13
18
23
28
33
38
43
b
TSP(ppb)
0
10000
20000
Depth (m)
3
4
5
6
7
8
9
c
TSP(ppb)
0
500
1000
1500
Depth (m)
3
8
13
18
23
28
d
TSP(ppb)
0
500
1000
1500
Depth (m)
3
5
7
9
11
13
15
17
19
21
February
November
May

Addendum E

Proceedings

Lijst met alle proceedings gepubliceerd in het kader van dit project gedurende de periode oktober 1992- september 1996.

1. Van Malderen H., De Bock L., Hoornaert S., Injuk J. en Van Grieken R., Chemical characterisation, source indentification and quantification of the input of atmospheric particulate matter into the North Sea, in *Dialogue between scientists and the users of the sea*, Proceedings of a Symposium held on the Occasion of the 10th Anniversary of the Civil Service Oceanographic Research Vessel Belgica, DWTC, Oostende, 17-19 oktober 1994, pp. 103-112.

2. Hoornaert S., Treiger B. en Van Grieken R., Trend analysis of the concentrations of metals in aerosols above the North Sea, in Proceedings of the Workshop "Progress in Belgian Oceanographic research", Royal Academy of Belgium, Brussel, 8-9 january 1996, pp. 103-106.

3. Injuk J. en Van Grieken R., Atmospheric inputs of heavy metals into the North Sea, in Proceedings of the Workshop "Progress in Belgian Oceanographic research", Royal Academy of Belgium, Brussel, 8-9 january 1996, pp. 111-113.

4. Jambers W. en Van Grieken R., Single particle characterization of inorganic North Sea suspension, in Proceedings of the Workshop "Progress in Belgian Oceanographic research", Royal Academy of Belgium, Brussel, 8-9 january 1996, pp. 115-117.

5. Van Grieken R., De Bock L., Hoornaert S., Jambers W., Koutsenogui P., Recent apllications of individual particle analysis in environmental research, in "Preservation of our World in the Wake of Change", Vol. VI A, Proceedings of the Sixth International Conference of the Israeli Society for Ecology & Environmental Quality Science, ISEEQS, Jerusalem, Israel, 30 juni- 4 juli 1996, pp. 67-70.

6. Injuk J. en Van Grieken R., Deposition of atmospheric Ni, Cu, Zn and Pb into the North Sea, based on coastal, ship and platform measurements and on modelled predictions, in "Preservation of our World in the Wake of Change", Vol. VI A, Proceedings of the Sixth International Conference of the Israeli Society for Ecology & Environmental Quality Science, ISEEQS, Jerusalem, Israel, 30 juni- 4 juli 1996, pp. 187-189.

Dialogue between Scientists and Users of the Sea

Proceedings of a symposium
held on the occasion of the 10th anniversary
of the civil service oceanographic research vessel
BELGICA
Ostend, 17-19 October 1994

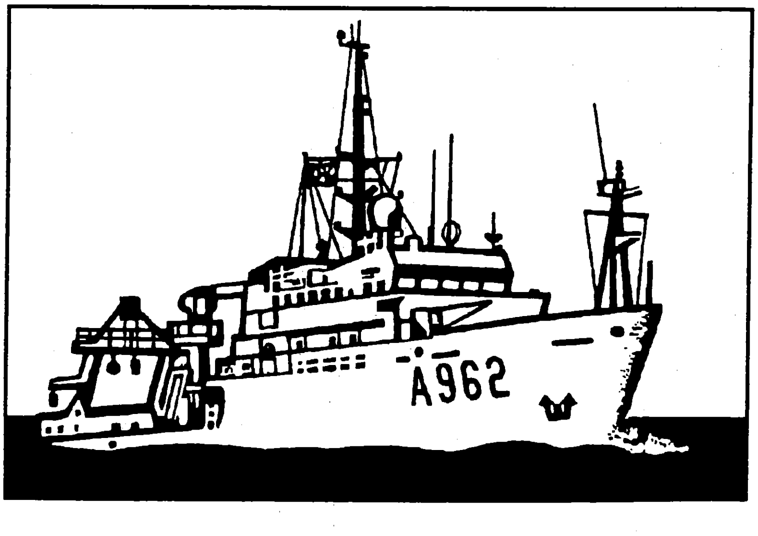

CHEMICAL CHARACTERISATION, SOURCE IDENTIFICATION AND QUANTIFICATION OF THE INPUT OF ATMOSPHERIC PARTICULATE MATTER INTO THE NORTH SEA

H. VAN MALDEREN, L. DE BOCK, S. HOORNAERT, J. INJUK and R. VAN GRIEKEN
Department of Chemistry, Micro- and Trace Analysis Centre (MiTAC)
University of Antwerp (UIA), Universiteitsplein 1
B-2610 Antwerp-Wilrijk, Belgium

1. Introduction

The North Sea is surrounded by highly industrialised countries and suffers input of waste material through several pathways, such as direct discharge, dumping activities and riverine input. Atmospheric input has only recently been recognised as a potentially major input source for contaminants. However, as yet this pathway has not been quantified fully. The few existing experimental values in the literature differ considerably, and particularly in comparisons between experimental data and model predictions discrepancies of a factor 10-15 have been noted for various heavy metals.

The major differences between modelled and experimental deposition fluxes are related to uncertainties in particle size distributions. The largest particle fraction, the so-called "giant" aerosols (these are particles with aerodynamic diameters larger than 2 μm) have hitherto nearly always been neglected. Yet it should be emphasised that, while giant particles are indeed numerically very scarce in the atmosphere, a particle of e.g. 10 μm has 1,000 times more mass than a 1 μm particle and, additionally, its deposition velocity is around 100 times higher. The presence of only a few of these giant particles will therefore influence the deposition flux enormously.

The major problem in nearly all previous past studies of aerosol deposition over the North Sea is precisely that the large particle fraction has not been adequately assessed because of the extreme difficulties in sampling these particles representatively. In order to achieve this, the particles should be sampled isokinetically. This means that the linear velocity of the particles in the atmosphere should be exactly the same as the air inlet speed in the sampling device. This problem has always been overlooked for various reasons, but mainly because the large particle fraction has always been thought of as negligible. Recently, collection of aerosols in wind tunnels under isokinetic conditions has been performed with both total filters and cascade impactors to collect atmospheric aerosols, including the largest fractions, as a function of particle size, under different atmospheric conditions and during different seasons.

Studies for the estimation of deposition fluxes from the atmosphere to the sea have made use of a variety of analytical techniques for the analysis of the bulk chemical composition of air and rain samples. Microanalysis techniques, however, have rarely been invoked, although they allow the determination of the distribution of elements in the aerosol and reveal whether a specific element is uniformly distributed over all the particles or whether it is a component of only a specific group of particles. The chemical analysis of individual aerosols makes it more straightforward to assign them to specific sources, while the abundance of a specific particle group is a measure of the source strength.

For some years our research group has been studying the North Sea environment intensively. We have focused our efforts primarily on heavy metal concentrations and deposition fluxes and on the physical and chemical characterisation of individual North Sea particles.

2. Recent North Sea sampling campaigns

Ships provide a stable platform for long-term sampling of marine aerosols over large areas. However, samples taken from a ship can easily be contaminated e.g. by sea spray under high wind conditions and by the engine exhaust of the ship itself. Aerosol sampling from aircraft can be done at both high altitudes and very low altitudes, down to 15-20 m above sea level, so that vertical profiles can be acquired. Ideally, the combined use of research vessels and aircraft for aerosol sampling makes it possible to study large areas, to obtain vertical profiles and to avoid contamination from local sources.

In the last eight years our group participated in numerous and extensive sampling campaigns using both ships and aircraft. Over a period of four years (1984-1987), aerosol samples were collected on board the R/V *Belgica* during various cruises on the North Sea, the English Channel and the Celtic Sea for analysis by energy-dispersive X-ray fluorescence (EDXRF), electron probe X-ray microanalysis (EPXMA) and laser microprobe mass analysis (LAMMA) (Bruynseels *et al.*, 1988; Xhoffer *et al.*, 1991, 1992; Otten, 1991). Special attention was also given to particles in the North Sea surface microlayer and underlying seawater (Xhoffer *et al.*, 1992).

From September 1988 to October 1989, a set of 108 aerosol samples was collected with the aid of an aircraft over the Southern Bight of the North Sea. Detailed information on the sampling instrumentation and sampling strategy can be found in Otten *et al.*, 1989. Briefly, after locating the inversion layer, six horizontal tracks were flown at six different altitudes equally spaced between the sea surface and the inversion layer. Particulate matter was sampled and deposited on various substrates and impactors for analysis with different techniques such as EPXMA, LAMMA, EDXRF and differential pulse anodic stripping voltammetry (DPASV). Special attention was given to the collection of giant aerosol particles. They were collected with a special sampling device, consisting of a cylindrical impaction surface (diameter 1 cm) covered with a particle-free sticky tape and supported by a vertical bar, which was exposed outside the aeroplane perpendicularly to the airflow around the aeroplane and directed upwind. Results of this sampling campaign can be found in publications by Rojas and Van Grieken (1992), Dierck *et al.* (1992), Injuk *et al.* (1992), Van Malderen *et al.* (1992), Rojas *et al.* (1993a) and Rojas *et al.* (1993b).

In September 1991 an extensive ship-based sampling programme was set up, covering the central area of the North Sea, within the framework of the EUROTRACK programme. Two research vessels (R/V *Belgica* and F/S *Alkor*) were positioned such that one ship was always about 200 km directly downwind from the other. An identical sampling scheme was thus performed at 200 km intervals on the same air masses as they crossed the North Sea. This allowed the researchers to study the changes in aerosol and rainwater composition due to deposition processes and chemical reactions. The ships changed position approximately every 8 hours. Special attention was given to isokinetic sampling of aerosols by making use of a wind tunnel in which the impactors and filter units were placed. The samples were analyzed by several X-ray emission techniques (EDXRF, EPXMA and proton-induced X-ray emission analysis or micro-PIXE) both for the bulk and individual particles. The results were presented elsewhere (Injuk *et al.*, 1993; Treiger *et al.*, 1994; De Bock *et al.*, 1994).

During 1993 and 1994 we participated in almost 10 cruises with the R/V *Belgica* in the North Sea. Special attention was given to sampling under isokinetic conditions, collection of North Sea aerosols for individual particle analysis by techniques such as Fourier transform infrared microscopy, secondary ion mass spectrometry and Raman spectroscopy, which have never been invoked in this context before, and to suspended particles in rainwater and seawater.

3. Bulk analysis versus single particle analysis

Throughout all these sampling campaigns, various techniques have been used in order to assess bulk concentrations of atmospheric particulate matter. These concentrations can then be used as input to deposition models which allow us to calculate atmospheric deposition fluxes. Several atmospheric studies of the North Sea atmosphere have dealt with the assessment of atmospheric concentrations and, to a lesser extent, deposition fluxes, but not with the microanalysis of individual atmospheric particles. Micro-analysis allows us to characterise the composition and morphology of individual particles. By investigating the presence of particular elements it is possible to discriminate between specific particle types. It is possible to follow their abundance as a function of the relevant parameters (e.g. wind direction, wind speed, location, humidity) and to identify their origin and sources. Additional information on reactions that particles undergo in the atmosphere may be inferred by micro-analytical techniques capable of selectively measuring the composition of the surface layer.

Bulk analysis techniques, which have been invoked in our contribution to the characterisation of the North Sea atmosphere, hardly need detailed explanation. EDXRF and PIXE, for instance, are so well-known, efficient and widely used as analytical techniques, with hundreds of applications reported yearly in environmental science and atmospheric chemistry journals, that any description is redundant. Elements as Cu, Zn, Cd and Pb were analyzed by DPASV, which has excellent sensitivities but which is, of course, time-consuming compared to EDXRF, since it involves a sample dissolution step.

Of all micro-analytical techniques, EPXMA is by far the most commonly used. When automated, EPXMA is a very efficient tool for analysing a large number of individual particles within a reasonably short time. In our laboratory, several hundreds of particles can be analyzed in a few hours by a JEOL Superprobe JXA-733 EPXMA unit, which is automated by a system for automated particle recognition and characterisation. The main disadvantage of EPXMA is its poor relative detection limit of about 0.1%. But combined with cluster analysis and/or multivariate techniques, EPXMA allows us to analyze a representative number of particles, e.g. more than 500 per sample, in a few hours. Using EPXMA we have analyzed more than 100,000 individual North Sea aerosols in the last few years.

The very low Bremsstrahlung in a Scanning Proton Microprobe (SPM or micro-PIXE) permits detection limits down to 10 ppm, *i.e.*, 100 to 1,000 times better than in EPXMA. This technique is still young and therefore not automated. To date only a very limited number of particles has been measured with this technique.

An alternative technique is LAMMA. The principle of LAMMA is based on vaporisation and ionisation of a particle by a focused laser beam. LAMMA has some interesting features: it can detect all elements, has very low detection limits compared to other techniques and can give information about organic compounds. On the other hand, the results are rather irreproducible and because of the low mass resolution, results are sometimes difficult to interpret. To overcome these problems we have acquired a new Fourier-transform Ion Cyclotron Resonance Mass Spectrometer (FTIR-ICR-MS) with a mass resolution 100 to 1,000 times better. Thousands of spectra have been measured by LAMMA over the last 10 years, but the new spectrometer is still at the experimental stage.

4. Results and discussion

It is beyond the scope of this article to present complete and detailed results acquired in all the sampling campaigns over the past decade, but we will however try to give a summary. Detailed results can be found in the articles published by MiTAC, which can be found in the reference list.

4.1. Average airborne concentrations and deposition fluxes of heavy metals to the North Sea

The average concentrations of the most relevant trace metals in the aerosols over the Southern Bight of the North Sea were found to be as follows (in ng m^{-3}): 2.1 ± 0.6 for Cd, 14 ± 3 for Cu, 61 ± 8 for Pb and 73 ± 10 for Zn. These data are in a reasonable agreement with those supplied by other groups. Presumably due to reduced emissions of Pb, a small decrease in Pb concentrations was noticed. To check the relation between element concentrations and wind direction, all samples were split up into 5 wind sectors according to the origin of the air masses. These results are presented in Table 1.

To calculate the deposition of these metals to the sea we used the fundamental concept that the flux is given by the product of a concentration term and a kinetic parameter, which controls the rate of mass transfer.

Table 1

Average heavy metal concentrations in ng m^{-3} according to the origin of the air masses.

Wind direction	Cd	Cu	Pb	Zn
W-SW	2.2 ± 0.7	20 ± 9	52 ± 7	53 ± 6
N-NW	0.2 ± 0.1	1.1 ± 0.3	7 ± 2	2.0 ± 0.3
E-NE	1.4 ± 1.0	5 ± 2	50 ± 7	73 ± 9
S-SE	4.1 ± 2.6	17 ± 4	123 ± 13	150 ± 4
Local	1.1 ± 0.5	14 ± 3	55 ± 15	60 ± 19

Dry deposition of particles to the sea surface is the sum of all physical removal processes that take place when there is no precipitation. Particles can reach the sea surface by gravitational settling, turbulent diffusion or impaction. Dry deposition velocities were calculated using a modified version (Rojas *et al.*, 1993c) of the model developed by Slinn and Slinn. The resulting dry deposition velocities have been mass weighted, *i.e.* the deposition velocity corresponding to a certain particle size has been scaled by the fraction of the mass accounted for by that particle size. The calculated average deposition velocities ranged from 0.25 ± 0.03 cm s^{-1} for Pb to 0.17 cm s^{-1} for Cu.

Wet deposition is the combination of rainout and washout. Wet deposition calculations were carried out using Slinn's model with an annual rainfall of 600 mm as given by the German Weather Service. The resulting scavenging rates have been calculated for the five wind sectors and weighted by mass and wind frequency in a similar fashion as for dry deposition. The calculated scavenging rates ranged from 2.3×10^{-6} s^{-1} for Pb to 3.7×10^{-6} s^{-1} for Cu. Table 2 summarises dry and wet deposition values of Cd, Cu, Pb and Zn into the Southern Bight of the North Sea, calculated as the weighted average for five different wind sectors. On average, wet deposition is a factor of 2 higher than dry deposition.

Table 2

Dry and wet deposition fluxes of heavy metals into the Southern Bight of the North Sea in kg km^{-2} yr^{-1}.

Deposition flux	Cd	Cu	Pb	Zn
Dry flux	0.16	1.58	5.08	7.94
Wet flux	0.43	3.46	5.67	19.8

The riverine input for the Southern Bight area of the North Sea contributes 70-80% of the total riverine input for the North Sea, which has been estimated quite accurately. Based on the deposition values listed in Table 2 and on the area of the Southern Bight of the North Sea, the total atmospheric input can be evaluated and compared with other input sources. The results are shown in Table 3.

The atmosphere appears to be a significant source, in particular for Pb and Cd. Although 40% of Pb enters the Southern North Sea through the atmosphere, this fraction will go down in the near future because of the increasing use of unleaded gasoline. On the other hand, the contribution from dumping has decreased significantly due to recent EC legislation, so that the total atmospheric contribution will be relatively more important. Our deposition estimates indicate that the atmosphere is a major source of pollution of the North Sea by heavy metals (Injuk *et al.*, 1990).

Table 3

Relative contribution (%) of various input routes to the Southern Bight of the North Sea.

Input	Cd	Cu	Pb	Zn
Rivers	23	30	14	28
Discharges	9	7	3	6
Dumping	13	39	43	44
Atmosphere	55	24	40	22

4.2. Composition, characterisation and source identification of individual aerosol particles

Using automated EPXMA of more than 100,000 single North Sea particles and their abundance, we were able to study their variation with altitude, location, meteorological conditions and air mass trajectories. Nine major particle types were identified. The source of each was determined unambiguously.

The release of sea salt into the atmosphere is dominated by the process of breaking waves and this is more effective as wind speed increases. Transformed sea salt particles rich in Cl and S are formed by the conversion of NaCl to Na_2SO_4, induced by SO_2 and other S compounds, implying the release of HCl into the atmosphere. S-rich particles of various compositions - H_2SO_4, $(NH_4)_2SO_4$, $(NH_4)HSO_4$ and $(NH_4)_3H(SO_4)_2$ - originate from anthropogenic sources and are probably formed by gas-to-particle conversion. The $CaSO_4$ particles over the North Sea, too, are predominantly emitted by anthropogenic sources such as combustion processes. $CaSO_4$ particles may be enriched in S and can therefore be partially identified as $CaSO_4(NH_4)_2SO_4$ resulting from coagulation of $CaSO_4$ with sub-micron sulphate aerosols. On the other hand, Ca-rich particles can originate both from the marine environment and from natural continental sources. Various dissolved salts begin to crystallise sequentially as sea water evaporates. Calcite ($CaCO_3$) and dolomite ($CaMg(CO_3)_2$) precipitate first, followed by $CaSO_4$ and Mg salts. It is possible that $CaMg(CO_3)_2$ undergoes further reaction with gaseous S-rich components. Aluminosilicate particles cannot be distinguished from fly-ash particles on the basis of chemical composition. Only morphology can differentiate these two species. Important differences in these typical, nearly perfect, spherical fly-ash particles were observed in samples taken over the North Sea in air masses originating from over Eastern Europe. A small quantity of quartz can be emitted during combustion of coal in power plants. The fact that quartz particles, as Fe-rich particles, have very small diameters ($< 0.8\ \mu m$) supports the hypothesis that they are formed during combustion processes. Titanium-rich particles over the North Sea most probably find originate on the continent; possible sources are paint spraying, soil dispersion, asphalt production and power plants. Continentally-derived aerosols are often found in marine environments. Using EPXMA, we found that high number concentrations of aluminosilicates, present as an internal mixture in sea salt aerosols, are more likely to result from coagulation of sea salt and silicate particles within clouds, including drop coalescence, than from re-suspension of silicate particles from the sea surface as a result of bubble bursting (Andreae *et al.*, 1986).

As an example, the results of hierarchical clustering on the data set for giant North Sea aerosols are shown in Tables 4a and 4b. The two tables show data from aircraft flights with, respectively, little and strong continental influence. More detailed information can be found elsewhere (Van Malderen *et al.*, 1992).

All the particle types that have been discussed above for the EPXMA results were also found by LAMMA. However, here the particles often appeared as internal mixtures: the image of this aerosol, as obtained with the much more sensitive LAMMA, is therefore much more complicated.

Table 4a
Particle types identified for sampling flights with little continental influence.

Group number	Abundance (%)	Average diameter (μm)	Elements detected	Identification
1	31	3.5	Na, Cl, S	S enriched seaspray
2	18	3.3	Na, Cl	Seaspray
3	16	2.9	Ca, S	Gypsum
4	10	2.0	Fe	Fe-rich
5	8	3.9	S, Cl	Sulphates
6	6	3.1	Ca, S, Cl	Cl-enriched gypsum
7	5	3.2	Al, Si, Cl	Aluminosilicates
8	5	3.1	none	Organic
9	1	1.9	Na	Na-rich

Table 4b
Particle types identified for sampling flights with strong continental influence.

Group number	Abundance (%)	Average diameter (μm)	Elements detected	Identification
1	36	3.1	Ca, (Si, P)	Ca-rich
2	17	2.1	none	Organic
3	12	3.3	Ca, S	Gypsum
4	11	4.3	Al, Si	Aluminosilicates
5	4	2.7	K, Cl, (Zn)	K, Zn-chlorides
6	4	3.7	Cl, Na	Seaspray
7	3	3.6	Fe	Fe-rich
8	2	2.6	Si	Quartz

LAMMA was applied to a number of representative particles from the previously-discussed particle types in order to elaborate trace element contents and surface layer composition. Applying low-energy laser shots to the spherical fly-ash particles revealed typical spectra that were interpreted as fingerprints for the desorption of polynuclear aromatic hydrocarbons (PAH). Spectra of pure sea salts are dominated by Na, K and typical Na/K/Cl cluster ions. Often sea salt particles are found to have been transformed to some extent; in that case, nitrate and sulphate coatings are readily detectable (Bruynseels and Van Grieken, 1985; Kolaitis *et al.*, 1989). Bruynseels *et al.* (1985) found the amount of nitrate-coated sea salt particles to increase significantly from a beach site towards an industrialised area, 30 km downwind from the ocean. Another advantage of LAMMA in aerosol research is its ability to detect ammonium compounds, which are very interesting from an environmental point of view. Otten *et al.* (1987) found the relative abundances of ammonium-rich particles in the North Sea aerosol to increase dramatically under the influence of polluted air masses. Examining the relative abundances of several compounds as a function of size and wind direction allowed some clear trends to be discerned. Ammonium was mainly present in the smallest particles, sea salt exhibited its typical size profile and predominated with marine air masses, while aluminosilicates and KCl prevailed for continental air masses. More detailed information can be found in a publication by Dierck *et al.* (1992).

The results involving micro-PIXE analysis on sixteen North Sea aerosol particles are presented in Table 5. At this preliminary stage the elemental concentrations are expressed in ng cm^{-2}. The sea-salt aerosol particles clearly predominate, with Cl and usually S, K and Ca as major components and several trace elements including Ti, V, Cr, Mn, Fe, Zn and Pb. Based on this data set, four different groups of particles can be distinguished. The first group is characterised by particles containing Cl as a major element with S, K and Ca as minor components. The second group contains particles with Cl as a major element, again, but enriched with S, Cr and Ca. The presence of Cr in the North Sea troposphere seems significant. In the third particle group, Ca is the predominant element but the particles are enriched with notable concentrations of Fe and heavy metals. They may partially correspond to the fly-ash particles found also by EPXMA and defined by their invariably high Al, Si and Fe content (Si and Al were not measured in micro-PIXE); trace elements cannot be found by EPXMA because of its high detection limits. Finally, particles containing only Ca, Cl and K form a fourth group; they are probably also of marine origin. Here it must be stressed that only a limited number of particles were analyzed by micro-PIXE and that statistical analysis was therefore impossible. The type and quality of information acquired by the different techniques is undoubtedly quite dissimilar, but complementary. More detailed information on micro-PIXE results can be found elsewhere (Injuk *et al.*, 1993).

Acknowledgements

This work was partially supported by the Belgian State - Prime Minister's Services - Federal Office for Scientific, Technical and Cultural Affairs, within the framework of the Impulse Programme *Marine Sciences* (under contract MS/06/050) and of the EUROTRAC project EU 7/08, and by the Belgian Ministry of Public Health and the Environment. The aircraft-based measurements were supported by *Rijkswaterstaat*, the Netherlands, under contracts NOMIVE*2, DGW-217 and DGW920. Wendy Jambers (UIA) collected some of the samples on the R/V *Belgica*. For the micro-PIXE analyses proton microprobes at the University of Lund, Sweden, and IBMM, Geel, Belgium, were used.

Table 5

Elemental composition of North Sea aerosols as obtained by micro-PIXE, with values in ng cm^{-2}.

Sample	S	Cl	K	Ca	Ti	V	Cr	Mn	Fe	Zn	Pb
B-18-2	118 ± 4	900 ± 80	23 ± 2	24 ± 3	-	-	-	-	-	-	-
B-18-2	53 ± 9	350 ± 30	12 ± 1	14 ± 1	-	-	-	-	-	-	-
B-18-2	27 ± 5	220 ± 20	7 ± 1	7 ± 1	-	-	-	-	-	-	-
B-18-2	76 ± 17	720 ± 60	15 ± 2	9 ± 1	0.8 ± 0.3	-	16 ± 1	-	0.7 ± 0.1	-	-
B-18-2	86 ± 11	300 ± 30	11 ± 2	57 ± 4	-	-	24 ± 2	-	2.2 ± 0.2	-	-
A-18-2	23 ± 3	92 ± 6	3 ± 1	4 ± 1	-	-	16 ± 1	-	0.6 ± 0.1	-	-
A-17-4	-	12800 ±900	16 ± 4	-	-	-	-	-	-	330 ± 30	-
A-17-4	430 ± 40	66 ± 14	510 ± 40	-	-	-	-	-	4.1 ± 0.5	320 ± 20	-
A-17-4	350 ± 30	104 ± 8	30 ± 4	400 ± 30	0.9 ± 0.3	-	-	0.7 ± 0.4	33 ± 3	107 ± 8	-
A-17-4	95 ± 9	310 ± 22	85 ± 6	64 ± 4	3.9 ± 0.5	-	-	1.8 ± 0.4	106 ± 7	185 ± 13	-
A-17-2	132 ± 21	1600 ± 100	-	9900 ± 700	-	-	-	10 ± 1	42 ± 3	-	-
A-17-4	182 ± 14	330 ± 30	103 ± 7	187 ± 13	3.2 ± 0.5	-	2.2 ± 0.3	5 ± 1	400 ± 30	310 ± 20	-
A-17-1	1460 ± 120	780 ± 60	-	8600 ± 600	10 ± 2	2.9 ± 0.6	5.2 ± 0.7	48 ± 4	480 ± 30	26 ± 3	28 ± 8
A-17-1	260 ± 20	65 ± 5	-	949 ± 3	5.7 ± 0.6	2.2 ± 0.5	20 ± 2	270 ± 20	890 ± 60	14 ± 1	-
A-18-1	-	39 ± 7	10 ± 1	1200 ± 100	-	-	-	-	-	-	-
A-18-1	-	240 ± 20	10 ± 1	160 ± 10	-	-	-	-	-	-	-

References

ANDREAE M., CHARLSON R., BRUYNSEELS F., STORMS H., VAN GRIEKEN R. and MAENHAUT W., 1986. *Internal mixture of sea salt, silicates, and excess sulphate in marine aerosols.* Science, 232: 1620-1623.

BRUYNSEELS F. and VAN GRIEKEN R., 1985. *Direct detection of sulphate and nitrate layers on sampled marine aerosols by laser microprobe mass analysis.* Atmos. Environ., 19: 1967-1974.

BRUYNSEELS F., STORMS H., TAVARES T. and VAN GRIEKEN R., 1985. *Characterization of individual particle types in coastal air by laser microprobe mass analysis.* Int. J. Environ. Anal. Chem., 23: 1-14.

BRUYNSEELS F., STORMS H., VAN GRIEKEN R. and VAN DER AUWERA L., 1988. *Characterization of North Sea aerosols by individual particle analysis.* Atmos. Environ., 22: 2593-2602.

DE BOCK L., VAN MALDEREN H. and VAN GRIEKEN R., 1994. *Individual aerosol particle composition variations in air masses crossing the North Sea.* Environ. Sci. Technol., 28: 1513-1520.

DIERCK I., MICHAUD D., WOUTERS L. and VAN GRIEKEN R., 1992. *Laser microprobe mass analysis of individual North Sea aerosol particles.* Environ. Sci. Technol., 26: 802-808.

INJUK J., OTTEN P., ROJAS C., WOUTERS L. and VAN GRIEKEN R., 1990. *Atmospheric deposition of heavy metals (Cd, Cu, Pb and Zn) into the North Sea.* Final Report to Rijkswaterstaat, Dienst Getijdewateren, 's Gravenhage, The Netherlands, in the framework of project NOMIVE*2 task No. DGW-920, University of Antwerp.

INJUK J., OTTEN Ph., LAANE R., MAENHOUT W. and VAN GRIEKEN R., 1992. *Atmospheric concentrations and size distributions of aircraft-sampled Cd, Cu, Pb and Zn over the Southern Bight of the North Sea.* Atmos. Environ., 26A: 2499-2508.

INJUK J., VAN MALDEREN H., VAN GRIEKEN R., SWIETLICKI E., KNOX J. and SCHOFIELD R., 1993. *EDXRS study of aerosol composition variations in air masses crossing the North Sea.* X-Ray Spectrometry, 22: 220-228.

KOLAITIS L., BRUYNSEELS F., VAN GRIEKEN R. and ANDREAE M., 1989. *Determination of methanesulfonic acid and non-seasalt sulphate in single marine aerosol particles.* Environ. Sci. Technol., 23: 236-240.

OTTEN Ph., BRUYNSEELS F. and VAN GRIEKEN R., 1987. *Study of inorganic ammonium compounds in individual marine aerosol particles by laser microprobe mass spectrometry.* Anal. Chim. Acta, 195: 177-183.

OTTEN Ph., ROJAS C., WOUTERS L. and VAN GRIEKEN R., 1989. *Atmospheric deposition of heavy metals (Cd, Cu, Pb and Zn) into the North Sea.* Second Report to Rijkswaterstaat, Dienst Getijdewateren, 's Gravenhage, The Netherlands, in the framework of project NOMIVE task No. DGW-920, University of Antwerp.

OTTEN Ph., 1991. *Transformation, concentrations and deposition of North Sea aerosols.* Ph.D. Dissertation, University of Antwerp (UIA).

ROJAS C. and VAN GRIEKEN R., 1992. *Electron microprobe characterization of individual aerosol particles collected by aircraft above the Southern Bight of the North Sea.* Atmos. Environ., 26A: 1231-1237.

ROJAS C., INJUK J., VAN GRIEKEN R. and LAANE R., 1993a. *Dry and wet deposition fluxes of Cu, Cd, Pb and Zn into the Southern Bight of the North Sea.* Atmos. Environ., 27A: 251-259.

ROJAS C., VAN GRIEKEN R. and MAENHAUT W., 1993b. *Elemental composition of aircraft-sampled aerosols above the Southern Bight of the North Sea.* Water, Air and Soil pollution, 71: 391-404.

ROJAS C., VAN GRIEKEN R. and LAANE R., 1993c. *Comparison of three deposition models applied to field measurements in the Southern Bight of the North Sea.* Atmos. Environ., 27A: 363-370.

TREIGER B., INJUK J., BONDARENKO I., VAN ESPEN P., VAN GRIEKEN R., BREITENBACH L. and WÄTJEN U., 1994. *Non-linear mapping of microbeam proton-induced X-ray emission data for source identification of North Sea aerosols.* Spectrochim. Acta 49B: 345-353.

VAN MALDEREN H., ROJAS C. and VAN GRIEKEN R., 1992. *Characterization of individual giant aerosol particles above the North Sea.* Environ. Sci. Technol., 26: 750-756.

XHOFFER C., BERNARD P., VAN GRIEKEN R. and VAN DER AUWERA L., 1991. *Chemical characterization and source apportionment of individual aerosol particles over the North Sea and the English Channel using multivariate techniques.* Environ. Sci. Technol., 25: 1470-1478.

XHOFFER C., WOUTERS L. and VAN GRIEKEN R., 1992. *Characterization of individual particles in the North Sea surface microlayer and underlying seawater: comparison with atmospheric particles.* Environ. Sci. Technol., 26: 2151-2161.

* * *

International Council of Scientific Unions

Scientific Committee on Oceanic Research

Royal Academy of Belgium

National Committee of Oceanology

Workshop

Progress in Belgian Oceanographic Research

(Brussels, January 8-9, 1996)

Published with the support of the Royal Academy of Belgium
and the Royal Society of Sciences of Liege

TREND ANALYSIS
OF THE CONCENTRATIONS OF METALS
IN AEROSOLS ABOVE THE NORTH SEA

Stefaan HOORNAERT, Boris TREIGER
and René VAN GRIEKEN

The variation of the concentrations of heavy metals in aerosols above the North Sea has been investigated for different areas of the North Sea region.

In the past 20 years much attention has been paid to the atmospheric deposition of airborne particles into the sea (NAS, 1978; GESAMP, 1980; GESAMP, 1989; Duce, 1991). In the case of the North Sea this is one of the major input routes of heavy metals into the seawater. In order to evaluate the amount of metals deposited into the sea airborne trace metal concentrations have been determined during several sampling campaigns on, above and around the North Sea. This has produced quite a lot of individual data sets which, up till now, have never been intercompared.

The aim of this work therefore was to gather all these data on airborne trace metal concentrations, to compare them and to look for possible trends in the concentrations as a function of time.

The statistical analysis was done on all data for the period 1971-1994. The attention was focused mainly on Cd, Cu, Pb and Zn and, to a lesser extent, on Ni and Cr. Because of the existence of a South-to-North decreasing trend in airborne trace metal concentrations above the North Sea, a distinction was made between measurements in four different regions: the English Channel, the Southern Bight, the central and the northern North Sea. A second distinction was made between measurements performed in marine areas (during cruises on the sea, on lightships or platforms and during flights above the sea) and coastal areas (land-based measurements but close to the sea). Additionally real land-based measurements in the UK were considered since this area is still closely related to the North Sea region.

The use of different sampling and analysis techniques as well as seasonal influences in the case of short sampling campaigns might cause some fluctuations in the observed concentrations but despite this some interesting concentration patterns are found.

Key words: heavy metals, airborne particles, atmospheric concentrations, trend analysis

For the English Channel and the marine area of the central North Sea not enough data are available to notice certain trends. In the case of the northern North Sea the concentration levels for the marine and the coastal area are very similar so that both regions have been discussed together. For the land-based measurements in the UK, data are only available for the seventies. In spite of this, similar concentration patterns are found as for the other regions in this period.

In all regions of the North Sea a strong decreasing trend is observed in the airborne Pb and Zn concentrations. In the case of the coastal area of the Southern Bight (including the Belgian coast), it can be seen that the average reported Pb concentrations have dropped from 270 ng/m³ in 1972 to 8 ng/m³ in 1994 while the average Zn concentrations have decreased from 306 ng/m³ to 22 ng/m³ (Figure 1). Since the majority of the data in the literature deals with the Southern Bight, the trends observed for this region are considered to be the most reliable. These lower concentrations also imply a lower input of Pb and Zn into the North Sea. Besides this similar trend for both elements, a strong correlation is found between their concentration patterns. Therefore the decrease in the airborne Pb (and Zn) concentrations should be attributed mainly to reduced industrial emissions rather than only to the use of unleaded gasoline since, in the latter case, this correlation would be non-existent.

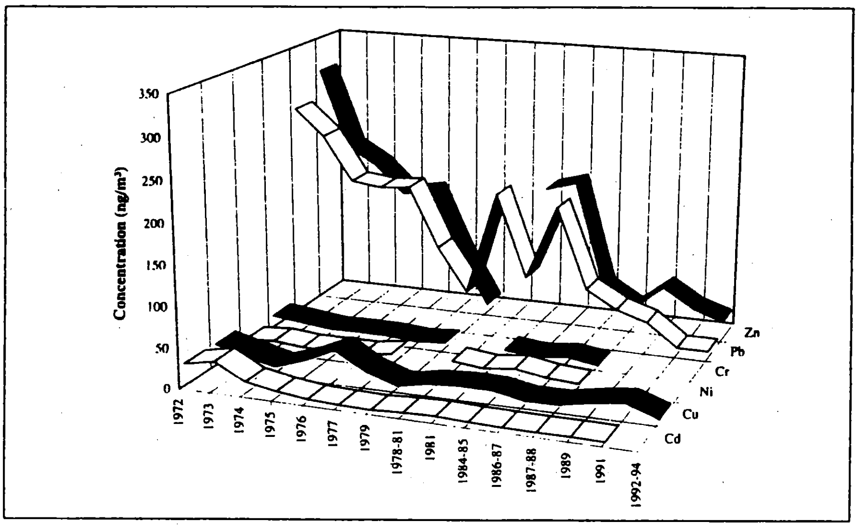

Figure 1 Average airborne trace metal concentrations (ng/m³) for the coastal area of the Southern Bight

For the other elements the situation is less clear. For Cr only few data are available for most regions so that it is impossible to speak about trends in the Cr concentrations. Only for the coastal area of the Southern Bight, enough data are present. However here the reported concentrations are fluctuating without a consistent decreasing or increasing pattern. A similar situation is true for the Cd concentrations. Very few data have been published on airborne Cd except for the case of the coastal area of the Southern Bight where the average airborne Cd concentrations have decreased significantly to less than 1 ng/m^3.

In contrast to Cd and Cr, enough data are available in literature on Ni and Cu concentrations. However also in the case of Ni and Cu no clear trends are detected. The meaning of this can be twofold: either no trends are present for these elements at all or the trends are so small that they cannot be seen due to the fluctuations in the concentrations caused by the use of different sampling and analysis techniques or seasonal changes. For Ni a consistent concentration pattern is only observed for the coastal area of the central North Sea where a slightly increasing trend is found in the Ni concentration level. The airborne Cu level is rather stable for the coastal area of the central North Sea. In all other cases the Cu concentrations do not show a particular pattern. However in the case of the marine area of the Southern Bight and the northern North Sea the most recent values (of the end of the eighties or the beginning of the nineties) appear to be the lowest values ever reported for these regions.

From the comparison of the most recently reported concentrations (in most cases also the lowest) with data on trace metal concentrations in some remote areas it can be seen that the values found for the North Sea region are still higher than those in the remote areas. However the differences are getting smaller.

References

Duce R.A., Liss P.S., Merrill J.T., Atlas E.L., Buat-Menard P., Hicks B.B., Miller J.M., Prospero J.M., Arimoto R., Church T.M., Ellis W., Galloway J.M., Hansen L., Jickells T.D., Knap A.H., Reinhardt K.H., Schneider B., Soudine A., Tokos J.J., Tsunogai S., Wollast R., Zhou M. (1991) The atmospheric input of trace species to the world ocean. Global Biogeochem. Cycles, 5, 193-259.

GESAMP (1980) Joint Group of Experts on the Scientific Aspects of Marine Pollution. Interchange of pollutants between the atmosphere and ocean. Reports and Studies No. 13.

GESAMP (1989) IMO/FAO/UNESCO/WMO/WHO/IAEA/UN/UNEP Joint Group of Experts on the Scientific Aspects of Marine Pollution. The atmospheric input of trace species to the world ocean. Reports and Studies No. 38.

NAS (1978) The tropospheric transport of pollutants and other substances to the oceans. National Academy of Sciences Press, Washington, D.C.

Acknowledgement

This work was supported by Rijkswaterstaat, Den Haag, The Netherlands, and by the Belgian State - Prime Minister's Service - Services for Scientific, Technical and Cultural Affairs (contract MS/06/050 of the Impuls Programme in Marine Sciences)

Affiliation and address

University of Antwerp (UIA), Department of Chemistry, Universiteitsplein 1, 2610 Antwerpen.

International Council of Scientific Unions

Scientific Committee on Oceanic Research

Royal Academy of Belgium

National Committee of Oceanology

Workshop

Progress in Belgian Oceanographic Research

(Brussels, January 8-9, 1996)

Published with the support of the Royal Academy of Belgium
and the Royal Society of Sciences of Liege

ATMOSPHERIC INPUTS OF HEAVY METALS INTO THE NORTH SEA

Jasna INJUK and René VAN GRIEKEN

The aim of this work was to estimate quantitatively from field measurements the atmospheric supply of trace elements into the North Sea and to evaluate the nature of the aerosol particles responsible for this flux. In principle, the best way to quantify atmospheric inputs to the sea surface would be by direct flux measurements. However, up to now these have generally been unsuccessful or meaning of the results open to significant doubt. When the aerosol concentration above the sea is known, the problem of calculating deposition fluxes is reduced to the calculation of the deposition velocity, using an appropriate model which is basically a function of particle size and wind speed. A major drawback in this context is the great uncertainty concerning the size distributions of trace elements over the sea. Certainly the contribution of the so-called "giant" aerosol particles has generally been underestimated, due to their inadequate collection.

The indirect deposition calculations in this work are based on the measured aerosol concentrations in the lower troposphere of the North Sea. Over a period of five years (1989 - 1994) aerosols were collected from an aircraft, on board of research vessels, from a platform and at the Belgian coast (pier of Blankenberge, about 100 m from the shore). Different ways of aerosol collection have been invoked; sampling was done on Nuclepore filters and quartz discs, by different types of cascade impactors and by the membrane type of filters. For all ship- and platform-sampling, the sampling equipment was placed in a wind-tunnel, with a forced internal air flow, which orients itself towards the wind by a wind vane, so that particles were collected isokinetically with a high efficiency.

Various sensitive multi-element bulk and single particle techniques [1] were implemented to measure the airborne concentrations and size distributions of micro- and trace- elements over the North Sea, namely: energy-dispersive X-ray fluorescence (EDXRF)

key words: North Sea, heavy metals, atmospheric deposition

and total-reflection X-ray fluorescence (TXRF), proton-induced X-ray emission (PIXE), anodic stripping voltametry (ASV), electron-probe X-ray microanalysis (EPXMA) andnuclear microprobe (NMP) combined with PIXE. The resulting huge data set was handled by multivariate techniques [2] like principal component analysis (PCA) and non-linear mapping (NLM).

The average airborne heavy metal concentrations for different sampling campaigns (from an aircraft, from research vessels and from the platform near the Belgian coast) in the Southern Bight of the North Sea were all in the same ranges: e.g. (in ng m^{-3}) 1-5 for V, 1-7 for Cr, 1-7 for Ni, 2-10 for Cu, 6-83 for Zn and 4-73 for Pb. A clear decreasing trend was observed from the southern to the northern parts of the North Sea. There is a strong dependence on the wind direction; the heavy metal concentrations originating from the south-southeast sector are about 20 times higher than for the north-northwest sector, when the air masses are from purely marine origin. Based on average data set, dry and wet deposition fluxes were calculated. The total dry and wet deposition is estimated to be (in tons y^{-1}): 560 for V, 1270 for Cr, 650 for Ni, 690 for Cu, 3480 for Zn and 1970 for Pb. Inferring the removal of aerosol from the differences in airborne concentration above two research vessels positioned 200 km downwind from each other yielded similar values; it was observed that the deposition velocities varied much from day to day and that they were particularly high under high wind speeds.

The atmospheric deposition fluxes were evaluated relative to the other input sources: those borne by rivers, dumping and incineration. It is clearly recognized that substantial inputs of metals are introduced into the North Sea through the rivers and the atmosphere. The atmospheric deposition balanced 34% (Ni), 18% (Cu), 17% (Zn) 32% (Pb) among all input sources. The determined total deposition fluxes have pointed out the importance of the atmosphere as a passage by which the pollutants are reaching the North Sea environment. It was found that the "giant" particles are by far the most important in this flux.

The NMP combined with PIXE was successfully applied to the analysis of individual giant aerosol particles for their elemental composition down to absolute masses of 50 fg for some trace metals [3]. Such single particle analysis combined with multivariate numerical analysis reveals three major particle types: (1) particles dominated by (Na)Cl, S, K and Ca, apparently seasalt, aged seasalt and gypsum, (2) particles with relatively high contents of Cr, Fe, Ni, Zn, V and Ti, probably fly ash and (3) mixed or aggregated marine/continental particles, which are internally heterogenous and contain e.g. Cr and seasalt elements in separated parts of the same giant particle. Collision of fly ash particles with abundant seaspray might explain the increased deposition velocities during stormy conditions.

Acknowledgement

This work was prepared in the framework of the Impulse Programme in Marine Sciences, supported by the Belgian State - Prime Minister's Service - Services for Scientific, Technical and Cultural Affairs (contract MS/06/050).

References

1. Injuk J. and Van Grieken R., Spectrochim. Acta. 1995, B50, 1787-1803.
2. Teiger B., Injuk J., Bondarenko I., Ven Espen P., Wätjen U., Bretienbach L. and Van Grieken R., Spectrochim. Acta, 1994, 49 B, 345-353.
3. Injuk J., Breitenbach L., Van Grieken R. and Wätjen U., Mikrochim. Acta, 1994, 114/115, 313-321.

Affiliation and address

University of Antwerp (UIA), Department of Chemistry, Universiteitsplein 1, 2610 Antwerpen.

International Council of Scientific Unions

Scientific Committee on Oceanic Research

Royal Academy of Belgium

National Committee of Oceanology

Workshop

Progress in Belgian Oceanographic Research

(Brussels, January 8-9, 1996)

Published with the support of the Royal Academy of Belgium
and the Royal Society of Sciences of Liege

SINGLE PARTICLE CHARACTERIZATION OF INORGANIC NORTH SEA SUSPENSION

Wendy JAMBERS and René VAN GRIEKEN

The variation of suspended matter in the Southern Bight of the North Sea has been studied by collecting samples at different depths and places and during the four seasons. The results are also used for comparison with aerosols and with suspension in rainwater collected above the North Sea.

During the last three years ten sampling campaigns were performed on board the R/V Belgica. Seawater was collected with a Niskin bottle and the suspension was filtered immediately after collection on aerosol grade polycarbonate Nuclepore filters with 0.4 µm pore size. A small amount of the water was either mixed with the hydrophilic Nanoplast resin and horizontally centrifuged onto a carbon coated electron microscopy grid or directly centrifuged onto a coated microscopy grid [1]. Rainwater was collected with a manual wet-only collected at the highest deck of the ship and this suspension was also filtered immediately after collection.

All samples have been studied with single particle micro-analytical techniques. The filters were analyzed with automated electron probe X-ray micro-analysis (EPXMA). Here EPXMA is associated with a particle recognition and characterisation programme, which allows the automatic analysis of up to 200 individual particles per hour. The analysis of large amounts of particles per sample (for this study 500 particles per sample) is necessary to ensure the statistical relevancy of the data. This results however in huge data matrices, which for interpretation were reduced with hierarchical cluster analysis.

In the JEOL 733 Superprobe automated EPXMA is preformed with an energy dispersive X-ray (EDX) detector with fixed beryllium window, which can only detect elements with $Z > 11$. Information about the organic fraction can be obtained by staining the filters with ruthenium tetroxide [2]. This is a strong oxidizer which reacts with a variety of organic compounds. The major problem with this staining is the overlap in the EDX-spectrum of the ruthenium L_α peak with the chlorine K_α peak. For marine suspension,

Key-words: suspension, individual particle, micro-analysis

however, chlorine is removed during the desalting of the filter and the overlap is thus avoided.

In EPXMA only X-ray spectra, thus the chemical compositions, and morphological characteristics of the particles are obtained. In a scanning transmission electron microscope (STEM), EDX can be combined with selected area electron diffraction (SAED), which allows the full characterisation of the particles, i.e. chemical composition, crystalline structure and morphological parameters. However, this technique cannot be automated and only 10 particles can be analyzed in one day.

At this moment about 75% of the samples have been analyzed and clustered. The aluminosilicate, silicon-rich and calcium-rich particles are overall the most important particles types. In most samples these groups represent more than 90% of the particles. Iron-rich and titanium-rich particles are also present in all samples, but in much lower abundances than the former particle types. Particles enriched in heavy metals are only found in very low concentration (< 1%), but will be studied separately in the near future.

The different particle types can be apportioned to different sources. Most aluminosilicate particles are clay minerals formed by erosion of soil. These clay minerals are known to absorb trace metals, as is the case for the detected iron rich and titanium rich aluminosilicates, and are also the transport medium for river suspension into estuaries and ocean systems. Aluminosilicate can also occur as fly ash particles, i.e. particles formed during combustion processes. These fly ashes have a composition which is comparable to that of mineral aluminosilicates and are thus classified into the same particle type. Silicon-rich and calcium-rich particles both have a mineral and a biological origin, which cannot be separated based on the X-ray peak intensities and are thus also classified into the same groups. Iron-rich and titanium-rich particles can also be apportioned to two different source, namely a mineral and an anthropogenic source.

The results of the ruthenium coated samples indicate that most particles contain at least a small amount of organic material. This can be explained by the spontaneous formation of organic coatings on particles in surface waters [5,6]. The calcium aluminosilicates and about 50 % of the calcium-rich particles have very large ruthenium X-ray intensities, which indicates the organic origin of these particles. The amount of biogenic silicon-rich particles was low. However, these samples were collected in winter and further analysis will be done on samples collected in spring and fall.

For most crystalline particle types, detected during automated EPXMA, electron diffraction patterns could be recorded. These determined crystalline particles are, however, not representative for the total suspended fraction, because STEM-SAED analysis is restricted in the size (about 1 µm) and the thickness (as thin as possible) of the particles. Another problem are the soluble salts which crystallise during the embedding in the resin. Especially sea salt, which has the tendency of crystallising onto suspended particles, interferes in the diffraction patterns and complicates the interpretation of these patterns.

These recrystallisation problems can be reduced by using a different preparation technique, that is direct centrifugation of the particles onto the electron microscopy grid [1,3,4]. However, this centrifugation preparation has four limitations: (a) it cannot be preformed in the field, which enlarges the risk of coagulation and absorption of particles during storage, (b) high centrifugation forces act upon the thin carbon carrier foil which is seriously damaged, (c) these samples are air-dried, during which important structural modification can occur and (d) particles are put on top of the carbon foil and can be lost during storage and transport of the grids. The last three limitations can be reduced by centrifuging on a nanoplast-carbon coated grid which is again coated with nanoplast after centrifugation (i.e. the particles are sandwiched between two nanoplast layers) [1], but these samples become so thick that difficulties occur during SAED analysis. Both preparations thus have their advantages and problems, but for the analysis of these sea water samples the direct centrifugation is preferred.

The suspension filtered from the rainwater mainly consist of aluminosilicates and organic particles (these are so dense that a large fraction is even detected without staining of the filter). Silicon-, iron- and titanium-rich particles are also found in all samples. During the collection in November 1995 all samples also contained small amounts of trace metal rich particles (manganese, zinc and chromium).

The results of both suspension in rain water and in sea water were compared with each other and with the results of aerosols collected above the North Sea. Most striking is the absence of calcium containing particles in rain water suspension. In aerosol samples, however, calcium was detected in gypsum particles and in calcium containing aluminosilicates. It thus seems that calcium containing aerosols are dissolved in rain water. Moreover, since no calcium rich particles were detected in fresh water sediments [6], the calcium containing particles in the North Sea must have a marine source or be produced by erosion of the calcite cliffs of Dover, England. The abundances of iron- and titanium-rich particles in rain water is also much higher than in sea water. This can be explained by the dilution of air transported particles with marine and riverine suspended matter.

References

1. Perret D., Leppard G.G., Muller M., Belzile N., De Vitre R. and Buffle J., Wat. Res., 1991, 25, 1333-1343.
2. Lavoie D.M., Deep-Sea Research, 1992, 39, 1655-1668.
3. Nomizu T. and Mizuike A., Mikrochim. Acta, 1986, I, 65-72.
4. Nomizu T., Nozue T. and Mizuike A., Mikrochim. Acta, 1987, II, 99-106.
5. Leppard G.G., In: Environmental Particles (Eds. Buffle J. and Van Leeuwen H.P.), Lewis, Chelsea MI, 1992, vol.1, pp.231-289.
6. Gibbs R.J., Environ. Sci. Technol., 1983, 17, 237-240.

Acknowledgement

This work was prepared in the framework of the Impulse Programme in Marine Sciences, supported by the Belgian State - Prime Minister's Service - Services for Scientific, Technical and Cultural Affairs (contract MS/06/050).

Affiliation and address

University of Antwerp (UIA), Department of Chemistry, Universiteitsplein 1, 2610 Antwerpen.

Preservation of Our World in the Wake of Change

Volume VI A

Proceedings of the

Sixth International Conference of the
Israeli Society for Ecology &
Environmental Quality Sciences

Jerusalem, Israel, June 30 - July 4, 1996

ISEEQS Publication
Jerusalem, Israel, 1996

Preservation of Our World in the Wake of Change, Vol. VI A/B
ISEEQS Pub., Jerusalem, Israel, 1996. Editor: Y. Steinberger

RECENT APPLICATIONS OF INDIVIDUAL PARTICLE ANALYSIS IN ENVIRONMENTAL RESEARCH

R.Van Grieken, L. De Bock, S. Hoornaert,
W. Jambers and P. Koutsenogui, Department of Chemistry, University of Antwerp (UIA), B-2610 Antwerpen, Belgium

INTRODUCTION

Application of micro-analysis techniques to particulate environmental samples, i.e. analysis of individual environmental particles, often allows to obtain valuable information that is complementary to bulk analysis. In principle, by single particle analysis techniques, detailed information concerning the origin, formation, transport, reactivity and transformation reactions of environmental particulate matter can be obtained in a more straightforward way than by bulk techniques. This paper will illustrate the potential of single particle analysis via some recent successful environmental application examples.

MICRO-ANALYSIS TECHNIQUES

In several recent reviews[1,2], the micro-analysis techniques that have already been invoked in environmental studies, have been discussed amply, together with the applications that were published in the recent literature. Hitherto, the most common techniques in this field, as generally in all micro-analysis, are the electron-beam methods, like scanning electron microscope analysis with energy-dispersive X-ray analysis attachment (SEM-EDX) or electron probe X-ray micro-analysis (EPXMA), which can advantageously be automated and offers chemical and morphological information for particles larger than 0.2 µm. Scanning transmission electron microscopy (STEM) with EDX allows to investigate much smaller particles, down to the nanometer range. These will also be the techniques used in the examples below, together with selected area electron diffraction (SAED) in STEM and with the micro-version of particle induced X-ray emission analysis (micro-PIXE). Other less common techniques for environmental single particle analysis are laser microprobe mass analysis, secondary ion mass spectrometry, Fourier-transform infrared analysis, Raman microscopy, electron energy loss spectrometry, etc.[1,2]

In automated EPXMA[3], the electron beam is scanned over e.g. a loaded filter (on which the individual particles are, of course, spatially separated), while the electron backscatter signal is monitored. For the pixels where a particle (and not the filter material) is hit by the electron beam during the scanning, the computer will memorise the co-ordinates. As soon as the contour of a particle has been filled, the system will stop scanning and measure the characteristic X-ray spectrum of the detected particle, which allows quantification of typically a dozen elements (excluding normally the low-Z elements, below Na or so). Also the average size and a shape factor of each particle will be calculated. Hundreds of particles can be characterised in this way in a few hours. To ensure the statistical relevance of the data, 500 or more particles are usually analysed per sample. This results in huge data matrices which are reduced by hierarchical clustering analysis (HCA) and/or factor analysis (FA) and/or other multivariate analysis techniques.

The combination of X-ray analysis in STEM with SAED allows the determination of both the chemical composition and the crystalline structure of the particles; however, this technique cannot be automated, implying that only a few particles can be analysed per day.

Micro-PIXE commonly makes use of a proton beam in the MeV range from an accelerator to excite characteristic X-rays in the particles. The detection limits are several orders of magnitude lower than for EPXMA, but the visualisation and automation of the technique is still poor at present.

CHARACTERISATION OF AQUEOUS NORTH SEA SUSPENSION

The variation of suspended matter in the Southern Bight of the North Sea has been studied by sampling at different depths and places and during the four seasons, followed by analysis with EPXMA and STEM-SAED. During the last three years ten sampling campaigns were performed on board the R/V Belgica. The samples were prepared immediately after collection by filtering the water through Nuclepore membranes or by mixing with a Nanoplast resin and horizontally centrifuging this mixture onto an electron microscopy grid. Information about the organic fraction can be obtain by staining the filters with a strong oxidiser like ruthenium tetroxide.

The EPXMA results show that aluminosilicates dominate in all the North Sea suspension samples. Together with the Si-rich and

Ca-rich particles, they represent over 90% of all the particles. Fe-rich and Ti-rich particles are also found in all analyzed samples, but always in low abundances. The ruthenium stained samples indicate that most particles contain at least small amounts of organic material. This proves the existence of spontaneously formed organic coatings on particles in surface water. About 75% of the Ca-containing particles have a very large ruthenium X-ray peak intensity, which indicates a biogenic source for these particles.

For most crystalline particles, detected during automated EPXMA, electron diffraction patterns could be recorded. However, these determined crystalline particles are not representative for the whole suspended fraction, because STEM-SAED analyses are restricted in the size (about 1 mm) and the thickness (as thin as possible) of the particles.

The suspension filtered from rainwater sampled over the North Sea mainly consists of aluminosilicates and organic particles (the latter are usually so dense that a large fraction is even detected without staining of the filter). Si-rich, Fe-rich and Ti-rich particles are also found in all samples. During the collection in November 1995, all samples also contained small amounts of trace metal rich particles (Mn, Zn and Cr).

The results of the suspensions in rain water and in sea water were compared with each other and with the results of aerosols collected above the North Sea. Most striking is the absence of Ca-containing particles in rain water suspension. In aerosol samples, however, Ca was detected in gypsum particles (which were most abundant in the atmosphere for air masses coming from over Germany, they are probably related to desulphurization processes in thermal power plants) and in Ca-containing aluminosilicates. It thus seems that Ca-containing aerosols are dissolved in rain water. Moreover, since no Ca-rich particles were detected in fresh water sediments, the Ca-containing particles in the North Sea must have a marine source or must be produced by erosion of e.g. calcite cliffs. The abundances of Fe- and Ti-rich particles in rain water is also much higher than in sea water. This can be explained by the dilution of air transported particles with marine and riverine suspended matter.

IDENTIFICATION OF INDIVIDUAL AEROSOL PARTICLES CONTAINING Cr, Pb AND Zn

Aerosol samples have been collected over the Southern Bight of the North Sea from an aircraft at different heights. Almost 45.000 individual particles were analysed with EPXMA. More than 5.000 of these were found to contain significant concentrations of one or more of the heavy metals Cr, Pb and Zn. These results provide ample evidence for the apparent existence of a heavy metal-containing North Sea aerosol. It was mainly overlooked in previous investigations using single particle analysis, because these particles are "drowned" in an excess of other, more abundant, particle types such as sea salt and aluminosilicates. The enormous number of particles obtained by the automated analysis method allows to acquire more statistically reliable results than by manual analysis. It is exactly this huge database that allows to focus on special, low-abundant particle types such as heavy metal-containing particles. With the help of HCA various heavy metal-containing particle types could be identified. Most of the particle types were directly of indirectly connected to emissions of the metallurgical industry, which is eminently present in the northern part of France, the German Ruhr area, and the industrial centers in the middle of the United Kingdom.

Significant differences in abundances were detected in the North Sea heavy metal aerosol, depending on the origin of the air masses. In samples with continental influence 50 times more Zn- and Pb-containing particles were found than in samples with a marine history. For Cr, on the other hand, the abundances in the marine area were found to be one-third of the values for the continental areas. This might point to a rather undefined marine source, which could be the recycling of previously deposited material by reinjection into the atmosphere by sea spray.

CHARACTERISATION OF INDOOR MUSEUM AEROSOLS

Indoor air pollution, a consequence of both indoor and outdoor factors, can cause chemical damage or soiling onto surfaces of paintings, frescoes, statues etc., by deposition of particulate material or absorption of present gases. The conservation of our cultural heritage and its protection against possible damage due to indoor air pollution has only recently received growing scientific interest.

To characterise the in- and outdoor airborne particle composition at the Correr museum, situated on San Marco square in Venice, Italy, two separate sampling campaigns were organised at the museum, in co-operation with aerosol physicists. The purposes of the first campaign were primarily the determination of the chemical composition and associated diameter of individual aerosol particles with a diameter range of 0.2-20 µm and secondly the investigation of the possible changes between successive sampling periods. Automated EPXMA and manual SEM-EDX were used. The classification of the analysed particles in separate particle types and the identification of different aerosol sources was obtained by HCA and FA, respectively. Additional aims for the second campaign were to characterise also particles below 0.2 µm using STEM-EDX, to map the internal compositional heterogeneity within individual micrometer-size particles, to obtain information on the trace elemental composition of the aerosols using micro-PIXE, and finally to compare between the in- and outdoor aerosol composition at the Correr museum.

Based on the relative abundances found by HCA, the majority of samples from both campaigns appeared to be composed of six to eight different particle types. The four most abundant types appeared to be Ca-rich particles in association with S, Si and Cl, aluminosilicate particles, particles derived from the sea and S-rich particles containing large amounts of organic material. The correlation between the abundance of the particle types and their diameters as well as between the sampling periods was investigated. FA revealed similar results.

The results of the SEM-EDX mapping of the elemental composition within the individual particles indicated that the simultaneous presence of several elements in e.g. Ca-Si-rich particles with diameters > 8 µm, was the result of different coagulation processes between Ca-Si-rich particles and a series of small particles present in the indoor environment. The heterogeneous nature of these giant particles was confirmed by micro-PIXE measurements. Due to the better detection limits of micro-PIXE relative to SEM-EDX, elements with Z=22-30 could also frequently be detected, down to ppm concentration levels.

A comparison between the in- and outdoor aerosol composition indicated the existence of an indoor source for relatively large Ca-rich aerosol source and a strong accumulation of this particle type inside the museum: the degradation of the rendering on the walls in the museum was thought to be responsible for this. The opposite effect was found for giant aluminosilicate particles: their abundance appeared to be double outside the museum. Generally, the abundance of particles became comparable in- and outdoors in the smallest size.

CHARACTERISATION OF AEROSOLS IN REMOTE AND POLLUTED AREAS OF SIBERIA

It has been demonstrated[4] that the aerosol particles formed over Siberia contribute noticeably to the deposition in the Arctic region. This is now becoming an important climatological factor, as since recently, in the context of "Global Change", the Arctic is considered to be the "weather kitchen" for all the Earth. However, there are only few measurements of atmospheric aerosols directly in Siberia, which covers about 13 mio. km^2 of continental area (9% of all continents) and may be considered as one of the main sources and sinks of continental aerosol on the global scale. The lack of knowledge about Siberian aerosols and their influence on the global radiation budget contributes to the uncertainties for climatological models. Siberia has a very low mean population density, about 2 people per km^2, but it is heavily industrialised in some regions, which may be considered as powerful point sources of pollution situated in rather clean surroundings. Because of it continental climate with rapid seasonal changes, Siberia is also a very promising "laboratory" for studying of specific aerosols, like bioaerosols, soil erosion or antropogenical aerosols. As the most of Siberian territory is frozen and covered with snow up to 8 months in a year, the production of biogenic particles or soil erosion is strongly suppressed in winter compared to summer. This allows studying specifically the antropogenical aerosol components or its fraction that has been subjected to long-range transport. Most of Siberia is also situated many hundred km away from the ocean, so that one may study continental aerosol with practically no marine influence.

Automated EXPMA and HCA were used for classifying aerosols collected in various campaigns, spread over the years 1992-1995, at many locations in different remote areas of Siberia. A few main particle type define the picture of the aerosols in Siberia (Table 1).

Table 1. Main groups of the aerosols, resulting from HCA of EPXMA-based elemental composition data for individual aerosols, sampled in West, Central and North Siberia and in the region of Lake Baikal.

Group No	Identification	Summer		Winter	
		W. Sib.	Baikal .	W. Sib.	N. Sib
1	Al, Si	45 ± 17	39 ± 10	57 ± 1	36 ± 8
2	Si-rich	5 ± 5	14 ± 2	18 ± 6	17 ± 2
3	biogenic	14 ± 11	8 ± 7	-	-
4	Ca, S	14 ± 4	-	8 ± 3	11 ± 2
5	Fe-rich	8 ± 5	5 ± 1	7 ± 4	11 ± 1
6	Ca-rich	2 ± 4	13 ± 5	-	-
7	S-rich	4 ± 4	10 ± 12	2 ± 2	8 ± 1
8	organic	3 ± 6	-	5 ± 5	6 ± 6
9	Pb-rich	2 ± 2	-	3 ± 3	4 ± 1

First of all are the aluminosilicates (totally about 60%), which are mainly fly-ash particles, produced by coal burning (the main energy source of Siberia) or soil dust generated at a local scale or transported from the South. Fly-ash particles may be distinguished from erosion particles by means of electron microscopy because of their morphology (mostly spherical). Si-rich or quartz particles may be provided by transport of desert dust from the South but also as the result of coal burning. This conclusion is based on the fact that numerous Si-rich particles are still observed in winter, although the surface in Siberia is then fully frozen and covered with snow. Other elements, which are also typical for erosion aerosols, are Fe and Ca.

One group of particles is observed only in the samples taken in summer; it is identified as biogenic material (8-25% of all particles) and is characterised by the simultaneous presence of such elements as K, Cl, P and S. Particles, which were only observed due to backscattered electrons but had no X-ray response, were identified as organic material; their main components are probably C, O and H, which do not provide X-ray peaks in the used analytical device. If organic particles are contaminated by coagulation of other particles containing S or Pb (auto exhaust), they make up separate groups of particles (S- or Pb -rich). Heterogeneous reactions of $CaCO_3$, arising from erosion processes, with atmospheric SO_2, are supposed to be the main source of $CaSO_4$-particles (Ca, S group in Table 1.)

REFERENCES

[1] Jambers W., De Bock L. and Van Grieken R. (1995): Recent advances in the analysis of individual environmental particles: a review. Analyst 120; 681-692

[2] Xhoffer C. and Van Grieken R. (1993): Environmental aerosol characterization by single particle analysis techniques, in "Environmental Particles, Vol.2"; J.Buffle and H.P. Van Leeuwen, Eds., Lewis Publ., Boca Raton, FL., 207-245

[3] Van Malderen H., Van Grieken R., Bufetov V. and Koutsenogii K. (1996): Chemical characterization of individual aerosol particles in Central Siberia. Envir. Sci. Technol. 30, 312-321.

[4] Rahn K.A. (1985): Progress in Arctic air chemistry, 1980-1984. Atmos. Environ. 19, 1987-1994.

ACKNOWLEDGMENTS

This work was partially supported by the Belgian State - Prime Minister's Service - Office for Scientific, Technical and Cultural Affairs (in the framework of the Impulse Programme Marine Sciences (contract MS/06/050) and the Co-operation Programme with East and Central Europe), by INTAS (grant 93-0182) and by the European Union (contract ENV4-CT95-0088).

3, 96 ?

Preservation of Our World in the Wake of Change

Volume VI A

Proceedings of the

Sixth International Conference of the
Israeli Society for Ecology &
Environmental Quality Sciences

Jerusalem, Israel, June 30 - July 4, 1996

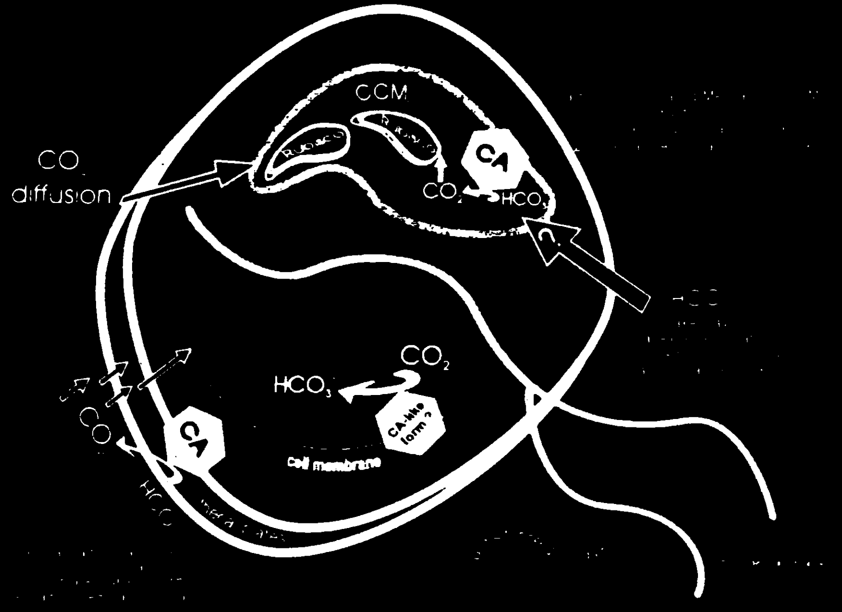

ISEEQS Publication
Jerusalem, Israel, 1996

Preservation of Our World in the Wake of Change, Vol. VI A/B
ISEEQS Pub., Jerusalem, Israel, 1996. Editor: Y. Steinberger

DEPOSITION OF ATMOSPHERIC Ni, Cu, Zn AND Pb INTO THE NORTH SEA, BASED ON COASTAL, SHIP AND PLATFORM MEASUREMENTS AND ON MODELLED PREDICTIONS

Jasna Injuk and Rene Van Grieken
Department of Chemistry, University of Antwerp (UIA), B-2610 Antwerp, Belgium

ABSTRACT

The atmospheric input of Ni, Cu, Zn and Pb into the North Sea is further assessed for comparison with the input by other pathways. Indirect deposition calculations are based on the ship, platform and coast based measured aerosol concentrations in the period spanning from 1992-1994 and on the use of Slinn and Slinn model. The magnitude of atmospheric dry and wet deposition fluxes to the North Sea environment is estimated to be (in tonnes per year): 650 for Ni, 690 for Cu, 3480 for Zn and 1970 for Pb. It was found that the "giant" particles are by far the most important in this flux. Of the total input into the North Sea through rivers and direct discharges, this atmospheric deposition balanced some 28% for Cu, 30% for Zn and 57% for Pb. Estimates of heavy metal inputs upon field measurements were evaluated versus modelling results for the same area and period of study. Such combined approach has not been attempted so far, and the agreement within 56% between these very different methods was considered as "satisfactory".

INTRODUCTION

The North Sea comprises only 0.18% of the world's oceans, yet it is surrounded by some of the world's largest industrial regions and cities. Approximately 164 million people live within its catchment area. The area is subject to the effects induced by the huge inputs of both natural and anthropogenic materials; they are transported by rivers and canals, both in solution and as particulate matter. Furthermore, various compounds such as nutrients, metals and organic micropollutants reach the North Sea from the atmosphere through different physical processes.

In this study, the reported dry deposition fluxes are based upon size-segregated airborne concentration data measured by Total-reflection X-ray fluorescence (TXRF) and dry deposition velocities calculated with the model of Slinn and Slinn (1980). Wet deposition fluxes are derived from the average measured aerosol concentrations, rainfall intensity and theoretical scavenging rates. In contrast to our previous work (Rojas et al., 1993) and similar studies from the literature (Ottley and Harrison, 1993), combined coastal, ship and platform based measurements are evaluated in relation to the modelled calculations for the same area and period of time. Supplementary, the use of TXRF as an appropriate analytical method for atmospheric research studies was confirmed; it allows a short sampling time of e.g. half an hour, implies virtually no sample preparation and yields simultaneous determinations of various elements with detection limits down to 0.2 ng m^{-3} (Injuk and Van Grieken, 1995).

EXPERIMENTAL

Sampling Strategy

The dry and wet deposition fluxes, reported here for the southern and central North Sea area, are based upon concentration data of aerosol samples collected in the lower troposphere in a period spanning from September 1992 to May 1994. A huge data set of more than 1000 mass-segregated airborne samples was collected during two research cruises aboard the R/V Belgica (August 21-27, 1993), on the research platform "Nordsee" (54°42'N, 7°10'E; NOSE Experiment'92, from September 2-21, 1992) and at a station located approximately 100 m from the Belgian coastal line in Blankenberge (from October 1992 to May 1994). The sampling procedure involved the use of a Battelle cascade-impactor (cut-off diameters 0.25, 0.5, 1, 2, 4, 8 and 16 µm; flow-rate 1.2 l min^{-1}) in a continuous forced air flow inside a wind tunnel (Vawda et al., 1992). By sampling from a portable wind tunnel, the problems of isokinetic sampling conditions are overcome since it allows quantitative collection of big particles (larger than 4 µm) without problems of a variable cut-off with wind direction and wind speed. The tunnel is directed into the ambient wind by means of a light wind vane and, as a ventilator produces a constant forced air stream inside the tunnel, the linear velocity of the particles in the air can be made the same as the intake velocity in the sampling device. Impactor stages were loaded with polished quartz discs (30 mm diameter, 3 mm thickness) that were also used directly as targets for

TXRF. The discs were specially cut in order to allow for appropriate mounting above the stage orifice. A steel spring presses them firmly against the three disc holders.

Sample Preparation and Analysis

A rather new method for aerosol collection and sample preparation was applied in this work, namely the use of the reflector holders of TXRF as a sample support for the direct impaction of size-segregated airborne matter. This method has not been widely attempted so far (Schneider, 1989). Prior to the collection, siliconizing of the quartz discs was achieved by dispersing a 5 μl drop of silicone solution (SERVA, Polylab) to reduce both blow-off and bounce-off effects. The airborne particle spots, collected on the quartz siliconised discs, were subsequently supplied with a Ga solution aliquot as an internal standard, dried in an exsiccator under reduced pressure and analyzed by TXRF. The economic so-called "Atominstitut" TXRF-module generally allows absolutely detection limits down to a few 100 pg. All samples were irradiated for 500 sec at 20 mA and 45 kV. X-ray spectrum evaluation was done with the computer programme AXIL (Van Espen et al., 1986).

RESULTS AND DISCUSSION

For the determination of atmospheric parameters describing the input of trace elements into the North Sea, elemental aerosol size distributions were measured, followed by calculation of deposition velocities and dry and wet deposition fluxes. The dry deposition flux, F_d (ng m^{-2} s^{-1}), of material to the water surface was calculated from the product of atmospheric concentrations, C_a (ng m^{-3}) and the dry deposition velocity, V_d (m s^{-1}). The dry deposition velocity of aerosols is strongly dependent on particle size and meteorological factors, primarily wind speed and humidity. Since dry deposition velocities are mass dependent (so-called granulometric approach), normalizing aerosol mass and particle size is necessary. In this study, we used the mass distribution given by the Battelle cascade-impactor. In calculation of dry fluxes to the sea, the total airborne concentration of an element within each cascade impactor was multiplied by the corresponding particle mass-weighted deposition velocity. The average dry deposition rates and the standard deviations, based on calculations from the different sampling campaigns in '92, '93 and '94, are given in Table 1. The values for the dry deposition fluxes determined in this work are typically less than previously published data (Injuk and Van Grieken, 1995), but still comparable. A primary cause of the higher values for the dry deposition flux derived by earlier workers stems from the extrapolation of point measurements to the whole North Sea, while here a spatial distribution of measurements was used. Furthermore, the generally higher levels previously reported, may also result from higher atmospheric concentrations prior to the many voluntary and enforced emission controls implemented in recent years. The uncertainty produced in the resultant dry deposition flux is strongly dependent upon the aerosol size distribution, especially their large size fraction.

Wet deposition calculations (Table 1) were carried out using the scavenging factors, recommended by GESAMP (1989): 500 (Ni, Cu, Zn, Pb). Also, an annual rainfall above the North Sea of 677 mm y^{-1} and the average elemental atmospheric concentrations of the whole data set, were included. The data presented in Table 1 suggest that on the average wet deposition fluxes are approximately a factor of 3 higher that dry deposition for all elements of interest. In Table 2, the estimates for total (dry and wet) atmospheric inputs to the North Sea based on this study are compared with the most recently published values given by OSPARCOM (1993).

Table 3 summarizes information on riverine, direct and atmospheric inputs to the North Sea together with the disposal at sea for some heavy metals. It is clearly recognized that substantial inputs of metals are introduced into the marine environment through the rivers and the atmosphere. The atmospheric deposition balanced 28% (Cu), 30% (Zn) and 57% (Pb) among all input sources. The impact of other smaller point sources can, however, be highly significant and should not be ignored. In order to reduce inputs via the atmosphere, reduction of emissions at the source will usually prove to be the most effective method. The atmospheric input data, presented here, must be used with a great care: the method of extrapolating measurements of coastal station (although this was not exclusively done here) is crude and can result in an overestimation of inputs to the open sea. Furthermore, the accuracy is dependent on the uncertainties in the concentration measurements (20%) and deposition calculations (50%) and also on the accuracy of the estimation of the other input routes (30%).

Comparison with model calculations

To validate indirect deposition calculations satisfactorily, the obtained results were compared with the modelling values, which represent the same area and period of time (Table 4). The model used was the so-called EUTREND model developed at the Dutch National Institute of Public Health and Environmental Protection (Van Jaarsveld and van Aalst, 1986). It is a statistical long-range version of the Gaussian plume model, what means that the dispersion from a source is assumed to follow the prevailing wind direction and wind speed within a sector of 30% in the horizontal plane. Atmospheric processes included in the model are: emission, dispersion, advection, chemical conversion and wet and dry deposition. With respect to the deposition, the model describes the behaviour of pollutants attached to particles as a function of particle size. The emission is considered to be distributed over 5 particle size classes: < 0.95, 0.95 - 4, 4 - 10, 10 - 20, >20 µm. The model calculates these classes separately, with specific deposition properties for each class. Chemical reaction rates are used in the model independently of concentrations levels. The model is applied here using a fixed receptor grid over the North Sea area with a 0.5° long. x 0.25° lat. resolution. Emission factors for heavy metals were taken from the PARCOM-ATMOS emission factor manual (Van der Most and Veldt, 1992).

The average discrepancies between the indirectly calculated deposition rates with the modelled ones are around 56%. Here, it must be recognized that the total uncertainty of the results implies uncertainties introduced by the model concept, in compound specific parameters and in the emission estimates. The uncertainty in the emissions ranges from a factor of 2 to 3.5. This range must be considered as a maximum margin (Baart and al., 1995). Also, there is a large uncertainty on experimental values. To sum up, it can be concluded that, on the basis of comparisons with measurements, a quite satisfactory agreement was achieved.

ACKNOWLEDGMENTS

We thank A. Baart (TNO Institute of Environmental Sciences, Delft, The Netherlands) for carrying out the model calculations. This work was supported by the a) Belgian State-Prime Minister's Service-Science Policy Office, in the framework of the Impulse Programme in Marine Sciences (Contract MS 06 050) and in the framework of the EUROTRAC Programme (Contract EU 7 08), b) Belgian Ministry of Public Health and the Environment, Department of Protection against Ionizing Radiation.

REFERENCES

Baart, A.C.; Berdowski, J.J.M.; van Jaarsveld, J.A.; Calculation of atmospheric deposition of contaminants on the North Sea. TNO Institute of Environmental Sciences, Delft, The Netherlands, Report No. TNO-MW-R95/138, **1995**.

GESAMP-IMO/FAO/UNESCO/WMO/WHO/IAEA/UN/UNEP Joint Group of Experts on the Scientific Aspects of Marine Pollution. The Atmospheric Input of Trace Species to the World Ocean. Rep. Stud. GESAMP (38) **1989**.

Injuk, J.; Van Grieken, R. Spectrochim. Acta. **1995**, 50B, 1787-1803.

Injuk, J.; Van Grieken, R. J. Atmos. Chem. **1995**, 20, 179-212.

OSPARCOM (1993) North Sea Assessment Report 2b. North Sea Task Force. Oslo and Paris Commissions, London. Olsen and Olsen, Fredensburg, Denmark.

Ottley, C.J.; Harrison, R.M. Atmos. Environ. **1993**, 5, 685-695.

Rojas, C.M.; Injuk, J.; Van Grieken, R.; Laane, R.M. Atmos. Environ. **1993**, 27A, 251-259.

Schneider, B. Spectrochim. Acta. **1989**, 44B, 519-523.

Slinn, S.A.; Slinn, W.G.N. Atmos. Environ. **1980**, 14, 1013-1016.

Van Espen, P.; Janssens, K.; Nobels, J. **1986**, Chemometrics Intelligent Lab. Syst., 1, 109-114.

Van Jaarsveld, J.A.; van Aalst, R.M.; Onderdelinden, D.; Deposition of metals from the atmosphere into the North Sea: Model calculations. RIVM, Bilthoven, Report No. 842015002, **1986**.

Van der Most, P.F.J.; and Veldt, C.; Emission factors manual PARCOM-ATMOS. Emission factors for air pollutants 1992. TNO Report 92-235, Apeldoorn, The Netherlands.

Vawda, Y.; Colbeck, I.; Harrison, R.M.; Nicholson, K.W. J. Aerosol Sci. **1992**, 23, 233-243.

Addendum F

Mededelingen
Posters
Licentiaats- en doctoraatstheses

Mededelingen

* Prof. R. Van Grieken, "Atmospheric deposition of heavy metals into the North Sea", tijdens "Congress on Progress in Belgian Oceanographic Research", Brussel, 21-22 januari 1993.

* Prof. R. Van Grieken,"Atmospheric deposition into the marine environment", tijdens "EC-Symposium on Marine Science and Technology", Brussel, 15-17 maart 1993 (invited lecture).

* W. Jambers, "Characterization of inorganic suspended matter with EPXMA", tijdens "EC-Advanced Study Cource: Analysis of Marine Particles", Bergen, Noorwegen, 1 - 12 juni 1993.

* Prof. R. Van Grieken, "Single particle analysis of marine aerosols", tijdens "12th Annual Meeting of the American Association for Aerosol Research", Oak Brook, IL, USA, 11-15 oktober 1993 (invited lecture).

* L. De Bock, "Individual aerosol particle composition variations in air masses crossing the North Sea", tijdens "IZWO-contactdag: De Noordzee", Brugge, 22 april 1994.

* Prof. R. Van Grieken, "Determination of atmospheric heavy metal inputs into the North Sea by TXRF and micro-PIXE", tijdens "European Conference of Energy Dispersive X-ray Spectrometry", Budapest, Hongarije, 30 mei - 3 juni 1994 (invited lecture).

* Prof. R. Van Grieken, "Characterization and assessment of environmental particles", tijdens "Second International Symposium on Speciation of Elements in Toxicology and in Environmental an Biological Sciences", Loen, Noorwegen, 15 - 18 juni 1994 (invited lecture).

* Prof. R. Van Grieken, "Atmospheric deposition of heavy metals into the North Sea as studied by micro and trace analysis", tijdens "6th International Conference on Environmental Contamination", Delphi, Griekenland, 10-12 oktober 1994 (invited lecture).

* Prof. R. Van Grieken, "De Noordzee: ook door de lucht verontreinigd", tijdens "Symposium 10 jaar Belgica: Dialoog tussen de Wetenschappers en de Gebruikers van de Zee", Oostende, 17-19 oktober 1994 (invited lecture).

* Prof. R. Van Grieken, "Individual aerosol particle analysis: new developments and environmental applications", tijdens "Symposium Analitika 94: Analytical Science towards the Welfare of People and the Environment", Stellenbosch, Zuid Afrika, 8-13 december 1994 (invited lecture).

* Prof. B. Treiger, "Studying the composition of atmospheric aerosols through the joint application of hierarchical, non-hierachical and fuzzy clustering to EPXMA data sets", tijdens "3rd Russian-German-Ukrainian Analytical Symposium", Sumy, Ukraine, 5-9 september 1994 (invited lecture).

* W. Jambers, "Characterization of inorganic North Sea suspension", tijdens "European Research Course on Atmospheres 1995", Grenoble, Frankrijk, 9 januari - 8 februari 1995.

* Dr. J. Injuk, "Assessment of atmospheric pollutant fluxes to the North Sea by X-ray emission analysis", tijdens Staff Exchange Tempus, Ljubljana, Slovenië, 3-7 juli 1995.

* Prof. R. Van Grieken, "Micro-analysis of individual environmental particles", tijdens "XXXIX Colloquium Spectroscopicium Internationale", Leipzig, Duitsland, 27 augustus - 1 september 1995 (invited lecture).

* S. Hoornaert, "Trend analysis of the concentrations of metals in aerosols above the North Sea", tijdens Workshop "Progress in Belgian Oceanographic Research", Brussel, 9 january 1996.

* Dr. J. Injuk, "Atmospheric inputs of heavy metals into the North Sea", tijdens Workshop "Progress in Belgian Oceanographic Research", Brussel, 9 january 1996.

* W. Jambers, "Single particle characterization of inorganic North Sea suspension", tijdens Workshop "Progress in Belgian Oceanographic Research", Brussel, 9 january 1996.

* W. Jambers, "Individuele deeltjes analyse van Noordzee suspensie", tijdens 3de Vlaams Jongeren Congres, J-KVCV, Gent, 10 april 1996.

* Prof. R.Van Grieken, "Recent applications of individual particle analysis in environmental research", tijdens "Preservation of our World in the Wake of Change", Sixth International Conference of the Israeli Society for Ecology & Environmental Quality Science, Jerusalem, Israel, 30 juni- 4 juli 1996 (invited lecture).

* Dr. J. Injuk, "Deposition of atmospheric Ni, Cu, Zn and Pb into the North Sea, based on coastal, ship and platform measurements and on modelled predictions", tijdens "Preservation of our World in the Wake of Change", Sixth International Conference of the Israeli Society for Ecology & Environmental Quality Science, Jerusalem, Israel, 30 juni- 4 juli 1996.

Posters

* "Study of the concentrations, sources and deposition of North Sea aerosols using X-ray spectrometric techniques", tijdens "Congress on Progress in Belgian Oceanographic Research", Brussel, 21-22 januari 1993.

* "Study of individual particle types and heavy metal deposition for North Sea aerosols", tijdens "IZWO-contactdag: De Noordzee", Brugge, 22 april 1994.

* "Individual aerosol particle composition variation in air masses crossing the North Sea", tijdens "Symposium 10 jaar Belgica: Dialoog tussen de Wetenschappers en de Gebruikers van de Zee", Oostende, 17-19 oktober 1994.

* "Study of individual particle types and heavy metal deposition for North Sea aerosols", tijdens "Symposium 10 jaar Belgica: Dialoog tussen de Wetenschappers en de Gebruikers van de Zee", Oostende, 17-19 oktober 1994.

* "De lucht vervuild de Noordzee", tijdens "Historische Tentoonstelling 10 jaar Belgica", Oostende, 20-23 oktober 1994.

* "Characterisation of inorganic North Sea suspension", tijdens "European Research Course on Atmospheres 1995", Grenoble, Frankrijk, 9 januari - 8 februari 1995.

Licentiaats- en doctoraatstheses

Zes licentiaats- en vijf doctoraatsstudenten hebben meegewerkt aan dit onderzoek.

Licentiaatsstudenten

A. Neuwirth, Characterization of aerosols using total reflection X-ray fluorescence spectrometry (TXRF), 1993.

H. Van de Rul, Analyse van aerosolen met totale reflectie X-stralen fluorescentie spektrometrie, 1993.

M. De Beuckeleer, Concentratiebepaling van Cd, Pb, Cu en Zn in Noordzee aerosolen met anodische heroplossingsvoltametrie, 1993.

S. Hoornaert, Gips en chroom-rijke deeltjes in de Noordzee atmosfeer, 1994.

K. Gysels, Vergelijkende studie over het gebruik van een wind tunnel bij het nemen van aerosolmonsters, 1995.

K. Maes, Analyse van aerosolen met GDMS, 1995.

Doctoraatsstudenten

J. Injuk, Assessment of atmospheric pollutant fluxes to the North Sea by X-ray emission analysis, 25 april 1995.

H. Van Malderen, Microanalytical X-ray techniques for single particle analysis of marine and remote aerosols, 11 september 1995.

H. Struyf, Fourier transform laser probe massaspectrometrie met externe bron; ontwikkeling, anorganische speciatie en toepassingen, 16 april 1996.

L. De Bock, Optimalisatie van micro-analysemethodes voor individuele milieupartikels, verdededigingi 1997.

W. Jambers, Individuele deeltjes analyse van aquatisch suspensie met EXPMA en STEM, verdediging 1997.